DESIGN, SYNTHESIS AND CHARACTERIZATION OF SELF-ORGANIZING CONJUGATED POLYMERS FOR USE IN ORGANIC ELECTRONIC APPLICATIONS

A Dissertation
Presented to
The Academic Faculty

By

Kathy Beckner Woody

In Partial Fulfillment
Of the Requirement for the Degree
Doctor of Philosophy in the
School of Chemistry and Biochemistry

Georgia Institute of Technology

May, 2011

DESIGN, SYNTHESIS AND CHARACTERIZATION OF SELF-ORGANIZING CONJUGATED POLYMERS FOR USE IN ORGANIC ELECTRONIC APPLICATIONS

Approved by:

Dr. David Collard, Advisor
School of Chemistry and Biochemistry
Georgia Institute of Technology

Dr. Seth Marder
School of Chemistry and Biochemistry
Georgia Institute of Technology

Dr. Stefan France
School of Chemistry and Biochemistry
Georgia Institute of Technology

Dr. Laren Tolbert
School of Chemistry and Biochemistry
Georgia Institute of Technology

Dr. Anselm Griffin
School of Polymer, Textile, and Fiber Engineering
Georgia Institute of Technology

Date Approved: March, 2011

To Jeff, my husband and best friend

ACKNOWLEDGEMENTS

I would like to thank my advisor, Dr. David Collard, for all of his support throughout my graduate career. From the start he encouraged independent thinking and always supported every educational endeavor that I pursued, in and out of the lab. I am deeply grateful for his commitment to teaching me to become a better scientist. I also need to thank my undergraduate advisor at the University of Kentucky, Dr. Mark D. Watson. He welcomed me into his lab and taught me excellent research skills, and largely influenced my decision to attend graduate school.

I would like to acknowledge current and former members of Team Collard for their assistance including Dr. Glen Brizius, Dr. Bradley Carson, Dr. David Noga, Dr. Rakesh Nambiar, Dr. Cianan Russell, Dr. Bing Wang, Whitney Komorner, Subodh Jagtap, Guillermo Alas and Stephen Zappitello. Thanks to Elizabeth Henry, a fantastic summer REU student. A special thanks to Dr. Shannon Watt whose friendship and mentorship has been more important to me than she will ever know, and Dr. Jenny Raynor who always brightened my day with baked goods, fun dog stories and great friendship.

I would like to thank my thesis committee members (Dr. Stefan France, Dr. Anselm Griffin, Dr. Seth Marder and Dr. Laren Tolbert) for their support and guidance throughout my graduate career.

My collaborators at Wright Patterson Air Force Research Labs, Dr. Benjamin Leever and Dr. Michael Durstock, who provided assistance with solar cell fabrication and characterization of materials presented in this thesis, and helped me attain a better understanding of what goes in to developing organic devices.

The School of Chemistry and Biochemistry faculty and staff have been very supportive, especially Dr. Cam Tyson, an excellent mentor and friend and Dr. Leigh Bottomley, who gives excellent advice. Dr. Art Ragauskas provided me with the opportunity to travel abroad to Portugal as part of a sustainability outreach, and this trip was one of the most fun and educational endeavors that I accounted in graduate school. Dr. Leslie Gelbaum has provided excellent NMR support, the Georgia Tech Mass Spectrometry Facility, Dr. Haskell Beckham and Ryan Kincer for providing access and help with GPC, DSC and TGA, and Dr. Angus Wilkinson for assistance with Wide Angle X-ray Diffraction.

I cannot thank my friends in the graduate program enough, especially Anthony Baldridge, Tina Dreaden, Kathryn Pigg, Katy Roege, Aubrey Smith, Nick Haase, and Chip Humphries. My non-Georgia Tech friends, Peter and Katie Balch, Nate and Allison Laird, and AK and Teresa Broyles, provided love, support and a wonderful escape from graduate school.

I thank my parents, Richard and Jane Beckner for always loving and supporting me, teaching me to be an independent thinker, and believing in me. Also my brother-in-law and sister, Jason and Karen Grace, for all of the support, prayers and encouragement. To my son, Caleb, you are such an inspiration and my only hope is that my achievements will provide you with everything you need in life.

Above all, I cannot adequately express the gratitude I feel toward my husband Jeff. He put my career and my dreams before his, and he believed in me more than I believed in myself. Jeff, in part I owe all of my achievements to you, and you will always be the most significant person in my life.

TABLE OF CONTENTS

LIST OF TABLES

LIST OF FIGURES

LIST OF SYMBOLS AND ABBREVIATIONS

Δ	chemical shift
Δ	reflux
ΔH	enthalpy
λ	wavelength
λ_{max}	wavelength at maximum intensity
μ	micro
A	acceptor
Å	Angstrom
AcOH	acetic acid
AFM	atomic force microscopy
AIBN	2,2-azo-bis(isobutyronitrile)
Ar	aromatic
ATIR	Attenuated total reflection infrared spectroscopy
br	broad
CCl_4	carbon tetrachloride
$CDCl_3$	deuterated chloroform
CH_2Cl_2	methylene chloride
CTCP	catalyst-transfer condensation polymerization
CuI	copper iodide
CV	cyclic voltammetry
D	donor
d	doublet
dd	doublet of doublets
DMF	dimethyl formamide
DMSO	dimethyl sulfoxide
DP	degree of polymerization
DSC	differential scanning calorimetry
d-spacing	domain spacing
E_g	bandgap

EI	electron ionization
em	emission
E_{ox}	oxidation potential
E_{red}	reduction potential
Et_2O	diethyl ether
EtOAc	ethyl acetate
EtOH	ethanol
FTIR	Fourier-Transform Infrared Spectroscopy
g	grams
GPC	gel-permeation chromatography
GRIM	Grignard metathesis
h	hour
H_2O	water
hh	head-to-head
HOMO	highest occupied molecular orbital
HRMS	high resolution mass spectroscopy
ht	head-to-tail
Hz	hertz
I_2	iodine
IR	infrared
J	coupling constant
kg	kilograms
KIO_3	potassium iodate
L	liter
LUMO	lowest unoccupied molecular orbital
M	molarity
M.P.	melting point
m/z	mass to charge ratio
M^+	molecular ion
MeOH	Methanol
$MgSO_4$	magnesium sulfate
mL	milliliter

mmol	millimoles
M_n	number average molecular weight
mol	moles
MS	mass spectroscopy
mV	millivolt
M_w	weight average molecular weight
N_2	nitrogen
NaH	sodium hydride
NBS	*N*-bromosuccinimide
$Ni(dppp)Cl_2$	[1,3-bis(diphenylphosphino)propane]dichloronickel(II)
nm	nanometer
NMR	nuclear magnetic resonance
OFETs	organic field effect transistors
OLEDs	organic light emitting diodes
OPVs	organic photovoltaics
p	pentet
P3HT	poly(3-hexylthiophene)
P3OT	poly(3-octylthiophene)
PAT	poly(3-alkylthiophene)
$Pd(PPh_3)_4$	tetraakis(triphenylphosphine)palladium(0)
PDI	polydispersity index
Ph	phenyl
PPE	poly(1,4-phenylene ethynylene)
PQE	poly(5,8-quinoxaline ethynylene)
PPh_3	triphenylphosphine
ppm	parts per million
PQ	poly(5,8-quinoxaline)
PThPY	poly(thienopyrazine)
R	alkyl
Rg	regioregular
Rn	regiorandom
RT	room temperature

s	second
s	singlet
t	triplet
T_c	crystallization temperature
T_g	glass transition temperature
Th	thiophene
THF	tetrahydrofuran
ThPy	thienopyrazine
$TiCl_4$	titanium tetrachloride
TLC	thin layer chromatography
T_m	melting temperature
TMS	trimethylsilyl
tt	tail-to-tail
UV-vis	ultraviolet-visible
V	volts
WAXD	wide angle X-ray diffraction

SUMMARY

Conjugated polymers comprise some of the most promising materials for new technologies such as organic field effect transistors, solar light harvesting technology and sensing devices. In spite of tremendous research initiatives in materials chemistry, the potential to optimize device performance and develop new technologies is remarkable. Understanding relationships between the structure of conjugated polymers and their electronic properties is critical to improving device performance. The design and synthesis of new materials which self-organize into ordered nanostructures creates opportunities to establish relationships between electronic properties and morphology or molecular packing. This thesis details our progress in the development of synthetic routes which provide access to new classes of conjugated polymers that contain dissimilar side chains that segregate or dissimilar conjugated blocks which phase separate, and summarizes our initial attempts to characterize these materials.

Variations of the side chains on the backbone of a conjugated polymer provide opportunities to tailor the molecular assembly and electronic properties of the material. The placement of side chains relative to one another can greatly influence the bulk properties of the polymer. For example regiorandom and regioregular PAT, which differs only in the placement of side chains with respect to one another on the conjugated backbone, have large differences in optical and electronic properties. In spite of these differences, the influence of regioregularity has not been investigated in many other types of materials. Poly(1,4-phenylene ethynylene)s (PPEs) have been used in a variety of organic electronic applications, most notably as fluorescent sensors. Using traditional

synthetic methods, asymmetrically disubstituted PPEs have irregular placement of side chains on the conjugated backbone. Herein, we establish the first synthetic route to an asymmetrically substituted regioregular PPEs. The initial PPEs in this study have different lengths of alkoxy side chains, and both regioregular and regiorandom analogs are synthesized and characterized for comparison.

The design of amphiphilic structures provides additional opportunities for side chains to influence the molecular packing and electronic properties of conjugated polymers. Regioregular side chain placement becomes even more important in conjugated polymers when the side chains are amphiphilic. A new class of regioregular, amphiphilic PPEs has been prepared bearing alkoxy and semifluoroalkoxy side chains, which have a tendency to phase separate. The optical properties are investigated using UV-visible absorption and fluorescence spectroscopy. Wide Angle X-ray Diffraction is used to better understand the molecular packing of these materials in the solid state.

Fully conjugated block copolymers can provide access to interesting new morphologies as a result of phase separation of the conjugated blocks. In particular, donor-acceptor block copolymers that phase separate into electron rich and electron poor domains may be advantageous in organic electronic devices such as bulk heterojunction solar cells, of which the performance relies on precise control of the interface between electron donating and accepting materials. The availability of donor-acceptor block copolymers is limited, largely due to the challenges associated with synthesizing these materials. In this thesis, two new synthetic routes to donor-acceptor block copolymers are established. These methods both utilize the catalyst transfer condensation polymerization, which proceeds by a chain growth mechanism. The first example entails the synthesis of

a monofunctionalized, telechelic poly(3-alkylthiophene) which can be coupled to electron accepting polymers in a subsequent reaction. The other method describes the first example of a one-pot synthesis of a donor-acceptor diblock copolymer. The methods of synthesis are described, and characterization of the block copolymers is reported.

Another limitation in the synthesis of donor-acceptor block copolymers is the availability of electron accepting polymers. Most conjugated polymers have low electron affinity, or are electron donating. The synthesis of new electron accepting polymers will provide opportunities to expose the utility of these materials in device applications. Poly(5,8-quinoxaline) is a known electron accepting polymer, however steric interactions between the quinoxaline units causes distortion of the backbone from planarity, which may be detrimental to the charge transport properties of the material. We report a new class of electron accepting quinoxaline-based conjugated polymer, poly(5,8-quinoxaline ethynylene)s where incorporating an alkyne between the quinoxaline units allows for planarization of the conjugated backbone.

CHAPTER 1: INTRODUCTION

1.1. Conjugated Polymers

In the 1970's, Heeger, MacDiarmid and Shirakawa first realized the ability of doped polyacetylene to conduct electricity,[1] spawning tremendous research efforts in the synthesis and development of new conjugated materials, and resulting in the award of a Noble Prize in 2000.[2] With the demonstration of the semiconducting properties of undoped conjugated materials, the driving force for this research became the potential to develop low-cost, flexible and light-weight organic electronic applications from these polymers for which the cost of materials processing is significantly lower than that of inorganic semiconductors. Some applications that conjugated polymers have been explored as the semiconductor include organic field effect transistors (OFETs),[3-6] organic photovoltaic cells (OPVs),[7-10] organic sensors,[11-13] and organic light emitting diodes (OLEDs).[14,15] The breadth of potential applications of conjugated polymers creates a constant need for the optimization of existing polymers and the design of new conjugated polymers with tunable properties.

While there are many types of conjugated polymers, this thesis focuses on four general classes: regioregular poly(3-alkylthiophene) (PAT), poly(1,4-phenylene ethynylene) (PPE), poly(5,8-quinoxaline) (PQ) and poly(thienopyrazine) (PThPy).

1.1.1. Regioregular Poly(3-alkylthiophene)

Poly(3-alkylthiophene)s (PATs) are important conjugated materials that have good stability and have potential applications in many areas. The ability of these

materials to assemble and planarize leads to better performance of organic electronic applications in comparison to many other conjugated materials. Oxidative polymerization of 3-alkylthiophene leads to three possible couplings between the 2- and 5- positions of the thiophene ring, including chemically distinct diads linked between the 2- and 2-position (head-to-head, *hh*), the 2- and 5- positions (head-to-tail, *ht*) and the 5- and 5-positions (tail-to-tail, *tt*), Figure 1.1. McCullough and Reike were the first to realize the importance of controlling the relative positions of the side chains along the backbones of these polymers.[16,17] They independently developed organometallic coupling reactions which afford PATs consisting of primarily *ht* dyads. This avoids the presence of *hh* coupling which lead to distortion of the backbone from planarity and a reduction of conjugation. Regioregular *ht* PATs however have a lower energy planar conformation, leading to higher crystallinity, red shifted optical absorptions, greater conductivity and smaller band gaps than their regiorandom analogs.[18]

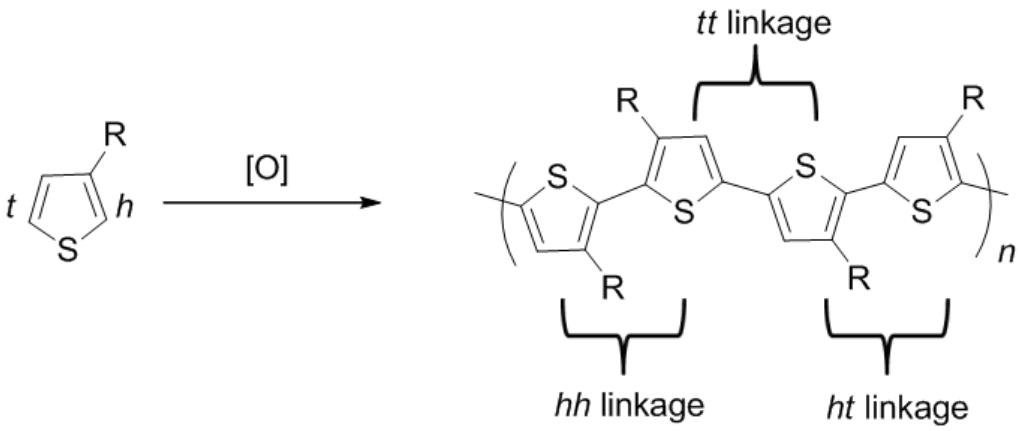

Figure 1.1. Oxidative polymerization of PATs lead to three chemically distinct diads containing *hh*, *ht* and *tt* coupling.

1.1.2. Poly(1,4-phenylene ethynylene)s

Poly(1,4-phenylene ethynylene)s (PPEs) are comprised of alternating para-phenylene and alkyne units in the conjugated backbone and have interesting properties resulting from their linear structure, strong fluorescence and solid state packing. PPEs have been employed in many organic electronic applications, most notably as chemical sensors.[11,12,19] The substitution of PPEs with flexible alkyl[20] or alkoxy[21,22] side chains imparts solubility and crystallinity to the polymers. These side chains influence the molecular packing of the PPE backbone in the solid state, and thereby affect the electronic structure of the close-packed conjugated systems. Thus, variation of the structure of the side chains provides opportunities to tailor the optical and electronic properties of this versatile class of polymers.

1.1.3. Electron Accepting Conjugated Polymers

Most conjugated polymers consist of electron-rich repeat units, whereby they have relatively low oxidation potentials and in that they are electron donating. Accordingly, they may serve as electron donating, or p-channel, semiconductors. There are few reports of electron accepting, n-channel semiconducting conjugated polymers. Such materials have not been extensively studied for use as the acceptor material in organic electronic applications; however, there is an example of a high performing solar cell which incorporates a conjugated polymer as the electron acceptor.[23]

Electron accepting conjugated polymers often contain electron withdrawing substituents such as fluorine or cyano groups,[24,25] or they consist of heteroaromatic units such as quinoline,[26] pyramidine,[27] pyridine,[28] thienopyrazine,[29] and quinoxaline.[30,31]

Poly(5,8-quinoxaline) (PQ) and poly(thienopyrazine) (PThPy) contain heteroaromatic repeat units in the conjugated backbone, and materials are easily solubilized by decorating them with flexible side chains, Figure 1.2. While these materials have not been extensively studied for organic electronic applications, they are subject to n-doping by reduction and are thus of potential use as electron accepting materials.[32]

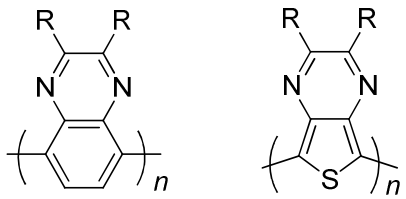

Figure 1.2. Electron accepting polymers poly(5,8-quinoxaline) and poly(thienopyrazine).

1.2. Amphiphilic Poly(3-alkythiophene)s with Alkyl and Semifluoroalkyl Side Chains

The design of amphiphilic structures allows for the manipulation of the packing and orientation of molecules in the solid state and at interfaces.[33] It is well established that the identity and relative position of side chains along the polymer backbone have a large impact on the properties of poly(alkylthiophene)s. These differences are most pronounced when these side chains impart amphiphilicity to the structure. The Collard research group has previously explored the impact of amphiphilicity in poly(3-alkylthiophene)s substituted with alternating alkyl and fluoroalkyl or semifluoroalkyl segments.[34,35]

Fluoroalkanes and hydrocarbons have a tendancy to phase separate. On a molecular scale, fluoroalkyl and alkyl segments of a small molecule or a polymer segregate to afford control over molecular packing. Unlike other common combinations of side chains

which give rise to amphiphilicity (e.g., combinations of alkyl, ionic, oligoether, siloxyl units), hydrocarbon and fluorocarbon segments are both hydrophobic and are of a similar size. The incorporation of semifluoroalkyl side chains in various polymers has led to enhanced thermal stability and chemical and oxidative resistance,[36-38] and formation of self-assembled architectures.[39-42] Poly(3-alkylthiophene)s (PATs) substituted with alternating alkyl and semifluoroalkyl side chains along the backbone adopt an all-anti configuration in the solid state, giving rise to a Janus-type amphiphilic structure. The ribbonlike conjugated backbone has fluoroalkyl groups on one side and alkyl side chains on the other. The segregation of dissimilar side chains gives rise to a highly ordered bilayer lamellar crystalline packing, Figure 1.3. In addition, by avoiding interaction of both of the disparate side chains with the substrate the polymeric molecules self-orient, leading to a packing in which the conjugated backbone assembles perpendicular to the substrate.[34]

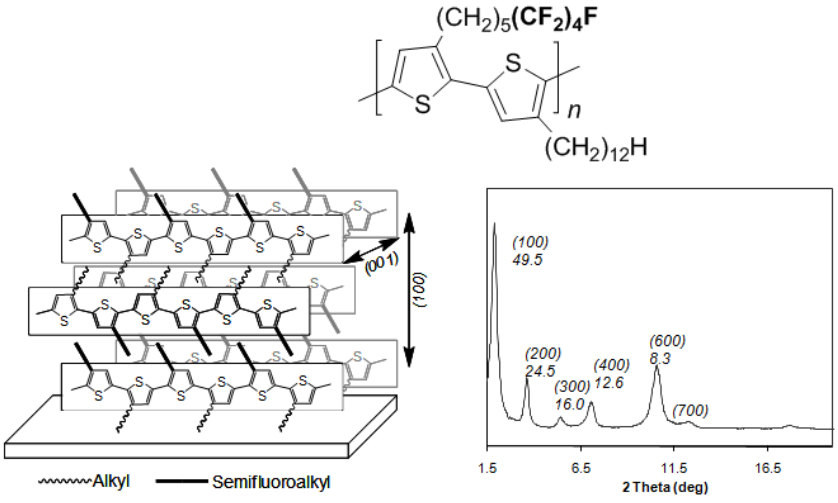

Figure 1.3. PATs with alternating alkyl and semifluoroalkyl substituents, which self-orient perpendicular to the substrate (left) and form bilayer lamellar structures (wide angle X-ray diffraction, right).[34]

1.3. Fully Conjugated Block Copolymers

In addition to the self-assembly of polymers in which each individual repeat unit has amphiphilic characteristics, block copolymers undergo microphase segregation of the two blocks to afford nanostructured materials. However, in spite of the potential advantages for using these types of materials to create new morphologies with interesting electronic properties, the majority of research on conjugated polymers to-date has focused on homopolymers and alternating copolymers.[43] Conjugated block copolymers are much less studied, which may be attributed to the challenges in synthesizing such materials.[44] The few reports of fully conjugated block copolymers suggest that these materials present interesting opportunities to impart new properties as a result of phase separation of the two blocks, with formation of morphologies which may be advantageous in new applications.[45-47]

1.3.1. Synthesis of Conjugated Diblock Copolymers by Step Growth Polymerizations

Conjugated polymers are often prepared by condensation polymerizations of aromatic dihalides and an appropriately substituted difunctional monomers, (e.g. bis-stannanes,[48] bisboronates,[49] and bisphosphonantes[50] or other organometallic reagents[51]). However, condensation polymerizations typically proceed with step growth kinetics that lead to polydisperse materials with polydispersity indices (PDI) greater than 2.[52] Such step growth processes do not lend themselves to formation of well-defined block copolymers.

Early approaches to the synthesis conjugated diblock copolymers proceeded by coupling of the individual blocks.[53] This requires the preparation of the individual

polymers with appropriate functionality at the termini, which are then coupled together in a subsequent reaction (Figure 1.4A).

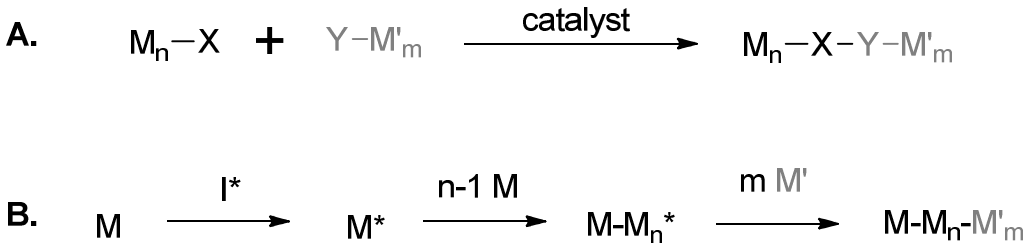

Figure 1.4. Preparation of diblock copolymers: (A) by coupling to two pre-formed monofunctional homopolymers; (B) By sequential chain-growth polymerization of two monomers.

There are several disadvantages with this synthetic approach. The functional end-groups of the two individual homopolymers are present in very low concentrations which might result in low yielding coupling reaction, leading to the presence of uncoupled homopolymer chains. In addition, the step growth polymerizations used to prepare the two precursor polymers give materials with high PDIs. Thus, coupling the two polydisperse polymer chains results in ill-defined materials such that it is difficult to tailor the lengths of the segments to attain control over copolymer assembly and properties.

Another challenge associated with synthesizing each precursor block using a step-growth polymerization is the inability to precisely control the end-groups of the polymers. Coupling two difunctional monomers can lead to polymer chains containing a

mixture of the two types functional group on each termini which could lead to triblock and other multiblock copolymers. Scherf addressed this issue by synthesizing a single monomer bearing each type of functional group (e.g., an A-B type monomer), such that there is always one type of each end group on every polymer chain. Poly(9,9-dialkylfluorene) was prepared by a Suzuki polymerization of the bromo-boronic acid substituted monomer, Figure 1.5.[54] At the end of the polymerization, bromo-terminated poly(3-alkyl thiophene) was added as an end-capper to afford poly(9,9-dialkylfluorene)-*block*-poly(3-alkyl thiophene) (**PF-*b*-PAT**). While gel permeation chromatography (GPC) demonstrated that the desired block copolymers are formed, there are significant drawbacks to this synthetic method including: (i) the use of a step-growth polymerization to prepare the two chains leading to block copolymers with high polydispersities (ii) the use of poly(3-alkylthiophene) with ill-defined end-groups[55] (i.e., not strictly monobrominated polymer chains) and (iii) potential coupling between polyfluorene chains.

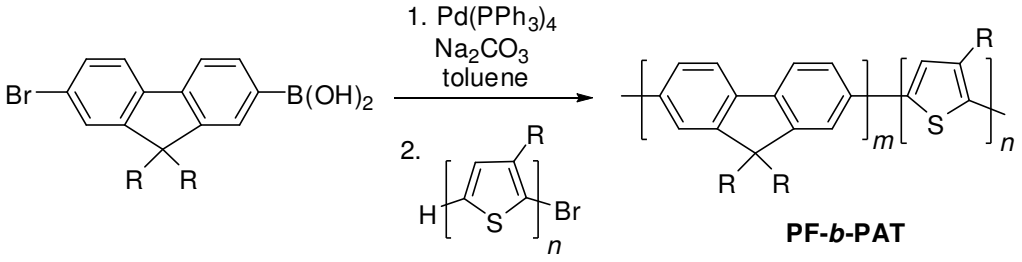

Figure 1.5. Synthesis of poly(9,9-dialkylfluorene)-*block*-poly(3-alkylthiophene).

Given the lack of control over the polydispersity of polymers prepared by step growth condensation polymerizations, and the inefficiency of coupling polymer end groups, the

recent development of chain-growth condensation polymerizations presents significant opportunities for the preparation of now well-defined conjugated block copolymers.

1.3.2. Chain Growth Condensation Polymerizations

In contrast to the step growth kinetics common to condensation polymerizations, addition polymerizations typically proceed by a chain growth process. In a chain growth polymerization, each polymer chain is grown from an initiator, and only reacts with subsequent monomer at the active termini. In the absence of pathways for termination or chain transfer this process leads to a "living" polymerization to afford well-defined polymers with narrow molecular weight distributions (PDI ≈ 1) and control over the molecular weight. The addition of a second monomer to a living polymerization after consumption of the first monomer allows for further extension of the polymer chain to afford a block copolymer, Figure 1.4B.

The conversion of a condensation polymerization from a process involving step growth kinetics to one that proceeds by a chain growth process has only been reported recently. This requires the use of catalysts which selectively transfer reactivity to the terminus of the polymer chain upon addition of each monomer to the chain end.[56]

In 1995, McCullough developed the Grignard metathesis (GRIM) polymerization in which 2,5-dibromo-3-alkylthiophene was treated with a Grignard reagent followed by addition of a transition metal catalyst, producing regioregular poly(3-alkylthiophene).[57] The pathway for these polymerizations was originally formulated in terms of a nickel catalyzed coupling proceeding with step growth kinetics, Figure 1.6B. However, evidence was soon collected to indicate that the polymerizations proceed with

characteristics of a quasi-living process.[58] Yokozawa and coworkers further modified this polymerization by synthesizing a 2-bromo-5-iodo-3-alkylthiophene which provided additional selectivity for the insertion of the metal, and demonstrated well-controlled polymerizations with narrow PDIs.[59] Investigation of this reaction revealed that the polymerization takes place by a chain growth process, or a catalyst-transfer condensation polymerization (CTCP).

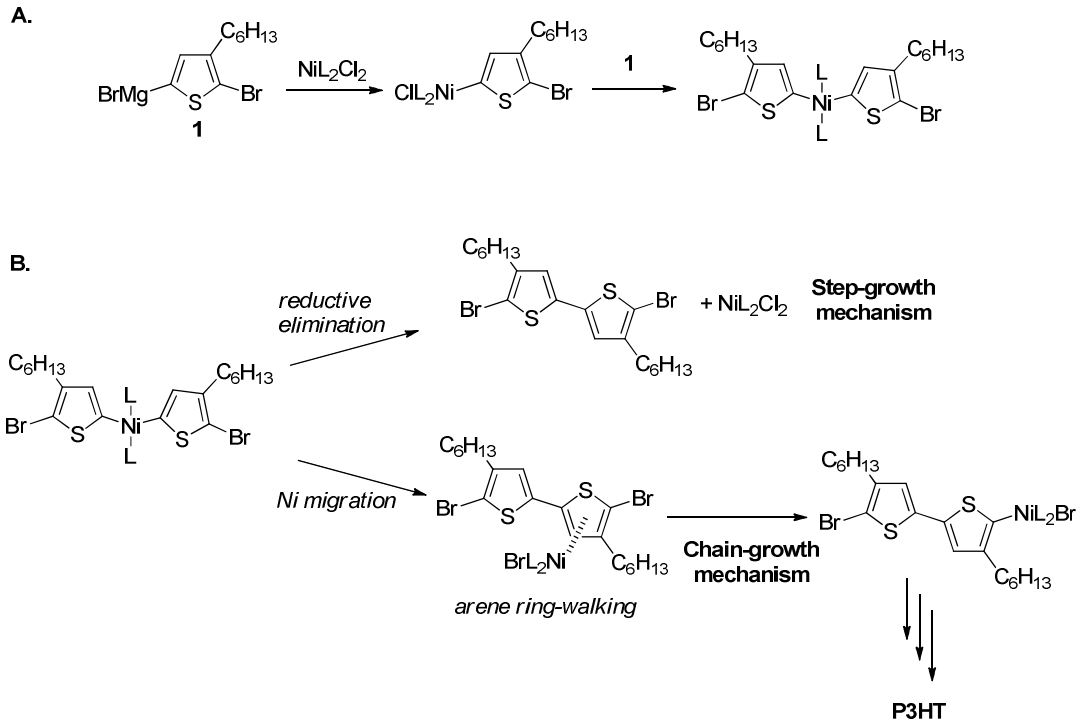

Figure 1.6. Nickel(II) catalyzed polymerization of 2-bromo-5-metallothiophene monomers: (A) Preparation of dithienyl nickel complex, (B) Top, original step-growth mechanism proposed by McCullough; bottom, mechanism for the chain-growth catalyst transfer polymerization of 3-alkylthiophene.

The polymerization of a 2-bromo-5-magnesiothiophene monomer proceeds by reaction of two equivalents of monomer with nickel(II) to form a dithienylnickel(II) complex. The propagation step of the chain gowth polymerization is a reductive elimination to form a thiophene-thiophene bond *with intramolecular transfer of the nickel to the chain end* by oxidative insertion into the thiophene-bromine bond. Thus, the reactive nickel center is transferred to the end of the growing polymer chain upon the addition of each monomer without dissociation of nickel from the chain (Figure 1.6B, bottom). The absence of termination or chain transfer during the process leads to control of the molecular weight of the polymer consistent with a living polymerization.

1.4. The Potential for use of Block Copolymers in Bulk Heterojunction Solar Cells

Bulk heterojunction solar cells make use of mixtures of electron donating and electron accepting materials in the active layer.[60] The conversion of light to energy begins with absorption of photons in the organic layer. Absorption of photons excites an electron in the electron rich (donor) material to form an exciton, or an electrically neutral electon-hole pair, Figure 1.7. The exciton randomly diffuses through the donor material, and if it reaches an interface between the donor and acceptor materials, dissociation of the electron-hole pair can occur by electron transfer from the donor to the LUMO of the acceptor, Figure 1.7. Dissociation occurs if the charge separated state is lower in energy and there is sufficient driving force to overcome the binding energy of the electron-hole pair, that is, the Coulomb attraction which in conjugated polymers is typically between 0.3-0.4 eV.[61] Migration of the electron and hole occurs by a hopping mechanism aided

by the potential created by the metal electrodes. If the electron and hole reach the anode and cathode respectively, a photocurrent is generated.

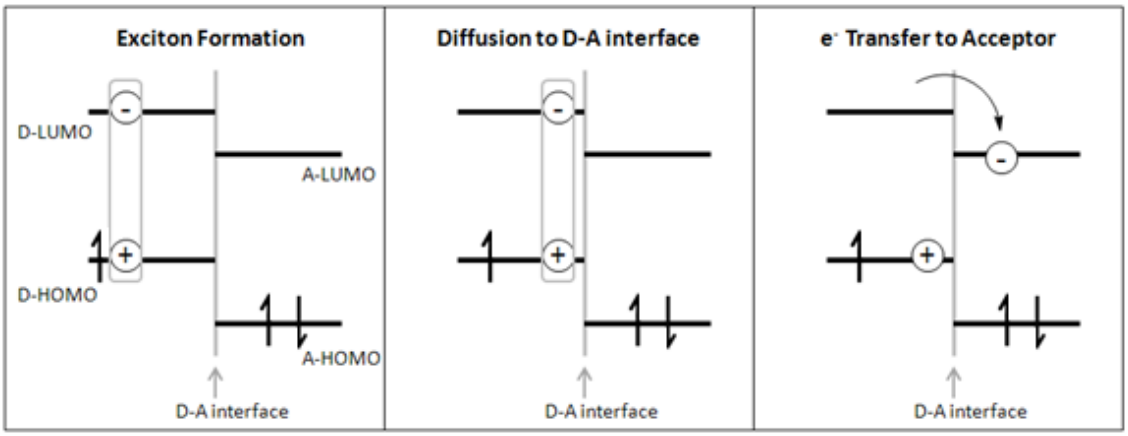

Figure 1.7. Light to energy conversion in an organic photovoltaic cell.

There are several challenges associated with these steps,[62] which to date have limited power conversion efficiencies of approximately 8%.[63] One challenge is associated with the exciton diffusion length, which occurs over distances of only 5-10 nm.[65] Excitons that do not reach an interface decay, often in the form of luminescence. Thus, bulk heterojunction solar cells require thorough blending of the donor and acceptor materials to increase the relative proportion represented by the diffusion zone, or the amount of material capable of producing charge carriers. Increasing the contact between the donor and acceptor by thoroughly blending the materials improves the performance of the solar cell; devices with phase separation on the scale of 10-20 nm outperform those with larger domains.[64,65]

Initiatives to improve the performance of bulk heterojunction solar cells largely focus on the design and synthesis of low band gap conjugated polymers[66,67] and changing the morphology of the blends.[68-70] Another possibility is to use block copolymers to better

control phase separation of the donor and acceptor.[25] Block copolymers phase separate on the nanoscale, where the size of the phases formed by the two blocks is directly related to the length of each block. Rod-coil block copolymers containing a combination of conjugated semi-rigid segments and flexible segments have been extensively studied and provide abundant opportunities to prepare materials with unique morphologies.[71,72] However, these materials contain only one electroactive segment and the flexible segment serves as an insulator. Block copolymers consisting of a combination of phase separating donor and acceptor conjugated segments would provide opportunities to control the scale and morphology of phases in bulk heterojunction solar cells and thereby influence the donor-acceptor interface.

1.5. Scope of work

Understanding relationships between the molecular and supermolecular structure of materials and their electronic properties is critical to improving the performance of organic electronic applications which make use of conjugated polymers as semiconductors. The design and synthesis of new materials which self-organize into ordered nanostructures creates opportunities to establish relationships between electronic properties and morphology or molecular packing. The work presented in this thesis provides molecular design and synthetic routes which creates access to new classes of conjugated polymers that self-assembly by virtue of substitution with dissimilar side chains or as a result of segregation of dissimilar conjugated blocks.

In Chapter 2, we establish the first general synthetic route to an asymmetrically substituted regioregular PPEs. The PPEs in this study have different lengths of alkoxy

side chains, and both regioregular and regiorandom analogs are synthesized and characterized. Regioregular side chain placement becomes even more important in conjugated polymers when the side chains impart an amphiphilic structure. In Chapter 3, we incorporate alkoxy and semifluoroalkoxy side chains onto the backbone of PPEs, Figure 1.8.

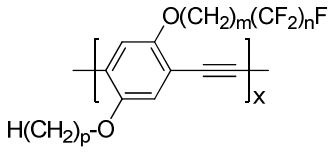

	regiorandom	*regioregular*
m = 6, n = 6, p = 12	**RnPPE(6,6/12)**	**RgPPE(6,6/12)**
m = 8, n = 4, p = 12	**RnPPE(8,4/12)**	**RgPPE(8,4/12)**
m = 10, n = 2, p = 12	**RnPPE(10,2/12)**	**RgPPE(10,2/12)**

Figure 1.8. Amphiphlic PPEs with semifluoroalkoxy and alkoxy side chains on each repeat unit (Chapter 3).

The development of chain growth CTCP provides a synthetic route which affords control over polymer structure, and affords access to novel all conjugated block copolymers. In Chapter 4, we utilize this type of polymerization to prepare a telechelic monofunctional poly(3-alkylthiophene) which was used in a subsequent coupling reaction with poly(5,8-quinoxline) to prepare donor-acceptor triblock copolymers, Figure 1.9. In Chapter 5, we utilize this type of polymerization to prepare diblock copolymers with poly(3-alkylthiophene) (donor) and poly(thienopyrazine) (acceptor) segments. This is the first example of donor-acceptor block copolymers prepared by a one-pot condensation polymerization, Figure 1.10.

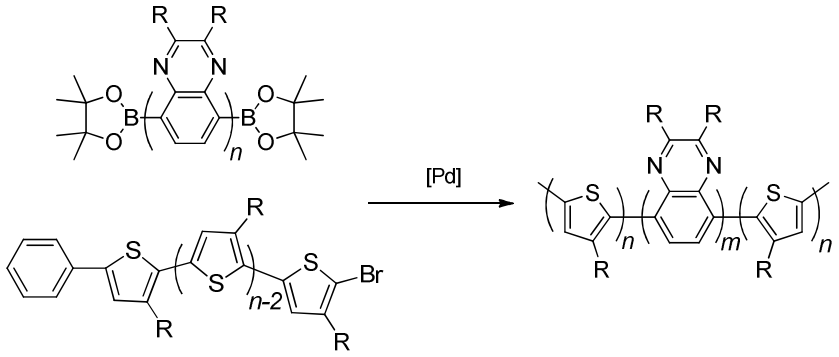

Figure 1.9. Coupling of a telechelic poly(3-alkylthiophene) with a single α-bromothienyl end group and poly(5,8-quinoxaline) (PQ) bearing two boronate ester end groups (Chapter 4).

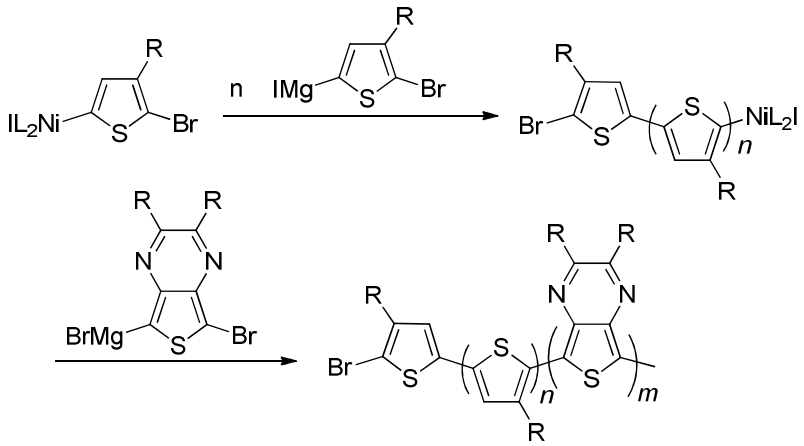

Figure 1.10. One-pot chain-growth condensation polymerization of donor-acceptor block copolymer with poly(3-alkylthiophene) and poly(thienopyrazine) segments (Chapter 5).

The limitation to the study of donor-acceptor conjugated polymers is presented by the amount of different electron accepting polymers is addressed in Chapter 6. Poly(5,8-quinoxaline) is an electron accepting polymer.[30] However steric interactions between the quinoxaline units causes distortion of the backbone from planarity, which may be detrimental to the charge transport properties of the material. We report a new class of

electron accepting quinoxaline-based conjugated polymer, poly(5,8-quinoxaline ethynylene)s in which incorporation of an alkyne beween the quinoxaline units allows for planarization of the conjugated backbone, Figure 1.11.

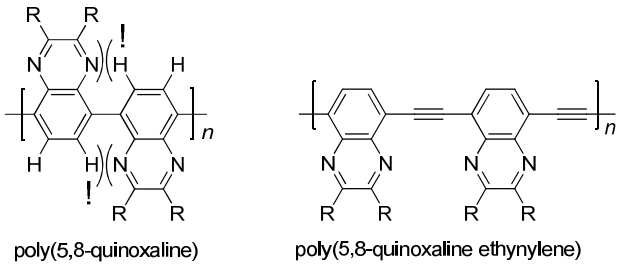

Figure 1.11. Poly(5,8-quinoxaline) based PPEs allow for planarization of the conjugated backbone (Chapter 6).

1.6. References

1. Chiang, C. K.; Fincher, C. R.; Park, Y. W.; Heeger, A. J.; Shirakawa, H.; Louis, E. J.; Gau, S.C.; MacDiarmid, A. G. *Phys. Rev. Lett.* **1977**, *39*, 1098-1101.

2. Shirakawa, H. *Angew. Chem. Int. Ed.* **2001**, *40*, 2574-2580.

3. Allard, S.; Forster, M.; Souharce, B.; Thiem, H.; Scherf, U. *Angew. Chem. Int. Ed.* **2008**, *47*, 4070-4098.

4. Garnier, F.; Hajlaoui, R.; Yassar, A.; Srivastava, P. *Science* **1994**, *265*, 1684-1686.

5. Zaumeseil, J.; Sirringhaus, H. *Chem. Rev.* **2007**, *107*, 1296-1323.

6. Dimitrakopoulos, C. D.; Malenfant, P. R. L. *Adv. Mater.* **2002**, *14*, 99-117.

7. Bundgaard, E.; Krebs, F. C. *Solar Energy Materials & Solar Cells* **2007**, *91*, 954-985.

8. Gunes, S.; Neugebauer, H.; Sariciftci, N. S. *Chem. Rev.* **2007**, *107*, 1324-1338.

9. Inganas, O.; Zhang, F. Andersson, M. R. *Acc. Chem. Res.* **2009**, *42*, 1731-1739.

10. Chen, J.; Cao, Y. *Acc. Chem. Res.* **2009**, *42*, 1709-1718.

11. McQuade, D. T.; Pullen, A. E.; Swager, T. M. *Chem. Rev.* **2000**, *100*, 2537-2574.

12. Thomas, S. W.; Joly, G. D.; Swager, T. M. *Chem. Rev.* **2007**, *107*, 1339-1386.

13. Basabe-Desmonts, L.; Reinhoudt, D. N.; Crego-Calama, M. *Chem. Soc. Rev.* **2007**, *36*, 993-1017.

14. Burroughes, J. H.; Bradley, D. D. C.; Brown, A. R.; Marks, R. N.; Mackay, K.; Friend, R. H.; Burns, L. P.; Holmes, A. B. *Nature* **1990**, *347*, 539-541.

15. Kraft, A.; Grimsdale, A. C.; Holmes, A. B. *Angew. Chem. Int. Ed.* **1998**, *37*, 402-428.

16. McCullough, R.D.; Lowe, R. D. *J. Chem. Soc. Chem. Comm.* **1992**, 70.

17. Chen, T.-A.; Rieke, R. D. *Syn. Metals* **1993**, *60*, 175-177.

18 . Chen, T.-A.; Wu, X.; Rieke, R. D. *J. Am. Chem. Soc.* **1995**, *117*, 233-244.

19. Weder, C.; Sarwa, C.; Bastiaansen, C.; Smith, P. *Adv. Mater.* **1997**, *9*, 1035-1039.

20. Francke, V.; Mangel, T.; Müllen, K. *Macromolecules* **1998**, *31*, 2447-2453.

21. Weder, C.; Wrighton, M. S. *Macromolecules* **1996**, *29*, 5157-5165.

22. Yang, J.-S.; Swager, T. M. *J. Am. Chem. Soc.* **1998**, *120*, 11864-11873.

23. Granström, M.; Petritsch, K.; Arias, A. C.; Lux, A.; Andersson, M. R.; Friend, R. H., *Nature* **1998**, *395*, 257-260.

24. Jin, Y.; Kim, K.; Park, S. H.; Song, S.; Kim, J.; Jung, J.; Lee, K.; Suh, H. *Macromolecules* **2007**, *40*, 6799-6806.

25. Greenham, N. C.; Moratti, S. C.; Bradley, D. D. C.; Friend, R. H.; Holmes, A. B., *Nature* **1993**, *365*, 628-630.

26 . Saito, N.; Kanbara, T.; Nakamura, Y.; Yamamoto, T.; Kubota, K. *Macromolecules* **1994**, *27*, 756-761.

27 . Kanbara, T.; Kushida, T.; Saito, N.; Kuwajima, I.; Kubota, K.; Yamamoto, T., *Chem. Lett.* **1992**, 21, 583-586.

28 . Yamamoto, T.; Maruyama, T.; Zhou, Z.; Ito, T.; Fukuda, T.; Yomeda, Y.; Begum, F.; Ikeda, T.; Sasaki, S.; Takezoe, H.; Fukuda, A.; Kubota,; K. *J. Am. Chem. Soc.* **1994**, *116*, 4832-4845.

29 . Wen, L.; Duck, B. C.; Dastoor, P. C.; Rasmussen, S. C. *Macromolecules* **2008**, *41*, 4576.

30 . Jonforsen, M.; Johansson, T.; Inganäs, O.; Andersson, M. R. *Macromolecules* **2002**, *35*, 1638-1643.

31 . Saito, N.; Kanbara, T.; Kushida, T.; Kubota, K.; Yamamoto, T. *Chem.Lett.* **1993**, *22*, 1775-1778.

32. Yamamoto, T.; Sugiyama, K.; Kushida, T.; Inoue, T.; Kanbara, T. *J. Am. Chem. Soc.* **1996**, *118*, 3930-3937.

33. Fazio, D.; Mongin, C.; Donnio, B.; Galerne, Y.; Guillon, D.; Bruce, D. W. *J. Mater. Chem.* **2001**, *11*, 2852-2863.

34. Wang, B.; Watt, S.; Hong, M.; Domercq, B.; Sun, R.; Kippelen, B.; Collard, D. M. M*acromolecules* **2008**, *41*, 5156-5165.

35. Li, L.; Collard, D. M. *Macromolecules* **2005**, *38*, 372-378.

36. Ren, Y.; Lodge, T. P.; Hillmyer, M. A. *Macromolecules* **2001**, *34*, 4780-4787.

37. Tran, H. V.; Hung, R. J.; Chiba, T.; Yamada, S.; Mrozek, T.; Hsieh, Y.-T.; Chambers, C. R.; Osborn, B. P.; Trinque, B. C.; Pinnow, M. J.; MacDonald, S. A.; Willson, C. G.; Sanders, D. P.; Conner, E. F.; Grubbs, R. H.; Conley, W. *Macromolecules* **2002**, *35*, 6539-6549.

38. Robitaille, L. Leclerc, M. *Macromolecules* **1994**, *27*, 1847-1851.

39. Wang, J.; Ober, C. K. *Macromolecules* **1997**, *30*, 7560-7567.

40. Johansson, G.; Percec, V. Ungar, G.; Zhou, J. P. *Macromolecules* **1996**, *29*, 646-660.

41. Hayakawa, T. Wang, J.; Xiang, M.; Li, X.; Ueda, M.; Ober, C. K.; Genzer, J.; Sivaniah, E.; Kramer, E. J.; Fischer, D. A. *Macromolecules* **2000**, *33*, 8012-8019.

42. Small, A. C.; Pugh, C. *Macromolecules* **2002**, *35*, 2105-2115.

43. *Handbook of Conducting Polymers*, 2 ed.; T. Skotheim, J. R., R. Elsenbamer, Ed. Marcel Dekker: New York, 1998.

44. Scherf, U.; Gutacker, A.; Koenen, N. *Acc. Chem. Res.* **2008**, *41*, 1086-1097.

45. Liang, Y.; Wang, H.; Yuan, S.; Lee, Y.; Gan, L.; Yu, L. *J. Mater. Chem.* **2007**, *17*, 2183-2194.

46. Güntner, R.; Asawapirom, U.; Forster, M.; Schmitt, C.; Stiller, B.; Tiersch, B.; Falcou, A.; Nothofer, H.–G. *Thin Solid Films* **2002**, *417*, 1-6.

47. Scherf, U.; List, E. J. W. *Adv. Mater.* **2002**, *14,* 477-487.

48. Bao, Z.; Chan, W. K.; Yu, L. *J. Am. Chem. Soc.* **1995**, *117*, 12426-12435.

49. Schlüter, A. D. *J. Polym. Sci. Part A.* **2001**, *39*, 1533-1556.

50. Suzuki, Y.; Hashimoto, K.; Tajima, K. *Macromolecules* **2007**, *40*, 6521-6528.

51. Chen, T.-A.; Wu, X.; Rieke, R. D. *J. Am. Chem. Soc.* **1995**, *117,* 233-244.

52. Flory, P. J. *Chem. Rev.* **1946**, *39*, 137-197.

53. Isomura, M.; Misumi, Y.; Masuda, T. *Polym. Bull.* **2001**, *46*, 291-297.

54. Tu, G.; Li, H.; Forster, M.; Heiderhoff, R.; Balk, L. J.; Sigel, R.; Scherf, U. *Small* **2007**, *3*, 1001-1006.

55. Beryozkina, T.; Senkovskyy, V.; Kaul, E.; Kiriy, A. *Macromolecules* **2008**, *41*, 7817-7823.

56. Yokoyama, A.; Yokozawa, T. *Macromolecules* **2007**, *40*, 4093-4101.

57. McCullough, R. D.; Williams, S. P.; Tristram-Nagle, S.; Jayaraman, M.; Ewbank, P. C.; Miller, L. *Syn. Metals* **1995**, *69*, 279.

58. Miyakoshi, R.; Yokoyama, A.; Yokozawa, T. *J. Am. Chem. Soc.* **2005**, *127*, 17542-17547.

59. Yokoyama, A.; Miyakoshi, R.; Yokozawa, T. *Macromolecules* **2004**, *37*, 1169-1171.

60. *Organic Photovoltaics, Mechanisms, Materials and Devices*; Sun. S.-S.; Sariciftci, N. S.; CRC Press: New York, 1995.

61 . Zhu, X.-Y.; Yang, Q.; Muntwiler, M. *Acc. Chem. Res.* **2009**, *42*, 1779-1787.

62 . Brédas, J.-L.; Norton, J. E.; Cornil, J.; Coropceanu, V. *Acc. Chem. Res.* **2009**, *42*, 1691-1699.

63. Kim, J. Y.; Lee, K.; Coates, N. E.; Mosees, D.; Nguyen, T.-Q.; Dante, M.; Heeger, A. J. *Nature* **2007**, *317*, 222-225.

64. McNeill, C. R.; Westenhoff, S.; Groves, C.; Friend, R. H.; Greenham, N. C. *J. Phys. Chem. C* **2007**, *111*, 19153-19160.

65 . Peet, J.; Heeger, A. J.; Bazan, G. C. *Acc. Chem. Res.* **2009**, *42*, 1700-1708.

66. Krebs, F. C.; Bundgaard, E. *Solar Energy Materials and Solar Cells* **2007**, *91*, 954-985.

67 . Chen, J.; Cao, Y. *Acc. Chem. Res.* **2009**, *42*, 1709-1718.

68. van Bavel, S. S.; Bärenklau, M.; With, G.; Hoppe, H.; Loos, J. *Adv. Funct. Mater.* **2010**, *20*, 1458-1463.

69. Hoppe, H.; Sariciftci, N. S. *J. Mater. Chem.* **2006**, *16*, 45-61.

70. Shaheen, S. E.l Brabec, C. J.; Sariciftci, N. S. *Appl. Phys. Lett.* **2001**, *78*, 841-843.

71. Liang, Y.; Wang, H.; Yuan, S.; Lee, Y.; Gan, L.; Yu, L. *J. Mater. Chem.* **2007**, *17*, 2183-2194.

72. Lee, M.; Cho, B.-K.; Zin, W.-C. *Chem. Rev.* **2001**, *101*, 3869-3892.

CHAPTER 2: SYNTHESIS AND CHARACTERIZATION OF UNSYMMETRICALLY SUBSTITUTED REGIOREGULAR POLY(1,4-PHENYLENE ETHYNYLENE)S*

2.1. Introduction

The performance of conjugated polymers in organic electronic devices can be enhanced by molecular design. Side chains are often substituted onto the backbone of conjugated polymers to impart solubility to facilitate processing. However, these substituents also provide opportunities to tailor the optical and electronic properties of the materials. Variation of the identity and placement of side chains on a conjugated polymer backbone has a large impact on the molecular assembly and electronic properties of the material. As described in Chapter 1, regioregular poly(3-alkylthiophenes) (PATs) with exclusively head-to-tail linkages adopt a more planar confirmation than regiorandom analogs, leading to higher crystallinity, red shifted optical absorptions, greater conductivity and smaller bandgaps then their regiorandom analogs.[1] The regiorandom PATs are distorted from planarity by the presence of a random sequence of head-to-head, head-to-tail and tail-to-tail linkages (Figure 1.1). While the influence of regioregularity has been widely explored in PATs, investigation of the influence of regioregularity in other classes of conjugated materials has been limited to poly(3-alkylthienylene vinylene)[2], poly[3-alkyl-2,5-thienylene-1,4-phenylene)[3], poly(1,4-phenylene vinylene)s[4] and poly(biphenylene vinylene).[5]

* PPEs with methoxy and dodecyloxy side chains (**PPE(1/12)**) and regiorandom PPE with hexyloxy and dodecyloxy side chains (**RnPPE(6/12)**) were synthesized by Rakesh Nambiar.

Poly(1,4-phenylene ethynylene)s (PPEs) have interesting properties resulting from their linear structure, strong fluorescence and packing in the solid state. This combination of properties has led to their use in a wide variety of applications including field effect transistors,[6] solar cells[7] and sensors.[8] While symmetrically substituted 2,5-disubstituted PPEs are inherently regioregular, there are numerous examples of PPEs prepared from monomers bearing pairs of dissimilar side chains on the phenylene rings where regioregularity becomes a concern.[9] For example, 2,5-dialkoxy PPEs are typically prepared by cross-coupling of symmetrically substituted 2,4-dialkoxy-1,4-diiodobenzenes and 2,4-dialkoxy-1,4-diethynylbenzenes (i.e., AA and BB type monomers). If each monomer is substituted with a pair of dissimilar alkoxy groups this polymerization results in an irregular placement of side chains along the PPE backbone with formation of head-head (*hh*), head-tail (*ht*) and tail-tail (*tt*) diads, Figure 2.1.

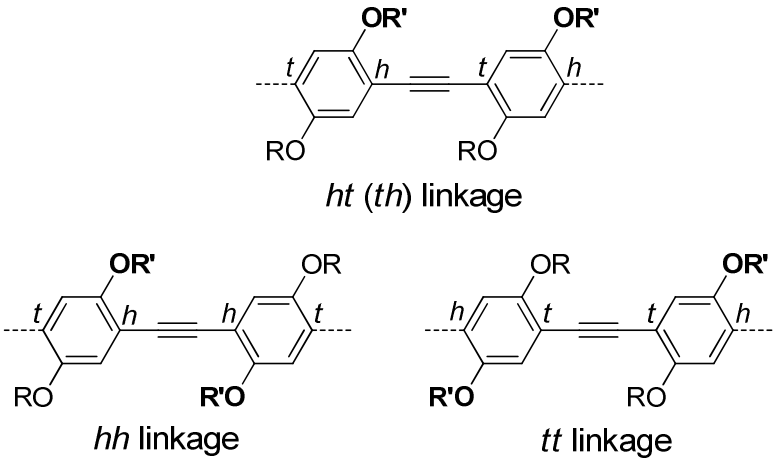

Figure 2.1. Three possible dyads occur when coupling AA and BB type monomers, where R does not equal R'.

In this Chapter, we report the preparation of the first regioregular asymmetrically substituted PPEs by the cross-coupling of asymmetrically substituted 2,4-dialkoxy-4-iodophenylacetylenes (i.e., a single AB type monomer containing both the ethynyl and iodo substituents).[10,11] This allowed us to compare the properties of PPEs with regioregular and regiorandom substitution.

2.2. Experimental

2.2.1. General Synthetic Methods

All starting materials were purchased from commercial sources and used without further purification unless stated otherwise. THF and Et_2O were dried over sodium benzophenone ketyl prior to distillation under argon. Column chromatography was performed on flash grade silica (32-60 Å, Sorbent Technologies, Atlanta, Georgia). Thin-layer chromatography was performed on 3×5 cm silica gel plates (0.2 mm thick, 60 F254) on an aluminum support (Sorbent Technologies). NMR analysis was performed on a Bruker DSX 400 or DSX 300 instruments using $CDCl_3$ as the solvent unless stated otherwise. Chemical shifts are reported relative to internal tetramethylsilane. ^{13}C NMR are proton decoupled. IR analyses were performed on a Nicolet 4700 FTIR with an ATR attachment from SmartOrbit Thermoelectronic Corporation. Ultraviolet-visible analysis was performed on a Perkin-Elmer Lambda 19 spectrophotometer. Elemental analyses were performed by Atlantic Microlab, Inc. (Norcross, GA). The X-ray diffraction data was obtained using a Scintag X1 diffractometer equipped with copper tube and a Peltier cooled solid state detector. The Bestman-Ohiro reagent ($CH_3COC(=N_2)PO(CH_3O)_2$) was

prepared using previously reported methods.[12] ^{1}H and ^{13}C NMR, IR and EI mass spectra are provided in Appendix A for compounds **II-1-4**, **RgPPE(6/12)** and **PPE(C12)**.

2.2.2. Monomer Synthesis

Synthetic procedures and spectroscopic data for the AB type, 2,5-dialkoxy-4-iodophenylacetylene monomers are given below.

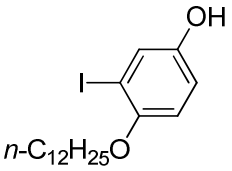

4-Dodecyloxy-3-iodophenol, II-1. This compound was synthesized by previously reported procedures (88% yield).[11] ^{1}H NMR (300 MHz, $CDCl_3$): δ 7.29 (d, $^{4}J_{ArH2\text{-}ArH6}$ = 2.89 Hz, 1H, Ar C2-H), 6.78 (dd, $^{3}J_{ArH5\text{-}ArH6}$ = 8.8 Hz, $^{4}J_{ArH2\text{-}ArH6}$ = 2.9 Hz, 1H, Ar C6-H), 6.68 (d, $^{3}J_{ArH5\text{-}ArH6}$ = 8.8 Hz, 1H, Ar C5-H), 6.0-6.25 (bs, 1H, OH), 3.92 (t, $^{3}J_{H1\text{-}H2}$ = 6.4 Hz, 2H, -OCH_2-), 1.73-1.85 (m, 2H), 1.2-1.6 (m, 18H), 0.89 (t, $^{3}J_{H11\text{-}H12}$ = 6.6 Hz, 3H, -CH_3). ^{13}C NMR (75 MHz, $CDCl_3$): δ 152.45, 150.38 (Ar C1,4), 126.4 (Ar C2), 116.33 (Ar C6), 113.8 (Ar C5), 87.3 (Ar C3), 70.68 (-O-CH_2-), 32.19, 29.94, 29.92, 29.87, 29.85, 29.63, 29.60, 29.51, 26.34, 22.97, 14.40. IR (ν, cm^{-1}): 3348 (O-H), 2920 (Ar C-H str.), 2850, 1701, 1600, 1583, 1487, 1465, 1434, 1388, 1377, 1273, 1206 (C-O str.), 1145, 1033, 1008, 906, 861, 799, 779. HRMS: calc. for $C_{18}H_{29}O_2I$ = 404.12123, obs. = 404.12155, Δ = 0.8 ppm. Elemental Analysis: Theoretical: C, 53.47 %; H, 7.23 %; Found: C, 53.83 %; H, 7.38 %.

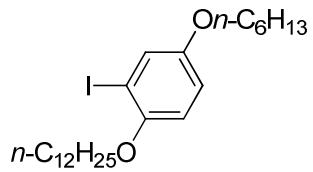

1-Dodecyloxy-4-hexyloxy-2-iodobenzene, II-2. Monoiodinated phenol, **II-1** (2.55 g, 6.30 mmol) was added to a stirred solution of PPh_3 (1.65 g, 7.55 mmol) and 1-hexanol (0.80 ml, 7.6 mmol) in Et_2O (40 mL) under Ar. Diethyl azodicarboxylate (DEAD) (1.15 mL, 7.55 mmol) was added dropwise by syringe and the resulting pale yellow solution was stirred at room temperature for 24 h. Et_2O (60 mL) was added and the solution was washed with 10% aqueous NaOH (200 mL) followed by H_2O (100 mL). The solution was dried over $MgSO_4$, the solvent was removed under reduced pressure, and the residue was subjected to flash column chromatography (20:80 v/v ethyl acetate:hexanes) to afford **II-2** (2.80 g, 91% yield) pale yellow oil. ^{1}H NMR (300 MHz, $CDCl_3$): δ 7.33 (d, $^4J_{HH}$ = 2.90 Hz, 1H, Ar C3-H), 6.83 (dd, $^3J_{HH}$ = 8.9 Hz, $^4J_{HH}$ = 2.9 Hz, 1H, Ar C5-H), 6.71 (d, $^3J_{HH}$ = 8.9 Hz, 1H, Ar C6-H), 3.93 (t, $^3J_{HH}$ = 6.4 Hz, 2H, -OCH_2-), 3.87 (t, $^3J_{HH}$ = 5.4 Hz, 2H, -CH_2-), 1.65-1.85 (m, 4H), 1.20-1.58 (m, 24H), 0.84-0.94 (m, 6H, 2 × -CH_3). ^{13}C NMR (75 MHz, $CDCl_3$): 153.97 (Ar C-O), 125.55, 115.62, 113.30 (Ar C-H), 87.22 (Ar C-I), 70.39, 69.05 (-O-CH_2-), 31.91, 31.59, 29.66, 29.62, 29.42, 29.34, 29.26, 26.01, 25.67, 22.68, 22.62, 14.11, 14.06 (three aliphatic carbons have coincident chemical shifts). IR (ν, cm^{-1}): 2920 (Ar C-H str.), 2851, 2030, 1733, 1597, 1568, 1486, 1466, 1387, 1350, 1271, 1209 (C-O str.), 1106, 1062, 935, 850, 801, 770, 721. HRMS: calc. for $C_{24}H_{41}O_2I$ = 488.21513, obs. = 488.21704, Δ = 3.9 ppm. Elemental Analysis: Theoretical: C, 59.01 %; H, 8.46 %; Found: C, 59.03 %; H, 8.29 %.

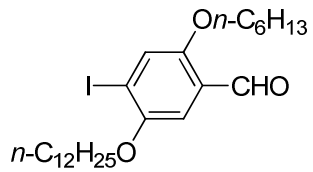

5-Dodecyloxy-2-hexyloxy-4-iodobenzaldehyde, II-3. $TiCl_4$ (11.7 g, 61.4 mmol) was added dropwise to a solution of monoiodinated diether **II-2** (5.0 g, 10 mmol) in dry CH_2Cl_2 (50 mL) at -40 °C in a dry flask under Ar. The mixture was stirred for 15 min at -40 °C and dichloromethyl methyl ether (2.35 g, 20.5 mmol) was added dropwise and stirring was continued for another 2h. The reaction mixture was poured into mixture of conc. HCl and ice. The mixture was extracted with CH_2Cl_2 (100 mL) and the extract was washed with water (100 mL). The organic layer was dried over $MgSO_4$ and the solvent was removed under reduced pressure. Column chromatography (silica gel, 30% CH_2Cl_2/hexanes) afforded **II-3** as a white solid (2.91 g, 55 % yield), m.p. = 57 °C. ^{1}H NMR (300 MHz, $CDCl_3$): δ 10.40 (s, 1H, -CHO), 7.43 (s, 1H, Ar C3-H), 7.16 (s, 1H, Ar C6-H), 3.95-4.02 (m, 4H, -OCH_2-), 1.77-1.81 (m, 4H), 1.24-1.44 (m, 24H), 0.85-0.88 (m, 6H, 2 × -CH_3). ^{13}C NMR (75 MHz, $CDCl_3$): δ 189.28 (-CHO), 155.77 (Ar C2), 152.12 (Ar C5), 125.11 (Ar C1), 124.51 (Ar C3), 108.81 (Ar C6), 96.78 (Ar C4), 69.90, 69.44 (-O-CH_2-), 31.90, 31.45, 29.63, 29.56, 29.54, 29.34, 29.26, 29.04, 29.00, 26.02, 25.66, 22.68, 22.54, 14.12, 14.00 (one aliphatic carbon missing due to coincident chemical shifts). IR (ν, cm^{-1}): 2912 (Ar C-H str.), 2847, 1670 (C = O str.), 1587, 1458, 1383, 1213 (C-O str.), 1032, 867, 827, 748, 715, 611. HRMS: calc. for $C_{25}H_{41}O_3I$ = 516.20893, obs. = 516.20592, Δ = 5.8 ppm. Elemental Analysis: Theoretical: C, 58.14%; H, 8.00 %; Found: C, 57.75 %; H, 8.07 %.

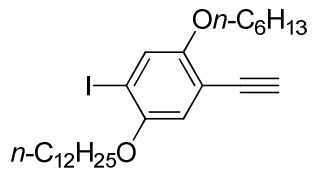

1-Dodecyloxy-5-ethynyl-4-hexyloxy-2-iodobenzene, II-4. Bestman-Ohiro reagent, $CH_3COC(=N_2)PO(CH_3O)_2$ (0.45 g, 2.3 mmol), was added dropwise to a mixture of aldehyde **II-3** (0.5 g, 0.9 mmol) and K_2CO_3 (0.19 g, 1.4 mmol) in 12 mL of a 1:5 v/v mixture of anhydrous CH_2Cl_2 and MeOH under argon and the mixture was stirred for 10 h. The solvent was removed under reduced pressure to obtain a pale yellow residue which was recrystallized from isopropanol to give ethyne **II-4** (0.22 g, 49 % yield) as a colorless solid, m.p. = 39-41 °C. ^{1}H NMR (300 MHz, $CDCl_3$): δ 7.28 (s, 1H, Ar C3-H), 6.86 (s, 1H, Ar C6-H), 3.92-3.95 (m, 4H, -OCH_2), 3.29 (s, 1H, -C≡C-H), 1.76-1.81 (m, 4H), 1.26-1.48 (m, 24H) 0.85-0.92 (m, 6H, 2 × -CH_3). ^{13}C NMR (75 MHz, $CDCl_3$): δ 154.81 (Ar C4), 151.65 (Ar C1), 123.73 (Ar C3), 116.64 (Ar C6), 112.19 (Ar C5), 88.28 (Ar C2), 81.74, 79.64 (-C≡C-), 70.04, 69.83(-O-CH_2-), 31.90, 31.46, 29.62, 29.56, 29.33, 29.27, 29.10, 29.04, 26.02, 25.52, 22.68, 22.54, 14.11, 13.99 (two aliphatic carbons have coincident chemical shifts. IR (ν, cm^{-1}): 3269 (C-H str), 2953 (Ar-H str.), 2914, 2845, 2091 (C≡C str), 1473, 1465, 1371, 1209 (C-O str.), 1026, 856, 818, 725, 687, 642. HRMS: calc. for $C_{26}H_{41}O_2I$ = 512.21402, obs. = 512.2139, Δ = 1.0 ppm. Elemental analysis: Theoretical: C, 60.93%; H, 8.06%; I, 24.76; O, 6.24%; Found: C, 60.92%; H, 7.94%; I, 24.61%; O, 6.29%.

2.2.3. Polymer Synthesis

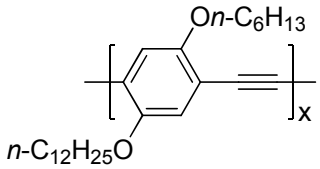

Regioregular dodecyloxy/hexyloxy, RgPPE(6/12). A solution of monomer **II-4** (428 mg, 0.84 mmol), toluene (10 mL) and diisopropylamine (2 mL) were added to a 50 mL flask and degassed via freeze/pump/thaw. $Pd(PPh_3)_4$ (50.0 mg, 0.86 mmol) and CuI (8.0 mg, 0.84 mmol) were added to the solution. The mixture was stirred at 60 °C for 2 days. Precipitation from MeOH and sequential extractions in a Soxhlet extractor with acetone, hexanes and chloroform gave a chloroform fraction as an orange solid (261 mg, 81% yield). GPC (THF, UV-vis detector): 15.12 kD. ^{1}H NMR (300 MHz, $CDCl_3$): δ 7.01 (br s, 2H), 3.97-4.05 (m, 4H), 1.81-1.90 (m, 4H), 1.24-1.66 (m, 24H), 0.84-0.91 (m, 6H). IR (AT-IR, neat): 2920, 2852, 2370, 1514, 1428, 1388, 1277, 1213, 1045, 858, 725. Elemental Analysis: Theoretical: C, 76.13 %; H, 9.88 %; Found: C, 76.26 %; H, 9.98 %.

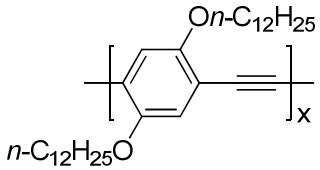

Poly(1,4-dialkoxyphenyene ethynylene), PPE(12/12). A solution of 1,4-bis(dodecyloxy)-2,5-diethynylbenzene (0.4g, 1.0 mmol) and 1,4-bis(dodecyloxy)-2,5-diiodobenzene (0.6 g, 1.0 mmol) in THF (20 mL) was degassed by freeze-pump-thaw cycles (2 x 15 min). Diisopropylamine (4 mL, 28 mmol), CuI (31 mg, 0.16 mmol), and $Pd(PPh_3)_4$ (0.18 g, 0.16 mmol) were added to the mixture and the solution was stirred for 24 h 45 °C. The solution was poured into methanol (200 mL) and filtered. The resulting

solid was subjected to extractions of acetone and chloroform in a Soxhlet extractor. The chloroform fraction was then placed under reduced pressure to remove solvent to afford the poly(1,4-dialkoxyphenylene ethynylene) (**PPE(12/12)**) as an orange solid (0.55 g, 72%): ^{1}H NMR (300 MHz, $CHCl_3$) δ 7.3-7.29 (2H), 7.0-6.9 (2H), 4.13-3.96 (8H), 1.89-1.80 (8H), 1.24 (72H), 0.87 (12H). IR (ATIR): 2954 (Ar C-H str.), 1198 (C-O str), 1375 (C-C str.), 2916, 793, 690 cm^{-1}. GPC (THF, UV-vis detector) M_n = 7 kg/mol, PDI = 2.4. Elemental Analysis: Theoretical: C, 73.74%; H, 10.18%. Found: C, 72.81%, H, 9.93%.

2.3. Results and Discussion

2.3.1. Polymer Design

To understand the influence of regioregularity on PPEs, both regioregular (Rg) and regiorandom (Rn) analogs of poly(2,5-dialkoxy-1,4-phenylene ethynylene)s were prepared where each analog contained a dodecyloxy substiuent, and either a methoxy or hexyloxy substituent (**PPE(m/12)**, *m=1 or 6, respectively*), Figure 2.2. Thus, any changes in the molecular assembly or electronic properties between analogs can be attributed to the regioregularity of the side chains. We also prepared a symmetrically substituted PPE with dodecyloxy side chains (**PPE(12/12)**) for comparison.

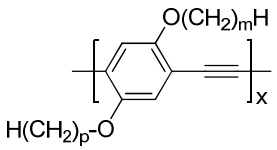

	regiorandom	*regioregular*
m = 6, p = 12	**RnPPE(6/12)**	**RgPPE(6/12)**
m = 1, p = 12	**RnPPE(1/12)**	**RgPPE(1/12)**
m = 12, p = 12	**PPE(12/12)**	

Figure 2.2. Regioregular and regiorandom PPEs examined in this study.

The regiorandom polymers in this study were prepared by the combination of diiodoarenes and diethynylarenes with appropriately substituted alkoxy chains. The regioregular analogs were prepared from AB type 2,5-dialkoxy-4-iodo-ethynylene monomers. This type of functionality only allows head-to-tail coupling of the monomer, which in turn restricts the relative placement of the substituents in the resulting polymer.

2.3.2. Synthesis of AB Type Monomers

The preparation of unsymmetrically substituted regioregular dialkoxy PPEs relies on the synthesis of monomer **II-4**, which contains both an iodo and ethynyl substiuent Figure 2.3. There is a challenge in installing the iodo and ethynyl groups in specific positions adjacent to the two dissimilar alkoxy substituents. This was achieved by the synthesis of 4-alkoxy-3-iodophenols (**II-1**). This compound was synthesized using previously reported methods by tosylation of 4-(dodecyloxy)phenol which lowers the electron donating ability of the oxygen and allows for subsequent monoiodination. The following detosylation gives compound **II-1**.[11] A Mitsunobu reaction was then used to install the second alkoxy side chain to give compound **II-2**. It was then necessary to find a synthetic approach which allowed the installation of an ethynyl group para to the iodine. We explored several routes to the alkyne,[11] and found that formylation of **II-2** followed by homologation allowed for successful synthesis of the 2,5-dialkoxy-4-iodo-phenylacetylene monomer **II-4**.

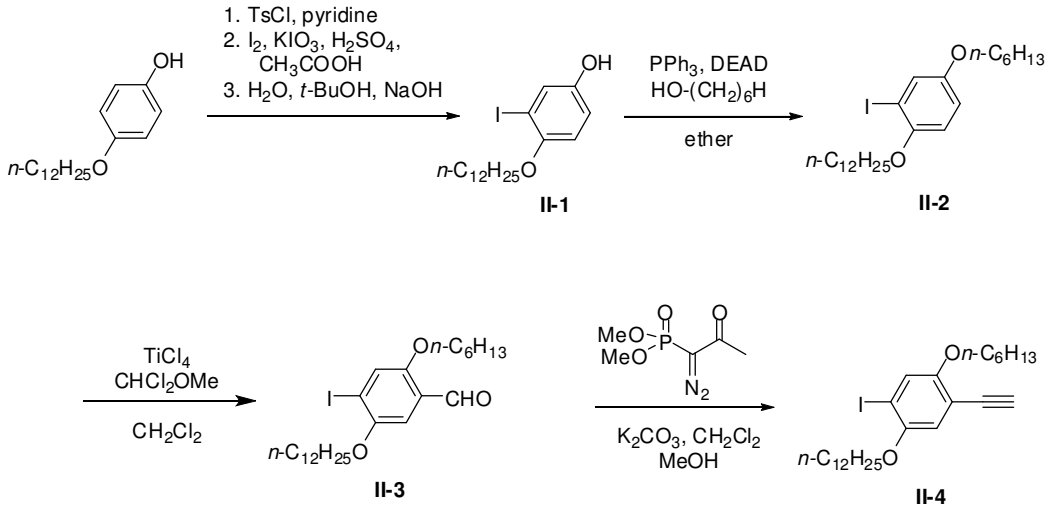

Figure 2.3. Synthetic route to AB type asymmetrically substituted dialkoxy monomers.

Formylation of monoiodobenzene **II-2** using $TiCL_4$ and $CHCl_2OCH_3$ at low temperatures (-15 to -40 °C) provided benzaldehyde **II-3**. Analysis of the crude reaction mixture indicated that the desired 2,5-dialkoxy-4-iodobenzaldehyde is the major product, but several byproducts are also formed. The crude reaction mixture gave a ^{1}H NMR spectrum indicating the prescence of three different aldehydes, Figure 2.4. Analysis of the aromatic region allowed for the identification of the byproducts. The desired product gives singlets at 7.45 and 7.18 ppm. The remaning signals in the aromatic region of the spectrum indicate the presence of a trisubstituted benzene: δ 7.30 (d, $^4J_{HH}$ = 3 Hz), δ 7.11 (dd, $^4J_{HH}$ = 3.3 Hz, $^3J_{HH}$ = 9 Hz), and 6.91 (d, $^3J_{HH}$ = 9 Hz). These protons are further downfield than the starting material, and are consistent with literature values for a 2,5-dialkoxy-benzaldehyde, which is formed by electrophilic aromatic substitution of the iodo substituent for a formyl group. The presence of a regioisomer of the desired product was shown by mass spectrometry, and can be identified from the appearance of a

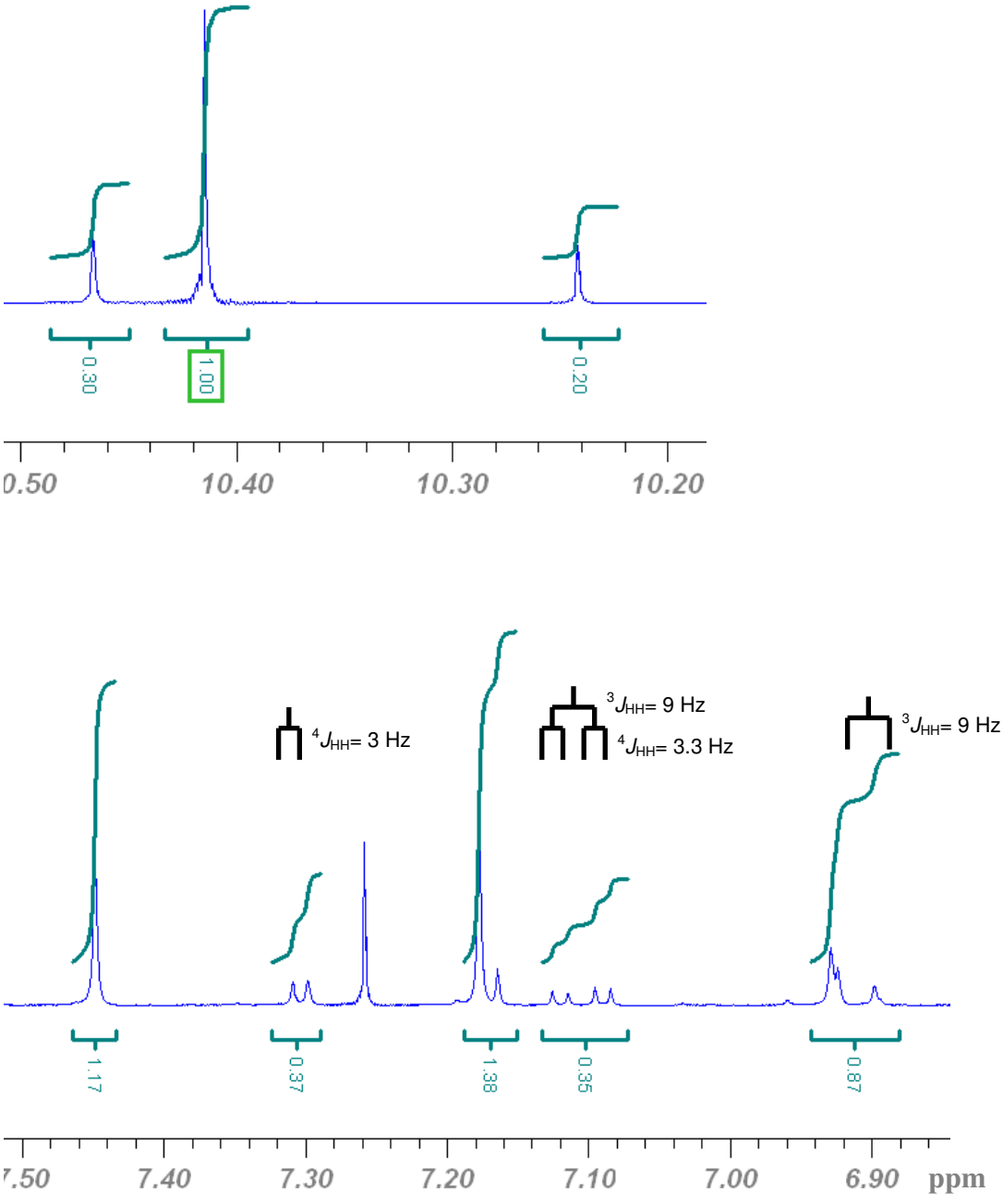

Figure 2.4: ^{1}H NMR spectra of crude reaction mixture obtained upon formylation of **II-2**. Top, formyl (-C*H*O) region of the spectrum. Bottom, aromatic region.

singlet at 6.93 ppm in the ^{1}H NMR spectrum as a 2,5-dialkoxy-3-iodobenzaldehyde (i.e., from formylation meta to the iodo substituent). The 3,6-dialkoxy-2-iodobenzaldehyde regioisomer (formed by formylation ortho to the iodosubstituent) is not formed, likely due to steric interactions with the iodine. Two other byproducts formed during this reaction are 1,4-dialkoxybenzene and 1,4-dialkoxy-2,5-diiodobenzene. The signals for the aromatic protons of these compounds occur at 6.80 ppm and 7.18 ppm respectively. The former arises from protonation of the starting material followed by electrophilic loss of iodine to a second molecule of starting material to give the diiodinated material. Column chromatography allowed for separation of each of these byproducts and mass spectroscopy was used to verify the molecular weights of the side products. The overall conversion to the desired product is 61%, and the remaining 39% is accounted for in the byproducts: 1,4-dialkoxy-2,5-diiodobenzene (6%), 1,4-dialkoxybenzene (3%), 2,5-dialkoxy-benzaldehyde (18%) and 2,5-dialkoxy-3-iodobenzaldehyde (12%), Figure 2.5.

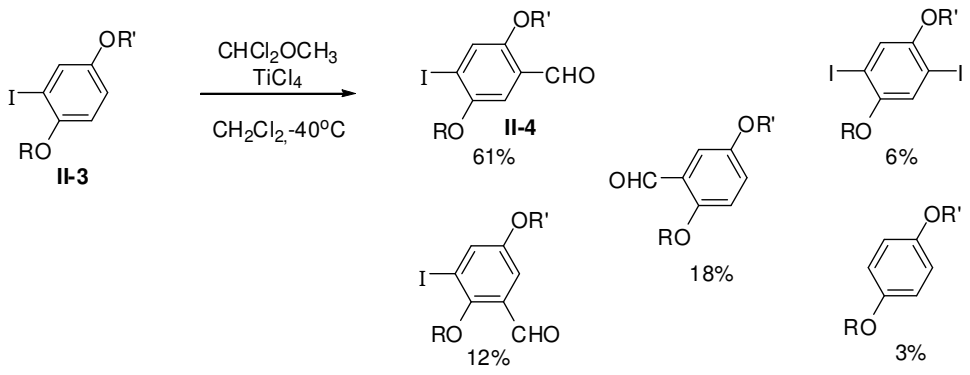

Figure 2.5. Formylation of **II-3** and byproducts that are formed.

The desired product was purified by column chromatography followed by recrystallization. Benzaldehyde **II-3** was then treated with $CH_3COC(=N_2)CPO(OCH_3)_2$ and K_2CO_3 in $MeOH/CH_2Cl_2$ (the Bestman-Ohiro homologation)[12] to give monomer **II-4**.

2.3.3. Synthesis of Regioregular and Regiorandom Dialkoxy PPEs

The regioregular PPEs with exclusively head-to-tail linkages were prepared from monomer **II-4** using palladium-catalyzed condensation polymerization, Figure 2.6a. The polymers were isolated and purified by precipitation from the reaction mixture by addition to a large volume of MeOH, followed by dissolution in chloroform and reprecipitation by addition to acetone, to give bright orange solids. The regiorandom analogs were prepared by coupling the AA and BB type diiodoarene and diethynylarene monomers, Figure 2.6b.[11] A symmetrically substituted dialkoxy-PPE, poly(2,4-dodecyloxy-1,4-phenylene ethynylene), **PPE(12/12)**, was synthesized by polymerization of the di(dodecyloxy) substituted diiodo- and diethynylbenzene monomers.[13] The polymers were characterized by ^1H and ^{13}C NMR, FT-IR, and UV-vis absorption spectroscopies, differential scanning calorimetry (DSC), gel permeation chromatography (GPC), and X-ray diffraction (XRD).

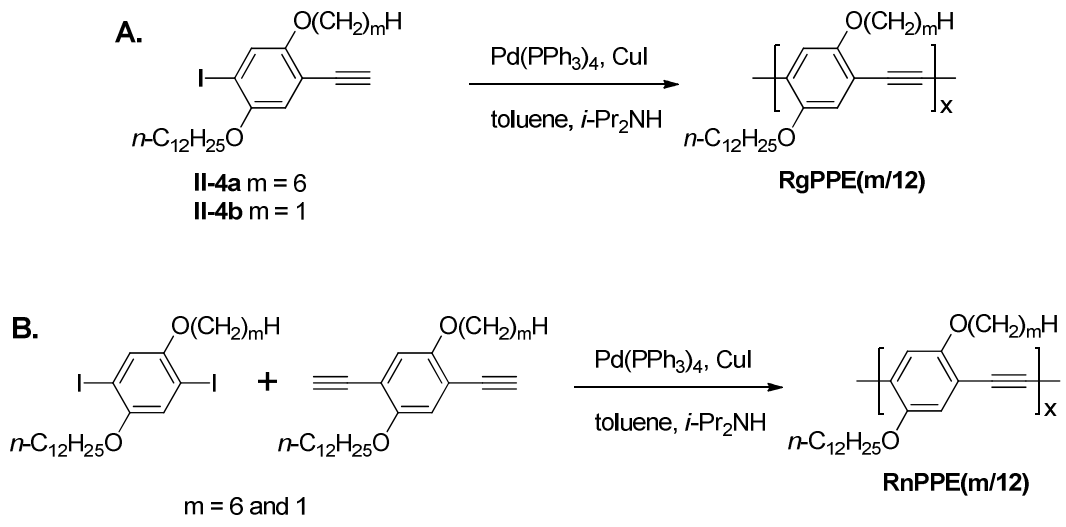

Figure 2.6. Polymerization of A, regioregular PPEs and B, regiorandom analogs.

2.3.4. Structural Characterization

Molecular weights of the polymers were determined by GPC and end group analysis by ^{1}H NMR spectroscopy. The PPE polymer chains have iodophenyl or phenylacetylene end groups. The chemical shift of the aromatic proton ortho to the iodide is further downfield (δ 7.3 ppm) than the protons on the polymer backbone (~δ 7.1). In contrast, the aromatic proton ortho to the alkyne end group is easily distinguished, occurring at around δ 6.9 ppm. The signals of the other proton associated with each of these end groups are coincident with signals for protons in the polymer backbone. In a traditional polymerization of diiodo and diethynyl monomers, a slight stoichiometric imbalance leads to different amounts of the iodo and ethynyl end groups. In this case the average amount of the two end groups was considered when calculating the number of repeat units present in the polymer. However, synthesis of regioregular polymers from A-B type 4-iodophenylacetylene monomers leads to chains bearing one end group of each type, as confirmed by the equal integrals for the peaks at δ 6.9 and δ 7.3 ppm for

polymers prepared in this manner. The molecular weights of the polymers obtained by ^{1}H NMR and GPC are shown in Table 2.1. The molecular weights obtained by GPC are consistently higher than those determined by end group analysis, which can be explained by the relatively large hydrodynamic volume of the rigid-rod PPE compared to the coiled conformation of the polystyrenes used as a standard for GPC measurements.[14]

Table 2.1. Physical Properties of **RgPPE(m/p)**, **RnPPE(m/p)** and **PPE(12/12)**

Polymer	M_n [a,b] (kg.mol^{-1})	M_n [b,c] (kg.mol^{-1})	M_w [c,d] (kg.mol^{-1})	PDI [c,e]	DP [b,f]
RgPPE(1/12)	8.2	12	30	2.5	26
RnPPE(1/12)	8.7	18	67	3.7	27
RgPPE(6/12)	6.2	15	42	2.8	16
RnPPE(6/12)	17	38	140	3.7	44
PPE(12/12)	14	49	134	2.73	29

[a] Number average molecular weight (M_n). [b] Determined by end group analysis. [c] Determined by gel permeation using polystyrene standards. [d] Weight average molecular weight (M_w). [e] Polydispersity index (PDI). [f] Degree of polymerization (phenyls as repeating units).

Analysis of the aromatic region of the ^{1}H provides insight to the impact of regioregularity on the molecular structure, Figure 2.7. The aromatic protons for both regioregular and regiorandom analogs of **PPE(6/12)** are coincident and appear as a sharp singlet at 7.01 ppm, Figure 2.7B. Similarly, **RgPPE(1/12)** has one sharp singlet in the aromatic region, which can be assigned to the aromatic protons in the 3-position (ortho to the dodecyloxy substituent) and in the 6-position (ortho to the methoxy substituent). This

is in contrast to the ^{1}H NMR spectra of **RnPPE(1/12)**. This analog has three singlets in the aromatic region, which arise from the presence of three diads, head-to-head, head-to-tail and tail-to-tail, Figure 2.7A.

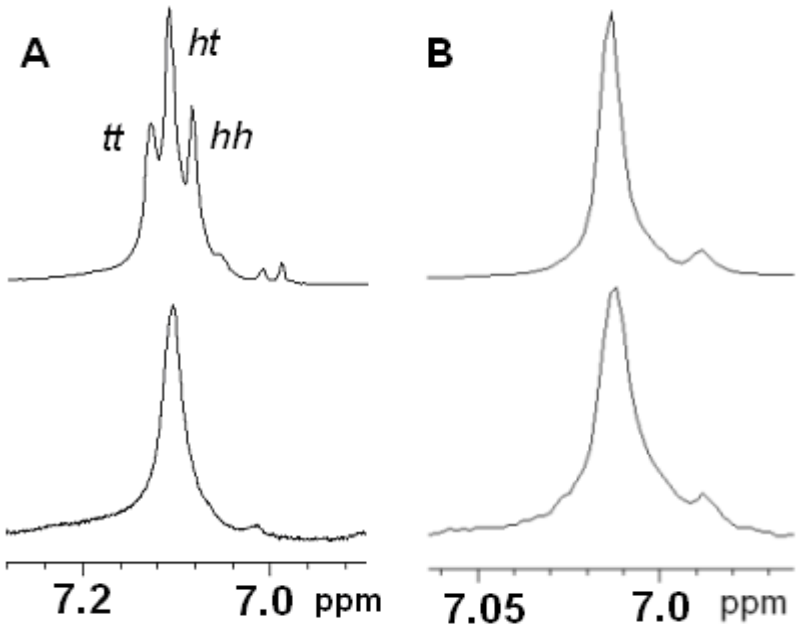

Figure 2.7. ^{1}H NMR (400 MHz, $C_2D_2Cl_4$) spectra of (A) **PPE(1/12),** Top, Regiorandom; Bottom, Regioregular (B) **PPE(6/12),** Top, Regiorandom; Bottom Regioregular.

The aromatic region has three singlets, with a peak ration of 1:2:1. The center peak corresponds with the protons in the head-to-tail diads, as observed in the regioregular analog. The other peaks can be assigned to the head-to-head and tail-to-tail diads. The peak furthest downfield at δ 7.04 ppm is a result of the head-to-head linkage, where the dodecyloxy side chains are pointed toward each other. These aromatic protons experience the highest steric crowding, resulting in the downfield shift. Likwise, the peak

upfield at δ 7.0 ppm is a result of the tail-to-tail linkage, where the methoxy side chains are pointing toward each other. These protons are shifted upfield because they experience the least amount of steric crowding. Although the **PPE(6/12)** PPEs have alkoxy side chains of different lengths, the chains are long enough to impart a similar steric environment around the respective nuclei of the backbone for all three types of diads. This results in identical ^{1}H NMR spectra for both the regioregular and regiorandom analogs of **PPE(6/12)**.

2.3.5. Electronic Structure

UV-vis absorption spectra were obtained for regioregular and regiorandom analogs of the asymmetrically substituted dialkoxy PPEs both in solution and as thin films. The absorption spectra for the PPEs in solution all show a broad absorption at around 450 nm, which is also characteristic of the symmetrically substituted dialkoxy-PPEs, Figure 2.8. The similarity of these spectra can be attributed to the low rotational barriers of PPEs in solution (estimated to be <1 kcal/mol),[14] and lack of aggregation of the polymer chains in $CHCl_3$ solution.

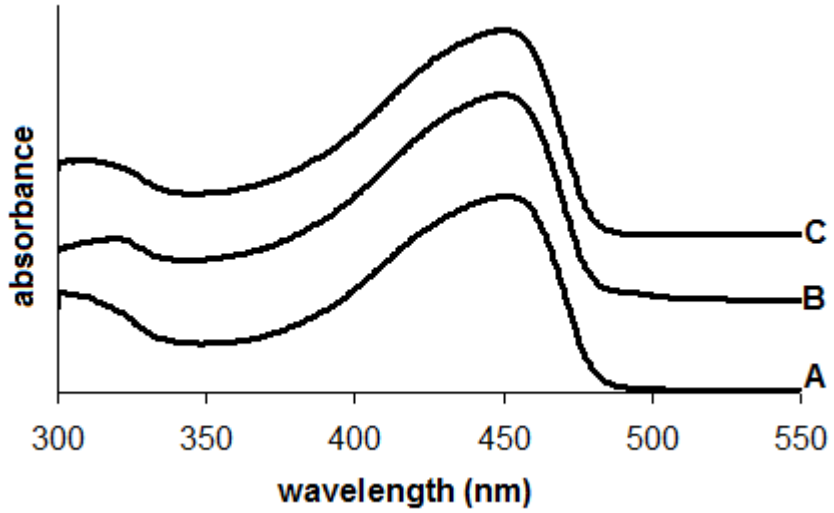

Figure 2.8. UV-vis spectra of polymer solutions ($CHCl_3$): A, **PPE(12/12)**; B, **RnPPE(6/12)**; C, **RgPPE(6/12)**.

The solid-state spectra of the PPEs were investigated using films prepared by drop-casting a solution of the polymer in $CHCl_3$ onto quartz slides followed by annealing at 120 ^oC under vacuum for 24 h. The absorption spectra are shown in Figure 2.9. In comparison to the soution spectra, the absorptions are broader and shifted to higher wavelengths, as a result of the interactions beween the conjugated polymer chains. **RgPPE(6,12)** has a slightly broader absorption than the regiorandom analog, Figure 2.10 (middle). Both hexyloxy/dodecyloxy analogs have more contribution at the maximum absorption at about 490 nm in comparison to **PPE(12/12)**, Figure 2.9 (bottom). The differences in the regioregular and regiorandom analogs of **PPE(1/12)** are more pronounced, Figure 2.9 (top). The regioregular analog has a red-shifted maximum absorption (475 nm in comparison to 460 nm) and greater contributions at the higher wavelengths. This may be attributed to the ordered arrangement of the side chains in

RgPPE(1/12) which leads to a more conjugated, planar conformation. The head-to-head and tail-to-tail couplings in **RnPPE(1/12)** causes steric interactions between side chains, impeding the formation of an ordered assembly. This is not observed in **PPE(6/12)**, indicating that regioregularity has a stronger influence on the electronic PPEs with dissimilar side chains (C1 and C12) than those bearing more similar side chains (C6 and C12).

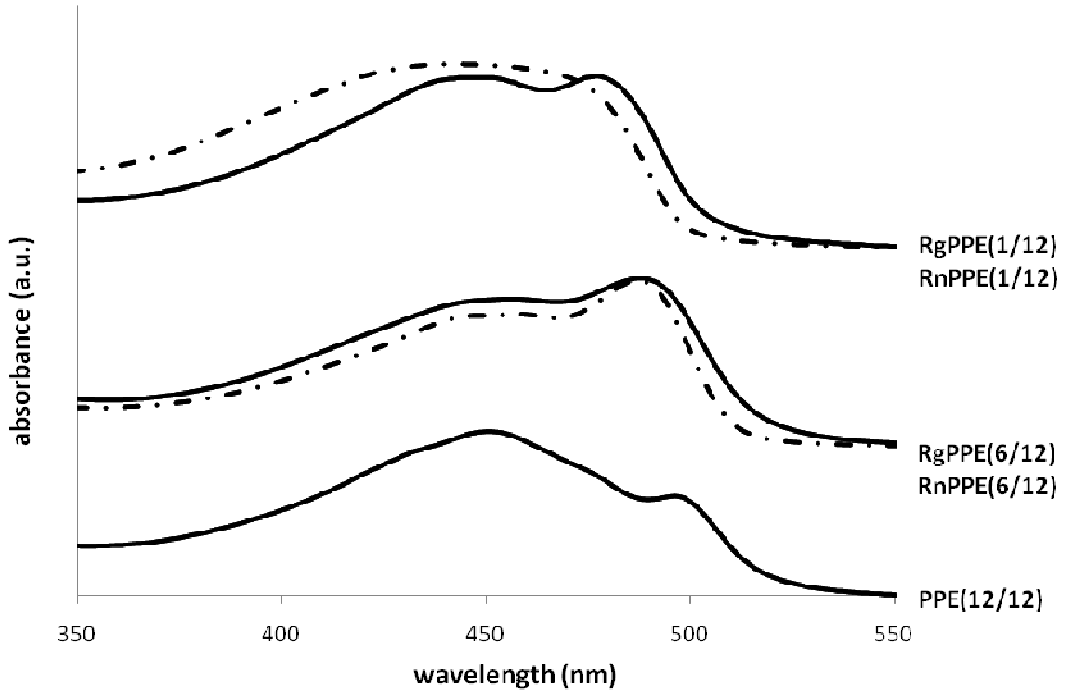

Figure 2.9. Thin-film UV-visible absorption spectrum of regiorandom and regioregular analogs of **PPE(1/12)** (top), **PPE(6/12)** and symmetrically substituted **PPE(12/12)** (bottom).

2.3.6. Molecular Assembly

Wide-angle X-ray diffraction was used to explore the effect of regioregularity on the molecular packing of the polymer chains in the solid state. Thin films were formed on silicon wafers by slow evaporation of the PPEs from xylene and annealed for 24 h at 120 ^{o}C, under vacuum. The X-ray diffractograms of **PPE(6/12)** regioisomers (regiorandom, Figure 2.10A; and regioregular, Figure 2.10B) both show a peak at $2\theta = 4.46^{o}$ (19.9 Å), and small peak at approximately 8.7^{o} (10.2 Å). For comparison, the diffractogram for the symmetrical **PPE(12/12)** material shows four peaks, at $2\theta = 3.54^{o}$, 7.0^{o}, 10.45^{o} and 17.45^{o}. These can be assigned as the (100), (200), (300) and (500) planes of a lamella crystal with an interlayer spacing of 24.9 Å.[32] The strong peaks for [*h*,0,0] relections when *h* is even, and weak peaks associated with the reflections when *h* is odd, can be interpreted as arising from an electron density within the unit cell consisting of planes with high electron density (i.e., the conjugated backbone) and low electron density (alkyl regions). Thus, by analogy, we assign the two diffraction peaks (one strong, one weak) in each of the **PPE(6/12)** materials to the (100) and (200) planes of a lamella structure with interlayer spacing of 19.9 Å, Figure 2.10 inset. The irregular placement of side chains would suggest that they are more likely interdigitated, and there is shorter-range order than in symmetrically substituted **PPE(12/12)**. Thus, as expected, the combination of hexyl and dodecyl side chains results in a smaller interlayer spacing than is observed for **PPE(12/12)**. The broader diffraction peaks for the regiorandom **RgPPE(6/12)** analog might indicate the presence of less order than for the regioregular analogue (width at half height for the (100) peak: **Rg**, 0.45°; **Rn**, 0.64°).

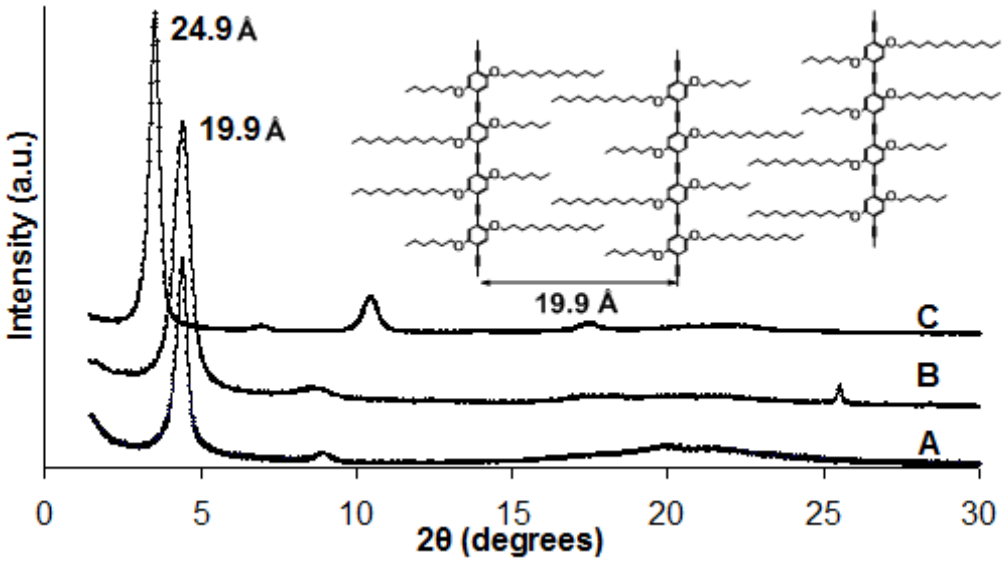

Figure 2.10. X-ray diffraction of annealed polymer films (annealed at 120 ^{o}C for 24h): A, regiorandom **RnPPE(6/12)**; B, regioregular **RgPPE(6/12)**; C, **PPE(12/12)**.

2.4. Conclusions

In conclusion, we have established synthetic routes to unsymmetrically substituted 2,5-dialkoxy-4-iodophenylacetylenes. Polymerization of these AB type monomers yields structurally homogenous regioregular unsymmetrically substituted PPEs. The placement of the substituents on the polymer backbone has an influence on the molecular assembly and the electronic structure of the PPEs. The effect of regioregularity on the properties of the unsymetrically substituted dialkoxy PPEs is greatest when there is a large difference in the side chain length. Thus, it is expected that distinctly different side chains will afford further level of control over the molecular packing and orientation of the conjugated polymer chains.

2.5. References

1. McCullough, R.D. *Adv. Mater.* **1998**, *10*, 93-116.
2. Loewe, R. S.; McCullough, R. D. *Chem. Mater.* **2000**, *12*, 3214-3221.
3. Ng, S. C.; Xu, J. M.; Chan, H. S.; Fujii, A.; Yoshiimo, K. *J. Mater. Chem.* **1999**, *9*, 381-385.
4. Suzuki, Y.; Hashimoto, K.; Tajima, K. *Macromolecules* **2007**, *40*, 6521-6528.
5. Krebs, F. C.; Jorgensen, M. *Macromolecules* **2002**, *35*, 10233-10237.
6. Xiao, X.; Nagahara, L. A.; Rawlett, A. M.; Tao, N. *J. Am. Chem. Soc.* **2005**, *127*, 9235-9240.
7. Mwaura, J. K.; Pinto, M. R.; Witker, D.; Ananthakrishnan, N.; Schanze, K. S.; Reynolds, J. R. *Langmuir* **2005**, *21*, 10119-10126.
8. K Weder, C.; Sarwa, C.; Bastiaansen, C.; Smith, P. *Adv. Mater.* **1997**, *9*, 1035-1039.
9. (a) Arnt, L.; Tew, G. N. *Langmuir* **2003**, *19*, 2404-2408. (b) Arnt, L.; Tew, G. N. *Macromolecules* **2004**, *37*, 1283-1288. (c) Breitenkamp, R. B.; Tew, G. N. *Macromolecules* **2004**, *37*, 1163-1165. (d) Clark, A. P. Z.; Shen, K. F.; Rubin, Y. F.; Tolbert, S. H. *Nano. Lett.* **2005**, *5*, 1647-1652.
10. Nambiar, R. R.; Brizius, G. L.; Collard, D. M. *Adv. Mater*. **2007**, *19*, 1234-1238.
11. Nambiar, R.; Woody, K. B.; Ochocki, J. D.; Brizius, G. L.; Collard, D. M., *Macromolecules* **2009**, *42*, 43-51.
12. Ghosh, A. K.; Bischoff, A.; Cappiello, J. *Eur. J. Org. Chem.* **2003**, 821-832.
13. Moroni, M.; Le Moigne, J.; Luzzati, S. *Macromolecules* **1994**, *27*, 562-571.
14. Bunz, U. H. F. *Chem. Rev.* **2000**, *100*, 1605-1644.

CHAPTER 3: SYNTHESIS AND CHARACTERIZATION OF REGIO-REGULAR, AMPHIPHILIC POLY(1,4-PHENYLENE ETHYNYLENE)S

3.1. Introduction

The regioregular PPEs described in Chapter 2 were limited to PPEs with different lengths of linear alkoxy side chains. It was expected that regioregularity would have greater influence on PPEs with amphiphilic side chains that have a tendancy to segregate on a molecular scale. To explore the role of such amphiphilicity on other classes of conjugated polymers we prepared PPEs that are substituted with alkoxy and semifluoroalkoxy side chains.

The design of amphiphilic structures allows for the manipulation of the packing and orientation of molecules in the solid state and at interfaces.[1] There are several examples of facially amphiphilic (i.e., "Janus-type") PPEs in the literature which have a combination of a hydrophobic alkyl side chain and a polar,[2] PEG [3,4] or cationic[5] side chains. These studies reveal that the interactions of the disparate side chains affect the molecular assembly of the polymers and their optoelectronic properties. While the segregation of these amphiphilic side chains affords the opportunity to influence molecular packing of conjugated polymers, the incorporation of hydrophilic side chains renders the materials sensitive to moisture.

Semifluoroalkyl and alkyl side chains are both hydrophobic and have a tendancy to phase separate. As discussed in Chapter 1, it was previously shown that alternating alkyl and semifluoroalkyl side chains substituted on the backbone of poly(3-alkylthiophene)s (PATs) provide an amphiphilic structure where the side chains segregate on a molecular scale.[6] Here we extend this method to prepare amphiphilic regiorandom and regioregular PPEs bearing both semifluoroalkoxy (-

$O(CH_2)_m(CF_2)_nF$ and alkoxy ($-O(CH_2)_pH$) side chains on each repeat unit, Figure 3.1, to explore the effect of amphiphilicity on the solid state assembly of the polymers. The hydrocarbon spacer ($(CH_2)_m$) of the semifluoroalkoxy chain insulates the conjugated polymer backbone from the electron-withdrawing inductive effects of the fluorocarbon segment. Accordingly, any changes in the electronic properties of the materials may be ascribed to changes in molecular packing arising from incorporation of fluoroalkyl segments and their relative placement, rather than an electronic substituent effect on the conjugated backbone.

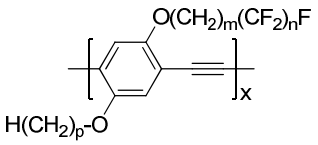

	regiorandom	*regioregular*
m = 6, n = 6, p = 12	**RnPPE(6,6/12)**	**RgPPE(6,6/12)**
m = 8, n = 4, p = 12	**RnPPE(8,4/12)**	**RgPPE(8,4/12)**
m = 10, n = 2, p = 12	**RnPPE(10,2/12)**	**RgPPE(10,2/12)**

Figure 3.1. Amphiphilic PPEs with semifluoroalkoxy and alkoxy side chains on each repeat unit.

The semifluoroalkoxy and alkoxy side chains are the same length (where m + n = p), and are almost isosteric with symmetrically-substituted dialkoxy PPEs (e.g. poly(2,4-dodecyloxy-1,4-phenylene ethynylene, **PPE(12/12)**).

3.2. Experimental

3.2.1. General Synthetic Methods

All starting materials were purchased from commercial sources and used without further purification unless stated otherwise. THF and Et_2O were dried over sodium benzophenone ketyl prior to distillation under argon. Column chromatography

was performed on flash grade silica (32-60 Å, Sorbent Technologies, Atlanta, Georgia). Thin-layer chromatography was performed on 3×5 cm silica gel plates (0.2 mm thick, 60 F254) on an aluminum support (Sorbent Technologies). NMR analysis was performed on a Bruker DSX 400 or DSX 300 instruments using $CDCl_3$ as the solvent unless stated otherwise. Chemical shifts are reported relative to internal tetramethylsilane. ^{13}C NMR are proton decoupled. IR analyses were performed on a Nicolet 4700 FTIR with an ATR attachment from SmartOrbit Thermoelectronic Corporation. Ultraviolet-visible analysis was performed on a Perkin-Elmer Lambda 19 spectrophotometer, and fluorescence spectroscopy was performed on a SPEX Fluorolog 1680/1681 0.22m spectrometer. Elemental analyses were performed by Atlantic Microlab, Inc. (Norcross, GA). The Bestman-Ohiro reagent (**III-10**) was prepared using previously reported methods.[7] ^{1}H and ^{13}C NMR, IR spectra and EI mass spectra are provided in Appendix B for all homologues.

3.2.2. Synthesis of Semifluoroalcohols

Synthetic procedures of the semifluoroalcohols in Figure 3.3. are given below. Compound **III-1** was synthesized using two different procedures modified from literature.[8,9] Compound **III-2** was synthesized using standard literature procedures.[6]

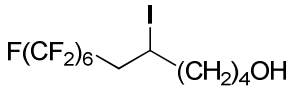

7,7,8,8,9,9,10,10,11,11,12,12,12-Tridecafluoro-5-iododododecan-1-ol, III-1a: ***Cu catalyzed method.*** A mixture of 5-hexen-1-ol (4.4 mL, 37 mmol), 1-perfluorohexyl iodide (25 g, 56 mmol) and Cu powder (0.36 g, 5.7 mmol) was heated to 120 °C for 24 h in a sealed thick-walled glass vessel under argon. Et_2O (50 mL) was added and the Cu catalyst was removed by filtration. The solvent was removed

under reduced pressure and the residue was subjected to flash column chromatography (silica gel, 20:80 v/v ethyl acetate:hexanes) to afford **III-1a** as a colorless liquid (9.91 g, 49%). ^{1}H NMR (300 MHz, $CDCl_3$): δ 4.27-4.36 (m, 1H, C5 CH), 3.65 (t, $^{3}J_{HH}$ = 6 Hz, 2H, -OCH_2-), 2.66-3.01 (m, 2H, C6 CH_2), 2.02 (br s, 1H, -OH), 1.47-1.87 (m, 6H). ^{13}C NMR (75 MHz, $CDCl_3$): δ 62.44 (C1), 41.59 (t, $^{3}J_{CF}$ = 20 Hz, C6), 40.00, 31.49, 25.97, 20.44 (6 CF_2 C's not visible above baseline due to splitting). IR (ATIR): 3350 (br, O-H str), 2947, 2884, 1749, 1367, 1195 (C-O str.), 1144, 1063, 812, 735, 698, 658, 509 cm^{-1}.

BEt_3 catalyzed method. A mixture of 5-hexen-1-ol (5.5 mL, 47 mmol) and 1-perfluorohexyl iodide (25 g, 56 mmol) was cooled to 0 °C under argon, and a solution of BEt_3 (2 mL, 2 mmol, 1 M in hexanes) was added via syringe. The mixture was stirred at 0ºC for 3 h, and MeOH (5 mL) was added, followed by H_2O (50 mL). The mixture was extracted with hexanes (200 mL) and dried over $MgSO_4$. The solution was filtered through a pad of silica gel (1:5 v/v EtOAc:hexanes) and the solvent was removed under reduced pressure to afford **III-1a** as a colorless liquid (21 g, 82%).

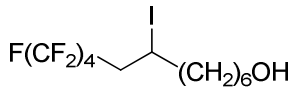

9,9,10,10,11,11,12,12,12-Nonafluoro-7-iododododecan-1-ol, III-1b. A mixture of 7-octen-1-ol (7.1 mL, 46 mmol) and perfluoro-*n*-butyl iodide (32 g, 92 mmol) was cooled to 0 °C under argon, and BEt_3 (0.3 mL, 1 mmol, 1 M in hexanes) was added by syringe. The mixture was stirred at 0 ºC for 3 h, and MeOH (5 mL) was added, followed by 50 mL H_2O. The mixture was extracted with hexanes (2 x 200 mL),the solution was dried over $MgSO_4$. The solution was filtered through a pad of silica gel (1:5 v/v EtOAc:hexanes) and the solvent was removed under reduced pressure to afford **III-1b** as a colorless liquid (21 g, 95%). ^{1}H NMR (300 MHz, $CDCl_3$): δ 4.28-

4.37 (m, 1H, C7), 3.62-3.67 (m, 2H, -OCH_2-), 2.66-3.01 (m, 2H, C8), 2.04 (bs, 1H, -OH), 1.75-1.85 (m, 2H), 1.37-1.60 (m, 8H). ^{13}C NMR (75 MHz, $CDCl_3$): δ 62.83 (C1), 41.51 (t, $^3J_{CF}$ = 22 Hz, C8), 40.17, 32.56, 29.49, 28.26, 25.48, 20.68 (4 CF_2 C's not visible above baseline due to splitting). IR (ATIR): 3352 (br, O-H str.), 2933, 2858, 1676, 1592, 1466, 1354, 1215 (C-O str.), 1132, 1051, 879, 719, 607, 515 cm^{-1}.

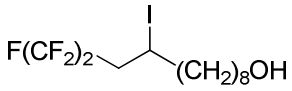

11,11,12,12,12-Pentafluoro-9-iododododecan-1-ol, III-1c. A dry Schlenk flask was fitted with a balloon and cooled to -75 °C, under argon. The flask was connected to a cylinder containing perfluoroethyliodide (25 g, 84 mmol) and the gas was slowly condensed into the flask. The liquid was allowed to warm to -20 °C and 9-decen-1-ol (10 mL, 56 mmol) was added, followed by dropwise addition of a solution of BEt_3 (1 mL of 1 a M solution in hexanes, 1 mmol) over 1 min. The mixture was stirred at -20 °C for 2 h, MeOH (10 mL) was added, and the resulting solution was allowed to warm to room temperature. The solution was poured into H_2O (50 mL) and extracted with hexanes (2 × 50 mL). The extracts were combined, dried over $MgSO_4$, and the solvent was removed under reduced pressure. The residue was subjected to column chromatography (silica gel, 2:1 v/v CH_2Cl_2:hexanes) to afford **II-1c** as a pale yellow liquid (19.55 g, 85%). ^{1}H NMR (300 MHz, $CDCl_3$): δ 4.26-4.31 (m, 1H, C9), 3.60 (t, $^3J_{HH}$ = 6.6 Hz, 2H, -OCH_2-), 2.61-2.94 (m, 2H, C8), 1.88 (s, 1H, -OH), 1.71-1.81 (m, 2H), 1.25-1.56 (m, 12H). ^{13}C NMR (75 MHz, $CDCl_3$): δ 62.80 (C1), 41.37 (t, $^3J_{CF}$ = 21 Hz, C9), 40.11, 32.62, 29.43, 29.24, 29.22, 28.34, 25.61, 20.79 (2 CF_2 C's not visible above baseline due to splitting). IR (ATIR): 3355 (br, O-H str.), 2931, 2858, 1465, 1436, 1323, 1189 (C-O str.), 1122, 1059, 723 cm^{-1}.

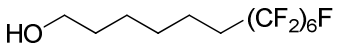

7,7,8,8,9,9,10,10,11,11,12,12,12-Tridecafluorododecan-1-ol, III-2a.

Iodide **III-1a** (9.0 g, 17 mmol) was added to a flask containing $NaBH_4$ (2.5 g, 66 mmol) and DMSO (150 mL). The mixture was heated to 80 °C for 24 h under argon, poured slowly into 10% aqueous HCl, and extracted with hexanes (2 × 100 mL). The combined extracts were dried over $MgSO_4$ and the solvent was removed under reduced pressure. The residue was subjected to flash column chromatography (30:70 v/v ethyl acetate:hexanes) to afford **III-2a** as a colorless liquid (5.8 g, 84%). ^{1}H NMR (300 MHz, $CDCl_3$): δ 3.62 (t, $^3J_{HH}$ = 6.6 Hz, 2H, -OCH_2-), 2.59 (bs, 1H, -OH), 1.94-2.12 (m, 2H), 1.38-1.82 (m). ^{13}C NMR (75 MHz, $CDCl_3$): δ 62.70 (C1), 32.41, 30.75 (t, $^3J_{CF}$ = 22 Hz, C6), 28.87, 25.40, 20.05 (6 CF_2 C's not visible above baseline due to splitting). IR (ATIR): 3332 (br, O-H str.), 2945, 2868, 1189 (C-O str), 1144, 1055, 845, 810, 731, 696, 654, 567, 534 cm^{-1}.

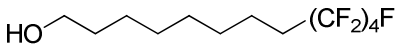

9,9,10,10,11,11,12,12,12-Nonafluorododecan-1-ol, III-2b. Reductive deiodination of **III-1b** (8 g, 17 mmol), according to the procedure provided above for the preparation of **III-2a,** afforded **III-2b** as a colorless liquid (4.5 g, 77%). ^{1}H NMR (300 MHz, $CDCl_3$): δ 3.60 (t, $^3J_{HH}$ = 6.6 Hz, 2H, -OCH_2-), 2.58 (bs, 1H, -OH), 1.92-2.10 (m, 2H), 1.49-1.58 (m, 2H), 1.31-1.49 (m, 10H). ^{13}C NMR (75 MHz, $CDCl_3$): δ 62.82 (C1), 32.61, 30.69 (t, $^3J_{CF}$ = 22 Hz, C8), 29.14, 28.98, 25.62, 20.04 (4 CF_2 C's not visible above baseline due to splitting). IR (ATIR): 3309 (br, O-H str.), 2923, 2854, 1496, 1464, 1369, 1213 (C-O str.), 1132, 1045, 1003, 879, 850, 719, 656, 600, 536 cm^{-1}.

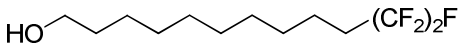

11,11,12,12,12-Pentafluorododecan-1-ol, III-2c. Reductive deiodination of **III-1c** (19 g, 47 mmol), according to the procedure provided above for the preparation of **III-2a**, afforded **III-2c** as a colorless liquid (10.64 g, 82%). ^{1}H NMR (300 MHz, $CDCl_3$): δ 3.63 (t, $^{3}J_{HH}$ = 6.6 Hz, 2H, -OCH_2-), 1.90-2.08 (m, 2H), 1.29-1.61 (m, 16H). ^{13}C NMR (75 MHz, $CDCl_3$): δ 63.01 (C1), 32.74, 31.50, 30.61 (t, $^{3}J_{CF}$ = 22 Hz), 29.46, 29.35, 29.27, 29.04, 25.79, 20.18 (2 CF_2 C's not visible above baseline due to splitting). IR (ATIR): 3340 (br, OH), 2931, 2860, 1469, 1344, 1190 (C-O str.), 1039, 715 cm^{-1}.

3.2.3. Synthesis of Symmetrically Substituted Alkoxy/Semifluoroalkoxy Monomers

Synthetic procedures and spectroscopic data for homologue A (*m = 6, n = 6*) and homologue B (*m = 8, n = 4*) of the asymmetrically substituted A-A and B-B type monomers in Figure 3.4. are given below.

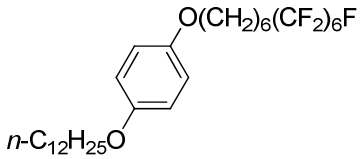

1-(Dodecyloxy)-4-(7,7,8,8,9,9,10,10,11,11,12,12,12-tridecafluorododecyl-oxy)benzene, III-3a. 4-(Dodecyloxy)phenol (2.5 g, 9.0 mmol) was added to a solution of **III-2a** (5.7 g, 14 mmol) and PPh_3 (3.5 g, 14 mmol) in Et_2O (100 mL) in a dry flask under argon. Diethylazodicarboxylate, DEAD (2.5 mL, 13.6 mmol) was added dropwise by syringe and the mixture was stirred for 48 h. The mixture was poured into 10% aqueous NaOH (200 mL), and the resulting solution was extracted with Et_2O (2 × 100 mL). The combined extracts were dried over $MgSO_4$ and the solvent was removed under reduced pressure. The residue was purified by flash

column chromatography (silica gel; 30:70 v/v CH_2Cl_2:hexanes) to afford **III-3a** as a colorless solid (3.08 g, 50 %): m.p. = 60-64 °C. ^{1}H NMR (300 MHz, $CDCl_3$): δ 6.82 (s, 4H, Ar-H), 3.88-3.93 (m, 4H, -OCH_2-), 1.98-2.16 (m, 2H, -CF_2CH_2-), 1.71-1.82 (m, 4H), 1.27-1.64 (m, 24H), 0.89 (t, $^3J_{HH}$ = 6.6 Hz, 3H, -CH_3). ^{13}C NMR (75 MHz, $CDCl_3$): δ 153.04 (coincident Ar C-O's), 115.37 (coincident Ar C-H's), 68.63 (C-O), 68.26 (C-O), 31.93, 30.81 (t, $^3J_{CF}$ = 22.8 Hz), 29.68, 29.65, 29.62, 29.44, 29.41, 29.36, 29.15, 28.86, 26.06, 25.78, 22.69, 20.08, 14.09 (6 CF_2 C's not visible above baseline due to splitting, 1 CH_2 missing due to coincident chemical shifts). IR (ATIR): 2920 (Ar-H str.), 2850, 1510, 1473, 1367, 1312, 1236, 1186, 1138 (C-O str.), 1045, 825, 773, 698, 648, 571, 534, 453 cm^{-1}. HRMS *calc*. for $C_{30}H_{41}F_{13}O_2$ = 680.28990, *obs*. = 680.28799, Δ = 2.8 ppm.

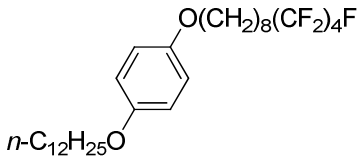

1-(Dodecyloxy)-4-(9,9,10,10,11,11,12,12,12-nonafluorododecyloxy)benzene, III-3b. A Mitsunobu reaction between of **III-2b** (3.8 g, 11 mmol) and 4-(dodecyloxy)phenol (2.5 g, 9.0 mmol), according to the procedure provided above for the preparation of **III-3a**, afforded **III-3b** as a colorless solid (2.76 g, 47%). m.p. = 60-62 °C. ^{1}H NMR (300 MHz, $CDCl_3$): δ 6.80 (s, 4H, Ar-H), 3.87 (t, $^3J_{HH}$ = 6.6 Hz, 4H, -OCH_2-), 1.94-2.12 (m, 2H, -CF_2CH_2-), 1.68-1.78 (m, 4H), 1.24-1.61 (m, 28H), 0.86 (t, $^3J_{HH}$ = 7.2 Hz, 3H). ^{13}C NMR (75 MHz, $CDCl_3$): δ 153.10 (coincident Ar C-O's), 115.35 (coincident Ar C-H's), 68.62 (coincient C-O's), 31.92, 30.73 (t, $^3J_{CF}$ = 22 Hz), 29.65, 29.58, 29.39, 29.35, 29.12, 29.01, 26.05, 25.98, 22.69, 20.03, 14.12 (4 CF_2 C's not visible above baseline due to splitting, 4 CH_2 C's have coincident chemical shifts with other signals). IR (ATIR): 2931 (Ar C-H str.), 2852, 1510, 1475,

1357, 1221 (C-O str.), 1132, 1026, 847, 825, 773, 719, 602, 532 cm^{-1}. HRMS *calc*. for $C_{30}H_{45}F_9O_2$ = 608.32759, *obs*. = 608.32720, Δ = 0.6 ppm.

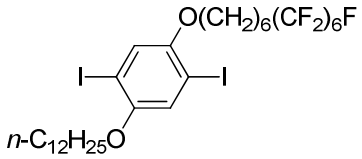

1-(Dodecyloxy)-4-(7,7,8,8,9,9,10,10,11,11,12,12,12-tridecafluorodo-decyloxy)-2,5-diiodo benzene, III-4a. A solution of dialkoxybenzene **III-3a** (1.7 g, 2.6 mmol), iodine (1.2 g, 4.7 mmol) and KIO_3 (0.46 g, 2.2 mmol) in a mixture of acetic acid (30 mL), water (2 mL) and H_2SO_4 (0.5 mL) was heated to reflux for 48 h. The mixture was cooled, diluted with CH_2Cl_2 (100 mL) and washed with saturated aqueous Na_2SO_3 until the mixture turned clear. The organic layer was washed with 10% aqueous NaOH (2 × 50 mL), dried over $MgSO_4$, and the solvent was removed under reduced pressure. The residue was dissolved in a 40:60 v/v mixture of CH_2Cl_2 and hexanes and the solution was passed through a pad of silica. The solvent was removed under reduced pressure and the residue was recrystallized from isopropanol to afford **III-4a** as a colorless crystalline solid (1.6 g, 70 %): m.p. = 48-52 °C. ^{1}H NMR (300 MHz, $CDCl_3$): δ 7.15 (s, 2H, Ar-H), 3.89-3.94 (m, 4H, -OCH_2-), 1.98-2.16 (m, 2H, -CF_2CH_2-), 1.73-1.85 (m, 4H), 1.25-1.69 (m, 24H), 0.86 (t, $^3J_{HH}$ = 7.2 Hz, 3H, -CH_3). ^{13}C NMR (75 MHz, $CDCl_3$): δ 153.08 (Ar C-O), 122.78 (Ar C-H), 86.28 (Ar C-I), 70.32 (C-O), 69.96 (C-O), 31.91, 30.78 (t, $^3J_{CF}$ = 22.8 Hz), 29.66, 29.57, 29.35, 29.26, 29.11, 28.87, 28.73, 26.01, 25.77, 22.68, 20.05, 14.11(6 CF_2 C's not visible above baseline due to splitting, 2 CH_2 C's have coincident chemical shifts with other signals). IR (ATIR): 2922 (Ar-H str.), 2854, 1485, 1464, 1348, 1207 (C-O str.), 1144, 1051, 984, 845, 696, 654, 569, 528, 432 cm^{-1}. HRMS *calc*. for $C_{30}H_{39}F_{13}I_2O_2$ = 932.08320, *obs*. = 932.08012, Δ = 3.3 ppm. Elemental Analysis: Theoretical: C,

38.64%; H, 4.22%; I, 27.22%; O, 3.43%; F, 26.49%; Found: C, 38.80%; H, 4.24%; I, 27.38%; O, 3.50%; F, 26.41%.

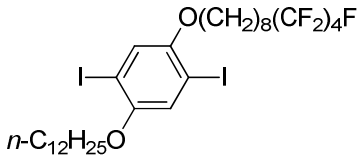

1-(Dodecyloxy-4-(9,9,10,10,11,11,12,12,12-nonafluorododecyloxy))-2,5-diiodobenzene, III-4b. Iodination of **III-3b** (2.7 g, 4.4 mmol), according to the procedure provided above for the preparation of **III-4a**, afforded **III-4b** as a colorless crystalline solid (2.3 g, 61%): m.p. = 50-52 °C. ^{1}H NMR (300 MHz, $CDCl_3$): δ 7.15 (s, 2H, Ar-H), 3.91 (t, $^{3}J_{HH}$ = 6.6 Hz, 4H, -OCH_2-), 1.95-2.12 (m, 2H, -CF_2CH_2-), 1.74-1.82 (m, 4H), 1.25-1.61 (m, 28H), 0.86 (t, $^{3}J_{HH}$ = 6.6 Hz, 3H, -CH_3). ^{13}C NMR (75 MHz, $CDCl_3$): δ 152.87 (Ar C-O), 122.75 (Ar C-H), 86.22 (Ar C-I), 70.33 (C-O), 31.90, 30.76 (t, $^{3}J_{CF}$ = 22 Hz), 29.64, 29.56, 29.33, 29.26, 29.12, 29.06, 28.98, 26.00, 25.94, 22.68, 20.05, 14.09 (4 CF_2 C's not visible above baseline due to splitting, 4 CH_2 C's have coincident chemical shifts with other signals). IR (ATIR): 2916 (Ar-H str.), 2848, 1487, 1458, 1392, 1354, 1215 (C-O str.), 1126, 1070, 997, 956, 845, 787, 717, 598, 528, 434 cm^{-1}. HRMS *calc*. for $C_{30}H_{43}F_9O_2I$ = 860.12089, *obs*. = 860.11577, Δ = 6.0 ppm. Elemental Analysis: Theoretical: C, 41.88%; H, 5.04%; I, 29.50%; O, 3.72%; F, 19.87%; Found: C, 41.95%; H, 4.94%; I, 29.80%; O, 3.98%; F, 19.61%.

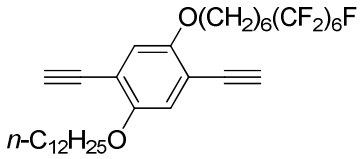

1-(Dodecyloxy)-2,5-diethynyl-4-(7,7,8,8,9,9,10,10,11,11,12,12,12-trideca-fluorododecyloxy)benzene, III-6a. Diiodide **III-4a** (1.5 g, 1.6 mmol) was added to a solution of $PdCl_2(PPh_3)_2$ (60 mg, 0.09 mmol) and CuI (20 mg, 0.11 mmol) in piperidine (19 mL). The mixture was degassed by freeze-pump-thaw and back-filled

with argon. Trimethylsilane acetylene (0.57 mL, 4.0 mmol) was added dropwise over 10 min and the mixture was stirred for 24 h. CH_2Cl_2 (100 mL) was added and the solution was passed through silica plug. The solvent was removed under reduced pressure to afford **III-5a** as a pale brown solid (1.23 g, 87 %). ^{1}H NMR (300 MHz, $CDCl_3$): δ 6.89 (s, 2H, Ar-H), 3.92-3.97 (m, 4H, -OCH_2-), 1.98-2.17 (m, 2H, -CF_2CH_2-), 1.74-1.86 (m, 4H), 1.26-1.66 (m, 24H), 0.88 (t, $^3J_{HH}$ = 7.2 Hz, 3H, -CH_3), 0.25 (s, 18H, -TMS). ^{13}C NMR (75 MHz, $CDCl_3$): δ 153.75 (Ar C-O), 117.12 (Ar C3-H), 113.85 (Ar C6-H), 100.95 (C≡C-TMS), 100.17 (C≡C-TMS), 69.37, 68.99, 31.91, 30.87 (t, $^3J_{CF}$ = 22.8 Hz), 29.62, 29.42, 29.32, 29.09, 28.89, 26.02, 25.75, 22.69, 20.14, 14.11, 0.01 (6 CF_2 C's not visible above baseline due to splitting, 4 CH_2 C's have coincident chemical shifts with other signals).

Tetra-*n*-butylammonium fluoride (1 M solution in THF, 2.5 mL, 2.5 mmol) was added dropwise to a solution of bis(trimethylsilane) **III-5a** (0.98 g, 1.1 mmol) in dry THF (40 mL), the mixture was stirred for 1 h, and poured into H_2O (50 mL). The mixture was extracted with CH_2Cl_2 (100 mL), the combined extracts were dried over $MgSO_4$, and the solvent was removed under reduced pressure. The residue was recrystallized from ethanol to afford **III-6a** as a yellow powder (0.55 g, 67 %): m.p. = 60-62 °C. ^{1}H NMR (300 MHz, $CDCl_3$): δ 6.95 (s, 1H, Ar-H), 6.94 (s, 1H, Ar-H), 3.94-4.00 (m, 4H, -OCH_2-), 3.33 (s, 1H, ≡C-H), 3.32 (s, 1H, ≡C-H), 1.98-2.16 (m, 2H, -CF_2CH_2-), 1.75-1.87 (m, 4H), 1.26- 1.69 (m, 24H), 0.88 (t, $^3J_{HH}$ = 7.2 Hz, 3H, -CH_3). ^{13}C NMR (75 MHz, $CDCl_3$): δ 154.02 (Ar C-O), 117.64 (Ar C3-H), 113.17 (Ar C6-H), 82.65(C≡C-H), 79.68(C≡C-H), 69.59 (C-O), 69.24 (C-O), 31.91, 31.04 (t, $^3J_{CF}$ = 22.8 Hz), 29.66, 29.63, 29.57, 29.28, 29.08, 28.81, 28.88, 28.73, 25.87, 25.62, 22.68, 14.11(6 CF_2 C's not visible above baseline due to splitting, 4 CH_2 C's have coincident chemical shifts with other signals). IR (ATIR): 3309 (≡C-H str.), 2922 (Ar-H str.),

2854, 2108 (C≡C str.), 1496, 1468, 1387, 1321, 1194 (C-O str.), 1144, 1068, 856, 787, 696, 652, 606, 571, 530 cm^{-1}. HRMS *calc*. for $C_{34}H_{41}F_{13}O_2$ = 728.28990, *obs*. = 728.29282, Δ = 4.0 ppm. Elemental Analysis: Theoretical: C, 56.04%; H, 5.67%; O, 4.39%; F, 33.89%; Found: C, 55.78%; H, 5.73%; O, 4.43%; F, 34.01%.

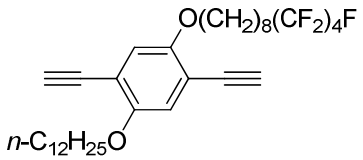

1-(Dodecyloxy)-2,5-diethynyl-4-(9,9,10,10,11,11,12,12,12-nonafluorododecyloxy)benzene, III-6b. Treatment of **III-4b** (1.5 g, 1.7 mmol) with trimethylsilyl acetylene followed by desilylation, according to the procedure provided above for the preparation of **III-6a**, afforded **III-6b** as a yellow powder (0.75 g, 91 %): m.p. = 50-52 ºC. ^{1}H NMR (300 MHz, $CDCl_3$): δ 6.95 (s, 2H, ArH), 3.97 (t, $^3J_{HH}$ = 6.6 Hz, 4H, -OCH_2-), 3.33 (s, 1H, ≡C-H), 3.32 (s, 1H, ≡C-H), 1.96-2.14 (m, 2H, -CF_2CH_2-), 1.75-1.84 (m, 4H), 1.26-1.62 (m, 28H), 0.88 (t, $^3J_{HH}$ = 6.6 Hz, 3H, -CH_3). ^{13}C NMR (75 MHz, $CDCl_3$): δ 153.84 (Ar C-O), 117.67 (Ar C3-H), 113.19 (Ar C6-H), 82.40 (C≡C-H), 79.74 (C≡C-H), 69.61 (C-O), 31.89, 30.75 (t, $^3J_{CF}$ = 22 Hz), 29.64, 29.57, 29.34, 29.11, 28.97, 25.87, 25.80, 27.67, 20.04, 14.10 (4 CF_2 C's not visible above baseline due to splitting, 6 CH_2 C's have coincident chemical shifts with other signals). IR (ATIR): 3307 (≡C-H str.), 2924 (Ar-H str.), 2854, 2106 (C≡C str), 1498, 1469, 1387, 1360, 1219 (C-O str.), 1132, 999, 856, 719, 652, 602, 534 cm^{-1}. HRMS *calc*. for $C_{34}H_{45}F_9O_2$ = 656.32759, *obs*. = 656.32432, Δ = 5.0 ppm. Elemental Analysis Theoretical: C, 62.18%; H, 6.76%; O, 4.87%; F, 26.04%; Found: C, 62.33%; H, 6.76%; O, 5.13%; F, 26.09%.

3.2.4. Synthesis of A-B type Alkoxy/Semifluoroalkoxy Monomers

Synthetic procedures and spectroscopic data for homologue A (*m = 6, n = 6*), homologue B (*m= 8, n = 4*) and homologue C (*m = 10, n = 2*) of the asymmetrically substituted A-B type monomers in Figure 3.6. are given below.

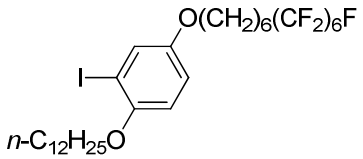

1-(Dodecyloxy)-4-(7,7,8,8,9,9,10,10,11,11,12,12,12-tridecafluorododecyl-oxy)-2-iodobenzene, III-7a. 4-(Dodecyloxy)-3-iodophenol (4.4 g, 11 mmol) was added to a solution of **III-2a** (5.5 g, 13 mmol) and PPh_3 (3.43 g, 13.1 mmol) in Et_2O (100 mL) in a dry flask under argon. DEAD (2.4 mL, 13 mmol) was added dropwise via syringe and the solution was stirred for 48 h. The mixture was poured into 10% aqueous NaOH (200 mL) and the resulting solution was extracted with Et_2O (2 × 100 mL). The combined extracts were dried over $MgSO_4$ and the solvent was removed under reduced pressure. The residue was subjected to flash column chromatography (silica gel; 10:90 v/v EtOAc:hexanes) to afford **III-7a** as a white solid (6.64 g, 76%): m.p.= 39-41°C. ^{1}H NMR (300 MHz, $CDCl_3$): δ 7.32 (d, $^4J_{ArH3\text{-}ArH5}$= 2.7 Hz, 1H, Ar C3-H), 6.83 (dd, $^3J_{ArH5\text{-}ArH6}$= 9 and $^4J_{ArH3\text{-}ArH5}$= 2.7 Hz, 1H, Ar C5-H), 6.72 (d, $^3J_{ArH5\text{-}ArH6}$= 9 Hz, 1H, Ar C6-H), 3.86-3.95 (m, 4H, -OCH_2-), 1.98-2.16 (m, 2H, -CF_2CH_2-), 1.72-1.85 (m, 4H), 1.27-1.69 (m, 24H), 0.88 (t, $^3J_{HH}$ = 6.6 Hz, 3H, -CH_3). ^{13}C NMR (75 MHz, $CDCl_3$): δ 153.59 (Ar C-O), 152.20 (Ar C-O), 125.25, 115.37, 113.03 (Ar C-H), 86.95 (Ar C-I), 70.15 (C-O), 68.44 (C-O), 31.91, 30.79 (t, $^3J_{CF}$= 22 Hz), 29.67, 29.57, 29.36, 29.33, 29.26, 29.03, 28.83, 26.08, 25.73, 22.69, 20.06, 14.12 (6 CF_2 C's not visible above baseline due to splitting, 2 CH_2 C's have coincident chemical shifts with other signals). IR (ATIR): 2916 (Ar C-H str., 2848, 1597, 1487, 1464, 1242,

1209 (C-O str.), 1142, 1047, 1005, 866, 783, 694, 640, 571, 530 cm^{-1}. HRMS *calc.* for $C_{30}H_{40}F_{13}IO_2$ = 806.18655, *obs.* =806.18250 Δ =5.0 ppm.

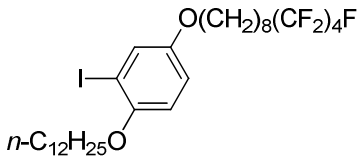

1-(Dodecyloxy)-4-(9,9,10,10,11,11,12,12,12-nonafluorododecyloxy)-2-iodobenzene, III-7b. Treatment of 4-(dodecyloxy)-3-iodophenol (6.8 g, 17 mmol) with **III-2b** (7.0 g, 20 mmol), according to the procedure provided above for the preparation of **III-7a**, afforded **III-7b** as a colorless solid (10.4 g, 84%): m.p.= 44-46°C. ^{1}H NMR (300 MHz, $CDCl_3$): δ 7.30 (d, $^4J_{ArH3\text{-}ArH5}$ = 2.7 Hz, 1H, Ar C3-H), 6.81 (dd, $^3J_{ArH5\text{-}ArH6}$ = 9.0 Hz, and and $^4J_{ArH3\text{-}ArH5}$ = 2.7 Hz, 1H, C-5 Ar-H), 6.71 (d, $^3J_{ArH5\text{-}ArH6}$= 8.7 Hz, 1H, C-6 Ar-H), 3.91 (t, $^3J_{H1\text{-}H2}$ = 6 Hz, 2H, -OCH_2-), 3.86 (t, $^3J_{H1'\text{-}H2'}$ = 6.6 Hz, 2H, -OCH_2-), 2.04 (m, 2H), 1.75 (m, 4H), 1.24-1.60 (m, 28H), 0.86 (t, $^3J_{HH}$ = 6.6 Hz, 3H, -CH_3). ^{13}C NMR (75 MHz, $CDCl_3$): δ 153.68 (Ar C-O), 152.16 (Ar C-O), 125.27, 115.39, 113.05 (Ar-C-H), 86.95 (Ar C-I), 70.15 (C-O), 68.69 (C-O), 31.91, 30.73 (t, $^3J_{CF}$ = 22 Hz), 29.64, 29.59, 29.56, 29.33, 29.23, 29.13, 29.08, 26.08, 25.91, 22.69, 20.04, 14.12 (4 CF_2 C's not visible above baseline due to splitting, 4 CH_2 C's have coincident chemical shifts with other signals). IR (ATIR): 2914 (Ar C-H str.), 2852, 1487, 1468, 1387, 1358, 1207 (C-O str.), 1130, 1047, 1020, 845, 783, 717, 600, 532 cm^{-1}. HRMS: *calc*. for $C_{30}H_{44}F_9O_2I$ = 734.22559, *obs*. =734.22424, Δ = 2.1 ppm.

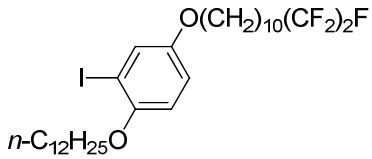

1-(Dodecyloxy)-4-(11,11,12,12,12-pentafluorododecyloxy)-2-iodobenzene, III-7c. Treatment of 4-(dodecyloxy)-3-iodophenol (6.01 g, 14.9 mmol) and **III-2c** (6.09 g, 22.5 mmol), according to the procedure provided above for the preparation of **III-7a**, afforded **III-7c** as a colorless solid (7.59 g, 77%): m.p.= 35-37 ^{o}C. ^{1}H NMR (300 MHz, $CDCl_3$): δ 7.31 (d, $^{4}J_{ArH3\text{-}ArH5}$= 3.3 Hz, 1H, Ar C3-H), 6.81 (dd, $^{3}J_{ArH5\text{-}ArH6}$= 9 and $^{4}J_{ArH3\text{-}ArH5}$= 6 Hz, 1H, Ar C5-H), 6.70 (d, $^{3}J_{ArH5\text{-}ArH6}$= 9 Hz, 1H, Ar C6-H), 3.85 (t, $^{3}J_{H1\text{-}H2}$ = 6Hz, 2H, -OCH_2-), 3.85 (t, $^{3}J_{H1'\text{-}H2'}$ = 6.6 Hz, 2H, -OCH_2-), 1.90-2.08 (m, 2H, -CF_2CH_2-), 1.67-1.83 (m, 4H), 1.25-1.59 (m, 32H), 0.86 (t, $^{3}J_{H11\text{-}H12}$ = 6.6 Hz, 3H, -CH_3). ^{13}C NMR (75 MHz, $CDCl_3$): δ 153.71 (Ar C-O), 152.12 (Ar C-O), 125.26, 115.37, 113.03 (Ar C-H), 86.94 (Ar C-I), 70.13 (C-O), 68.75 (C-O), 31.91, 30.62 (t, $^{3}J_{CF}$ = 22 Hz), 29.64, 29.56, 29.42, 29.35, 29.24, 29.15, 29.04, 26.08, 25.96, 22.68, 20.20, 14.11(2 CF_2 C's not visible above baseline due to splitting, 6 CH_2 C's have coincident chemical shifts with other signals). IR (ATIR): 2916 (Ar C-H str.), 2852, 1574, 1487, 1469, 1390, 1271, 1196 (C-O str.), 1047, 995, 862, 783, 715 cm^{-1}. HRMS: *calc.* for $C_{30}H_{48}F_5IO_2$ = 662.26192, *obs.* = 662.25778 Δ = 6.3 ppm.

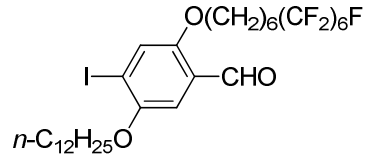

5-(Dodecyloxy)-2-(7,7,8,8,9,9,10,10,11,11,12,12,12-tridecafluorododecyl-oxy)-4-iodobenzaldehyde, III-8a. $TiCl_4$ (46 mL of a 1M solution in CH_2Cl_2, 46 mmol) was added in three portions to monoiodinated diether **III-7a** (6.2 g, 7.6 mmol) in dry flask at -40 ºC under argon. The mixture was stirred for 15 min and

dichloromethyl methyl ether (1.36 mL, 15.3 mmol) was added dropwise. The mixture was stirred for another 1.5 h at -40 ºC and then poured into a mixture of 1N HCl and ice. The mixture was extracted with CH_2Cl_2 (2 × 50 mL)and the combined organic extracts were washed with H_2O (100 mL), dried over $MgSO_4$. The solvent was removed under reduced pressure and the residue was subjected to column chromatography (silica gel, 30:70 CH_2Cl_2:hexanes) followed by recrystallization from isopropanol to afford **III-8a** as a colorless crystalline solid (2.72 g, 43%): m.p. = 66-68 ºC. ^{1}H NMR (300 MHz, $CDCl_3$): δ 10.39 (s, 1H, -CHO), 7.43 (s, 1H, ArC3-H), 7.16 (s, 1H, ArC6-H), 3.95-4.03 (m, 4H, -OCH_2-), 1.97-2.15 (m, 2H, -CF_2CH_2-), 1.74-1.87 (m, 4H), 1.24-1.66 (m, 24H), 0.86 (t, $^3J_{HH}$ = 7.2 Hz). ^{13}C NMR (75 MHz, $CDCl_3$): δ 155.68 (Ar C-O), 152.20 (Ar C-O), 125.12 (Ar C-CHO), 124.45 (Ar C3-H), 108.87 (Ar C6-H), 96.73 (Ar C-I), 69.91 (C-O), 69.12 (C-O), 31.91, 30.77 (t, $^3J_{CF}$ = 22 Hz), 29.63, 29.57, 29.54, 29.34, 29.25, 28.99, 28.88, 28.79, 26.01, 25.75, 22.68, 20.09, 14.10 (6 CF_2 C's not visible above baseline due to splitting, 1 CH_2 C's missing due to coincident chemical shifts). IR (ATIR): 2922 (Ar C-H str.), 2852, 1676 (C=O str.), 1591, 1464, 1390, 1321, 1209 (C-O str.), 1144, 1039, 980, 872, 845, 791, 698, 654, 607, 571, 534, 449 cm^{-1}. HRMS *calc.* for $C_{31}H_{40}F_{13}IO_3$ = 834.18146, *obs.* = 834.18235 Δ = 1.1 ppm.

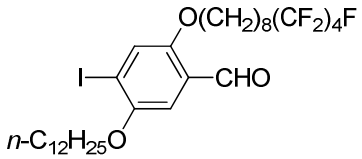

5-(Dodecyloxy)-2-(9,9,10,10,11,11,12,12,12-nonafluorododecyloxy)-4-iodo benzaldehyde,III- 8b. Formylation of **III-7b** (7.0 g, 9.5 mmol), according to the procedure provided above for the preparation of **III-8a**, afforded **III-8b** as a colorless crystalline solid (4.19 g, 58%): m.p.= 62-64 °C. ^{1}H NMR (300 MHz, $CDCl_3$):

δ 10.40 (s, 1H, CHO), 7.43 (s, 1H, ArC3-H), 7.16 (s, 1H, ArC6-H), 3.98 (m, 4H, -OCH_2-), 2.05 (m, 2H, -CF_2CH_2-), 1.81 (m, 4H), 1.26-1.58 (m, 28H), 0.88 (t, $^3J_{HH}$ = 6.6 Hz, 3H, -CH_3). ^{13}C NMR (75 MHz, $CDCl_3$): δ189.19 (Ar C-O), 155.70 (Ar C-O), 152.19 (Ar C-CHO), 125.13 (ArC3-H), 108.83 (ArC6-H), 96.76 (ArC-I), 69.90 (C-O), 69.33 (C-O), 31.90, 30.73 (t, $^3J_{CF}$ = 22 Hz), 29.65, 29.57, 29.35, 29.27, 29.14, 29.06, 29.01, 26.01, 25.92, 22.67, 20.04, 14.10 (4 CF_2 C's not visible above baseline due to splitting, 4 CH_2 C's have coincident chemical shifts with other signals). IR (ATIR): 2922 (Ar-H str.), 2850, 1674 (C=O str.), 1591, 1464, 1390, 1211 (C-O str.), 1132, 1041, 997, 883, 721, 606 cm^{-1}. HRMS: *calc*. for $C_{31}H_{44}F_9IO_3$ = 762.21915, *obs*. = 762.21996, Δ = 1.1 ppm.

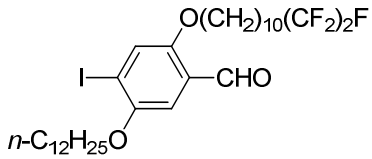

5-(Dodecyloxy)-2-(11,11,12,12,12-pentafluorododecyloxy)-4-iodobenzaldehyde, III-8c. Formylation of **III-7c** (6.5 g, 9.8 mmol), according to the procedure provided above for the preparation of **III-8a**, afforded **III-8c** as a colorless crystalline solid (2.79 g, 41%): mp = 50-54 ºC. ^{1}H NMR (300 MHz, $CDCl_3$): δ 10.39 (s, 1H, -CHO), 7.43 (s, 1H, ArC3-H), 7.16 (s, 1H, ArC6-H), 3.95-4.02 (m, 4H), 1.89-2.07 (m, 2H, -CF_2CH_2-), 1.75-1.84 (m, 4H), 1.24-1.59 (m, 32H), 0.86 (t, $^3J_{HH}$ = 6.6 Hz, 3H, -CH_3). ^{13}C NMR (75 MHz, $CDCl_3$): δ 189.25 (-CHO), 155.74 (Ar C-O), 152.14 (Ar C-O), 125.11 (Ar C-CHO), 124.51 (Ar C3-H), 108.81 (Ar C6-H), 96.77 (Ar C-I), 69.90 (C-O), 69.39 (C-O), 31.91, 30.61 (t, $^3J_{CF}$ = 22 Hz), 29.63, 29.56, 29.54, 29.40, 29.34, 29.26, 29.23, 29.15, 29.07, 29.04, 29.00, 26.01, 25.98, 22.69, 14.11 (2 CF_2 C's not visible above baseline due to splitting, 3 CH_2 C's have coincident chemical shifts with other signals). IR (ATIR): 2920 (Ar C-H str.), 2848, 1674 (C=O

str.), 1591, 1466, 1392, 1192, 1037, 1011 (C-O str.), 974, 872, 717, 607 cm^{-1}. HRMS *calc.* for $C_{31}H_{48}F_5IO_3$ = 690.25683, *obs.* = 690.25891 Δ = 5.5 ppm.

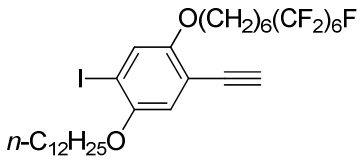

1-(Dodecyloxy)-5-ethyny-4-(7,7,8,8,9,9,10,10,11,11,12,12,12-tridecafluoro-dodecyloxy)-2-iodobenzene, III-9a. The Bestman-Ohiro reagent (**10**) $(MeO)_2P(=O)C(=N_2)COCH_3$ (1.4 g, 7.3 mmol) was added dropwise to a mixture of aldehyde **III-8a** (2.5 g, 3.0 mmol) and K_2CO_3 (0.62 g, 4.5 mmol) in a 1:1 v/v mixture of anhydrous CH_2Cl_2 and MeOH (20 mL). The mixture was stirred for 48 h at room temperature, poured into 10% aqueous HCl (50 mL), and extracted with CH_2Cl_2 (2 × 50 mL). The combined organic extracts were dried over $MgSO_4$ and the solvent was removed under reduced pressure. The residue was recrystallized twice from isopropanol to afford **III-9a** as a colorless solid (1.58 g, 64 %): m.p. = 59-61 °C. ^{1}H NMR (300 MHz, $CDCl_3$): δ 7.28 (s, 1H, ArC3-H), 6.86 (s, 1H, ArC6-H), 3.91-3.99 (m, 4H, -OCH_2-), 3.28 (s, 1H, ≡C-H), 1.98-2.16 (m, 2H, -CF_2CH_2-), 1.75-1.86 (m, 4H), 1.26-1.69 (m, 24H), 0.88 (t, $^3J_{HH}$ = 6.6 Hz, 3H). ^{13}C NMR (75 MHz, $CDCl_3$): δ 154.87 (Ar C-O), 152.03 (Ar C-O), 124.00 (Ar C6-H), 116.93 (Ar C3-H), 112.49 (Ar C2), 88.53 (Ar C-I), 81.98 (C≡C-H), 79.85 (C≡C-H), 70.31 (C-O), 69.76 (C-O), 32.15, 31.00 (t, $^3J_{CF}$ = 22 Hz), 29.89, 29.80, 29.58, 29.52, 29.36, 29.07, 28.96, 26.27, 25.85, 22.93, 20.27, 14.34 (6 CF_2 C's not visible above baseline due to splitting, 2 CH_2 C's have coincident chemical shifts with other signals). IR (ATIR): 3313 (≡C-H str.), 2924 (Ar C-H str.), 2854, 1495, 1460, 1367, 1321, 1209 (C-O str.), 1146, 1068, 984, 918, 850, 785, 748, 696, 654, 602, 569, 530 cm^{-1}. HRMS *calc.* for $C_{32}H_{40}F_{13}IO_2$ =

830.18655, *obs.* = 830.18624 Δ = 0.4 ppm. Elemental Analysis: Theoretical: C, 46.28%; H, 4.85%; I, 15.28%; O, 3.85%; F, 29.74%; Found: C, 46.06%; H, 4.71%; I, 15.42%; O, 4.13%; F, 29.48%.

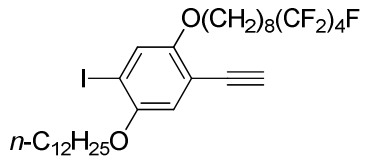

1-(Dodecyloxy)-5-ethynyl-4-(9,9,10,10,11,11,12,12,12-nonafluorododecyloxy)-2-iodobenzene, III-9b. Treatment of **III-8b** (2.7 g, 4.0 mmol) with the Bestman-Ohiro reagent (**III-10**), according to the procedure provided above for the preparation of **III-9a**, afforded **III-9b** as a yellow crystalline solid (1.40 g, 52%): m.p. = 43-45 °C. ^{1}H NMR (300 MHz, $CDCl_3$): δ 7.26 (s, 1H, ArC6-H), 6.85 (s, 1H, ArC3-H), 3.93 (m, 4H, O-CH_2), 3.27 (s, 1H, C≡C-H), 2.03 (m, 2H, -CF_2CH_2-), 1.78 (m, 4H), 1.18-1.58 (m, 28H), 0.86 (t, $^{3}J_{HH}$ = 6.9 Hz, 3H, -CH_3). ^{13}C NMR (75 MHz, $CDCl_3$): δ 154.73 (Ar C-O), 151.71 (Ar C-O), 123.75 (Ar C6), 116.66 (Ar C3), 112.21 (Ar C2), 88.28 (Ar C-I), 81.71 (C≡C-H), 79.65 (C≡C-H), 70.07 (C-O), 69.72 (C-O), 31.90, 30.73 (t, $^{3}J_{CF}$ = 22 Hz), 29.65, 29.55, 29.35, 29.27, 29.11, 29.00, 26.03, 25.78, 22.68, 20.03, 14.09 (4 CF_2 C's not visible above baseline due to splitting, 6 CH_2 C's have coincident chemical shifts with other signals). IR (ATIR): 3309 (≡C-H str.), 2925 (Ar-H str.), 2854, 2110, 1495, 1464, 1369, 1213 (C-O str.), 1132, 1001, 849, 717, 650, 598 cm^{-1}. HRMS: *calc*. for $C_{32}H_{44}F_9IO_2$ = 758.22424, *obs.* =758.22057, Δ = 3.7 ppm. Elemental analysis: Theoretical: C, 50.67%; H, 5.85%; I, 16.73%; O, 4.22%; F, 22.52%; Found: C, 50.69%; H, 5.88%; I, 16.47%; O, 4.48%; F, 22.38%.

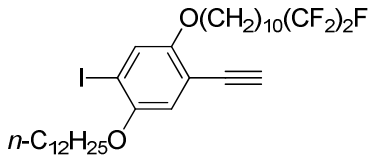

1-(Dodecyloxy)-5-ethynyl-4-(11,11,12,12,12-pentafluorododecyloxy)-2-iodobenzene, III-9c. Treatment of **III-8c** (1.55 g, 2.20 mmol) with the Bestman-Ohiro reagent (**III-10**), according to the procedure provided above for the preparation of **III-9a**, afforded **III-9c** as a white solid (1.1 g, 71%): m.p. = 37-38 °C. ^{1}H NMR (300 MHz, $CDCl_3$): δ 7.28 (s, 1H, ArC6-H), 6.86 (s, 1H, ArC3-H), 3.94 (m, 4H, -OCH_2-), 3.29 (s, 1H, ≡C-H), 1.98 (m, 2H, -CF_2CH_2-), 1.79 (m, 4H), 1.30 (m, 32H), 0.88 (t, 3H J = 6.6 Hz). ^{13}C NMR (75 MHz, $CDCl_3$): δ154.76 (Ar C-O), 151.67 (Ar C-O), 123.73 (Ar C6), 116.66 (Ar C3), 112.18 (Ar C2), 88.28 (Ar C-I), 81.73 (C≡C-H), 79.65 (C≡C-H), 70.06 (C-O), 69.79 (C-O), 64.41, 31.90, 30.60 (t, $^{3}J_{CF}$ = 22 Hz), 29.62, 29.56, 29.53, 29.35, 29.26, 29.24, 29.15, 29.10, 29.06, 26.01, 25.81, 25.32, 22.67, 20.19, 14.11 (2 CF_2 C's not visible above baseline due to splitting, 2 CH_2 C's have coincident chemical shifts with other signals). IR (ATIR): 3317 (≡C-H str.), 2924 (Ar C-H str.), 2854, 1468, 1371, 1192 (C-O str.), 1049, 1030, 1014, 862, 821, 715, 650, 617 cm^{-1}. HRMS *calc.* for $C_{32}H_{48}F_5IO_2$ = 686.26192, *obs.* = 686.26447 Δ = 3.7 ppm. Elemental Analysis: Theoretical: C, 55.98%; H, 7.05%; I, 18.48%; O, 4.66%; F, 13.83%; Found: C, 55.63%; H, 7.12%; I, 18.72%; O, 4.34%; F, 13.71%.

3.2.5. Synthesis of Regioregular Alkoxy/Semifluoroalkoxy PPEs

Polymerization procedures and spectroscopic data for regioregular PPEs in Figure 3.7. are given below.

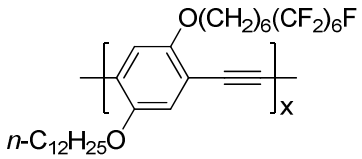

RgPPE(6,6/12). Monomer **III-9a** (551 mg, 663μmol), was added to a mixture of toluene (8 mL) and piperdine (3 mL) followed by the addition of $Pd(PPh_3)_4$ (38 mg, 33 μmol) and then CuI (6.0 mg, 32 μmol) The mixture was degassed by two freeze-pump-thaw cycles and backfilled with argon. The solution was heated at 70 °C for 3 d, and poured into MeOH (50 mL) to precipitate the polymer. The solid was filtered from the mixture, dissolved in $CHCl_3$ (20 mL) and precipitated twice into acetone (100 mL). The resulting orange solid (358 mg, 77%) was dried under vacuum. ^{1}H NMR (300 MHz, $CDCl_3$): δ 7.02 (s, 1H, Ar-H), 7.01 (s, 1H, Ar-H), 4.03-4.08 (m, 4H, -OCH_2-), 1.98-2.11 (m, 2H, -CF_2CH_2-), 1.80-1.89 (m, 4H), 1.26-1.68 (m, 24H), 0.87 (t, $^3J_{HH}$ = 6.9 Hz, 3H, -CH_3). ^{13}C NMR (75 MHz, $CDCl_3$): δ 154.06 (Ar C-O), 153.69 (Ar C-O), 118.01 (Ar C-H), 91.63 (C≡C), 70.11 (C-O), 31.91, 31.02 (t, $^3J_{CF}$ = 23.3 Hz), 29.65, 29.48, 29.33, 29.23, 28.98, 26.09, 25.81, 22.63, 20.27, 13.92 (6 CF_2 C's not visible above baseline due to splitting, 4 CH_2 C's have coincident chemical shifts with other signals). IR (ATIR): 2922 (Ar-H str.), 2854, 2368 (C≡C str.), 1516, 1471, 1431, 1419, 13232, 1215 (C-O str.), 1144, 1074, 1051, 856, 700, 654, 569, 534 cm^{-1}.

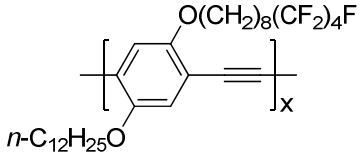

RgPPE(8,4/12). Polymerization of monomer **III-9b** (462 mg) was performed according to the procedure provide above for the preparation of **RgPPE(6,6/12)** to afford **RgPPE(8,4/12)** as an orange solid (367 mg, 95%). ^{1}H NMR (300 MHz, $CDCl_3$): δ 7.01 (bs, 2H, ArH) , 4.01-4.05 (m, 4H, -OCH_2-), 1.97-2.11 (m, 2H, -

CF_2CH_2-), 1.81-1.89 (m, 4H), 1.59-1.24 (m, 34H), 0.87 (t, $^3J_{HH}$ = 6.9 Hz, 3H, -CH_3). ^{13}C NMR (75 MHz, $CDCl_3$): δ 153.96 (Ar C-O), 117.96 (Ar C-H), 114.86 (Ar C-H), 91.64 (C≡C), 70.00 (C-O), 31.93, 30.93 (t, $^3J_{CF}$ = 22.6 Hz), 29.09, 29.49, 29.27, 29.20, 26.09, 25.99, 22.65, 20.19, 13.98 (4 CF_2 C's not visible above baseline due to splitting, 6 CH_2 C's have coincident chemical shifts with other signals). IR (ATIR): 2924 (Ar-H str.), 2854, 1516, 1510, 1431, 1419, 1390, 1217 (C-O str.), 1132, 1010, 879, 854, 837, 719, 606, 534, 507 cm^{-1}.

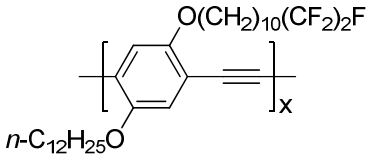

RgPPE(10,2/12). Polymerization of monomer **III-9c** (390 mg) was performed in a mixture of toluene (3 mL) and diisopropylamine (1 mL) according to the procedure provided above for the preparation of **RgPPE(6,6/12)** to afford **RgPPE(10,2/12)** as an orange solid (268 mg, 87%). ^{1}H NMR (300 MHz, $CDCl_3$): δ 6.99 (bs, 2H), 3.99-4.03 (m, 4H), 1.91-2.00 (m, 2H), 1.79-1.86 (m, 4H), 1.23-1.55 (m, 32H), 0.85 (t, 3H *J* = 7.2 Hz). ^{13}C NMR (75 MHz, $CDCl_3$): δ 154.07 (Ar C-O), 118.43(Ar C-H), 115.15 (Ar C-H), 91.90 (C≡C), 70.26 (C-O), 32.05, 30.97 (t, $^3J_{CF}$ = 22.0 Hz), 29.79, 29.65, 29.62, 29.53, 29.34, 29.26, 26.23, 22.77, 20.44, 14.08 (2 CF_2 C's not visible above baseline due to splitting, 6 CH_2 C's have coincident chemical shifts with other signals). IR (ATIR): 2922 (Ar-H str.), 2850, 2372 (C≡C str.), 1516, 1514, 1434, 1419, 1278, 1193 (C-O str.), 1043, 1045, 858, 812, 719, 534 cm^{-1}.

3.2.6. Synthesis of Regiorandom Alkoxy/Semifluoroalkoxy PPEs

Polymerization procedures and spectroscopic data for regiorandom PPEs in Figure 3.5 are given below.

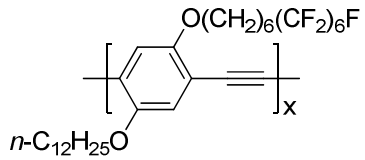

RnPPE(6,6/12). Monomers **III-4a** (463 mg, 497 μmol) and **III-6a** (362 mg, 497 μmol) were added to a mixture of toluene (8 mL) and diisopropylamine (2 mL), followed by the addition of $Pd(PPh_3)_4$ (29 mg, 25 μmol) and then CuI (5 mg, 26 μmol). The mixture was degassed by two freeze-pump-thaw cycles, the flask was backfilled with argon, and the solution was heated at 70 °C for 3 d. The mixture was poured into 50 mL of MeOH to precipitate the polymer. The solid was filtered from the mixture, dissolved in $CHCl_3$ and precipitated twice into acetone. The resulting orange solid (532 mg, 76%) was dried under vacuum. ^{1}H NMR (300 MHz, $CDCl_3$): δ 7.02 (bs, 2H, Ar-H), 4.01-4.11 (m, 4H, -OCH_2-), 1.95-2.11 (m, 2H, -CF_2CH_2-), 1.80-1.91 (m, 4H), 1.25-1.67 (m, 24H), 0.87 (t, $^3J_{HH}$ = 6.9 Hz, 3H, -CH_3), see Results and Discussion. ^{13}C NMR (75 MHz, $CDCl_3$): δ 154.18 (Ar C-O), 153.85 (Ar C-O), 118.21 (Ar C-H), 115.14 (Ar C-H), 91.83 (C≡C), 70.27 (C-O), 70.04 (C-O), 32.03, 31.14 (t, $^3J_{CF}$ = 23.3 Hz), 29.77, 29.60, 29.35, 29.09, 26.20, 25.92, 22.74, 20.37, 14.02 (6 CF_2 C's not visible above baseline due to splitting, 5 CH_2 C's have coincident chemical shifts with other signals). IR (ATIR): 2929 (Ar-H str.), 2858, 2368 (C≡C str.), 1515, 1431, 1214 (C-O str.), 1188, 1072, 858, 850, 696, 692, 571, 532 cm^{-1}.

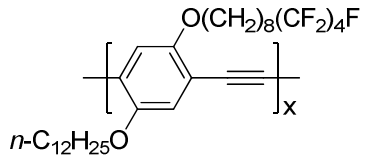

RnPPE(8,4/12). Polymerization of monomers **III-4b** (406 mg, 472 μmol) and **III-6b** (313 mg, 472 μmol) was performed according to the procedure provided above for the preparation of **RnPPE(6,6/12)** to afford **RgPPE(8,4/12)** as an orange solid (278 mg, 94%). ^{1}H NMR (300 MHz, $CDCl_3$): δ 7.01 (bs, 2H, ArH) , 4.01-4.07 (m, 4H, -OCH_2-), 1.96-2.11 (m, 2H, -CF_2CH_2-), 1.81-1.90 (m, 4H), 1.60-1.24 (m, 34H), 0.86 (t, $^{3}J_{HH}$ = 6.9 Hz, 3H, -CH_3). ^{13}C NMR (75 MHz, $CDCl_3$): δ 154.08 (Ar C-O), 118.42 (Ar C-H), 115.35 (Ar C-H), 91.61 (C≡C), 70.30 (C-O), 32.04, 31.11 (t, $^{3}J_{CF}$ = 22.4 Hz), 29.80, 29.57, 29.45, 29.25, 26.21, 26.12, 22.75, 20.34, 14.05 (4 CF_2 C's not visible above baseline due to splitting, 6 CH_2 C's have coincident chemical shifts with other signals). IR (ATIR): 2927 (Ar-H str.), 2856, 1516, 1471, 1431, 1390, 1381, 1217 (C-O str.), 1132, 1026, 879, 858, 714, 607, 534, 501 cm^{-1}.

3.3. Results and Discussion

3.3.1. Amphiphilicity of Alkoxy/Semifluoroalkoxy Benzene

The aim of substituting each phenylene ring of PPE with alkoxy and semifluoroalkyloxy groups was to impart amphiphilicity so that the polymer adopts a Janus type structure leading to self-organization. 1-Nonyloxy-4-(4,4,5,5,6,6,7,7,8,8,9,9,9-tridecafluorononyloxy)benzene serves as a small molecule model to illustrate the packing expected for the alkyloxy/semifluoro-alkoxy PPEs (e.g., **PPE(3,6/9)**). The unit cell of the single crystal X-ray structure of this compound, Figure 3.2., shows the clear segregation of the fluorinated and non-fluorinated side chains. The two types of side chains segregate so that they interact side-by-side and

end-on-end with like side chains. This leads to a bilayer lamellar structure with a repeat distance of 54 Å, approximately twice the length of the conformation of a single molecule in an extended all-trans conformation. The benzene rings form stacks in the direction perpendicular to the view shown in Figure 3.2.*

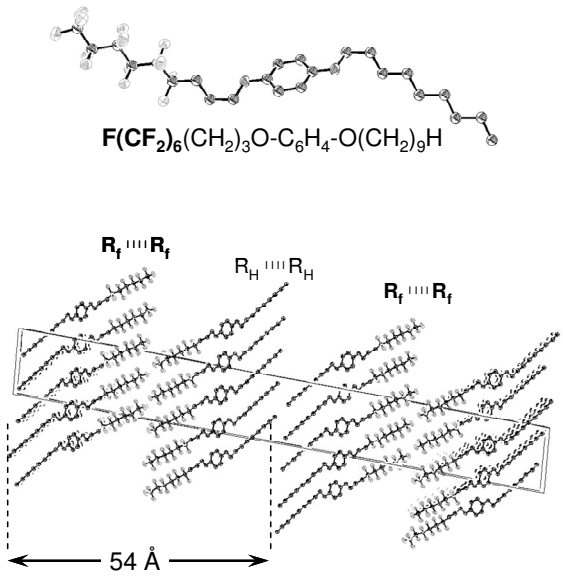

Figure 3.2. Amphiphilic 1-nonyloxy-4-(4,4,5,5,6,6,7,7,8,8,9,9,9-tridecafluoro-nonyloxy)benzene: Top, Molecular structure; bottom, unit cell. Hydrogen atoms have been omitted for clarity.

3.3.2. Synthesis of Regiorandom PPEs

We envisaged a synthetic approach to asymmetrically substituted PPEs whereby a semifluoroalkoxy chain would be incorporated into a monomer using a Mitsunobu etherification between suitably substituted phenols and commercially available semifluorinated alcohols. To explore the effect of variation of the fluoroalkyl chain length (*n*) while keeping the total length of the semifluoroalkoxy

* The synthesis of the model compound in Figure 3.2. and the data collection for this model study was carried out by Dr. Glen L. Brizius.

side chain constant (i.e., $m + n$), and therefore isosteric with the alkoxy substituent ($-O(CH_2)_pH$, $p = 12$ in most cases), we needed to develop a general route to semifluoroalcohols ($(HO-(CH_2)_m(CF_2)_nF$) where $m + n = 12$. They were successfully prepared by a radical addition reaction between a perfluoroalkyl iodide and ω-alken-1-ol, Figure 3.3. Initially, we explored the use of copper powder to facilitate the regiospecific addition of perfluoroalkyl iodides across the terminal alkene.[8] However, long reaction times were required to form only moderate yields (<60%), and the use of high temperatures required for this reaction presented a major limitation for the low boiling perfluoroethyl iodide (b.p.= 13ºC). Other common radical initiators such as $Pd(PPh_3)_4$,[10] dibenzoyl peroxide[11] and AIBN[12] also require high temperatures and often give low yields. We chose instead to use triethylborane as a catalyst, which has been shown to catalyze the addition reaction at low temperatures, but which has not gained widespread use for the preparation of semifluorinated chains.[9] This method proved to be highly effective, resulting in quantitative addition of the perfluoroalkyl iodides to the ω-alken-1-ols to give the iodo-substituted semifluoroalcohols, **III-1**, at temperatures as low as -20ºC within two hours. Conversion of **III-1** to the semifluoroalcohol **III-2** was achieved via reductive deiodination using sodium borohydride in dry DMSO.

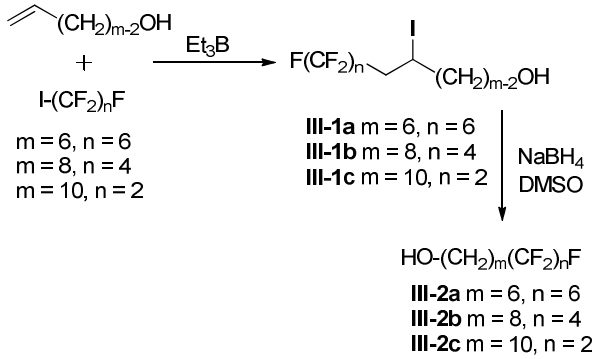

Figure 3.3. Synthesis of semifluoroalcohols.

A Mitsunobu reaction was used to install the semifluoroalkoxy chain onto 4-(dodecyloxy)phenol to afford the unsymmetrically substituted 1,4-dialkoxybenzenes **III-3**, Figure 3.4. Subsequent iodination of **III-3** yields the diiodinated monomers **III-4**. Palladium catalyzed coupling of TMS acetylene to **III-4**, followed by desilylation in the presence of tetra-*n*-butylammonium fluoride gave the diethynyl monomers **III-6**.

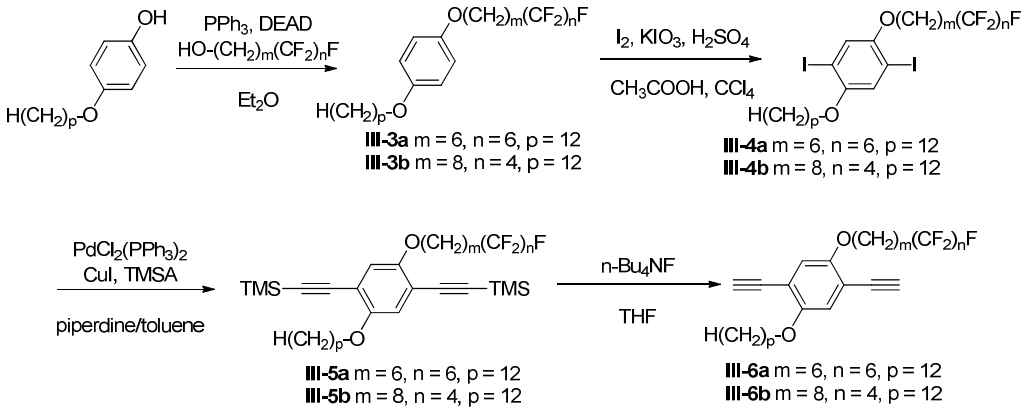

Figure 3.4. Synthesis of asymmetrically substituted diiodobenzenes **III-4** and diethynylbenzenes **III-6**: Monomers for the preparation of regiorandom PPEs.

The palladium catalyzed Sonogashira cross-coupling condensation polymerization of diiodo (AA) and diethynyl (BB) monomers **III-4** and **III-6** produced the amphiphilic, regiorandom PPEs, Figure 3.5.

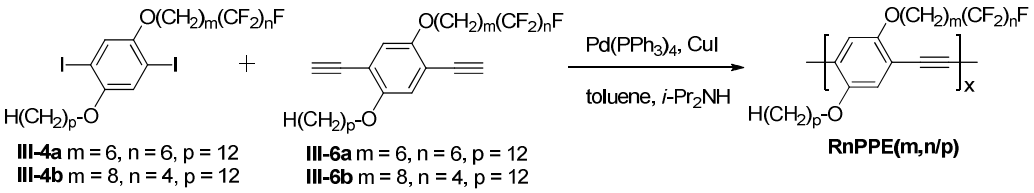

Figure 3.5. Preparation of regiorandom amphiphilic semifluoroalkoxy/alkoxy-substituted polymers, **RnPPE(*m,n*/p)**.

3.3.3. Synthesis of Regioregular PPEs

The synthesis of regioregular PPEs required a single monomer, **III-9**, bearing both an iodo and an ethynyl group (i.e., an AB monomer), Figure 3.6. The substitution pattern of the monomers was established by the regioselective iodination of 4-alkoxyphenols using previously reported methods to give 4-alkoxy-3-iodophenols.[13] A Mitsunobu reaction was then used to install the semifluoroalkyl side chains to provide **III-7a-c**. To generate the AB type monomer **III-9** it was necessary to selectively place an ethynyl group para to the iodine of **III-7**. A formylation reaction produced benzaldehyde **III-8**, which was then transformed to alkyne **III-9** using the Bestman-Ohiro homologation (treatment with $(MeO)_2P(=O)C(=N_2)COCH_3$). While the formylation reaction was not completely regiospecific,[13] the desired 1,2,4,5-tetrasubstituted isomer was easily separable from the byproducts by column chromatography followed by recrystallization.

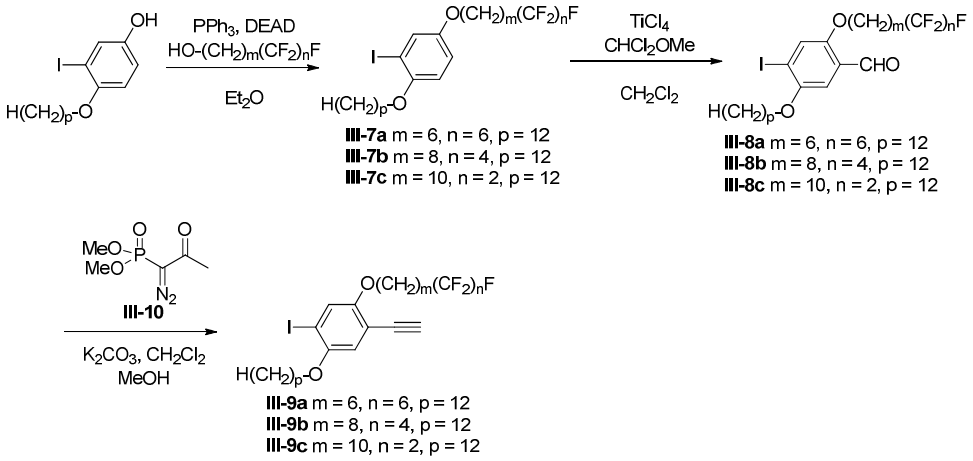

Figure 3.6. Synthesis of asymmetrically substituted A-B type alkxoy/semifluoro-alkoxy monomers.

The AB type monomer **III-9** was polymerized using the palladium catalyzed condensation polymerization to produce regioregular PPEs containing exclusively head-to-tail linkages, Figure 3.7.

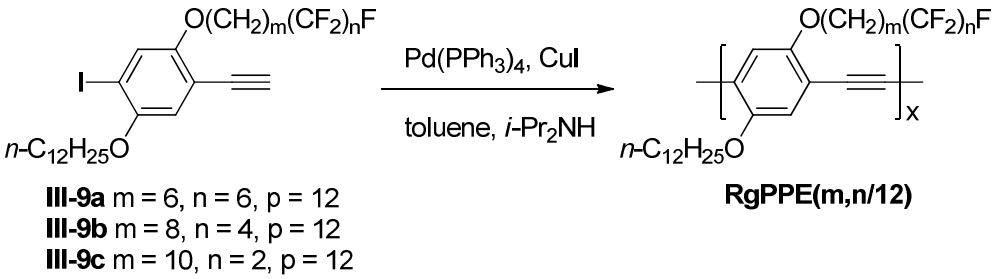

Figure 3.7. Preparation of regioregular amphiphilic semifluoroalkoxy/alkoxy-substituted polymers, **RnPPE(*m,n*/p)**.

Both regioregular and regiorandom PPEs were isolated and purified by precipitation from the reaction mixture by addition to a large volume of MeOH, followed by dissolution in chloroform and reprecipitation by addition to acetone, to give bright orange solids. Efforts to prepare PPEs from semifluoroalcohols with short

carbon spacers (m = 3) afforded completely insoluble materials, thus were not characterized further. The remaining polymers were wholly soluble in chloroform and THF, with the exception of **RgPPE(6,6/12)** of which only the chloroform soluble portion was used for characterization. An isosteric symmetrically substituted dialkoxy-PPE, poly(2,4-dodecyloxy-1,4-phenylene ethynylene), **PPE(12/12)**, was synthesized by polymerization of the di(dodecyloxy) substituted diiodo- and diethynylbenzene monomers.[13,14] The polymers were characterized by ^{1}H and ^{13}C NMR, FT-IR, and UV-vis absorption spectroscopies, differential scanning calorimetry (DSC), gel permeation chromatography (GPC), and X-ray diffraction (XRD).

3.3.4. Structural Characterization

The molecular weights of the PPEs were determined both by end group analysis and GPC, Table 3.1. The number average molecular weights (M_n) was determined by ^{1}H NMR spectroscopy by virtue of the distinct chemical shifts of the protons ortho to the iodo substituent (δ7.3) and ethynylene group (δ6.9) of the two end groups. PPEs synthesized from AB type monomers bear one end group of each type, as confirmed by the equal integrals of the two signals. Polymers prepared from coupling AA and BB type monomers have different amounts of these end groups, due to slight stoichiometric imbalances of the monomers in the polymerization reaction mixture. The degrees of polymerization (*DP*) range between 21-33 repeat units with the exception of **RgPPE(6,6/12)** which had a *DP* of only 12 as a result of poor solubility of the polymer in chloroform. However, the molecular weights of all of the PPEs in this study are higher than the effective conjugation length of PPEs (approximately 11 repeat units).[15] Regioregular **RgPPE(6,6/12)** and **RgPPE(8,4/12)**

are much less soluble then their regiorandom counterparts, likely a result of higher crystallinity arising from their more regular structures.

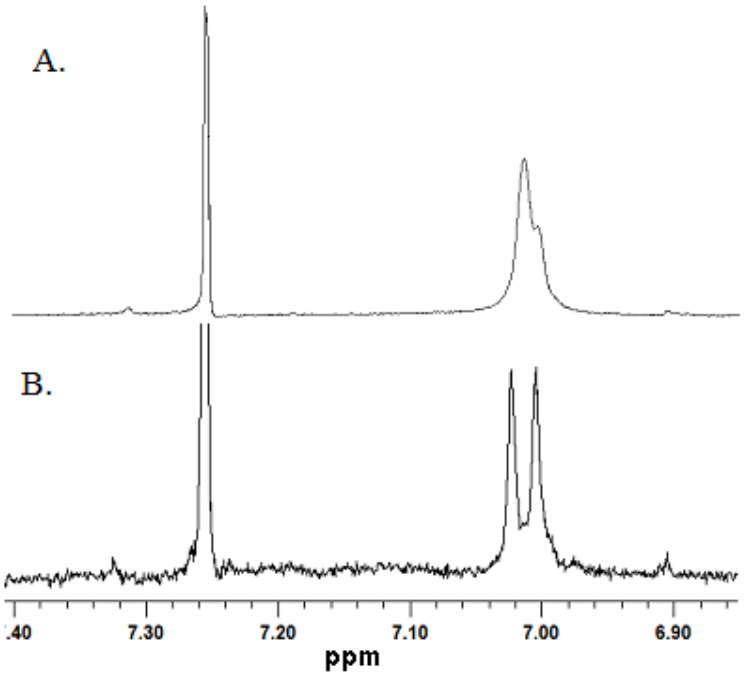

Figure 3.8. ^{1}H NMR spectra of **PPE(6,6/12)**: A, regiorandom (**Rn**)**;** B, regioregular (**Rg**).

Differences in the appearance of the aromatic region of the ^{1}H NMR spectra for **RgPPE(6,6/12)** and **RnPPE(6,6/12)** illustrate the regioregularity on the polymer structure. Three types of linkages can be formed when coupling AA and BB type monomers: head-to-tail (*ht*), head-to-head (*hh*) and tail-to-tail (*tt*), Figure 3.8.

The aromatic region in the ^{1}H NMR spectrum of **RgPPE(6,6/12)** has two sharp singlets at δ7.0 and δ7.1 ppm, corresponding to the protons ortho to the alkyl and semifluoroalkyl chain, respectively, Figure 3.8 B. However, only one broad signal is observed for the regiorandom analog (Figure 3.8 A) as a result of the overlap of

peaks occurring for protons in different environments on the aromatic backbone arising from *hh*, *ht* and *tt* diads.

3.3.5. Thermal Transitions

Thermal transition temperature and enthalpies (ΔH) of the PPEs in this study were determined by differential scanning calorimetry (DSC), Table 3.1. A single endothermic peak is observed for each of the polymers upon heating, which is similar to the melting transition observed for symmetrically substituted dialkoxy-PPEs.[16]

Table 3.1. Physical Properties of **RgPPE(m,n/p)**, **RnPPE(m,n/p)** and **PPE(12/12)** [a]

Polymer	M_n [b,c] (kg.mol^{-1})	M_n [b,d] (kg.mol^{-1})	M_w [d,e] (kg.mol^{-1})	PDI [d,f]	*DP* [c,g]	T_m [h] (^{o}C)	ΔH (kJ.mol^{-1}) [i]
RgPPE(6,6/12)	8.4	9.0 [j]	18	2.02	12	235	5.7
RnPPE(6,6/12)	15	– [k]	–	–	21	215	3.6
RgPPE(8,4/12)	21	8.6 [l]	17	2.03	33	198 [m]	3.2
RnPPE(8,4/12)	19	18	38	2.13	30	198 [m]	2.9
RgPPE(10,2/12)	13	36	88	2.41	24	194	2.1
PPE(12/12)	14	49	134	2.73	29	188	4.5

[a] **RgPPE(3,3/12)** and **RgPPE(3,6/9)** were insoluble in common organic solvents and not characterized by these methods. [b] Number average molecular weight (M_n). [c] Determined by end group analysis. [d] Determined by gel permeation using polystyrene standards. [e] Weight average molecular weight (M_w). [f] Polydispersity index (PDI). [g] Degree of polymerization (phenyls as repeating units). [h] Melting temperatures (T_m) determined by DSC at a scan rate of 10 ^{o}C.min^{-1}. [i] kJ per mole of repeat unit. [j] Chloroform soluble portion only, fractionation occurred. [k] **RnPPE(6,6/12)** forms a gel in THF so its molecular weight cannot be determined by this method. [l] Not all of the polymer sample was soluble in THF, fractionation occurred. [m] **RgPPE(8,4/12)** and **RnPPE(8,4/12)** show a very broad thermal transition in the DSC measurement.

The transition temperatures all occur at higher temperatures than for the 2,4-(didodecyloxy)-substituted PPE, **PPE(12/12)**, (188 ºC) and depend on the relative length of the fluorinated segment in the semifluoroalkoxy side chain. The temperature of the transition is highest for polymers with longer fluorinated segments (i.e., larger values of *n*). The thermal transition temperatures also depend on the regioregularity of the material. The regioregular **RgPPE(6,6/12)** has a significantly higher thermal transition than the regiorandom analog, **RnPPE(6,6/12)** (235 ºC versus 215 ºC) in spite of having a lower molecular weight. The regioregular and regiorandom analogs of **PPE(8,4/12)** homolog have identical melting points (198 ºC), although the transitions are very broad. The enthalpies of the transition (ΔH) provide additional insight into the effect of regioregularity. The enthalpies for the regioregular (**Rg**) analogs of both the **(6,6/12)** and **(8,4/12)** homologs are higher than for the corresponding regiorandom (**Rn**) analogs, demonstrating an increase in thermal stability of the crystalline phase of the regioregular homologs.

No thermal transitions are observed in the cooling scan in the differential scanning calorogram; the lack of an exothermic peak indicates that the material does not crystallize on the time scale of the cooling scan. Reheating the sample reveals the absence of cold crystallization and no melting transition. Annealing the samples just below the T_m, cooling and reheating does not reveal an endothermic transition, nor does letting the samples sit at room temperature for several weeks. The lack of thermal transitions after first melting is not due to thermal degradation, as supported by the ability to redissolve the PPE samples in chloroform, and the unchanged IR and ^{1}H NMR spectra of the samples.

3.3.6. Electronic Structure

UV-vis absorption spectra were obtained for regioregular and regiorandom analogs of the amphiphilic alkoxy/semifluoroalkoxy-PPEs both in solution and as thin films. The absorption spectra for the PPEs in solution all show a broad absorption at around 450 nm, which is also characteristic of the symmetrically substituted dialkoxy-PPEs, Figure 3.9. The similarity of these spectra can be attributed to the low rotational barriers of PPEs in solution (estimated to be <1 kcal/mol),[17] and lack of aggregation of the polymer chains in $CHCl_3$ solution.

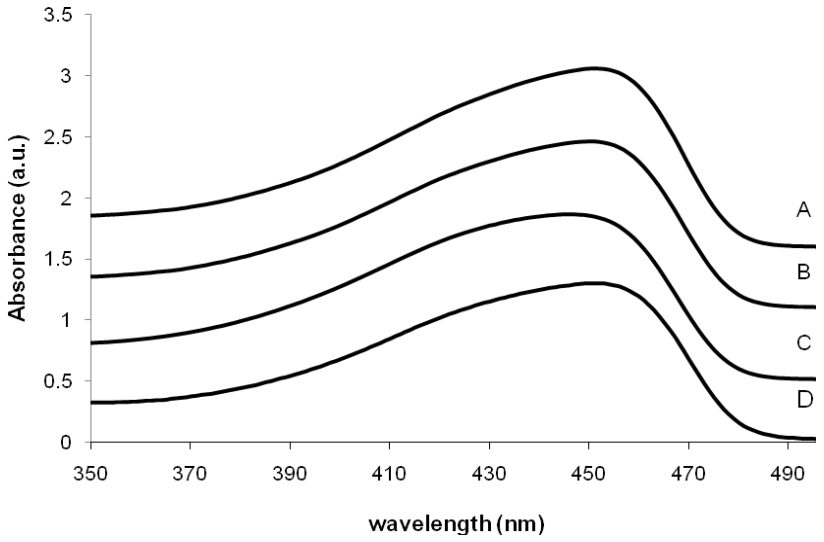

Figure 3.9. Solution UV-vis absorption in $CHCl_3$: A, **RnPPE(8,4/12)**; B, **RgPPE(8,4/12)**; C. **RgPPE(10,2/12);** and D, **PPE(12/12)**.

Larger differences were observed between the spectra of thin films of the materials, Figure 3.10. Films were prepared by drop-casting a chloroform solution of the polymers (approximately 0.1 $mg.mL^{-1}$) onto glass slides, allowing the solvent to evaporate. The films were then annealed at 110 °C under vacuum for 24 h. The symmetrically substituted **PPE(12/12)** (solid line in Figure 10A) has an absorption

with contributions at 460, 480 and 500 nm. Peaks at these wavelengths also contribute to the absorption of the amphiphilic alkoxy/semifluoroalkoxy-PPEs. Whereas for **PPE(12/12)** the peak at the lowest wavelength is the strongest, it is the peak at highest wavelength that is strongest for the regioregular homologs of **PPE(6,6/12)**, **PPE(8,4/12)**, and **PPE(10,2/12)**. The peak at 500 nm is absent in the spectrum of the regiorandom analog **RnPPE(8,4/12)**, Figure 3.10 A, and relatively weak in the spectrum of **RnPPE(6,6/12)**.

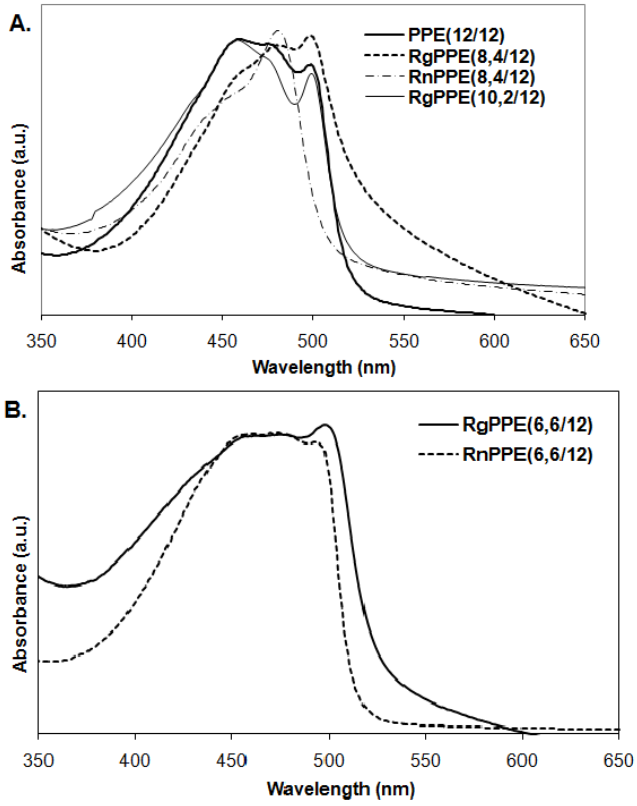

Figure 3.10. UV-vis spectra of annealed thin films of PPEs: A, symmetrically substituted **PPE(12/12)**, regioregular and regiorandom analogs of **PPE(8,4/12)** and **RnPPE(10,2/12)**; and B, regioregular and regiorandom analogs of **PPE(6,6/12)**.

We attribute the peak at higher wavelength to a portion of the materials that has a greater conjugation length arising from a more ordered, planar structure. The symmetrically substituted alkoxy-PPEs (e.g., **PPE(12/12)**) form a planar, highly conjugated structure by virtue of side chain crystallization of the regularly placed linear alkoxy chains (Figure 3.11 A). The observation that the regioregular materials give a stronger absorption at 500 nm suggests that these films have a higher portion of the most highly conjugated material. For the regiorandom analogs the absence of a

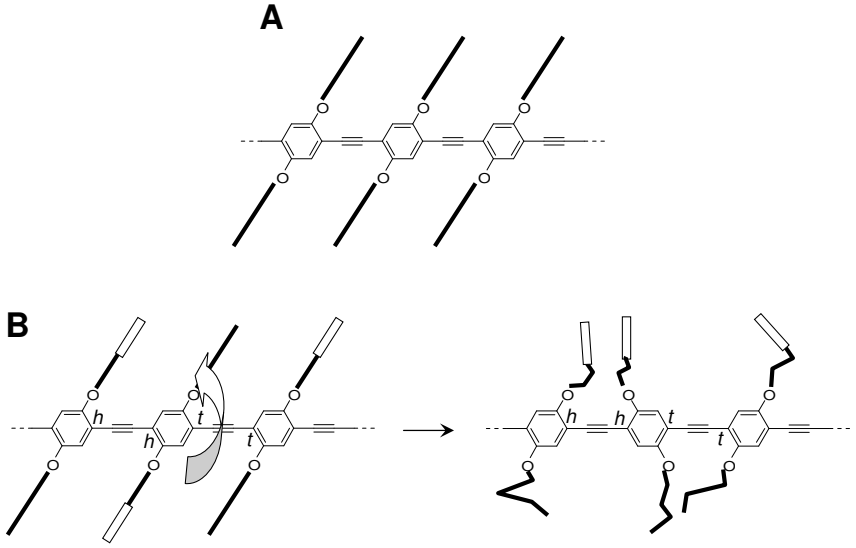

Figure 3.11. While regiorandom **RnPPE(*m*,*n*/*p*)** is isosteric with **PPE(*p*/*p*)**, amphiphilicity disrupts molecular packing. A, Side chain crystallization of symmetrically-substituted dialkoxy-PPE, e.g., **PPE(12/12)**. B, In regiorandom amphiphilic analog, crystalline packing of the side chains is impeded by packing of dissimilar chains (left); rotation about the backbone segregates the two types of side chains, but leads to steric hindrance, thereby disrupting molecular packing and inducing disorder.

peak at 500 nm arises from the irregular placement of alkoxy and semifluoroalkoxy This irregularity hinders side chain crystallization (Figure 3.11 B, left). While rotation of individual repeat units around the polymeric main chain allows the dissimilar side chains to segregate (Figure 3.11 B, right), this would result in steric hindrance between repeat units, thereby leading to a disordered structure and a hindrance of planarization.

The UV-vis absorption spectra of the PPEs are affected by annealing at different temperatures, Figure 3.12. Annealing **RgPPE(8,4/12)** at 110 ºC for 12 h (i.e., below the melting temperature of 198 ºC) and then cooling to room temperature results an increase in the intensity of the peak at 500 nm relative to the other peaks, indicating the formation of a more conjugated structure giving rise to absorptions at lower energy. Upon holding the sample just above the melting point at 200 ºC and then cooling gives rise to a broad blue-shifted absorption with λ_{max} = 433 nm.

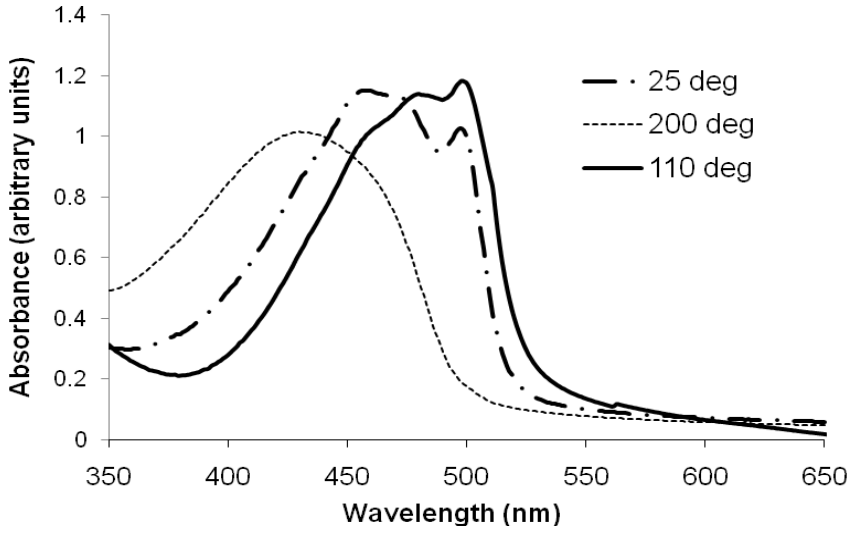

Figure 3.12. UV-vis absorption of thin films of **RgPPE(8,4/12)** at room temperature, before annealing (25 ºC) and after heating at110 ºC and 200 ºC for 2 h (m.p. = 198 ºC).

Dissolving and recasting the film gives spectra identical to those of the original unannealed absorption samples. Thus, annealing a semicrystalline as-cast film results in an increase in the 500 nm absorption due to formation of greater amounts of the crystalline phase. However, cooling from the melt results in an amorphous material that gives a blue shifted absorption corresponding to a material with less conjugation. This agrees with the observation from the thermal analysis experiment that the materials cooled from the melt do not crystallize, even after extensive annealing.

3.3.7. Molecular Packing

The supramolecular structures of the amphiphilic semifluoroalkoxy/alkoxy-substituted PPEs in this study were characterized using wide-angle X-ray diffraction (WAXD). A film of **PPE(12/12)** was prepared by drop-casting a xylene solution onto a silicon substrate. However, attempts to process the amphiphilic PPEs using this method provided cracked and irregular films that were not suitable for x-ray diffraction. In order to overcome this problem, the silicon substrates were first modified with a self assembled monolayer by treatment with either dodecyldimethylchlorosilane or (heptadecafluorodecyl)dimethylchlorosilane (see Appendix C). Suitable films of **RgPPE(6,6/12)**, **RnPPE(6,6/12)** and **RgPPE(8,4/12)** could only be formed on slides modified with a fluoroalkyl monolayer, whereas **RgPPE(10,2/12)** and **RnPPE(8,4/12)** formed the best films on the alkylated surfaces. Thus, the interaction between the polymer and substrate has a strong influence on film quality, with polymers bearing fluorine-rich side chains forming better films on fluorous surfaces, and those with low content of fluorine form better films on the oleophilic alkylsilane monolayer.

X-ray diffraction experiments were performed on both pristine and annealed 100 μm-thick films. The WAXD patterns of the annealed amphiphilic PPEs and the symmetrically substituted **PPE(12/12)** are shown in Figure 3.13. A-F. In each case, annealing the drop-cast films under vacuum at 110 °C for 24 h the peaks in the diffraction pattern become sharper and more resolved, but do not change in position, indicating an increase in crystallinity.

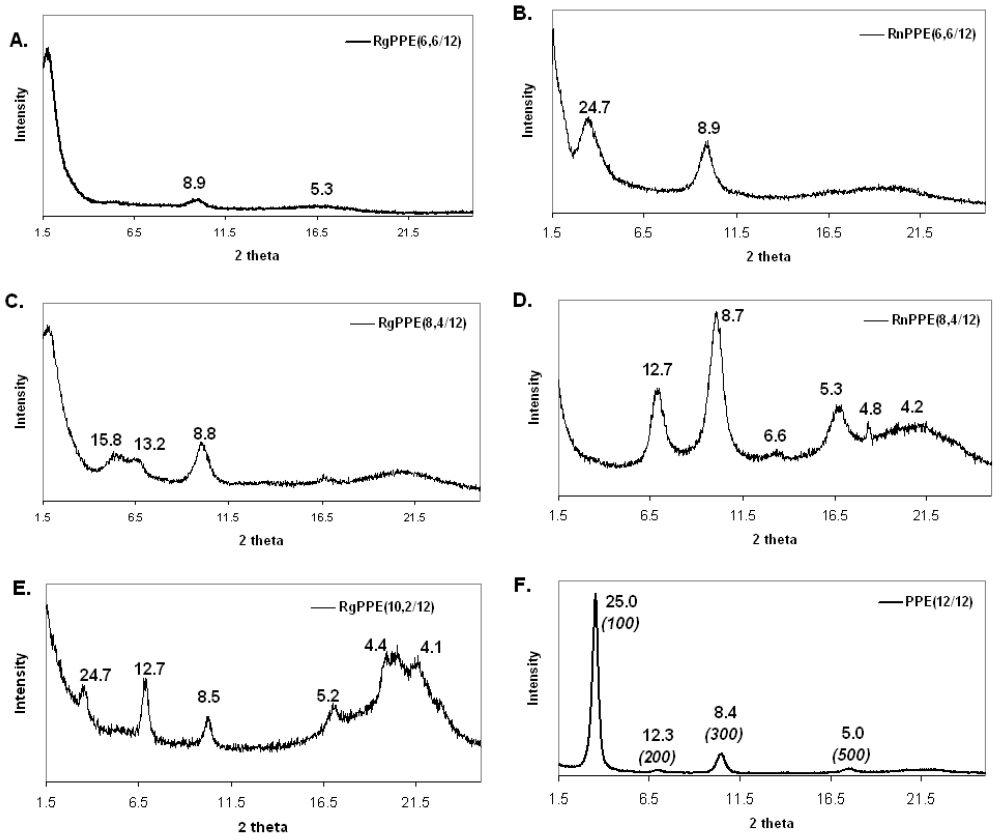

Figure 3.13. Wide angle X-ray diffraction patterns for annealed films: A, **RgPPE(6,6/12)**; B, **RnPPE(6,6/12)**; C, **RgPPE(8,4/12)**, D, **RnPPE(8,4/12)**; E, **RgPPE(10,2/12)**; and F, **PPE(12/12)**. Peaks are labeled with *d* spacings in Ångstroms.

Symmetrically substituted **PPE(12/12)** shows a sharp first order diffraction peak at 25 Å, and less intense higher order reflections at 12.3, 8.4 and 5.0 Å, corresponding to the (100), (200), (300) and (500) reflections arising from a lamellar crystalline morphology.[18] There is a monotonic decrease in the size of the reflections with odd indices (i.e., (100), (300), (500)), and those with even indices (i.e., (200), and (400), which is not observed) are significantly weaker. Introducing amphiphilicity has a significant impact on the molecular packing of the PPEs. However, in contrast to the Janus type polythiophenes,[6] in which imparting amphiphilicity gave rise to highly ordered and oriented crystalline phases, this change in molecular structure disrupts the lamellar packing of the PPE backbone. The peaks in the diffractograms of all of the amphiphilic PPEs are broader than those of the isosteric **PPE(12/12).** For the most part, the peaks which appear in the diffractograms of the amphiphilic PPEs correspond to peaks given by **PPE(12/12)**. For example, all of the diffractograms display a reflection at between 8.5-8.9 Å. However, none of the fluoroalkyl-substituted polymers show all of the reflections present in the symmetrical dialkoxy material. In addition, the relative intensities of peaks in the diffractogram of the amphiphilic are quite distinct from those in the symmetrical analog. For example, in the diffractorgram of **RgPPE(10,2/12)** the peak at d = 12.7 Å is significantly stronger than those at d = 24.7 and 8.5Å, the reverse of the situation for **PPE(12/12)**. Surprisingly, given the important role of regioregularity of side chain substitution of PATs and PPEs, the regiorandom materals (Figure 3.13. B and D) give stronger diffraction peaks than the corresponding regioregular materials (Figure 3.13. A and C). The diffraction peak at d = 12.3 Å is very weak for **PPE(12/12)**, but the diffractograms of **RgPPE(10,2/12)** and **RnPPE(8,4/12)** have significant peaks in this region. The strong reflection at 25 Å in the diffractogram of **PPE(12/12)** is missing,

or weak, for the other materials. The diffractograms of the amphiphilic PPEs which have been cooled to room temperature from the melt indicate a complete loss of crystallinity, consistent with DSC results.

The disordered nature of the amphiphilic PPEs is in contrast to similar facially-amphiphilic Janus-type alkyl/semifluoroalky-substituted polybithiophenes.[6] The spacing between side chains on the PPE backbone leads to interdigitation of side chains on adjacent polymer chains, Figure 3.14. A. However, similar interpenetration of the semifluoroalkyl chains would result in alkyl-fluoroalkyl contacts (Figure 3.14..B, left). Segregation of the alkyl and fluoroalkyl segments would require that the side chains do not fully interdigitate. Thus, we postulate that a disordered structure is formed to accommodate the segregation of the side chains (Figure 3.14. B, right).

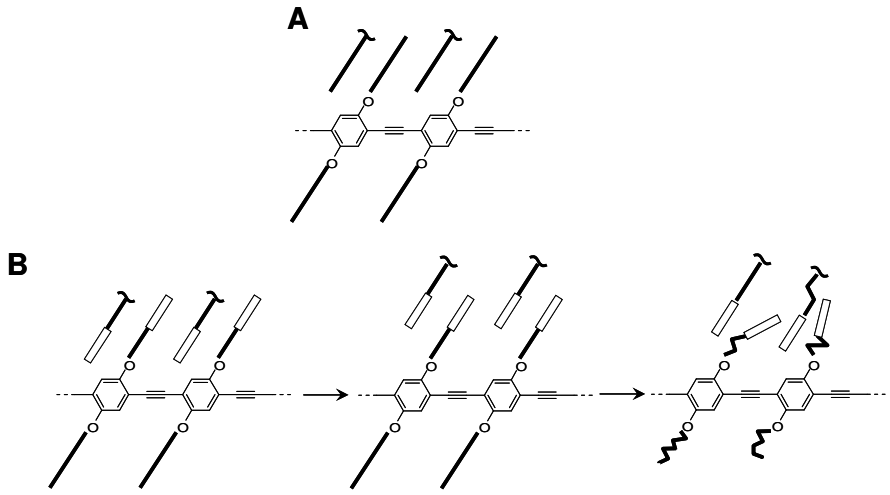

Figure 3.14. Incorporation of amphiphilic side chains imparts disorder to the structure of PPEs. A, The side chains of symmetrically-substituted dialkoxyl-PPEs, e.g., **PPE(12/12)** interdigitate to form a lamellar structure. B, Aggregation of fluoroalkyl segments limited extent of interpenetration of side chains, requiring that the alkylene spaces, $(CH_2)_m$, undergo conformational disordering to fill space efficiently, thereby introducing molecular disorder.

The similarity of the *d*-spacings for the peaks of all members of the series of alkoxy/semifluroalkoxy-substituted polymers, **PPE(*m*,*n*/12)**, to those in the diffractograms of the symmetrical isosteric analog **PPE(12/12)** suggests that the amphiphilic materials form crystalline phases with a similar lamella packing. However, the relative intensities of the peaks in the diffractograms are quite distinct. The relative intensity of the peaks arises from the electron density profile within the unit cell (the electron density profile is the Fourier transform of the diffractogram.) The form of the electron density profile of a polyphilic polymers in a bilayer architecture is unusual compared to conjugated materials (i.e., semirigid polymer chains bearing a single type of alkyl side chain, e.g., **PPE(12/12)**,) and resembles that of a lipid bilayer.[19-21] The relative intensities of the peaks in the diffractogram relate to the relative size and electron density of the separate microenvironments formed by segregation of the alkylene spacers (*m*), semifluoroalkyl chains (*n*), alkyl chains (*p*), and 1,4-phenylene units (Figure 3.15.).

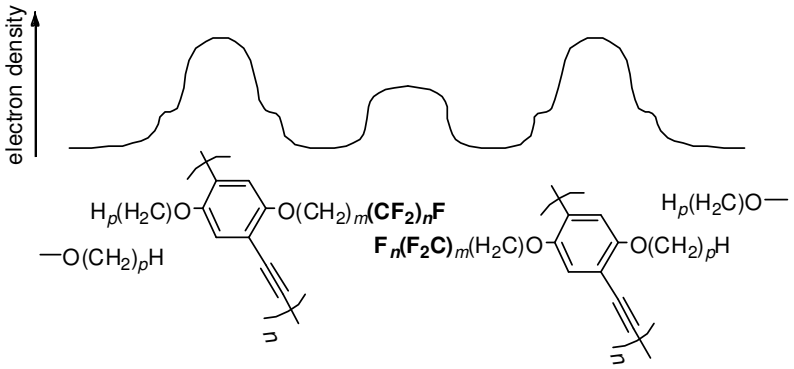

Figure 3.15. Electron desity profiles of regioregular alkoxy/semifluoroalkoxy PPEs.

3.4. Conclusions

A synthetic route to regioregular and regiorandom amphiphilic Janus-type PPEs bearing a semifluoroalkoxy and an alkoxy side chain on each phenyl ring has been described. Characterization of these amphiphilic PPEs reveals that thermal transitions in these polymers are affected both by the length of the fluorocarbon segment as well as regioregularity. In comparison to symmetrically substituted dialkoxy PPEs, the amphiphilic PPEs have a red shifted optical absorption and no longer display a simple lamellar morphology, as indicated by the X-ray diffraction patterns. Annealing the polymers above the melting temperature leads to a blue-shifted optical absorption and loss of all crystallinity. Thus, the alkoxy/semifluoroalkoyl-substitution pattern of the amphiphilic PPEs impedes crystallization. This is in contrast to the highly ordered and oriented solid phases formed by alkyl/semifluoroalkyl substituted poly(bithiophene)s. The difference in the behavior of these polymers may arise from the extent to which the side chains of dialkoxy-PPEs interdigitate. Segregation of the dissimilar side chains of the amphiphilic PPEs impedes this interdigitation and thereby disrupts crystallization.

3.5. References

1. Fazio, D.; Mongin, C.; Donnio, B.; Galerne, Y.; Guillon, D.; Bruce, D. W. *J. Mater. Chem.* **2001**, *11*, 2852-2863.
2. Breitenkamp R. B.; Tew, G. N. *Macromolecules* **2004**, *37*, 1163-1165.
3. Kim, J.; Swager, T. M. *Nature* **2001**, *411*, 1030-1034.
4. Kim, J.; Levitsky, I. A.; McQuade, D. T.; Swager, T. M. *J. Am. Chem. Soc.* **2002**, *124*, 7710-7718.
5. Clark, A. P-Z.; Cadby, A. J.; Shen, C. K-F.; Rubin, Y.; Tolbert, S. H. *J. Phys. Chem. B.* **2006**, *110*, 22088-22096.

6. Wang, B.; Watt, S.; Hong, M.; Domercq, B.; Sun, R.; Kippelen, B.; Collard, D. M. M*acromolecules* **2008**, *41*, 5156-5165.

7. Ghosh, A. K.; Bischoff, A.; Cappiello, J. *Eur. J. Org. Chem.* **2003**, 821-832.

8. Kotora, M.; Hácek, M.; Ameduri, B.; Boutevin, B. *J. Fluor. Chem.* **1994**, *68*, 49-56.

9. (a) Ren, Y.; Lodge, T. P.; Hillmyer, M. A. *Macromolecules* **2001**, *34*, 4780-4787. (b) Takeyama, Y.; Ichinose, Y.; Oshima, K.; Utimoto, K. *Tetrahedron Lett.* **1989**, *30*, 3159-3162. (c) Delon, L.; Laurent, P.; Blancou, H. *J. Fluor. Chem.* **2005**, *126*, 1487-1492.

10. Bonafoux, D.; Hua, Z.; Wang, B.; Ojima, I. *J. Fluor. Chem.* **2001**, *112*, 101-108.

11. Brace, N. *J. Fluor. Chem.* **1982**, *20*, 313-327.

12. Hong, X.; Tyson, J. C.; Middlecof, J. S.; Collard, D. M. *Macromolecules* **1999**, *32*, 4232-4239.

13. Nambiar, R.; Woody, K. B.; Ochocki, J. D.; Brizius, G. L.; Collard, D. M., *Macromolecules* **2009**, *42*, 43-51.

14. Moroni, M.; Le Moigne, J.; Luzzati, S. *Macromolecules* **1994**, *27*, 562-571.

15. Xue, C.; Luo, F.-T. *Tetrahedron* **2004**, *60*, 6285-6294.

16. Ofer, D.; Swager, T. M.; Wrighton, M. S. *Chem. Mater.* **1995**, *7*, 418-425.

17. Bunz, U. H. F. *Chem. Rev.* **2000**, *100*, 1605-1644.

18. Bunz, U. H. F.; Enkelmann, V.; Kloppenburg, L.; Jones, D.; Shimizu, K. D.; Claridge, J. B.; Loye, H.-C. Z.; Lieser, G. *Chem. Mater.* **1999**, *11*, 1416-1424.

19. McIntosh, T. J.; Simon, S. A. *Biochemistry* **1993***, 32*, 8374-8384.

20. Ionov, R.; Angelova, A. *Thin Solid Films* **1996**, *284-285*, 809-812.

21. Takahashi, H.; Ohta, N.; Hatta, I. *Chem. Phys. Lipids* **2001**, *112*, 93-97.

CHAPTER 4: SYNTHESIS AND CHARACTERIZATION OF FULLY CONJUGATED POLYTHIOPHENE-POLYQUINOXALINE-POLYTHIOPHENE D-A-D TRIBLOCK COPOLYMERS

4.1. Introduction

In bulk-heterojuction (B-H) organic solar cells donor (D) and acceptor (A) materials are blended to provide the photoactive layer. Absorption of photons leads to the formation of excitons, and diffusion of these excitons to the D-A interface leads to formation of charge carriers.[1] For example, prototype photovoltaic cells incorporating a regioregular poly(3-alkylthiophene) as the donor and [6,6]-phenyl-C_{61}-butyric acid methyl ester (PCBM) as the acceptor display relatively high efficiencies.[2] Initiatives to improve the performance of organic solar cells largely focus on the design and synthesis of new low band gap conjugated polymers[3] and changing the morphology of the blends.[4] Thoroughly blending of the donor and acceptor materials improves device performance by reducing the size of the phase-separated domains such that they are on the order of the exciton diffusion length (10 – 20 nm).[5]

Block copolymers phase separate on the nanoscale and the size of the phases formed by the two blocks is directly related to the length of each block. Rod-coil block copolymers containing a semi-rigid conjugated segment and a flexible segment have been extensively studied and provide abundant opportunities to prepare materials with unique morphologies[6-10] However, these materials contain only one electroactive segment and the flexible segment serves as an insulator. However, there are few reports of donor-acceptor conjugated block copolymers[11] This can largely be attributed to the synthetic challenges in preparing such materials and the paucity of electron accepting polymers, which generally contain heteroaromatic units in the

conjugated backbone (e.g., pyridine,[12] quinoxaline,[13] quinoline,[14] or thienopyrazine[15]) or are substituted with electron withdrawing substituents (e.g., fluorine[16] or cyano substituents[17]). Such block copolymers could provide opportunities to control the scale and morphology of phases in B-H solar cells.

The development of new synthetic methodologies is required to provide access to donor-acceptor block polymers that make use of the phase separation of the two blocks to impart new or enhanced electronic properties. One approach to such fully conjugated block copolymers is to couple the termini of two separate prepolymers that bear complementary functionality.[11,18,19] More recently, with the advent of catalyst-transfer condensation polymerizations (CTCP) of haloarylmagnesium halides,[20] similar block copolymers architectures have become accessible by chain extension of the active end of quasi-living polymers with a second monomer.[21-26] In this Chapter, we describe the use of CTCP to prepare a telechelic poly(3-octylthiophene) (P3OT) bearing a single bromine-substituted end group that is of potential use in the preparation of well-defined block copolymers We demonstrate the utility of this new well-defined monofunctional polythiophene by coupling it under Suzuki coupling conditions to a poly(quinoxaline) (PQ) that has two boronate ester end groups. This provides a D-A-D triblock copolymer, Figure 4.1. Poly(3-alkylthiophene)s are commonly employed as a donor material in B-H solar cells.[27] For this study we chose poly(5,8-quinoxaline) as an electron-poor acceptor block because it is susceptible to n-doping by reduction (E_{red} = –1.98 V versus Ag/Ag^{+})[28] and the polymer is rendered soluble by decoration of the backbone with flexible side chains.[13] The structural and optical properties of the polymers are described.

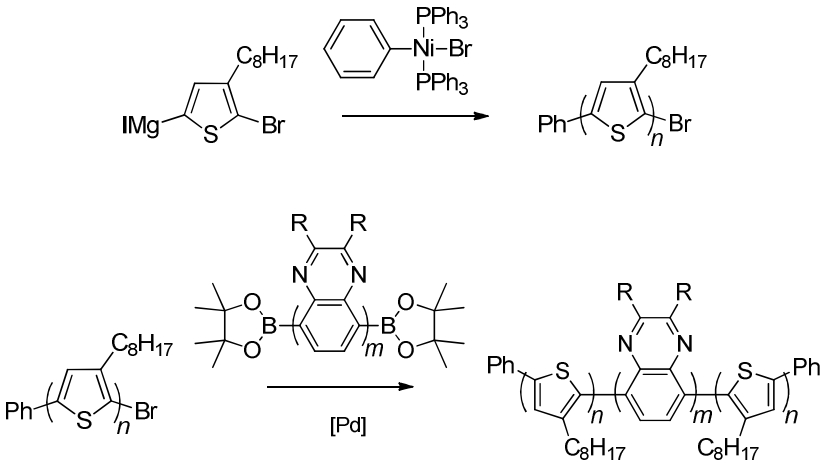

Figure 4.1. Preparation of a telechelic poly(3-octylthiophene) with a single α-bromothienyl end group, and coupling to a poly(5,8-quinoxaline) (PQ) bearing two boronate ester end groups to afford a triblock copolymer.

4.2. Experimental

4.2.1. General Synthetic Methods

All starting materials were purchased from commercial sources and used without further purification unless otherwise stated. THF and Et_2O were dried over sodium benzophenone ketyl prior to distillation under argon. Column chromatography was performed on flash grade silica (32-60 Å, Sorbent Technologies, Atlanta, GA). NMR analysis was performed on a Bruker DSX 300 instrument using $CDCl_3$ as the solvent. Chemical shifts are referenced to internal tetramethylsilane. ^{13}C NMR are proton decoupled. IR analyses were performed on a Nicolet 4700 FTIR with an ATIR attachment from Smart-Orbit Thermoelectronic Corporation. Ultraviolet-visible analysis was performed on a Shimadzu UV-2401PC spectrometer, and fluorescence spectroscopy was performed on a Shimadzu RF-5301PC spectrofluorophotometer. AFM scans were conducted using a Veeco Dimension V AFM Each sample was analyzed in tapping mode with a Nanosensors silicon AFM probe (model PPP-

NCHR) prepared from dichlorobenzene and chloroform solutions (20mg/mL). Elemental analyses were performed by Atlantic Microlab, Inc. (Norcross, GA). 4,7-Dibromobenzo[*c*][1,2,5]thiadiazole (**IV-1**),[29] $Ni(PPh_3)_4$,[30] and 2-bromo-5-iodo-3-octylthiophene[31] were prepared using previously reported methods. Synthesis of analogues **a** (R = $-C_6H_4-OC_8H_{17}$) and **b** (R = 2-ethylhexyl) are described below.

4.2.2. Synthesis of Monomers and Trimers

Synthetic procedures and spectroscopic data for the diketones, quinoxaline monomers and thiophene-quinoxaline-thiophene timer are below.

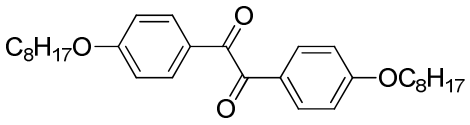

1,2-Bis(4-(octyloxy)phenyl)ethane-1,2-dione, IV-3a. Potassium carbonate (15.2 g, 110 mmol) and tetrabutylammonium bromide (8.0 g, 25 mmol) were added to a solution of 1-bromooctane (15 mL, 88 mmol) and 1,2-bis(4-hydroxyphenyl)ethane-1,2-dione (10.6 g, 41.4 mmol) in anhydrous DMF (150 mL) under argon. The mixture was heated at 80 °C for 24 h, cooled and poured into H_2O (700 mL). The resulting mixture was filtered and the filtrand was recrystallized from ethanol to afford **IV-3a** as a colorless solid (10.6 g, 52%): mp = 63-64 °C. ^{1}H NMR (300 MHz, $CDCl_3$) δ 7.92 (d, $^3J_{HH}$ = 8.7 Hz, 4H, Ar C2-H), 6.93 (d, $^3J_{HH}$ = 8.7 Hz, 4H, Ar C3-H), 4.02 (t, $^3J_{HH}$ = 6.6 Hz, 4H, $-OCH_2-$), 1.74-1.84 (m, 4H), 1.28-1.47 (m, 20H), 0.88 (t, $^3J_{HH}$ = 6.6 Hz, 6H). ^{13}C NMR (75 MHz, $CDCl_3$) δ 193.52 (C=O), 164.43 (Ar C4), 132.31 (Ar C2 and C6), 126.00 (Ar C1), 114.65 (Ar C3 and C5), 68.42 (C-O), 31.74, 29.25, 29.16, 28.96, 25.89, 22.61, 14.07. IR (ATIR): 2916 (Ar C-H str.), 2844, 1664, 1597, 1573, 1508, 1463, 1421, 1251 (C-O str.), 1162, 1058, 1014, 956, 889, 842, 759, 649,

617 cm^{-1}. HRMS *calc.* for $C_{30}H_{42}O_4$ = 466.3083, *obs.* = 466.3091, Δ = 1.7 ppm. Elemental Analysis: Theoretical: C, 77.21%; H, 9.07%; Found: C, 76.38%; H, 8.90%.

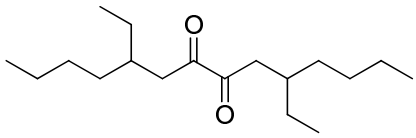

5,10-diethyltetradecane-7,8-dione, IV-3b. Prepared a solution of 2-ethylhexylmagnesium bromide by adding 2-ethylhexyl bromide (17.3 mL, mol) dropwise to a solution of Mg (2.61 g, mol) in THF (250 mL) and let stir for 1 h at room temperature. In a separate flask, added LiBr (17 g, mol) in THF (100 mL) to a solution of CuBr (14 g, mol) in THF (150 mL) by syringe. Cooled the mixture to -96 ºC by a pentane/liquid nitrogen slurry. Added 2-ethylhexylmagnesium bromide solution to the mixture dropwise over 1 h. Added oxalyl chloride (5.0 g, mol) to the mixture and let warm slowly to room temperature over 2 h. Quenched the reaction by pouring the mixture into saturated ammonium chloride (aq, 500 mL). Extracted organic layer, and washed aqueous layer repeatedly with diethyl ether (3 x 300 mL), combined the extracts and removed solvent under reduced pressure. The resulting residue was purified by column chromatography (10:90 v/v CH_2Cl_2:hexanes) to obtain **IV-3b** as a yellow liquid (5.01 g, 45%). ^{1}H NMR (300 MHz, $CDCl_3$) δ 2.64 (d, $^3J_{HH}$ = 6.6 Hz, 4H) 1.81-1.89 (m, 2H), 1.16-1.36 (m, 16H) 0.81-0.89 (m, 12H). ^{13}C NMR (75 MHz, $CDCl_3$) δ 200.59 (C=O), 40.24, 34.94. 33.22, 28.81, 26.46, 22.86, 14.03, 10.81. IR (ATIR): 2931, 2919, 2854, 1705 (C=O str.), 1456, 1377, 997, 925, 719, 690, 687, 578.

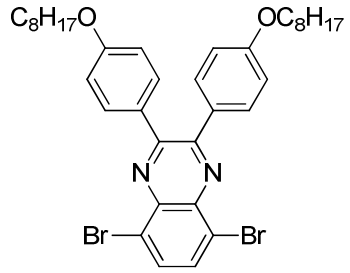

5,8-Dibromo-2,3-bis(4-(octyloxy)phenyl)quinoxaline, IV-4a. $NaBH_4$ (9 g, 238 mmol) was added in four equal portions 20 minutes apart to a solution of 4,7-dibromobenzo[c][1,2,5]thiadiazole (**IV-1**) (6.1 g, 21 mmol) and $CoCl_2 \cdot 6H_2O$ (0.1 g, 0.4 mmol) in EtOH (100 mL) under argon. The solution was stirred for an additional 30 min and the solvent was removed under reduced pressure. The residue was taken up in H_2O (100 mL) and the mixture was neutralized with 10 % HCl (50 mL) and extracted with CH_2Cl_2 (2 x 200 mL). The organic extracts were combined and the solvent was removed under reduced pressure to afford **IV-2** as a colorless solid (3.5 g). ^{1}H NMR (300 MHz, $CDCl_3$) δ 6.16 (s, 2H), 3.37 (br s, 4H). The crude solid is unstable in light and air, and was used immediately without further purification.

A solution of 3,6-dibromobenzene-1,2-diamine (**IV-2**) (3.5 g, 13 mmol) and **IV-3a** (5.0 g, 11 mmol) in acetic acid (200 mL) was heated to reflux for 24 h. The solution was cooled to room temperature and poured into H_2O (200 mL). The mixture was filtered and the filtrand was purified by column chromatography (30:70 v/v CH_2Cl_2:hexanes) to afford **IV-4a** as a yellow solid (4.4 g, 56%), mp = 81-83 °C . ^{1}H NMR (300 MHz, $CDCl_3$) δ 7.83 (s, 2H, quinioxaline C-H), 7.65 (d, $^3J_{HH}$ = 8.7 Hz, 4H, phenyl C2-H), 6.87 (d, $^3J_{HH}$ = 8.7 Hz, 4H, phenyl C3-H), 3.99 (t, $^3J_{HH}$ = 6.6 Hz, 4H, -OCH_2-), 1.78-1.82 (m, 4H), 1.28-1.49 (m, 20H), 0.89 (t, $^3J_{HH}$ = 7.2 Hz, 6H). ^{13}C NMR (75 MHz, $CDCl_3$) δ 160.41 (phenyl C4), 153.53 (quinoxaline C2 and C3), 138.95 (quinoxaline C1 and C4), 132.44 (quinoxaline C6 and C7), 131.63 (phenyl C2), 130.26 (phenyl C1), 123.38 (quinoxaline C5 and C8), 114.31 (phenyl C3), 68.05

(C-O), 31.79, 29.33, 29.21, 29.16, 26.00, 22.63, 14.09. IR (ATIR): 2912 (Ar C-H str.), 2846, 1600, 1512, 1468, 1377, 1242, 1173 (C-O str.), 985, 821, 717, 656, 540 cm^{-1}. HRMS *calc.* for $C_{36}H_{44}Br_2N_2O_2$ = 694.1770, *obs.* = 694.1767 Δ = 0.4 ppm. Elemental Analysis: Theoretical: C, 62.07%; H, 6.37%; N, 4.02%. Found: C, 61.81%; H, 6.31%; N, 4.21%.

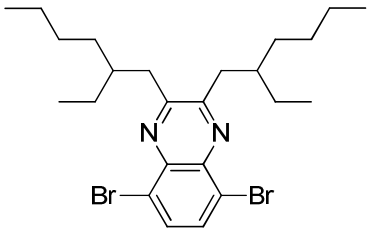

5,8-dibromo-2,3-bis(2-ethylhexyl)quinoxaline, IV-4b. A solution of 3,6-dibromobenzene-1,2-diamine (**IV-2**) (5.6 g, 21 mmol) and **IV-3b** (6.0 g, 21 mmol) in acetic acid (200 mL) was heated to reflux for 24 h. The solution was cooled to room temperature and poured into H_2O (200 mL), neutralized with 10 % KOH (aq) and extracted with diethyl ether (3 x 100 mL). The organic extracts were combined and the solvent was removed under reduced pressure. The resulting residue was purified by column chromatography (20:80 v/v CH_2Cl_2:hexanes) to afford **IV-4b** as a viscous yellow liquid (6.7 g, 47 %). ^{1}H NMR (300 MHz, $CDCl_3$) δ 7.81 (s, 2H), 2.99 (d, = 6.9 Hz, 4H), 2.12-2.20 (m, 2H), 1.23-1.46 (m, 16H), 0.85-0.96 (m, 12H). ^{13}C NMR (75 MHz, $CDCl_3$) δ 158.13 (quinoxaline C2 and C3), 138.96 (quinoxaline C1 and C4), 131.87 (quinoxaline C6 and C7), 123.34 (quinoxaline C5 and C8), 38.80, 38.05, 32.76, 28.84, 26.00, 23.04, 14.12, 10.90. IR (ATIR): 2908, 2842, 1585, 1465, 1394, 1301, 1259, 1168, 1097, 1018, 935, 811, 723, 656, 588, 430. HRMS *calc.* for $C_{24}H_{36}Br_2N_2$ = 510.1245, *obs.* = 510.1233 Δ = 2.4 ppm.

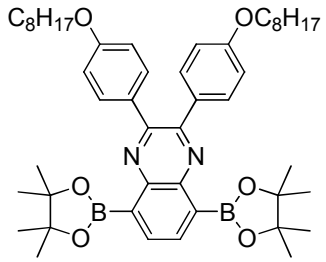

2,3-Bis(4-(octyloxy)phenyl)-5,8-bis(4,4,5,5-tetramethyl-1,3,2-dioxaborolan-2-yl)quinoxaline, IV-7. Dibromide **IV-4a** (3.85 g, 5.5 mmol) was added to anhydrous 1,4-dioxane (70 mL) under argon. Bis(pinacolato)diboron (3.5 g, 14 mmol), Pd(dppf)Cl_2 (0.4 g, 0.5 mmol) and potassium acetate (1.35 g, 13.8 mmol) were added to a solution of dibromide **IV-4a** (3.85 g, 5.5 mmol) in anhydrous 1,4-dioxane (70 mL) under argon. The solution was degassed by freeze-pump-thaw (2 x 15 min cycles) and heated to 100 °C for 24 h. The solution was cooled to room temperature and the solvent was removed under reduced pressure. The residue was dissolved in CH_2Cl_2 (100 mL) and the solution was extracted with H_2O (100 mL). The organic layer was concentrated under reduced pressure and the residue was subjected to column chromatography (30:70 v/v EtOAc:CH_2Cl_2) to afford **IV-7** as a white solid (2.5 g, 58%): mp = 96-98 °C. ^{1}H NMR (300 MHz, $CDCl_3$) δ 7.93 (s, 2H, quinoxaline C-H), 7.68 (d, $^3J_{HH}$ = 8.7 Hz, 4H, phenyl C2-H), 6.83 (d, $^3J_{HH}$ = 9.0 Hz, 4H, phenyl C3-H), 3.97 (t, $^3J_{HH}$ = 6.6 Hz, 4H, -OCH_2-), 1.79 (p, $^3J_{HH}$ = 7.5 Hz, 4H), 1.47 (s, 24H), 1.27-1.44 (m, 20H), 0.89 (t, $^3J_{HH}$ = 6.9 Hz, 6H). ^{13}C NMR (75 MHz, $CDCl_3$) δ 159.71 (phenyl C4), 150.77 (quinoxaline C2 and C3), 143.02 (quinoxaline C1 and C4), 134.98 (quinoxaline C6 and C7), 131.90 (phenyl C2), 131.56 (quinoxaline C5 and C8), 113.82 (phenyl C3), 84.11 (-O-$\underline{C}(CH_3)_2$-), 67.98 (-O$\underline{C}H_2$-), 31.82, 29.38, 29.28, 29.25, 26.05, 25.06, 22.67, 14.12. IR (ATIR): 2929 (Ar C-H str.), 2865, 1608, 1513, 1475, 1367, 1309, 1245 (C-O str.), 1178, 1143, 1025, 1022, 987, 858, 831, 817, 688, 604, 543 cm^{-1}.

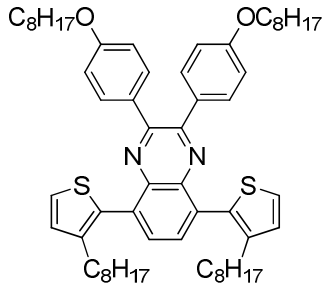

2,3-Bis(4-(octyloxy)phenyl)-5,8-bis(3-octylthiophen-2-yl)quinoxaline, IV-8. 2-Bromo-3-octylthiophene (0.62 g, 2.2 mmol) was added to a mixture of **IV-7** (0.45 g, 0.56 mmol) in THF (9 mL) and 2 M aqueous Na_2CO_3 (4 mL). The solution was degassed by freeze-pump-thaw (2 x 15 min each cycle) and $Pd(PPh_3)_4$ (0.1 g, 0.1 mmol) was added. The solution was stirred under argon at 70 °C for 24 h, poured into H_2O (50 mL) and extracted with CH_2Cl_2 (2 x 100 mL). The combined extracts were concentrated under reduced pressure and the residue was subjected to column chromatography (20:80 v/v CH_2Cl_2:hexanes) to afford **IV-8** as a viscous yellow liquid (0.48 g, 92%). ^{1}H NMR (300 MHz, $CDCl_3$) δ 7.75 (s, 2 H, quinoxaline C-H), 7.58 (d, $^3J_{HH}$ = 8.7 Hz, 4H, phenyl C2-H), 7.45 (d, $^3J_{HH}$ = 4.9 Hz, 2H, thiophene C5-H), 7.10 (d, $^3J_{HH}$ = 4.8 Hz, 2H, thiophene C4-H), 6.81 (d, $^3J_{HH}$ = 8.7 Hz, 4H, phenyl C3-H), 3.96 (t, $^3J_{HH}$ = 6.3 Hz, 4H, -OCH_2-), 2.68 (t, $^3J_{HH}$ = 8.1 Hz, 4H, Th-CH_2-), 1.79 (p, $^3J_{HH}$ = 7.2 Hz, 4H), 1.56-1.66 (m, 4H), 1.16-1.48 (m, 40H), 0.84-0.92 (m, 12H). ^{13}C NMR (75 MHz, $CDCl_3$) δ 159.79, 151.18, 141.10, 138.98, 133.32, 132.95, 131.58, 131.38, 130.47, 128.53, 125.66, 114.03, 67.98, 31.84, 30.85, 29.55, 29.38, 29.24, 26.05, 22.68, 22.65, 14.13, 14.11 (5 aliphatic carbons have coincident chemical shifts with other signals). IR (ATIR): 2924 (Ar C-H str.), 2852, 1604, 1511, 1467, 1384, 1334, 1294, 1247 (C-O str.), 1174, 1029, 966, 836, 723, 671, 547 cm^{-1}. Elemental Analysis: Theoretical: C, 77.70%; H, 8.91%; N, 3.02%; S, 6.91%. Found: C, 77.80%; H, 8.98%; N, 2.98%; S, 6.78%.

4.2.3. Synthesis of Poly(5,8-quinoxaline)s

Synthetic procedures and spectroscopic data for the poly(5,8-quinoxaline)s in this study are described below.

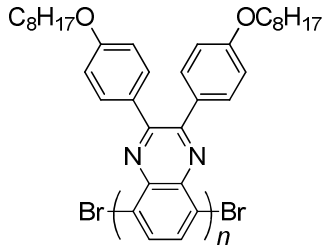

Poly(2,3-(4-octyloxyphenyl)quinoxaline-5,8-diyl), PQ(C8)Br$_2$. In an argon filled glove-box, Ni(COD)$_2$ (0.71 g, 2.6 mmol) was added to a Shlenk flask containing a solution of dibromide **IV-4a** (1.5 g, 2.2 mmol), 2,2'-bipyridine (0.44 g, 2.8 mmol) 1,5-cyclooctadiene (1 mL, 8 mmol) in anhydrous *N*,*N*-dimethyformamide (25 mL). The mixture was stirred at 60 °C for 48 h, and then poured into MeOH (100 mL). The solution was filtered and the resulting gray precipitate was dissolved in $CHCl_3$ (50 mL) and the solution was stirred with 10% aqueous HCl (20 mL) for 30 min. The organic layer was separated and then stirred with 10% KOH (20 mL) for 30 min. The organic layer was separated and the polymer was precipitated by pouring the solution into MeOH (200 mL). The solution was filtered and **PQ(C8)Br$_2$** was obtained as a yellow solid. ^{1}H NMR (300 MHz, $CDCl_3$) δ 8.33 (br s, 2H, quinoxaline C-H), 6.60 (b, 4H, phenyl C-H), 3.7 (b, 4H, -OCH_2-), 1.54-1.87 (m, 4H), 1.15-1.42 (m, 20H), 0.87 (b, 6H). IR (ATIR): 2927, 2856, 1604, 1511, 1467, 1384, 1342, 1294, 1243, 1172, 1027, 977, 831, 736, 665, 592, 540 cm^{-1}. GPC (THF, UV-vis detector) 4.28 kDa, PDI = 1.93.

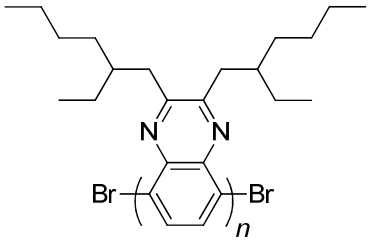

Poly(2,3-(2-ethylhexyl)quinoxaline-5,8-diyl), PQ(EH)Br$_2$. Polymerization of monomer **IV-4b** (2.0 g, 3.9 mmol) was carried out according to the procedure provided above to afford **PQ(EH)Br$_2$** as a yellow solid (1.1 g, 73%). ^{1}H NMR (300 MHz, $CDCl_3$) δ 8.14 (b, 2H, quinoxaline C-H), 2.79 (b, 4H, Ar-CH_2-), 1.92 (b, 2H, -CH_2C<u>H</u>$(CH_2)_2$-), 1.07-1.36 (m, 16H) 0.67-0.87 (m, 12H). IR (ATIR): 2954, 2921, 2854, 1580, 1460, 1377, 1308, 1205, 1172, 1094, 923, 827, 767, 726, 653, 567, 445 cm^{-1}. GPC (THF, UV-vis detector) 5.7 kDa, PDI = 2.1. Elemental Analysis: Theoretical: C, 79.51 %; H, 10.01 %; N, 7.73 %. Found: C, 79.10 %; H, 10.10 %; N, 7.30 %.

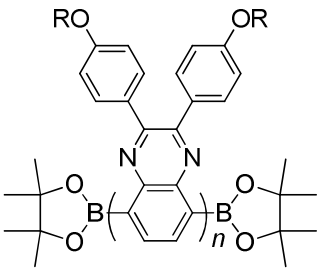

Boronate-ester modified poly(2,3-(4-octyloxyphenyl)quinoxaline-5,8-diyl), PQ(C8)-B(OR)$_2$. In a dry Schlenk flask under argon, bis(pinacolato)diboron (0.4 g, 1.6 mmol), potassium acetate (0.18 g, 1.8 mmol) and Pd(dppf)Cl_2 (0.06 g, 0.08 mmol) were added to a solution of **PQ(C8)Br$_2$** (0.67 g, 0.02 mols Br end groups) in anhydrous 1,4-dioxane (30 mL). The solution was stirred at 50 °C for 48 h, and then poured into MeOH (100 mL). The mixture was filtered and the residue was washed with MeOH (200 mL) to afford **PQ(C8)-B(OR)$_2$** as a yellow solid (0.60 g, 90%). ^{1}H

NMR (300 MHz, $CDCl_3$) δ 8.33 (b, 2H, quinoxaline C-H), 6.60 (b, 4H, phenyl C-H), 3.7 (b, 4H, -OCH_2-), 1.54-1.87 (m, 4H), 1.15-1.42 (m, 20H), 0.87 (b, 6H). IR (ATIR): 2924, 2852, 1600, 1512, 1471, 1382, 1342, 1294, 1249, 1170, 1027, 979, 831, 665, 592, 538 cm^{-1}.

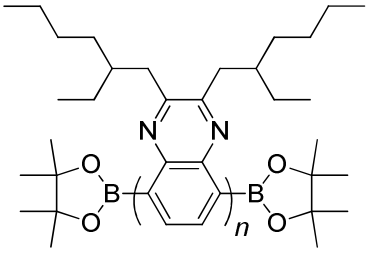

Boronate-ester modified poly(2,3-(2-ethylhexyl)quinoxaline-5,8-diyl), PQ(EH)-B(OR)$_2$. Modification of **PQ(EH)Br$_2$** (0.52 g 0.014 moles of Br end group) was carried out according to the procedure provided above to afford **PQ(EH)-B(OR)$_2$** as a yellow solid (0.47 g, 94%). ^{1}H NMR (300 MHz, $CDCl_3$) 8.14 (b, 2H, quinoxaline C-H), 2.79 (b, 4H, Ar-CH_2-), 1.92 (b, 2H, -C2 CH), 1.07-1.36 (m, 16H) 0.67-0.87 (m, 12H). IR (ATIR): 2954, 2921, 2854, 1580, 1460, 1377, 1308, 1248 (C-O str.), 1205, 1172, 1094, 923, 827, 767, 726, 653, 567, 445 cm^{-1}.

4.2.4 Synthesis of Initiated Poly(3-octylthiophene)

The synthetic procedure and spectroscopic data for the telechelic PAT in this study is described below.

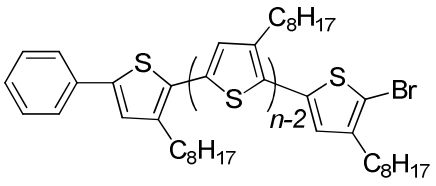

Monofunctional telechelic polythiophene, Ph-P3OT-Br. In a argon-filled glove box, bromobenzene (1 mL, 1.5 g, 9.5 mmol) was added to a solution of $Ni(PPh_3)_4$ (1.3 g, 1.17 mmol) and anhydrous toluene (8 mL). The mixture was stirred

overnight, and the solution turned from red to yellow. The mixture was filtered and the solid was washed with toluene (30 mL) to afford the arylnickel(II) initiator (**IV-5**) as a yellow solid (0.5 g, 57%). In a separate oven-dried Schlenk flask, iPrMgCl (1M in THF, 3.5 mL, 7.0 mmol) was added to a solution of 2-bromo-5-iodo-3-octylthiophene (2.8 g, 7.0 mmol) in THF (30 mL) at 0 °C. After 1 h, a solution of the phenylnickel(II) initiator (**IV-5**) (0.10 g, 0.14 mmol) in THF (2 mL) was added to the reaction mixture. The mixture was stirred for 1 h at 0 °C and transferred to a freezer (-20 °C) for 12 h. Hexanes (20 mL) was added and the mixture was poured into MeOH (100 mL). The resulting precipitate was sequentially extracted in a Soxhlet extractor with acetone, hexanes and chloroform to afford **Ph-P3OT-Br** as a purple solid: the hexanes extracted fraction (350 mg, 26%); the chloroform extracted fraction (637 mg, 47%). ^{1}H NMR (300 MHz, $CDCl_3$) δ 7.01 (br s, 1H), 2.74-2.89 (m, 2H), 1.71-1.82 (m, 2H), 1.32-1.44 (m, 10H), 0.89-0.91 (m, 3H). IR (ATIR): 2922, 2850, 1662, 1563, 1509, 1456, 1377, 1055, 823, 754, 723, 661 cm^{-1}. GPC (THF, UV-vis detector) hexanes fraction: 2.4 kDa, PDI= 1.3; chloroform fraction: 2.9 kDa, PDI= 1.0. Elemental Analysis: Theoretical: C, 64.48 %; H, 7.58 %; S, 17.22 %. Found: C, 64.79 %; H, 8.02 %; S, 17.02 %

4.2.5. Synthesis of D-A-D triblock copolymers

The synthetic procedures and spectroscopic data for the D-A-D triblock copolymers in this study are described below.

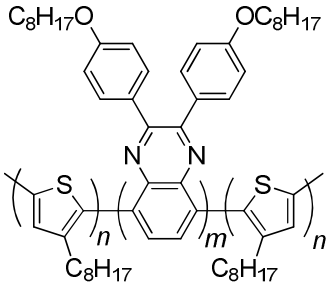

ABA triblock copolymer, P3OT-PQ(C8)-P3OT. K_2CO_3 (2 M, aq, 5 mL) was added to a solution of **PQ(C8)-B(OR)$_2$** (0.55 g) and hexanes-soluble **Ph-P3OT-Br** (0.61 g) in THF (20 mL), and the mixture was degassed by freeze-pump-thaw (2 x 15 min cycles). $Pd(PPh_3)_4$ (0.10 g, 0.09 mmol) was added and the solution was heated to 60 ºC for 3 d. The mixture was poured into MeOH (100 mL) and filtered. The resulting solid was sequentially extracted in a Soxhlet extractor with MeOH, acetone, hexanes and $CHCl_3$. The solvent from the $CHCl_3$ fraction was removed under reduced pressure to afford **P3OT-PQ(C8)-P3OT** as a purple solid (0.62 g, 52%). ^{1}H NMR (300 MHz, $CDCl_3$) δ 8.56 (br s, 2H, quinoxaline C-H), 7.24 (br s, 2H, thiophene C-H), 6.85 (b, 4H, phenyl C-H), 4.03 (b, 4H, -OCH_2-), 3.06 (b, 4H, thiophene CH_2-), 1.61-1.76 (m, 8H), 1.10-1.41 (m, 40H), 0.73-0.89 (m, 12H). IR (ATIR): 2924, 2854, 1604, 1509, 1467, 1384, 1342, 1294, 1240, 1170, 1112, 1025, 979, 831, 723, 663, 632, 590, 536 cm^{-1}. GPC (THF, UV-vis detector) 10.3 kDa, PDI = 2.8.

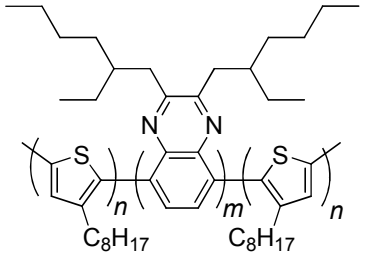

ABA triblock copolymer, P3OT-PQ(EH)-P3OT. Coupling of hexanes soluble **Ph-P3OT-Br** (0.38 g) and **PQ(EH)-B(OR)$_2$** (0.46 g) was carried out according to the procedure provided above to prepare **P3OT-PQ(EH)-P3OT** and the product was isolated as a purple solid (0.55 g, 67%). ^{1}H NMR (300 MHz, $CDCl_3$) δ 8.14 (bs, 2H, quinoxaline C-H), 6.98 (s, 2H, thiophene C-H), 2.80 (m, 8H, thiophene -CH_2-), 1.83-1.95 (m, 2H), 1.56-1.69 (m, 4H), 1.06-1.44 (m, 36H), 0.66-0.93 (m, 18H). IR (ATIR): 2956, 2927, 2856, 1495, 1379, 1261, 1095, 1018, 923, 800, 725, 696, 673, 622, 541, 443 cm^{-1}. GPC (THF, UV-vis detector) 10.0 kDa, PDI = 2.6.

4.3. Results and Discussion

4.3.1. Synthetic Approach

Our synthetic approach to the triblock copolymers involves three steps: (*i*) the synthesis of a well-defined monofunctional telechelic donor block, (*ii*) the synthesis of an acceptor block bearing complimentary functionality at both ends and (*iii*) coupling of the two polymer chains. In this study, we utilized an efficient Suzuki cross coupling between an electron poor (i.e. acceptor) poly(5,8-quinoxaline) block bearing boronate esters at both ends and an electron rich (donor) poly(3-alkylthiophene) bearing a single α-bromothienyl endgroup, Figure 4.1.

4.3.2. Telechelic bromine-terminated poly(3-alkylthiophene) donor block

We explored several methods to attain well-defined telechelic poly(3-alkylthiophene)s (PATs) that bear a single α-bromothienyl end group which could be used as the donor block in subsequent coupling reactions to the poly(5,8-quinoxaline) block. It is well established that poly(3-alkylthiophene)s with low polydispersity can be prepared by nickel(II)-catalyzed polymerization of 5-bromo-4-alkyl-2-thienylmagnesium iodides.[13] Unlike most condensation polymerizations, this reaction proceeds by a catalyst-transfer chain growth mechanism, in which the Ni remains associated with the polymer chain upon addition of each monomer to the chain, Figure 4.2.[32] The quasi-living nature of this polymerization relies on the rate of propagation being substantially greater than that of dissociative reductive elimination of nickel from the propagating chain end. While significant details about this process have been elucidated, quenching of the polymerization, typically by pouring the reaction mixture into an acidic aqueous solution, affords a mixture of α-bromothienyl and unfunctionalized thienyl end groups, Figure 4.2.[33]

In an effort to attain further control over the preparation of poly(3-alkylthiophene), several groups have explored the use of pre-formed arylnickel(II) complexes as initiators, thereby resulting in the installation of the aryl group at the initiated end of the chain.[34 - 36] We chose to prepare poly(3-octylthiophene) by employing phenylnickel(II) bromide as an initiator, and then focus on the retention of the α-bromothienyl functionality at the terminus derived from the propagating chain end. This was guided, in part, by the proposed mechanistic origins of the different combinations of end groups.[35]

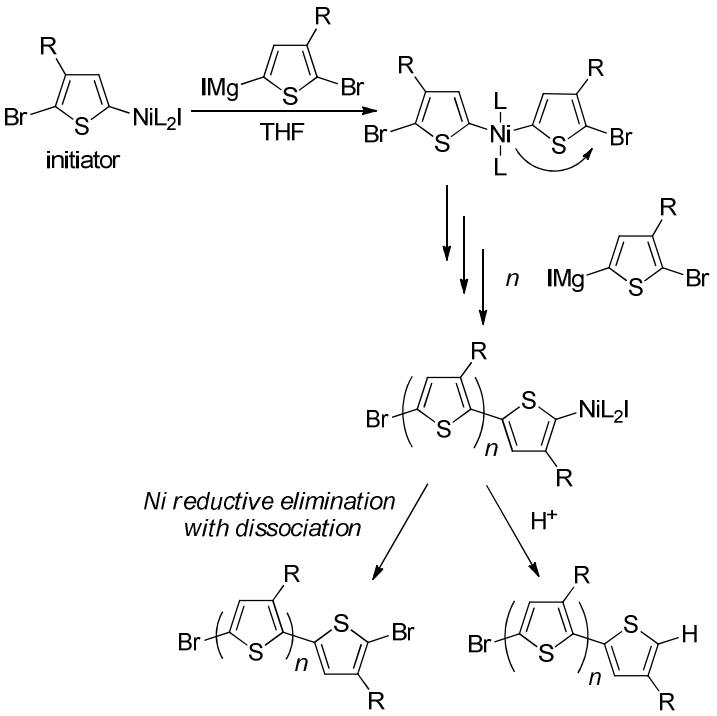

Figure 4.2. The origin of two types of end groups in the catalyst-transfer condensation polymerization (CTCP) of 5-bromo-4-alkyl-2-thienylmagnesium bromides.

Addition of bromobenzene to a solution of $Ni(PPh_3)_4$ in toluene led to the precipitation of the bright yellow initiator **5** that was collected by filtration, Figure 4.3.[37] Initiation of the polymerization of 2-bromo-3-octyl-5-iodothiophene (**IV-6**) with **IV-5** at 0 ºC resulted in the formation of the phenyl initiated poly(3-alkylthiophene) with either bromine or hydrogen groups at the terminus derived from the propagating chain end (i.e, **Ph-P3OT-X**) Figure 4.3. Kiriy has previously shown that if low temperatures are maintained during this polymerization the resulting polymers are exclusively propagated from the phenyl initiator. At room temperature there is evidence for chain transfer in which nickel dissociates from one chain and initiates a new chain that lacks the aryl end group derived from the initiator.[35] Even in

the absence of chain transfer, the α-bromothienyl end groups derived from the propagating chain end form as a result of some reductive elimination with dissociation of the nickel from the polymer backbone which could occur during the polymerization or after consumption of the monomer.

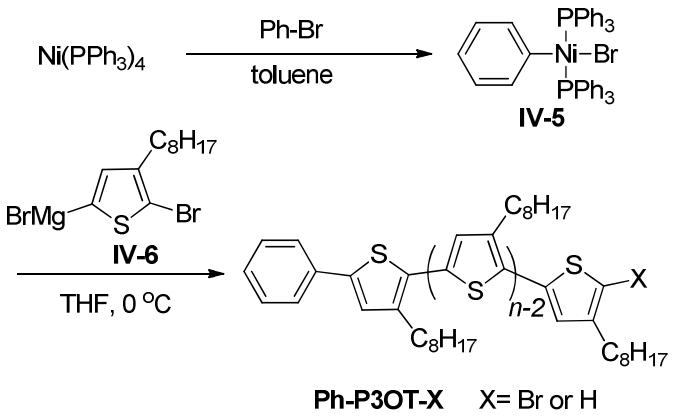

Figure 4.3. Initiation of the polymerization of 2-bromo-3-octyl-5-iodothiophene (**IV-6**) with phenylnickel(II) initiator (**IV-5**) leads to phenyl initiated P3OT.

Analysis of the aromatic region of the ^{1}H NMR allows for characterization of the two termini of the phenyl-initiated polymers, Figure 4.4A. The protons of the phenyl end groups derived from the initiator appear as a distinct set of multiplets at 7.61 (d), 7.38 (t) and 7.27 (m) ppm, with integrals of 2:2:1 respectively corresponding to the AM_2X_2 spin system of the phenyl end group. The β-hydrogen of the thiophene unit adjacent to the phenyl end group (H_d, Figure 4.4A) appears as a singlet at 7.16 ppm; the integral of this peak reveals a 1:1 ratio with the phenyl end groups. The thiophene at the other end of the polymer chain bears either an α-thienyl bromide or hydrogen atom (X = H or Br, Figure 4.4A). The relative amounts of these two types of terminal thiophenes can be determined by ^{1}H NMR. The β-proton on the terminal thiophene appears at 6.90 ppm if it bears an α-hydrogen atom (proton f, Figure 4.4),

and at 6.83 ppm if the polymer is terminated with a bromine atom (proton f').[38] Initial attempts at this polymerization resulted in a mixture of polymers with bromine (56%) and proton (44%) end groups, Figure 4.4A. The sum of the integral of protons f and f' (i.e. from the propagating chain end) is equal to that of the β-proton on the thiophene adjacent to the phenyl end group (proton d of the initiating end), consistent with efficient initiation of the polymerization by the phenylnicklel(II) complex **IV-6** and chain growth without termination or chain transfer prior to quenching.

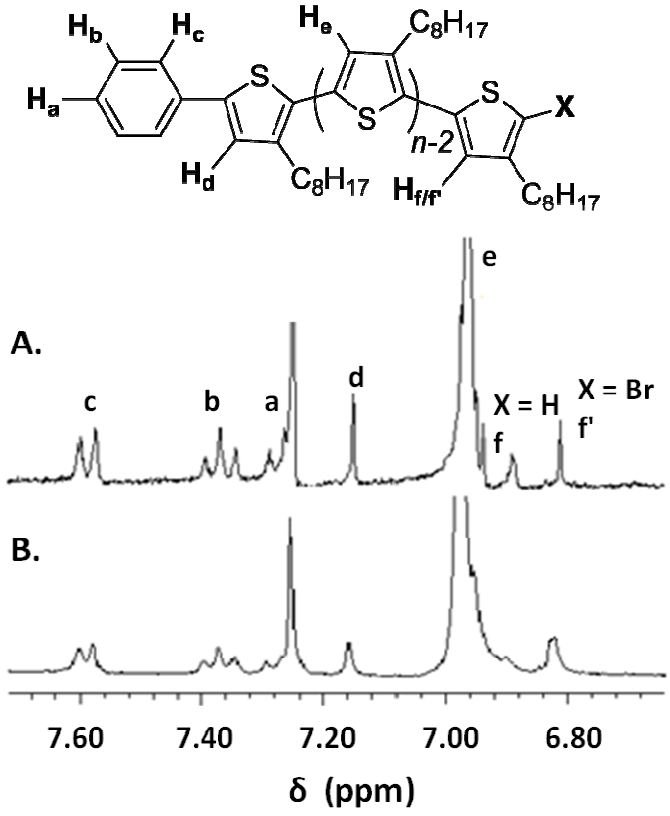

Figure 4.4. ^{1}H NMR (300 MHz, $CDCl_3$) of phenylnickel(II)-initiated poly(3-octylthiophene), allowed to react for 1 h and then: A, quenched by pouring reaction mixture into MeOH; and B, maintained for 12 h at -15 °C and poured into MeOH. The β-hydrogen of the terminal thiophene unit appears as signal f when X = H and as f' when X = Br.

This result is in contrast to a previous report in which polymerizations were conducted at room temperature. At this higher temperature a significant portion of the isolated polymers lacked the aryl end group derived from the initiator,[36] suggesting the occurrence of chain transfer whereby nickel dissociates from one propagating chain and reinitiates chain growth from another monomer. While initiation of the polymerization with the phenylnickel(II) complex installs a phenyl group at one end of the P3OT chain, the mixture of termini derived from the propagating chain end presents a significant hindrance to the preparation of block copolymers since it is important that all of the polymer chains have identical functionality. Polymers bearing an unfunctionalized thienyl end group would not undergo a subsequent coupling reaction to provide block copolymers, thereby leading to homopolymer impurities. In our hands, modifications of reaction time, temperature and quenching conditions were unsuccessful in completely preventing dissociative reductive elimination, and the polymerization reactions always gave a mixture of α-bromothienyl and thienyl termini derived from the propagating chain end. Since efforts to prevent this dissociation from occurring were unsuccessful, we decided instead to simply allow time for the dissociative reductive elimination of the nickel(II) from the polymer chain at the end of the polymerization to provide α-bromothienyl end groups. Rather than following the commonly-used procedure of quenching the polymerization by pouring the reaction mixture into methanol after a relatively short reaction time (i.e., upon consumption of the monomer), the reaction mixture was placed in a freezer at –15 °C for 12 h prior to precipitation into methanol. Holding the reaction at low temperatures for an extended period after consumption of the monomer allowed for almost complete reductive elimination and dissociation of the nickel from the polymer backbone to provide P3OT terminated with α-bromothienyl end groups (**Ph-P3OT-**

Br). Thus, while propagation is significantly faster than chain transfer during the polymerization, which is important to the success of this procedure, reductive elimination with dissociation of nickel from the chain does take place, albeit slowly, once the monomer is consumed. The ^{1}H NMR of the polymer reveals a 1:1 ratio of the β-proton on the thiophene adjacent to the phenyl propagating group (proton d, Figure 4.4B) and the α-bromothienyl group (proton f', Figure 4.4B), consistent with a polymer containing a high proportion of phenyl groups at the initiated end and and α-bromothienyl end groups derived from the propagating terminus.

The precipitated solid was subjected to sequential extraction in a Soxhlet extractor with methanol, acetone, hexanes and chloroform. From this procedure, extracts into hexanes consisted of a material with a lower degree of polymerization (DP = 14), and the chloroform fraction provided polymer with higher molecular weight (DP = 22), and low polydispersity indices (1.2 and 1.3, respectively). In these polymerizations we employed a 1:20 initiator to monomer ratio. Thus, the molecular weights are consistent with the living nature of the polymerization in which the chain length is controlled by the molar ratio of the initiator and monomer.[21]

4.3.3. Functionalized poly(5,8-quinoxaline)s

The difunctional electron-accepting blocks in this study, poly(2,3-(4-octyloxyphenyl)quinoxaline-5,8-diyl) **PQ(C8)** and poly(2,3-(2-ethylhexyl)quinoxaline-5,8-diyl) **PQ(EH)** were prepared by condensation polymerizations of 5,8-dibromoquinoxalines **IV-4a** and **IV-4b** using Yamamoto coupling conditions as previously reported, Figure 4.5.[13] Monomer **IV-4** was synthesized according to modified published procedures.[39] 4,7-Dibromobenzothiadiazole (**IV-1**) was reduced with sodium borohydride to afford

diamine **IV-2**, which was used without purification in a subsequent condensation with diketone **IV-3** to give 5,8-dibromoquinoxaline **IV-4**. Polymerization of monomer **IV-4** resulted in the dibromo-terminated quinoxaline polymers **PQ(C8)Br$_2$** and **PQ(EH)Br$_2$**, respectively. The protons of the quinoxaline rings at the termini of the chains appear as two distinct doublets in the ^{1}H NMR at 6.98 and 7.73 ppm (see Appendix D for spectra). This is consistent with unsymmetrically substituted quinoxaline groups, and is in contrast to the signal for the symmetrically substituted quinoxaline rings in the backbone of the polymer that appear as a singlet at 8.33 ppm. The degree of polymerization of the polymer was determined by comparing the relative integrals of the protons of the end groups and those of the polymer backbone. The **PQ(C8)Br$_2$** sample prepared in this study had a DP of eight, and the **PQ(EH)Br$_2$** analog had a DP of 14, where the degree of polymerization is limited by solubility of the respective polymers.

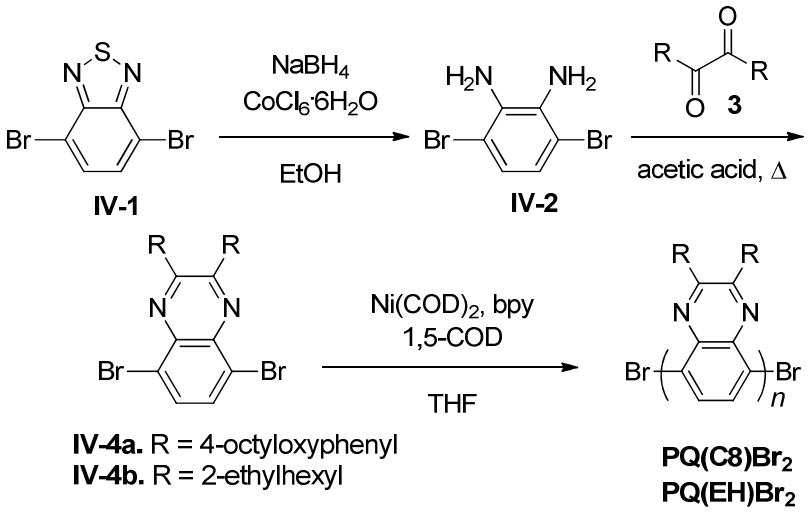

Figure 4.5. Synthesis of boronate ester terminated poly(5,8-quinoxaline) (**PQBr$_2$**).

4.3.4. Coupling of donor and acceptor blocks

We chose to convert the end groups of **$PQBr_2$** into boronate esters that could be coupled to the α-bromine terminated poly(3-octylthiophene), **Ph-P3OT-Br**, by a Suzuki cross-coupling reaction to couple the two blocks together. In order to test this approach, 5,8-dibromoquinoxaline (**IV-4a**) was treated with an excess of bis(pinacolato)diboron. This led to rapid and quantitative conversion to bisborolane **IV-7**, as confirmed by ^{1}H NMR (the singlet for the aromatic hydrogen of **IV-4a** at 7.83 ppm disappeared, and a new singlet appeared at 7.93 ppm for the bisborolane-quinoxaline), Figure 4.6. The palladium catalyzed Suzuki cross-coupling reaction between bisborolane **IV-7** and 2-bromo-3-octylthiophene afforded bisthienylquinoxaline **IV-8** with an isolated yield of 92% and serves as a model for the coupling of the donor and acceptor blocks.

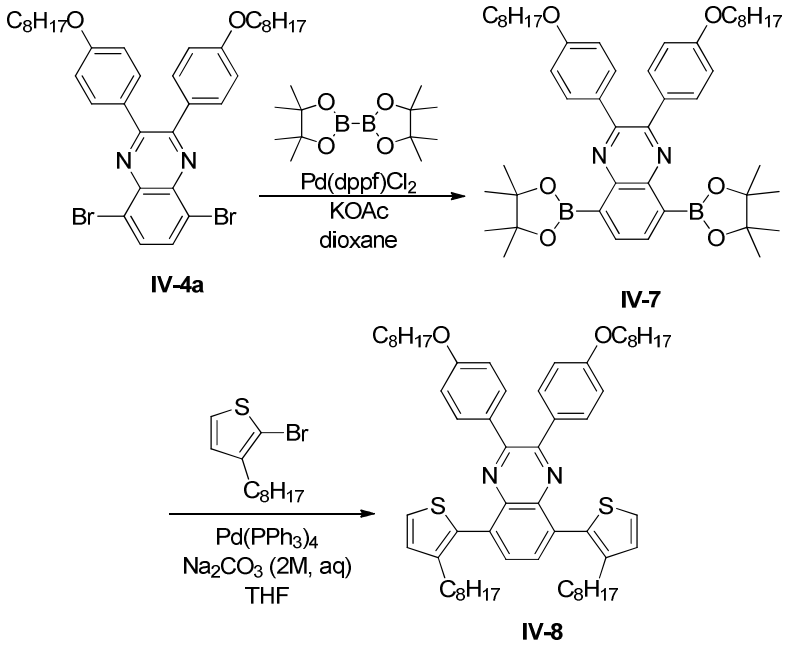

Figure 4.6. Synthesis of thiophene-quinoxline-thiophene trimer by Suzuki cross-coupling.

Treatment of **$PQBr_2$** with a large excess of bis(pinicolatediboron) afforded the boronate ester-terminated poly(quinoxaline), **PQ-B(OR')$_2$** as a yellow powder, Figure 4.7. While the aromatic end groups of the boronate ester terminated polyquinoxalines had coincident chemical shifts in the ^{1}H NMR with the dibromo-substituted analog, the presence of these end groups in **PQ(EH)-(BOR')$_2$** was confirmed by the appearance of a C-O stretching band at 1248 cm^{-1} in the IR spectrum, Figure 4.8.

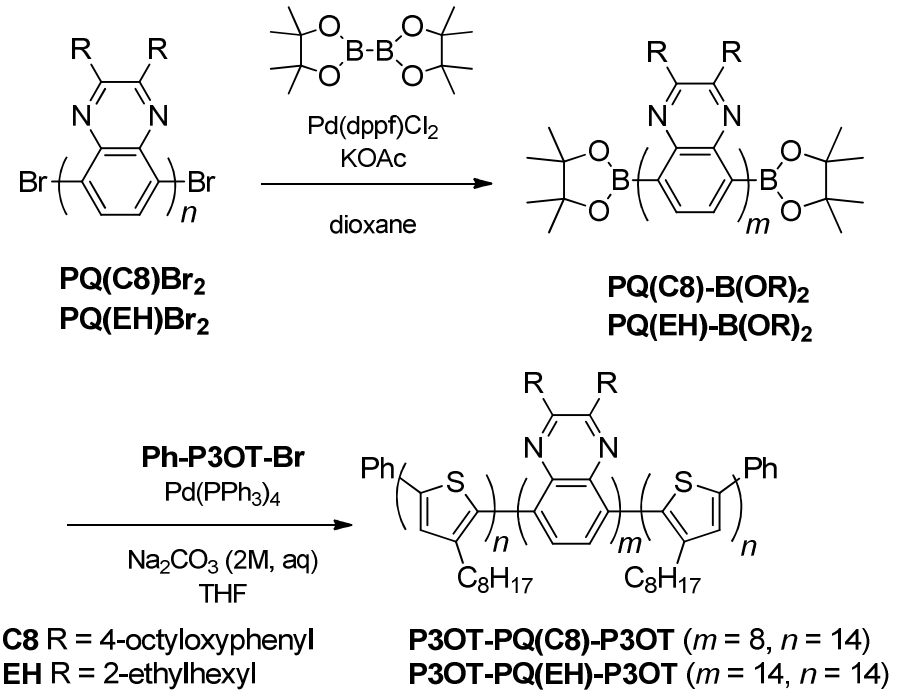

Figure 4.7. Synthesis of donor-acceptor-donor triblock copolymers by Suzuki cross-coupling.

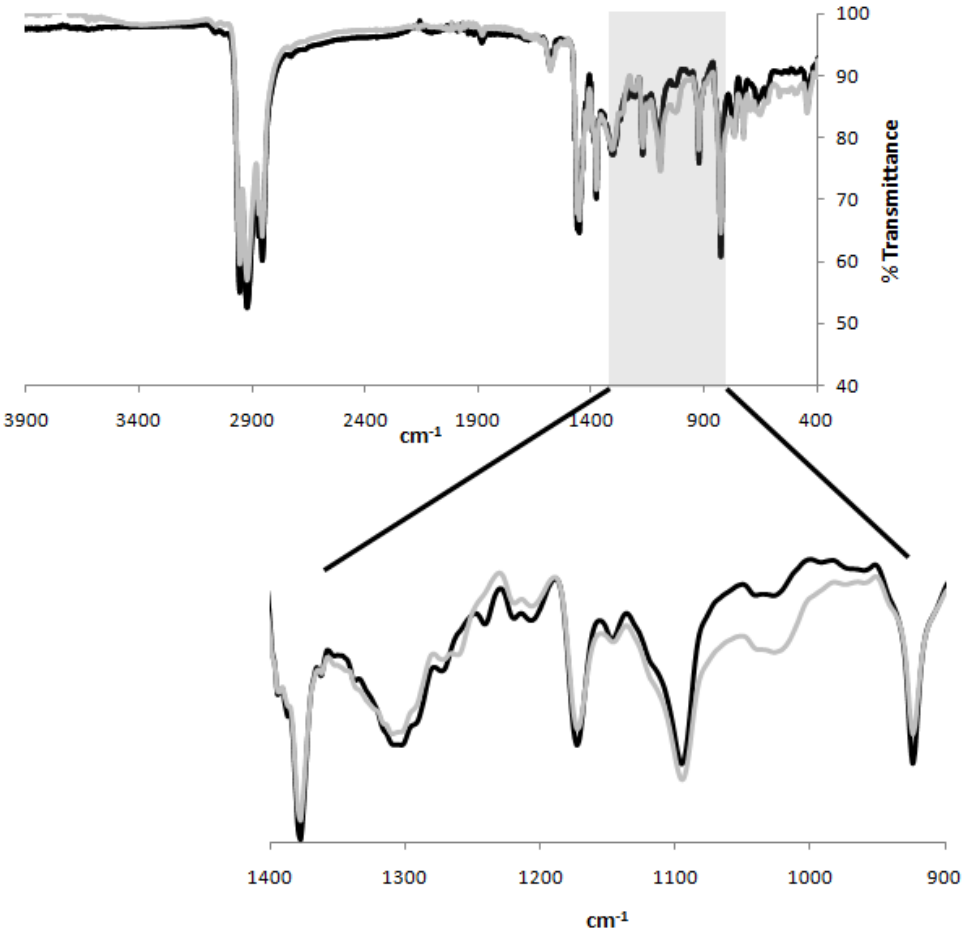

Figure 4.8 IR spectra of **PQ(EH)Br$_2$** (gray line) and **PQ(EH)-(BOR')$_2$** (black line).

The D-A-D triblock copolymers were prepared by combining the boronate ester terminated poly(quinoxaline)s, **PQ-B(OR')$_2$**, with 4 equivalents of the hexanes-soluble **Ph-P3OT-Br** under Suzuki cross-coupling conditions, Figure 4.7. The lower molecular weight hexanes-soluble fraction of the poly(3-alkylthiophene) donor block was used in order to simplify the purification process after the coupling reaction whereby any unreacted polymer could be washed out of the mixture by extraction. After coupling the resulting block copolymers were precipitated by addition of the reaction mixture to a large volume of cold methanol, and the resulting solid was purified by successive extractions in a Soxhlet extractor with methanol, acetone,

hexanes and chloroform. Any unreacted **Ph-P3OT-Br**, which was used in excess, was extracted into hexanes, and the block copolymer was extracted into the chloroform fraction.

4.3.5. Polymer characterization

The number (M_n) and weight (M_w) average molecular weights and polydispersity (PDI) of the homopolymers and triblock copolymers were determined by GPC and ^{1}H NMR spectroscopy, Table 4.1. The relative segment lengths of the block copolymers were determined by integration of the ^{1}H NMR signals of the protons of the aromatic rings: The β–hydrogen atoms of the thiophene backbone of P3OT gives a singlet at 7.0 ppm and the poly(quinoxaline) gives a singlet at 8.0 ppm (see Appendix D for spectra).

Table 4.1. Properties of **Ph-P3OT-Br** (D), **PQBr$_2$** (A) and D-A-D triblock copolymers.

Polymer	M_w [a,b] (kg.mol^{-1})	M_n [b,c] (kg.mol^{-1})	PDI [b,d]	DP [e,f]	T_m [g] (^{o}C)	T_c [h] (^{o}C)
Ph-P3OT-Br hexanes extract	3.1	2.7	1.2	12	176	157
Ph-P3OT-Br $CHCl_3$ extract	5.3	4.2	1.3	20	185	159
PQ(EH)Br$_2$	12.0	5.7	2.1	14	110	-
PQ(C8)Br$_2$	8.3	4.6	1.8	8	72(br)	-
P3OT-PQ(EH)-P3OT	26.0	10.0	2.6	42	75,115	92
P3OT-PQ(C8)-P3OT	28.8	10.3	2.8	36	-	-

[a]Weight average molecular weight (M_w). [b]Determined by gel permeation using polystyrene standards. [c]Number average molecular weight (M_n). [d]Polydispersity index (PDI) [e]Degree of polymerization (aryl repeat units). [f]Determined by end group analysis. [g]Melting temperatures determined by a DSC scan rate of 10 ^{o}C.min^{-1}. [h]Recrystallization temperatures determined by a DSC scan rate of 10 ^{o}C.min^{-1}.

Figure 4.9 shows the GPC profiles of **Ph-P3OT-Br**, **PQ(C8)Br$_2$** and the resulting D-A-D triblock copolymer. The elution curve of the hexanes-soluble fraction of **Ph-P3OT-Br** (dotted line) corresponds to an M_n of 2.4 kDa. The dibromopoly(quinoxaline), **PQ(C8)Br$_2$** (dashed line), has an M_n of 5.8 kDa. After Suzuki coupling of the donor and acceptor polymers and subsequent extractions, the chloroform fraction gives an elution curve corresponding to an M_n of 10.3 kDa (solid line). Taken together the ^{1}H NMR spectra and GPC data are consistent with formation of the D-A-D triblock copolymer, **P3OT-PQ(C8)-P3OT**.

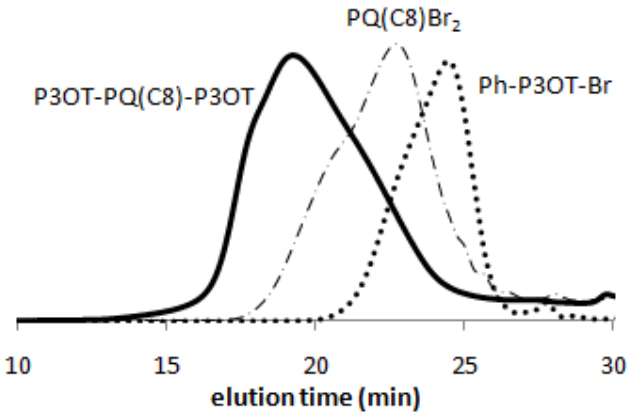

Figure 4.9. GPC profiles of **Ph-P3OT-Br** (dotted line), **PQ(C8)Br$_2$** (dashed line) and **P3OT-PQ(C8)-P3OT** (solid line).

The thermal transition temperatures of the polymers prepared in this study were measured by differential scanning calorimetry (DSC) in a nitrogen atmosphere, Table 4.1. DSC heating scans of **Ph-P3OT-Br** and **PQ(EH)Br$_2$** and corresponding triblock copolymer are shown in Figure 4.10. The hexanes soluble fraction of **Ph-P3OT-Br** has a single endothermic peak on heating at 176 ºC and a supercooled crystallization transition at 157 °C upon cooling. The melting transition of

PQ(EH)Br$_2$ occurs at 110 ºC. The corresponding triblock copolymer, **P3OT-PQ(EH)-P3OT** has two melting transitions at 75 and 115 °C, and one crystalization peak upon cooling at 92 °C. Depression of melting points of the separate components in other conjugated block copolymers has been previously observed.[40,41] Accordingly, the endothermic transitions of the triblock copolymer may correspond to melting of the **PQ(EH)** and **P3OT** segments, respectively. The triblock copolymer **P3OT-PQ(C8)-P3OT** does not show any thermal transitions, indicating hat this polymer is largely amorphous.

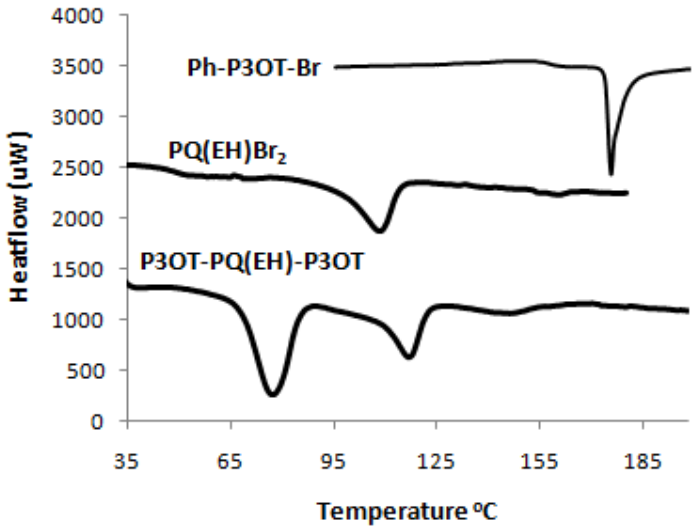

Figure 4.10. DSC heating scans of **Ph-P3OT-Br**, **PQ(EH)Br$_2$** and **P3OT-PQ(EH)-P3OT** (10 ºC.min^{-1}).

The solution UV-visible absorption spectra of **PQBr$_2$**, **Ph-P3OT-Br** and D-A-D triblock copolymers **P3OT-PQ(C8)-P3OT** and **P3OT-PQ(EH)-P3OT** are shown in Figure 4.11. The solution spectra were recorded for solution of the polymer in chloroform (5 mg/100 mL). The precursors for the polyquinioxaline blocks, **PQ(C8)Br$_2$** and **PQ(EH)Br$_2$** absorb at 392 nm and 376 nm respectively. The

telechelic poly(3-octylthiophene) bearing phenyl and α-bromothienyl termini absorbs at 450 nm. These absorptions are similar to previously reported values for related homopolymers.[14,42] The spectra of the D-A-D triblock copolymers display absorption bands that are similar to those of the constituent blocks. For example, the **P3OT-PQ(EH)-P3OT** triblock copolymer has absorption bands at 378 nm and 450 nm. As the block copolymer spectrum is, for the most part, a superposition of the homopolymer spectrum, there is no apparent ground state interaction between the donor and acceptor segments.

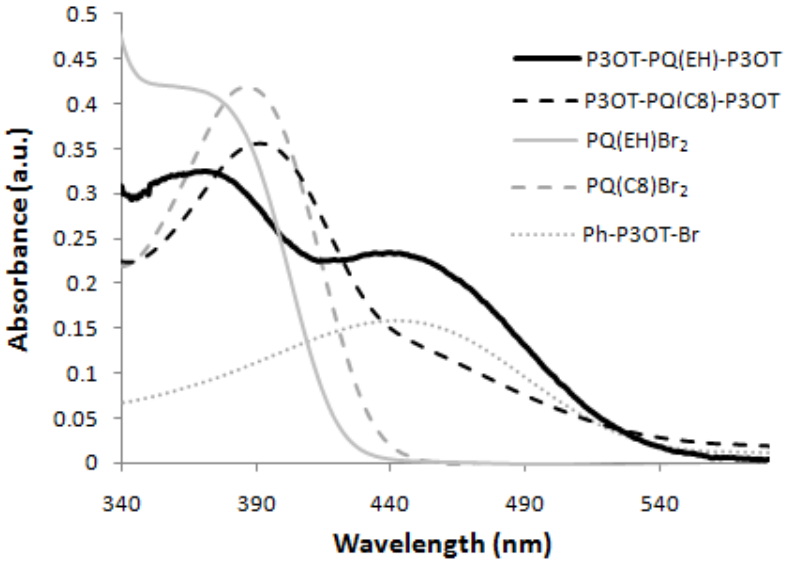

.

Figure 4.11. UV-visible absorption spectra in chloroform (5 mg/100 mL) for **Ph-P3OT-Br** (dotted line), **PQ(C8)Br$_2$** (gray dashed line), **PQ(EH)Br$_2$** (black dashed line), and D-A-D triblock copolymers **P3OT-PQ(C8)-P3OT** (gray solid line) and **P3OT-PQ(EH)-P3OT** (black solid line).

The solid state absorptions are broader and red-shifted for all of the materials, Figure 4.12. The absorption maxima for the homopolymers occur at 396 nm for **PQ(C8)Br$_2$** and at 501 nm for **Ph-P3OT-Br**. In the solid state D-A-D triblock **P3OT-PQ(C8)-P3OT** there are two absorption transitions that may be ascribed to the donor and acceptor segments, occurring at 490 nm and 407 nm respectively.

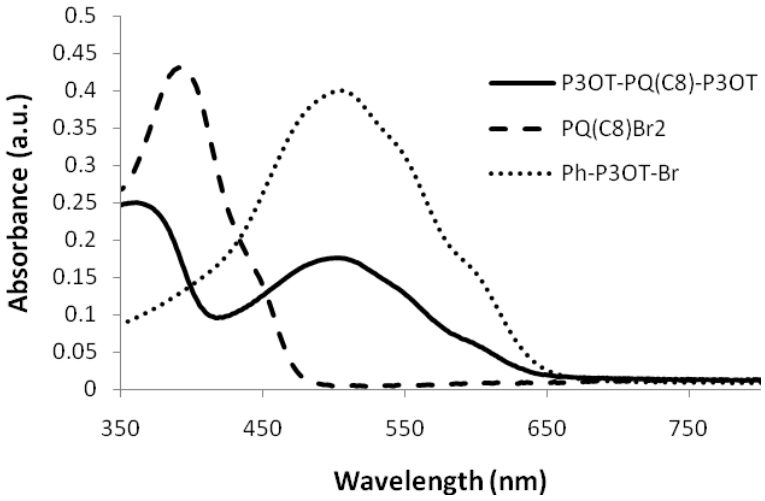

Figure 4.12. Solid state absorption spectra of **Ph-P3OT-Br** (dotted line), **PQ(C8)Br$_2$** (dashed line) and **P3OT-PQ(C8)-P3OT** (solid line), solutions (10 mg/mL in chloroform) cast onto quartz slides.

While the absorption spectra of the block copolymers have transitions that are similar those of the constituent homopolymers, the fluorescence spectra have much more noticeable differences. The solution and thin film fluorescence spectra are shown in Figure 4.13. The emission of a solution of the precursor poly(3-octylthiophene) block occurs at 560 nm, and the emission of the poly(5,8-quinoxaline) precursor occurs at 455 nm, consistent with previously reported results for related homopolymers.[14,41] However, the emission spectra of the block copolymer shows almost complete quenching of the fluorescence, consistent with electron

transfer from the donor to the acceptor segment. The solid state fluorescence spectra were measured on films prepared by casting 15 mg/mL of the polymers in 1,4-dichlorobenzene onto quartz slides. The emission of poly(3-octylthiophene) occurs at 770 nm and the emission of poly(5,8-quinoxaline) occurs at 500 nm. As with the solution spectra, films of the block copolymer show almost complete quenching of the fluorescence.

To investigate the morphology of the D-A-D triblock copolymers, thin films of **P3OT-PQ(EH)-P3OT** were cast from chloroform and dichlorobenzene. Atomic force microscopy height and phase images on the films are presented in Figure 4.14. The nanostructure apparent in these images may be attributed to phase separation of the crystalline poly(3-octylthiophene) segments and the amorphous poly(5,8-quinoxaline) segments. This is consistent with other reports of block copolymers that suggest nanostructure formation is a result of separation of crystalline and amorphous blocks.[14,43] Films of homopolymer cast under the same conditions did not show such textures.

4.4. Conclusions

In conclusion, we have established new synthetic routes to a monofunctional, telechelic poly(3-octylthiophene) where the single bromine end group can be used as a functional handle in subsequent coupling reactions. This was achieved by CTCP of 2-bromo-3-octylthienylmagnesium iodide from a phenylnickel(II) initiator at 0 °C, and delaying quenching of the polymerization rather than precipitation as soon as the monomer has been consumed. Working at low temperature slows down the dissociative reductive elimination of nickel from the polymer during propagation, insuring placement of phenyl groups at the initiated terminus of the chains in favor of

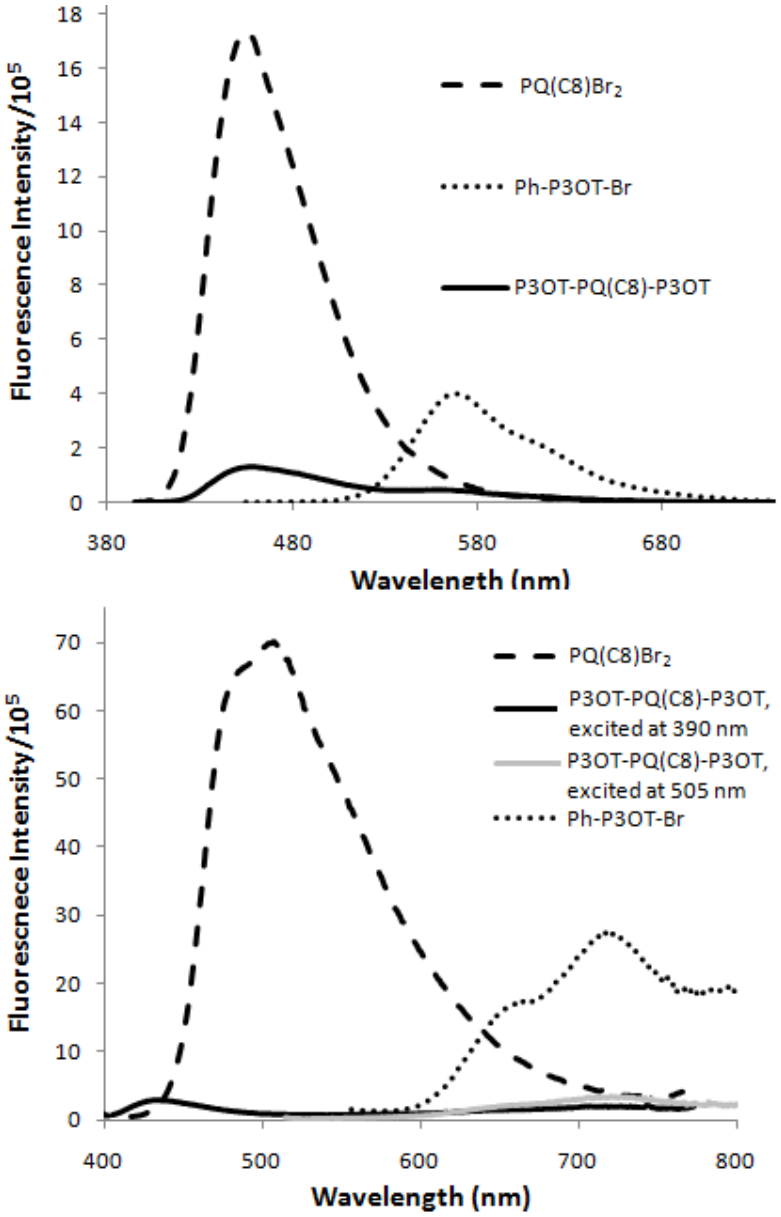

Figure 4.13. Fluorescence spectra of solutions (top; 5 mg/100 mL) and solid state (bottom; films cast from 15 mg/mL solutions in 1,4-dichlorobenzene) of **PQ(C8)Br$_2$** (dashed line), **Ph-P3OT-Br** (dotted line) and D-A-D triblock copolymer **P3OT-PQ(C8)-P3OT** excited at 390 nm (black line) and excited at 505 nm (gray line).

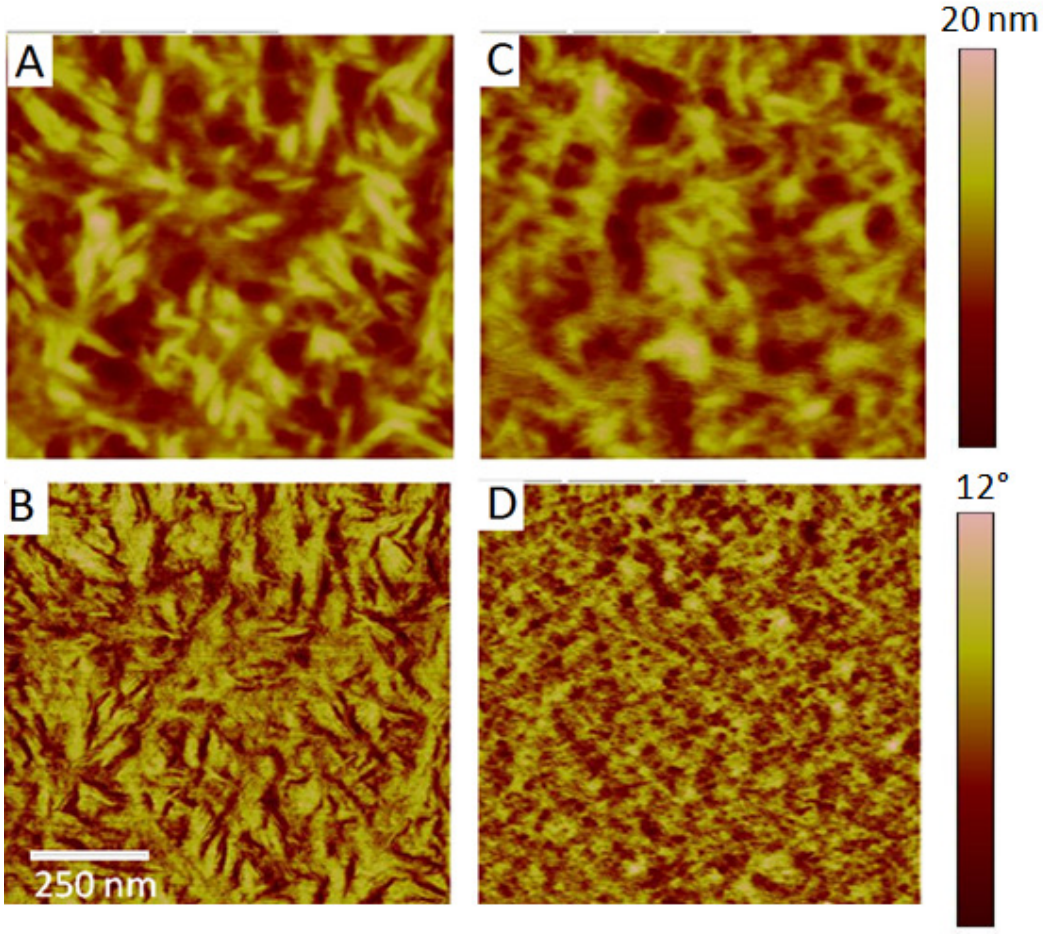

Figure 4.14. Tapping-mode atomic force microscopy (AFM) images of spin-coated thin films of **P3OT-PQ(EH)-P3OT** onto ITO. Films cast from chloroform: A, height and B, phase. Films cast from dichlorobenzene: C, height and D, phase.

competing chain transfer processes. The delay in quenching of the polymerization after consumption of the monomer allows time for reductive elimination of nickel and installation of the α-bromothienyl terminal functionality. The telechelic **Ph-P3OT-Br** block was coupled to a poly(5,8-quinoxaline) bearing boronic esters at each end to prepare a new class of D-A-D triblock copolymers with poly(3-octylthiophene) donor and poly(5,8-quinoxaline) acceptor blocks. The synthetic methods established in this study might be applicable to the preparation of a broad array of new materials.

Characterization of the D-A-D triblock copolymers in this study reveals efficient fluorescence quenching of the polymers in the solid state, supporting the occurrence of electron transfer.

4.5. References

1. Bredas, J.-L.; Norton, J. E.; Cornil, J.; Coropceanu, V. *Acc. Chem. Res.* **2009**, *42*, 1691–1699.
2. *Organic Photovoltaics, Mechanisms, Materials and Devices*; Sun. S.-S.; Sariciftci, N. S.; CRC Press: New York, 1995.
3. Krebs, F. C.; Bundgaard, E. *Solar Energy Materials and Solar Cells* **2007**, *91*, 954–985.
4. (a) van Bavel, S. S.; Bärenklau, M.; With, G.; Hoppe, H.; Loos, J. *Adv. Funct. Mater.* **2010**, *20*, 1458–1463. (b) Hoppe, H.; Sariciftci, N. S. *J. Mater. Chem.* **2006**, *16*, 45–61. (c) Shaheen, S. E.; Brabec, C. J.; Sariciftci, N. S. *Appl. Phys. Lett.* **2001**, *78*, 841–843.
5. McNeill, C. R.; Westenhoff, S.; Groves, C.; Friend, R. H.; Greenham, N. C. *J. Phys. Chem. C* **2007**, *111*, 19153–19160
6. (a) Liang, Y.; Wang, H.; Yuan, S.; Lee, Y.; Gan, L.; Yu, L. *J. Mater. Chem.* **2007**, *17*, 2183–2194. (b) Lee, M.; Cho, B.-K.; Zin, W.-C. *Chem. Rev.* **2001**, *101*, 3869–3892.
7. Iovu, M. C.; Jeffries-El, M.; Zhang, R.; Kowalewski, T.; McCullough, R. D. *J. Macromol. Sci. Part A* **2006**, *43*, 1991–2000.
8. Dai, C.-A.; Yen, W.-C.; Lee, Y.-H.; Ho, C.-C.; Su, W.-F. *J. Am. Chem. Soc.* **2007**, *129*, 11036–11038.

9. Craley, C. R.; Zhang, R.; Kowalewski, T.; McCullough, R. D.; Stefan, M. C. *Macromol. Rapid Commun.* **2009**, *30*, 11–16.

10. Iovu, M. C.; Craley, R.; Jeffries-El, M.; Krankowski, A. B.; Zhang, R.; Kowalewski, T.; McCullough, R. D. *Macromolecules*, **2007**, *40*, 4733–4735.

11. Scherf, U.; Gutacker, A.; Koenen, N. *Acc. Chem. Res.* **2008**, *41*, 1086–1097.

12. Yamamoto, T.; Maruyama, T.; Zhou, Z.; Ito, T.; Fukuda, T.; Yomeda, Y.; Begum, F.; Ikeda, T.; Sasaki, S.; Takezoe, H.; Fukuda, A.; Kubota, K. *J. Am. Chem. Soc.* **1994**, *116*, 4832–4845.

13. Yamamoto, T.; Sugiyama, K.; Kushida, T.; Inoue, T.; Kanbara, T. *J. Am. Chem. Soc.* **1996**, *118*, 3930–3937.

14. Saito, N.; Kanbara, T.; Nakamura, Y.; Yamamoto, T. *Macromolecules* **1994**, *27*, 756–761.

15. Wen, L.; Duck, B. C.; Dastoor, P. C.; Rasmussen, S. C. *Macromolecules* **2008**, *41*, 4576.

16. Jin, Y.; Kim, K.; Park, S. H.; Song, S.; Kim, J.; Jung, J.; Lee, K.; Suh, H. *Macromolecules* **2007**, *40*, 6799–6806.

17. Greenham, N. C.; Moratti, S. C.; Bradley, D. D. C.; Friend, R. H.; Holmes, A. B. *Nature* **1993**, *365*, 628–630.

18. Tu, G.; Li, H.; Forster, M.; Heiderhoff, R.; Sigel, R.; Balk, L.; J.; Scherf, U. *SMALL* **2007**, *3*, 1001–1006.

19. Scherf, U.; Adamczyk, S.; Gutacker, A.; Koenen, N. *Macromol. Rapid Commun.* **2009**, *30*, 1059–1065.

20. Yokoyama, A.; Miyakoshi, R.; Yokozawa, T. *Macromolecules* **2004**, *37*, 1169–1171.

21. Zhang, Y.; Tajima, K.; Hirota, K.; Hashimoto, K. *J. Am. Chem. Soc.* **2008**, *130*, 7812–7813.

22. Javier, A. E.; Varshney, S. R.; McCullough, R. D. *Macromolecules* **2010**, *43*, 3233–3237.

23. Ohshimizu, K.; Ueda, M. *Macromolecules* **2008**, *41*, 5289–5294.

24. Wu, P.-T.; Ren, G.; Li, C.; Mezzenga, R. Jenekhe, S. A. *Macromolecules* **2009**, *42*, 2317–2320.

25. Miyakoshi, R.; Yokoyama, A.; Yokozawa, T. *Chem. Lett.* **2008**, *37*, 1022–1023.

26. Yokoyama, A.; Kato, A.; Miyakoshi, R.; Yokozawa, T. *Macromolecules* **2008**, *41*, 7271–7273.

27. *Organic Photovoltaics, Mechanisms, Materials and Devices*; Sun. S.-S.; Sariciftci, N. S.; CRC Press: New York, 2005.

28. Yamamoto, T.; Sugiyama, K.; Kushida, T.; Inoue, T.; Kanbara, T. *J. Am. Chem. Soc.* **1996**, *118*, 3930–3937.

29. Neto, B. A. D.; Lopes, A. S. A.; Edeling, G.; Gonçalves, R. S.; Costa, V. E. U.; Quina, F. H.; Dupont, J. *Tetrahedron* **2005**, *61*, 10975-10982.

30. Senkovskyy, V.; Khanduyeva, N.; Komber, H.; Oertel, U.; Stamm, M.; Kuckling, D.; Kiriy, A. *J. Am. Chem. Soc.* **2007**, *129*, 6626-6632.

31. Yokoyama, A.; Miyakoshi, R.; Yokozawa, T. *Macromolecules* **2004**, *37*, 1169-1171.

32. Miyakoshi, R.; Yokoyama, A.; Yokozawa, T. *J. Am. Chem. Soc.* **2005**, *127*, 17542-17547.

33. Liu, J.; Loewe, R. S.; McCullough, R. D. *Macromolecules* **1999**, *32*, 5777–5785.

34. Beryozkina, T.; Senkovskyy, V.; Kaul, E.; Kiriy, A. *Macromolecules* **2008**, *41*, 7817–7823.

35. Smeets, A.; Van den Bergh, K.; Winter, J. D.; Gerbaux, P.; Verbiest, T.; Koeckelberghs, G. *Macromolecules* **2009**, *42*, 7638–7641.

36. Doubina, N.; Ho, A.; Jen, A. K-Y; Luscombe, C. K. *Macromolecules* **2009**, *42*, 7670–7677.

37. Senkovskyy, V.; Khanduyeva, N.; Komber, H.; Oertel, U.; Stamm, M.; Kuckling, D.; Kiriy, A. *J. Am. Chem. Soc.* **2007**, *129*, 6626–6632.

38. McCullough, R. D. *Adv. Mater.* **1998**, *10*, 93-116.

39. Tsami, A.; Bunnagel, T. W.; Farrell, T.; Scharber, M.; Choulis, S. A.; Brabec, C. J.; Scherf, U. *J. Mater. Chem.* **2007**, *17*, 1353-1355.

40. Tu, G.; Li, H.; Forster, M.; Heiderhoff, R.; Balk, L. J.; Scherf, U. *Macromolecules* **2006**, *39*, 4327–4331.

41. Wu, P.-T.; Ren, G.; Kim, F.; Li, C.; Mezzenga, R.; Jenekhe, S. A. *J. Poly. Sci Part A*, **2010**, *48*, 614–626.

42. McCullough, R. D., *Adv. Mater.* **1998**, *10*, 93–116.

43. Zhang, Y.; Tajima, K.; Hirota, K.; Hashimoto, K. *J Am. Chem. Soc.* **2008**, *130*, 7812–7813.

CHAPTER 5: PREPARATION OF DONOR-ACCEPTOR BLOCK COPOLYMERS BY CHAIN-GROWTH CATALYST TRANSFER CONDENSATION POLYMERIZATION

5.1. Introduction

The majority of research on conjugated polymers to-date has focused on homopolymers and alternating copolymers.[1] Much less studied are all-conjugated block copolymers. This can be attributed to the challenges in synthesizing these types of materials. The few reports of fully conjugated block copolymers suggest that these materials present interesting opportunities to impart new properties as a result of phase separation of the two blocks with formation of morphologies which may be advantageous in new applications.[2]

Rod-coil block copolymers comprised of a conjugated and a flexible segment have been prepared by a chain extension reaction where a pre-prepared end-functionalized conjugated polymer serves as a macroinitiator in a subsequent polymerization.[3-7] However, the living addition polymerizations used to synthesize these types of materials are not suitable for the preparation of fully conjugated block copolymers. Conjugated polymers are often prepared by condensation polymerizations of dihaloarenes and difunctional monomers such as stannanes,[8] organozinc reagents,[9] boronate esters[10], and phosphonantes.[11] Condensation polymerizations typically proceed with step-growth kinetics that leads to materials with polydispersity index (PDI) of greater than 2.[12] As described in Chapter 1, step-growth processes do not lend themselves to formation of well-defined block copolymers. Advances in synthetic methodologies are required to provide access to well-defined block polymers which might aid in exploiting the potential of these

materials in organic electronic applications. Of particular interest is the possiblity of forming donor-acceptor block copolymers that might be useful in the development of nanostructured dual-channel heterojunction devices.

In Chapter 4 we described a new synthetic route to prepare fully-conjugated donor-acceptor block copolymers by coupling a difunctional electron accepting conjugated polymer to a monofunctional telechelic poly(3-alkylthiophene) (PAT) with a single bromine end group. However there are some disadvantages associated with the coupling chemistry used to prepare the block copolymers in this study. While the individual polymers are well-defined materials, they must be synthesized separately and purified, and post-polymerization modifications are required (i.e. metalation of the chain ends of one of the polymers) before the chains can be coupled together. If the subsequent coupling reaction does not go to high conversion, or if there is a stoichiometric imbalance of the two polymers in the reaction mixture, there will be unreacted homopolymer impurities which may be difficult to separate from the block copolymers.

The well-defined PAT used in the study above was prepared by utilizing the catalyst-transfer condensation polymerization (CTCP) of 5-bromo-2-thienylmagnesium iodide. This polymerization proceeds by a chain growth mechanism whereby the nickel stays associated with the living chain end, which is analagous to a living polymerization. An important attribute of living polymerizations is the ability to form block copolymers by the sequential addition of monomers in a one-pot reaction. In 2008, Hashimoto and coworkers reported the first example of a one-pot synthesis of a fully conjugated diblock conjugated polymer by utilizing CTCP.[13] In this study, sequential addition of 5-bromo-2-thienylmagnesium iodides bearing hexyl and ethylhexyl side chains underwent polymerization to afford poly(3-

hexylthiophene)-*block*-poly(3-(2-ethylhexylthiophene), **P3HT-*b*-P3EHT**, Figure 5.1. Synthesis of a block copolymer in this manner provided control over the segment lengths (by variation of the amount of each monomer added), and each block has a narrow polydispesity as a result of the chain-growth mechanism. Characterization of the resulting polymer, **P3HT-*b*-P3EHT** revealed nanoscale segregation of the amorphous **P3EHT** blocks and the highly crystalline **P3HT** blocks. Varying the relative lengths of the two blocks produced different nanoscale morphologies. The polymerization is carried out in a one-pot reaction sequence, with no need to modify the individual blocks post polymerization.

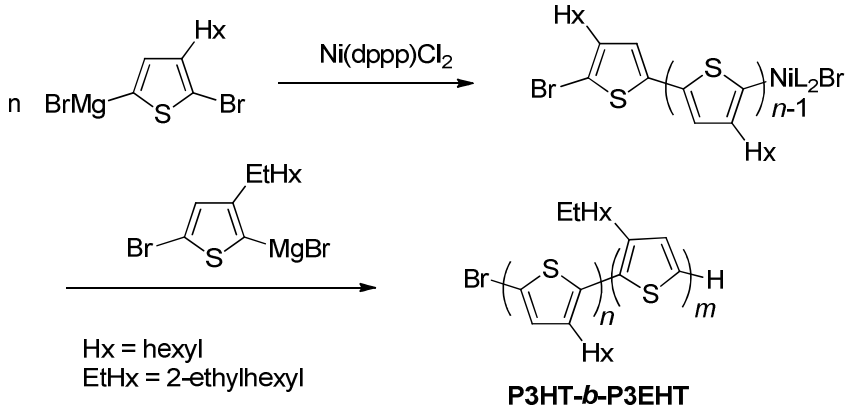

Figure 5.1. One-pot synthesis of a fully conjugated diblock conjugated polymer, poly(3-hexylthiophene)-*block*-poly(3-(2-ethylhexylthiophene).

Hashimoto's initial report was soon followed by publications from Ueda describing a block copolythiophene consisting of crystalline poly(3-hexylthiophene and amorphous poly(3-phenoxymethylthiophene blocks),[14] and from Jenekhe reporting (poly(3-butylthiophene)-*block*-poly(3-octylthiophene).[15] In the latter case the segments undergo microphase separation to form nanostructured materials even

though both blocks are crystalline. The CTCP synthetic method has also been applied to prepare block copolymers containing polyphenylene,[16] polyfluorene[17] and polypyrolle[18] segments.

The quasi-living nature of these polymerizations mean that the segment lengths of the block copolymers can be controlled, and the resulting polymers have narrow polydispersities. Other advantages of this method to prepare block copolymers are that the process is performed in a one-pot reaction and there is no need to perform post-polymerization modifications of the individual blocks. However, these reports are limited to conjugated blocks that have low-electron affinity (i.e. electron donating materials which are only p-channel semiconductors). Expansion of this method to the preparation of donor-acceptor block copolymers would provide access to materials that would have interesting electronic properties and may prove useful in organic electronic applications. Herein, we explore the use of a one-pot, chain growth catalyst-transfer condensation polymerization to prepare donor-acceptor diblock copolymers.

For our initial studies in this area, we have selected to use poly(3-alkylthiophene) as the electron rich block and poly(thieno[3,4-*b*]pyrazine) as the electron poor block. The preparation of poly(3-alkylthiophene) by chain growth condensation polymerizations is well-established,[19] and this polymer is commonly employed in devices such as bulk heterojunction solar cells as an electron donor.[20] The acceptor poly(thieno[3,4-*b*]pyrazine) block has a low-band gap (E_g = 0.93 eV) and high electron affinity (E_{red} = -0.90 V vs Ag wire).[21] The preparation of poly(thieno[3,4-*b*]pyrazine) has also been described using the catalyst transfer condensation polymerization.[21]

5.2. Experimental

5.2.1. General Synthetic Methods

All starting materials were purchased from commercial sources and used without further purification unless otherwise stated. THF and Et_2O were dried over sodium benzophenone ketyl prior to distillation under argon. Column chromatography was performed on flash grade silica (32-60 Å, Sorbent Technologies, Atlanta, GA). NMR analysis was performed on a Bruker DSX 300 instrument using $CDCl_3$ as the solvent. Chemical shifts are referenced to internal tetramethylsilane. ^{13}C NMR are proton decoupled. IR analyses were performed on a Nicolet 4700 FTIR with an ATIR attachment from Smart-Orbit Thermoelectronic Corporation. GPC analyses were performed on a Waters 2690 Separations Module with a Waters 2410 refractive index detector at a flow rate of 1 mL/min. Elemental analyses were performed by Atlantic Microlab, Inc. (Norcross, GA). The synthesis and characterization of diketone **V-1b** is provided in Chapter 4. The synthesis and characterization of all other compounds is provided below, and the ^{1}H and ^{13}C NMR, IR spectra and EI mass spectra can be found in Appendix E.

5.2.2. Synthesis of Thienopyrazine Monomers

Synthetic procedures and characterization of the monomers in Figure 5.2. and diketones in Figure 5.3. are given below. Compounds **V-1a**[22] and **V-2**[23] were synthesized according to literature procedures. Compounds **V-3** and **V-4** were synthesized by modification of literature procedures.[21,24]

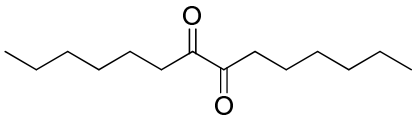

Tetradecane-7,8-dione,[22] **V-1a.** 1-Bromohexane (17 mL, 0.12 mol) was added dropwise to a solution of magnesium turnings (3.5 g, 0.14 mol) in THF (300 mL) to prepare the Grignard reagent. After the addition was complete, the mixture was placed in a sonicator for 1 hour. LiBr (20.8, 0.239 mol) was added to a solution of CuBr (17.2 g, 0.119 mol) and THF (200 mL) in a dry 1 L three neck flask, and the mixture was cooled to -96 °C in a pentane/liquid nitrogen bath. The solution of the Grignard reagent was added dropwise to the mixture over 2 hours. Oxalyl chloride (6.0 g, 47 mmol) was added to the solution dropwise and the mixture was allowed to slowly warm to room temperature, and then poured into saturated aqueous ammonium chloride (1000 mL). The mixture was extracted with Et_2O (4 x 500 mL). The organic extracts were combined and the solvent was removed under reduced pressure. The resulting residue was purified by column chromatography (30:70 v/v CH_2Cl_2:hexanes) to afford diketone **V-1a** as a yellow liquid (5.6 g, 52%).^{1}H NMR (300 MHz, $CDCl_3$) δ 2.72 (t, $^3J_{HH}$ = 7.5 Hz, 4H, C6 and C9 CH_2), 1.54-1.60 (m, 4H, C5 and C10 CH_2), 1.25-1.34 (m, 12H), 0.87 (t, $^3J_{HH}$ = 6.6 Hz, 6H, $–CH_3$). ^{13}C NMR (75 MHz, $CDCl_3$) δ 200.18 (C=O), 36.08, 31.50, 28.80, 22.99, 22.45, 14.12. IR (ATIR): 2919, 2854, 1704 (C=O str.), 1456, 1378, 1135, 763, 694, 688, 588 cm^{-1}.

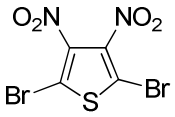

2,5-Dibromo-3,4-dinitrothiophene,[23] **V-2.** Sulfuric acid (100 mL) was added to a ventilated three neck flask equipped with an addition funnel. Fuming sulfuric acid (20 %, 120 mL), and fuming nitric acid (90 %, 70 mL) were slowly added to the flask and cooled to 0 °C. 2,5-Dibromothiophene (50 g, 24 mL) was added dropwise to the solution over 1 h and the mixture was stirred at 0 °C for an additional 2 h. The reaction mixture was slowly poured over ice (500 g) to afford a yellow solid that was

collected by filtration. The solid was washed with DI water (400 mL) and dried under reduced pressure to afford 2,5-dibromo-3,4-dinitrothiophene, **V-2**, as a yellow solid (54 g, 79%): mp = 136-138 °C. ^{13}C NMR (75 MHz, $CDCl_3$) δ 122.44 (C3 and C4), 113.73 (C2 and C5). IR (ATIR): 1529, 1490, 1452, 1342, 1311, 1072, 898, 746, 732, 663, 490. HRMS *calc.* for $C_4Br_2N_2O_4S$ = 329.7946, *obs.* = 329.7968, Δ = 6.7 ppm.

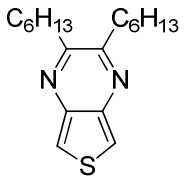

2,3-Dihexylthieno[3,4-b]pyrazine, V-3a. To a solution of 2,5-dibromo-3,4-dinitrothiophene **V-2** (10.2 g, 30.7 mmol) in concentrated HCl (150 mL) at 0 °C, tin powder (25 g, 0.21 mol) was added in small portions over 1 h and the reaction was stirred at 0 °C for 24 h. The resulting mixture was filtered and the recovered solid was washed with cold Et_2O (20 mL) and cold acetonitrile (20 mL). The resulting colorless solid was imediately added to EtOH (100 mL) and a mixture of KOH in EtOH was added dropwise until all of the white solid had dissolved. Diketone **V-1a** (3.48 g, 15.4 mmol) was added to the solution and the mixture was stirred overnight. The solvent was removed under reduced pressure and the resulting residue was purified by column chromatography (60:40 v/v CH_2Cl_2:hexanes) to afford thienopyrazine **V-3a** as a tan solid (2.5 g, 53 %) which is unstable in light and air. ^{1}H NMR (300 MHz, $CDCl_3$) δ 7.80 (s, 2H, thienopyrazine C-H), 2.89 (t, $^3J_{HH}$ = 7.8 Hz, 4H, Ar-CH_2–), 1.73-1.83 (m, 4H), 1.25-1.48 (m, 12H), 0.90 (t, $^3J_{HH}$ = 7.2 Hz, 6H, –CH_3). ^{13}C NMR (75 MHz, $CDCl_3$) δ 158.15, 139.31, 103.07, 35.33 (Ar-CH_2), 31.65, 29.23, 27.91, 22.58, 14.07 cm^{-1}.

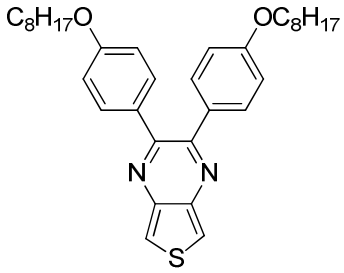

2,3-Bis(4-(octyloxy)phenyl)thieno[3,4-b]pyrazine, V-3b. To a solution of 2,5-dibromo-3,4-dinitrothiophene **V-2** (7.1 g, 21 mmol) in HCl (90 mL) at 0 °C, tin powder (15 g, 0.13 mol) was added in small portions over 1 h and the reaction was stirred at 0 °C for 24 h. The resulting mixture was filtered and the recovered solid was washed with cold Et_2O (20 mL) and cold acetonitrile (20 mL). The resulting white solid was added to EtOH (100 mL) and a mixture of KOH in EtOH was added dropwise until all of the white solid dissolved in the solution. Diketone **V-1b** (3.0 g, 6.4 mmol) was added to the solution and the mixture was stirred overnight. The solvent was removed under reduced pressure and the resulting residue was purified by column chromatography (90:10 v/v CH_2Cl_2:hexanes) to afford thienopyrazine **V-3b** as a tan solid (2.6 g, 69%) which decomposed at 72 °C. ^{1}H NMR (300 MHz, $CDCl_3$) δ 7.96 (s, 2H, thienopyrazine C–H), 7.37 (d, $^3J_{HH}$ = 8.7 Hz, 4H, Ar C2-H and C6-H), 6.82 (d, $^3J_{HH}$ = 8.7 Hz, 4H, Ar C3-H and C5-H), 3.96 (t, $^3J_{HH}$ = 6.6 Hz, 4H, –OCH_2–), 1.73-1.80 (m, 4H), 1.28-1.46 (m, 20H), 0.89 (t, $^3J_{HH}$ = 6.6 Hz, 6H, –CH_3). ^{13}C NMR (75 MHz, $CDCl_3$) δ 159.73, 153.03, 141.57, 131.54, 131.07, 116.82, 114.113, 68.01, 31.81, 29.38, 29.24, 29.20, 26.02, 22.67, 14.13. IR (ATIR): 2916, 2348, 1602, 1508, 1465, 1303, 1259, 1240 (C-O str.), 1172, 1007, 966, 829, 788, 736, 590, 541 cm^{-1}. HRMS *calc.* for $C_{34}H_{44}N_2O_2S$ = 544.1233, *obs.* = 544.1245, Δ = 2.4 ppm.

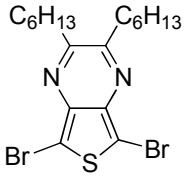

5,7-Dibromo-2,3-dihexylthieno[3,4-b]pyrazine, V-4a. A solution of *N*-bromosuccinimide (1.47 g, 8.25 mmol) in anhydrous DMF (10 mL) was added dropwise by syringe to a solution of thienopyrazine **V-3a** (1.0 g, 3.3 mmol) in DMF (40 mL) at -78 °C. The mixture was allowed to warm slowly to -15 °C and stirred at this temperature for 4 h. The reaction mixture was filtered and the recovered solid was washed with cold water (100 mL). The solid was subjected to column chromatography (10:90 v/v EtOAc:hexanes) to afford the thienopyrazine monomer **V-4a** as a yellow solid (1.05 g, 70 %), which decomposed at 50 °C and was not stable in light and air. ^{1}H NMR (300 MHz, $CDCl_3$) δ 2.89 (t, $^{3}J_{HH}$ = 7.5 Hz, 4H, Ar-CH_2–), 1.72-1.84 (m, 4H), 1.35-1.47 (m, 12H), 0.90 (t, $^{3}J_{HH}$ = 7.2 Hz, 6H, –CH_3). ^{13}C NMR (75 MHz, $CDCl_3$) δ 158.13, 139.30, 102.23, 35.32, 31.64, 29.22, 27.90, 22.57, 14.06.

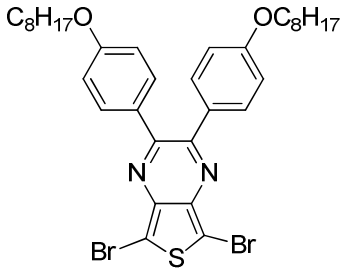

5,7-Dibromo-2,3-bis(4-(octyloxy)phenyl)thieno[3,4-b]pyrazine, V-4b. A solution of *N*-bromosuccinimide (1.45 g, 8.15 mmol) in anhydrous DMF (10 mL) was added dropwise by syringe to a solution of thienopyrazine **V-3b** (1.77 g, 3.25 mmol) in DMF (50 mL) at -78 °C. The mixture was allowed to warm slowly to -15 °C and stirred at this temperature for 24 h. The reaction mixture was filtered and the recovered solid was washed with cold water (100 mL). The resulting solid was subjected to column chromatography (30:70 v/v CH_2Cl_2:hexanes) to afford the

thienopyrazine monomer **V-4b** as a yellow solid (1.63 g, 71 %), decomposed at 128-130 °C. ^{1}H NMR (300 MHz, $CDCl_3$) δ 7.45 (d, $^{3}J_{HH}$ = 8.7 Hz, 4H, Ar C2-H and C6-H), 6.82 (d, $^{3}J_{HH}$ = 9 Hz, 4H, Ar C3-H and C5-H), 3.96 (t, $^{3}J_{HH}$ = 6.6 Hz, 4H, –OCH_2–), 1.73-1.80 (m, 4H), 1.29-1.47 (m, 20H), 0.89 (t, $^{3}J_{HH}$ = 6.6 Hz, 6H, –CH_3). ^{13}C NMR (75 MHz, $CDCl_3$) δ160.29, 154.27, 139.20, 131.42, 130.65, 114.13, 91.57, 68.07, 34.65, 31.80, 29.23, 26.00, 25.26, 22.65 (2 coincident CH_2 peaks), 14.11. IR (ATIR): 2911, 2846, 1598, 1463, 1392, 1245 (C-O str.), 1176, 998, 973, 823, 721, 609, 512, 516 cm^{-1}. HRMS *calc.* for $C_{34}H_{42}Br_2N_2O_2S$ = 700.1334, *obs.* = 700.1353, Δ = 2.7 ppm. Elemental Analysis: Theoretical: C, 58.12%; H, 6.03%; N, 3.94%; S, 4.56%; Found: C, 58.17%; H, 6.15%; N, 3.96%; S, 4.63%.

5.2.3. Synthesis of Homopolymers and D-A Block copolymers

Synthetic procedures and spectroscopic data for poly(3-octylthiophene) and poly(thieno[3,4-b]pyrazine) homopolymers and a sample experimental for the synthesis of blcok copolymers containing poly(3-octylthiophene) and poly(thieno[3,4-b]pyrazine) segments is provided below

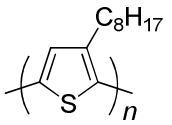

Poly(3-octylthiophene), P3OT. *i*-Propylmagnesium chloride (2 M in THF, 1.58 mL, 3.16 mmol) was added to a solution of 2-bromo-5-iodo-3-octylthiophene (1.21 g, 3.01 mmol) in anhydrous THF (11 mL) at 0 °C. After stirring for 15 min the solution was allowed to warm to room temperature. A suspension of Ni(dppp)Cl_2 (33 mg, 60 μmol) in anhydrous THF (14 mL) was added to the solution and the mixture was stirred for 4 h. The mixture was poured into MeOH (100 mL) and the resulting

precipitate was sequentially extracted in a Soxhlet extractor with acetone, hexanes and chloroform and the solvent was removed from the chloroform fraction to afford **P3OT** as a purple solid in the chloroform extracted fraction (458 mg, 78 %). GPC (THF, UV-vis detector): 13.4 kDa, PDI = 1.27. ^{1}H NMR (300 MHz, $CDCl_3$) δ 6.98 (br s, 1H, Ar C-H), 2.79-2.83 (m, 2H, Ar-CH_2–), 1.68-1.73 (m, 2H) 1.35-1.50 (m, 10H), 0.90-0.94 (m, 3H, –CH_3). IR (ATIR): 2910, 2844, 1419, 1371, 1033, 813, 664, 609, 545 cm^{-1}.

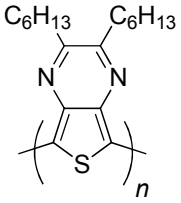

Poly(2,3-dihexylthieno[3,4-*b*]pyrazine), PThPy(C6). *i*-Propylmagnesium chloride (2 M in THF, 1.52 mL, 3.14 mmol) was added to a solution of thienopyrazine **4a** (1.38 g, 2.99 mmol) in anhydrous THF (20 mL) and the mixture was stirred for 1 h at room temperature. A suspension of Ni(dppp)Cl_2 (0.03 g, 0.06 mmol) in anhydrous THF (10 mL) was added to the solution and the mixture was stirred for 2 h. The mixture was poured into MeOH (100 mL) and the resulting precipitate was sequentially extracted in a Soxhlet extractor with acetone, hexanes and chloroform. The solvent was removed from the chloroform fraction to afford **PThPy(C6)** as a black solid (0.79 g, 88 %). GPC (THF, UV-vis detector): 6.4 kDa, PDI = 1.49. ^{1}H NMR (300 MHz, $CDCl_3$) δ 2.70-2.98 (m, 4H, Ar-CH_2–), 1.26-1.79 (m, 24H), 0.85-0.91 (m, 6H, –CH_3). IR (ATIR): 2908, 2848, 1625, 1509, 1384, 1374, 1226, 1085, 923, 833, 686, 482 cm^{-1}.

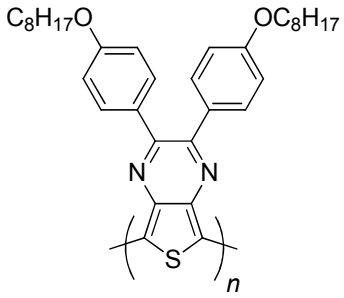

Poly(2,3-bis(4-(octyloxy)phenyl)thieno[3,4-*b*]pyrazine), **PThPy(ArC8).**

i-Propylmagnesium chloride (2 M in THF, 0.48 mL, mmol) was added to a solution of thienopyrazine **4b** (0.638 g, 0.91 mmol) in anhydrous THF (18 mL) and stirred for 1 h at room temperature. A suspension of Ni(dppp)Cl_2 (0.005 g, 0.01 mmol) in anhydrous THF (24 mL) was added to the solution and the mixture was allowed to stir for 2 h and the mixture was poured into MeOH (100 mL). The resulting precipitate was sequentially extracted in a Soxhlet extractor with acetone, hexanes and chloroform to afford **PThPy(ArC8)** as a black solid in the chloroform extracted fraction (0.338 g, 68.9 %). GPC (THF, UV-vis detector) chloroform fraction: 15.6 kDa, PDI= 1.92. ^{1}H NMR (300 MHz, $CDCl_3$) δ 7.81 (br, 4H, Ar C-H), 6.58 (br, 4H, Ar C-H), 3.82 (br, 4H, –OCH_2–), 1.63-1.80 (m, 4H), 1.21-1.53 (m, 20H), 0.90 (br, 6H, –CH_3). IR (ATIR): 2911, 2842, 1614, 1598, 1494, 1384, 1378, 1288, 1211, 1151, 948, 800, 647, 559, 470 cm^{-1}.

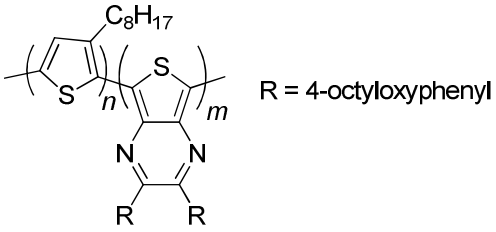

Poly(3-octylthiophene)-*block*-poly(thieno[3,4-*b*]pyrazine), BCP2.

Isopropylmagnesium chloride (2 M in THF, 0.55 mL, 1.10 mmol) was added to a solution of thienopyrazine **4b** (0.74 g, 1.05 mmol) in anhydrous THF (20 mL) and the mixture was stirred for 1 h at room temperature (Solution A). In a separate flask,

isopropylmagnesium chloride (2 M in THF, 1.32 mL, 2.64 mmol) was added to a solution of 2-bromo-5-iodo-3-octylthiophene (1.02 g, 2.51 mmol) in anhydrous THF (12 mL) at 0 °C (Solution B). After 15 min the solution was allowed to warm to room temperature. A suspension of Ni(dppp)Cl_2 (0.005 g, 0.01 mmol) in anhydrous THF (12 mL) was added to the solution containing the 5-bromo-2-thienylmagnesium iodides and the mixture was allowed to stir for 25 min at room temperature. A 12 mL portion of the reaction mixture was removed by syringe and poured into MeOH (50 mL) and charaterized as the P3OT prepolymer. To the remaining mixture, the solution containing (7-bromo-thieno[3,4-*b*]pyrazin-5-yl)magnesium bromide was added to the mixture in one portion and the mixture was allowed to stir for 30 min, and poured into MeOH (100 mL). The resulting precipitate was sequentially extracted in a Soxhlet extractor with acetone, hexanes and chloroform and the solvent was removed from the chloroform fraction to afford **BCP2** as a black solid (0.68 g, 64 %). GPC (THF, UV-vis detector): 17.2 kDa, PDI = 1.32. ^{1}H NMR (300 MHz, $CDCl_3$) δ 7.60 (br, 4H), 6.98 (br s, 1H), 6.81 (br, 4H), 4.03 (m, 4H, –OCH_2–), 2.78 (m, 2H thiophene-CH_2), 1.68-1.76 (m 6H), 1.29-1.42 (m, 30H), 0.87-0.88 (m, 9H). IR (ATIR): 2902, 2840, 1668, 1599, 1492, 1374, 1334, 1288, 1240, 1164, 1027, 1008, 788, 667, 549, 507 cm^{-1}.

5.3. Results and Discussion

5.3.1. Monomer Synthesis

The synthesis of the monomers used in this study proceeds by condensation of diketone **V-1** with 3,4-diaminothiophene, followed by bromination of the thienopyrazine, Figure 5.2.

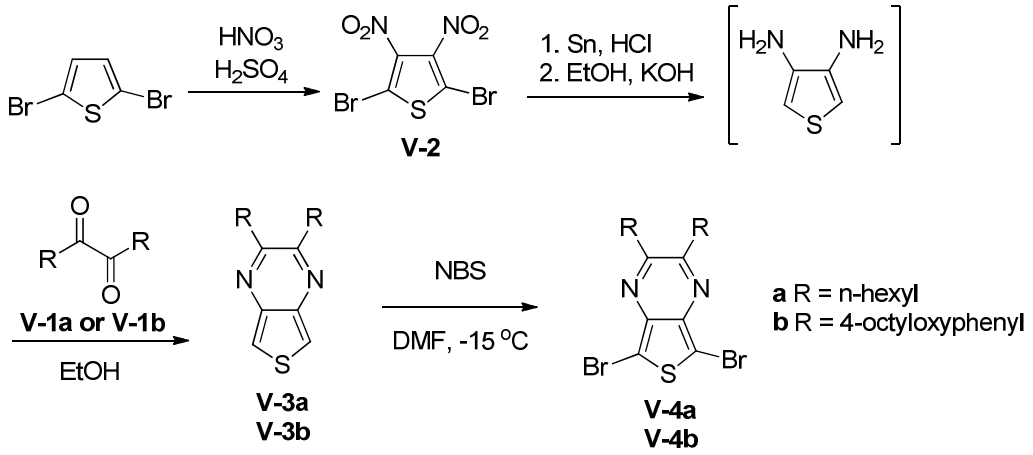

Figure 5.2. Synthesis of alkoxyl and aryl substituted dibromothieno[3,4-*b*]pyrazine monomers.

The two diketones used in the monomer synthesis, tetradecane-7,8-dione, **V-1a**,[22] and 1,2-bis(4-(octyloxy)phenyl)ethane-1,2-dione, **V-1b**,[25] were prepared by modifications of published procedures. Diketone **V-1a** was prepared from reaction of oxalyl chloride with the organocuprate generated in-situ from 1-hexylmagnesium bromide, Figure 5.3. A Williamson ether reaction was used to alkylate 1,2-bis(4-hydroxyphenyl)ethane-1,2-dione to provide diketone **V-1b**.

The synthesis of the thienopyrazine monomer begins with the nitration of 2,5-dibromothiophene to afford 2,5-dibromo-3,4-dinitrothiophene (**V-2**) which is then reduced with tin and HCl to provide thiophene-3,4-diamine, Figure 5.2. Due to the instability of this compound in light and air it was immediately used in the subsequent condensation reactions with diketones **V-1a** and **V-1b** to give thienopyrazines **V-3a** and **V-3b**, respectively. Bromination of thienopyrazines **V-3** using *N*-bromosuccinimide provided the thienopyrazine dibromides, **V-4a** and **V-4b**.

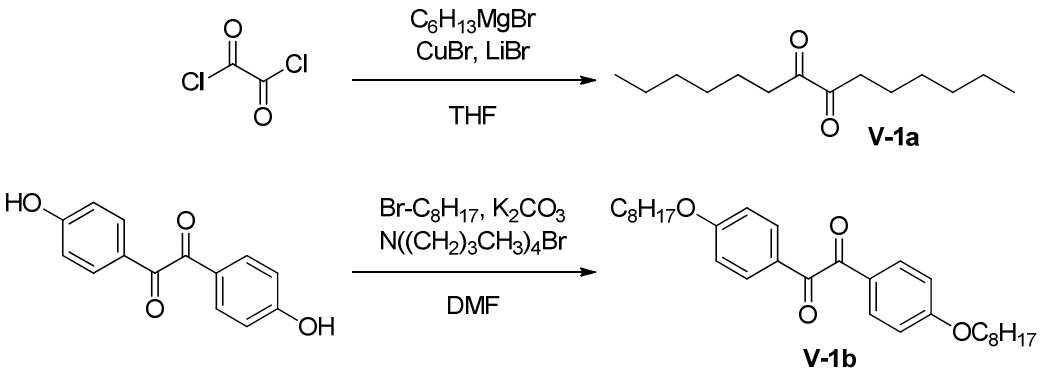

Figure 5.3. Synthesis of diketones used in the preparation of thienopyrazine monomers.

We found that in contrast to initial reports where the 5,7-dibromothieno[3,4-b]pyrazine **V-4a** was simply precipitated by adding the reaction mixture to water to afford a green solid that was used directly in the polymerization,[22] purification of the dibromothieno[3,4-b]pyrazine monomer by column chromatography removes impurities and yields a bright yellow solid. The thienopyrazine compounds **V-3a** and **V-4a** containing alkyl side chains (R = *n*-C_6H_{13}) had to be used immediately after purification, as they are unstable in light and air. However, we found that the aryl substituted thienopyrazines **V-3b** and **V-4b** were stable and could be purified and then stored for weeks at a time, indicating aromatic units directly attached to the thienopyrazine unit leads to improved stability to oxidation.

5.3.2 Homopolymer Synthesis

The catalyst-transfer condensation polymerization of (7-bromo-thieno[3,4-*b*]pyrazin-5-yl)magnesium bromides was first reported by Rasmussen and coworkers in 2008.[22] However, NMR analysis of the resulting polythieno[3,4-b]pyrazines in this study revealed that the isolated materials were low molecular weight oligomers. In

order to use this method to prepare block copolymers, it was first necessary to optimize the conditions for the polymerization of the thienopyrazine homopolymer. We found that removing impurities from the monomer by column chromatography prior to polymerization is crucial to obtaining higher molecular weight polymers using this method. Treatment of a 0.02 M THF solution of the purified monomer **V-4** with 1.05 equivalent of isopropylmagnesium chloride in a followed by addition of 1 mol % Ni(dppp)Cl_2, dppp = 1,2-bis(diphenyl-phosphimo)propane, resulted in polythieno[3,4-*b*]pyrazines, Figure 5.4. The molecular weights of the resulting polymers are summarized in Table 5.1. Poly(thieno[3,4-b]pyrazine)s with hexyl side chains (R = C_6H_{13}), **PThPy(C6)**, and aryl side chains (R = 4-octyloxyphenyl), **PThPy(ArC8)**, had a molecular weight of 6.4 kDa and 15.6 kDa, respectively. In both cases, the degree of polymerization is limited by solubility, as the polymers begin to precipitate from the solution within one hour of catalyst addition. Impurities from the polymerization, including unreacted monomer and low molecular weight oligomers, were removed from the polymer by washing with acetone and hexanes in a Soxhlet extractor. Subsequent extraction of the remaining solid into chloroform afforded the PThPy homopolymers. The instability of the alkyl substituted thienopyrazine **V-4a** required that this monomer be used immediately upon isolation for the polymerization to be successful. Thus, for convenience, we explored the use of the aryl substituted thienopyrazine **V-4b** for the synthesis of block copolymers.

Poly(3-octylthiophene), **P3OT**, was synthesized by the addition of 2% Ni(dppp)Cl_2 to a 0.1 M solution of 5-bromo-4-octyl-2-thienylmagnesium iodide in THF followed by precipitation of the polymer into a large volume of methanol. The polymer was purified by successive Soxhlet extractions with acetone, hexanes and

chloroform. The chloroform fraction contained **P3OT** which had a molecular weight of 13.4 kDa and a PDI of 1.27, Table 5.1.

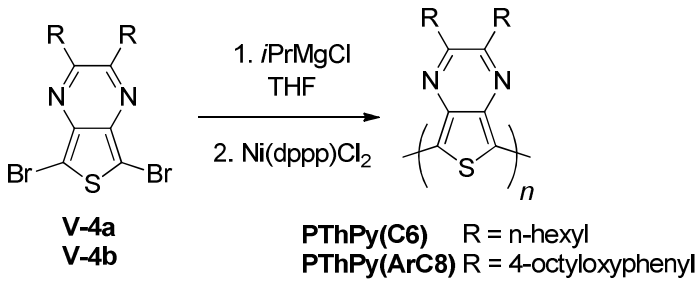

Figure 5.4. Synthesis of polythieno[3,4-*b*]pyrazine)s in this study.

Table 5.1. Molecular Weights and Polydispersity Indices of Homopolymers

Polymer	M_n[a,b] (kDa)	DP[b,c]	PDI[b,d]
P3OT	13.4	69	1.27
PThPy(C6)	6.4	21	1.49
PThPy(ArC8)	15.6	29	1.92

[a] Number average molecular weight (M_n). [b] Determined by gel permeation chromatography using polystyrene standards. [c] degree of polymerization. [d] Polydispersity index.

5.3.3. Synthesis of Block Copolymers

There are two possible pathways to consider for a one-pot polymerization of block copolymers consisting of poly(3-alkylthiophene) and poly(thieno[3,4-b]pyrazine) segments, Figure 5.5. Path A describes the initial polymerization of (7-bromo-thieno[3,4-*b*]pyrazin-5-yl)magnesium bromides followed by chain extension with 5-bromo-2-thienylmagnesium iodides, and in Path B the monomers are added in the reverse order.

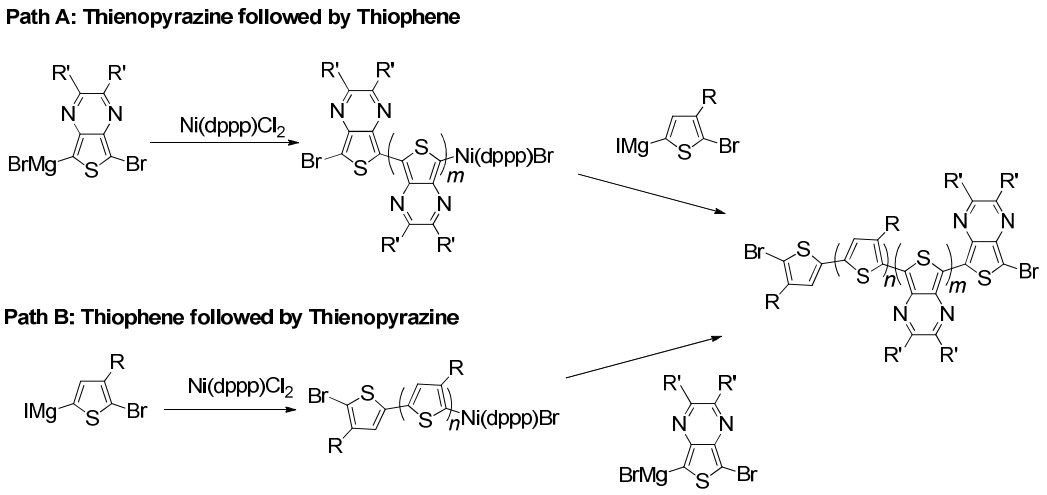

Figure 5.5. Possible synthetic pathways to block copolymers containing poly(3-alkylthiophene) and poly(thieno[3,4-b]pyrazine) segments.

It has previously been shown that the order of addition of monomers in the synthesis of block copolymers by catalyst-transfer condensation polymerization is important.[16] In order to form the second block by chain extension of the first block the nickel chain end must undergo reaction with the second monomer and then transfer to the new chain end without dissociation from the chain. The importance of the order of addition is illustrated in the block copolymerization of poly(3-alkylthiophene) and poly(*p*-phenylene).[16] It was shown that the phenylene monomer must be polymerized prior to the addition of the thiophene monomer; the reverse reaction produces polymer with broad molecular weight distribution and a multimodal GPC elution curve. The authors attribute the propensity of the reactive nickel endgroup to react with the second monomer to the π-donor ability of the monomer. The nickel more easily transfers from polymer endgroups with low π-donor to a monomer with high π-donor ability, but not the reverse. This would suggest that in the block copolymerization of poly(3-alkylthiophene) and poly(thieno[3,4-b]pyrazine), the thienopyrazine monomer

should be polymerized first, since it has a lower π-donor ability, (Path A, Figure 5.5). However, we found that when the poly(thieno[3,4-b]pyrazine) segment was prepared first the polymer precipitated prior to the addition of the thiophene monomer, and the second block was not formed.

We next studied the block copolymerization of the thiophene followed by the thienopyrazine monomer (Path B, Figure 5.5). In the initial experiment, Ni(dppp)Cl_2 was added to a solution of 5-bromo-2-thienylmagnesium iodides and allowed to stir at room temperature for one hour followed by addition of (7-bromo-thieno[3,4-*b*]pyrazin-5-yl)magnesium bromide prepared from **V-4b**. The **PThPy(ArC8)** segment was successfully polymerized by chain extension from the prepolymer as confirmed by the GPC elution curve. The polymer isolated after addition of the second ThPy monomer had a narrow molecular weight distribution and a higher molecular weight, Figure 5.6. This experiment indicates the successful transfer of the nickel complex to (7-bromo-thieno[3,4-*b*]pyrazin-5-yl)magnesium bromide without dissociation from the polymer chain, resulting in the formation of poly(3-octylthiophene)-*block*-poly(thieno[3,4-b]pyrazine), **BCP1**. The prepolymer had a molecular weight of 5.3 kDa and the block copolymer had a molecular weight of 12.7 kDa.

While the increase in molecular weight of the polymer after the addition of the second monomer supports the formation of a block copolymer in this experiment, the elution curve of the postpolymer also shows a small peak at 23 minutes that is similar to the elution time as the prepolymer, Figure 5.6. This suggests that some of the prepolymer does not initiate polymerization of the second monomer, possibly due to dissociation of the nickel from the chains end. In Chapter 4 we establish that the nickel complex slowly dissociates from the polymer backbone, especiallly if the

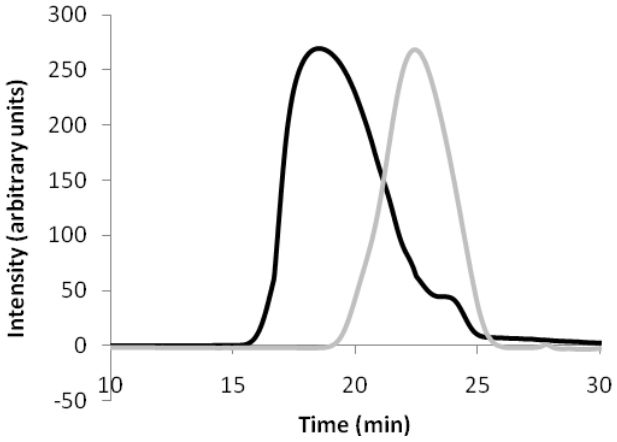

Figure 5.6. GPC elution curves of the poly(3-octylthiophene) prepolymer (gray line) and the postpolymer, poly(3-alkylthiophene)-*block*-poly(thieno[3,4-b]pyrazine), **BCP1** (black line).

polymerization is conducted for extended periods. Accordingly, using a shorter reaction time for the polymerization of the first monomer to minimize the amount of chain termination arising from the dissociation of nickel was investigated. A study of the conversion of monomer consumption versus time provides insight into the course of the polymerization, Figure 5.7. In this experiment, aliquots were taken from the polymerization mixture at various times and analyzed by ^{1}H NMR to compare the relative amounts of the polymer repeat units to unreacted monomer. A plot of monomer consumption versus time shows a linear increase, and then levels off as the concentration of the monomer decreases. From the shape of the curve for polymerization of 0.1 M 5-bromo-2-thienylmagnesium iodide in the presence of 2 mol % Ni(II), the rate of the polymerization slows considerably when approximately 70% of the monomer is consumed.

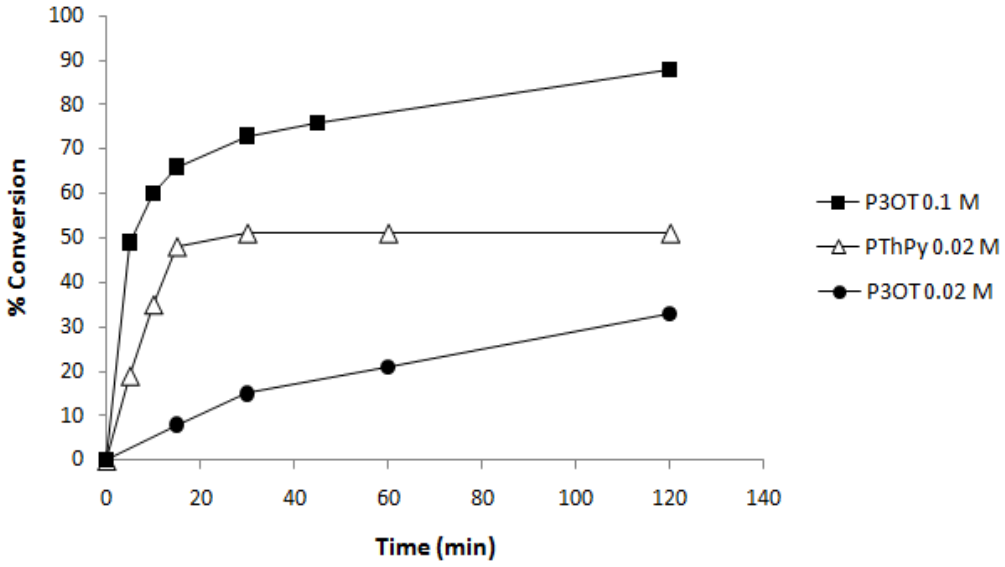

Figure 5.7. Conversion of monomer consumption versus time of **P3OT** at a concentration of 0.1 M (■) and 0.02 M (●) and of **PThPy(ArC8)** at a concentration of 0.02 M (Δ).

In a subsequent polymerization of the preparation of the block copolymers, we conducted the polymerization of 0.1 M 5-bromo-2-thienylmagnesium iodide for 25 min (corresponding to 70% monomer conversion). At this stage, a solution of (7-bromo-thieno[3,4-*b*]pyrazin-5-yl)magnesium bromide was added, diluting the concentration of the reaction to 0.02 M. At the point of addition, the remaining thiophene monomer was present in a concentration of 0.004 M, and the thienopyrazine monomer is present in a 7 fold excess. GPC analysis of the resulting polymerization revealed the first polythiophene block had a molecular weight of 12.9 kDa and the block copolymer had a molecular weight of 17.2 kDa (**BCP2**). To determine if the second block is a mixture of the two active monomers remaining in the solution or exclusively made up of thienopyrazine units, we explored the rates of the polymerization 0.02 M solutions of each of the monomers for a comparison of the

relative rates, Figure 5.7. The conversion of monomer versus time of **PThPy(ArC8)** proceeds at a much faster rate than the thiophene monomer at the same concentration. Taken together with the relative concentration of the two monomers after addition of thienopyrazine to the reaction, it is unlikely that thiophene defects are present in the second block.

To verify this assumption, we carried out a test reaction in which Ni(dppp)Cl_2 was added to a solution containing equimolar amounts of the thieophene and thienopyrazine monomers. After 30 min the mixture was poured into MeOH and the precipitated polymer was washed with acetone to remove unreacted monomers. The composition of the polymer was determined by ^{1}H NMR analysis by comparing the integrals of the peaks corresponding to the α-methylene of the octyl side chains on the thiophene repeat units (2.5 ppm) and the oxymethylene unit on the ThPy repeat units (3.8 ppm). The analysis revealed that only a trace amount of thiophene monomer is incorporated into the polymer. Accordingly, this supports the assumption that there would be little incorporation of thiophene defects in the second block of the copolymer.

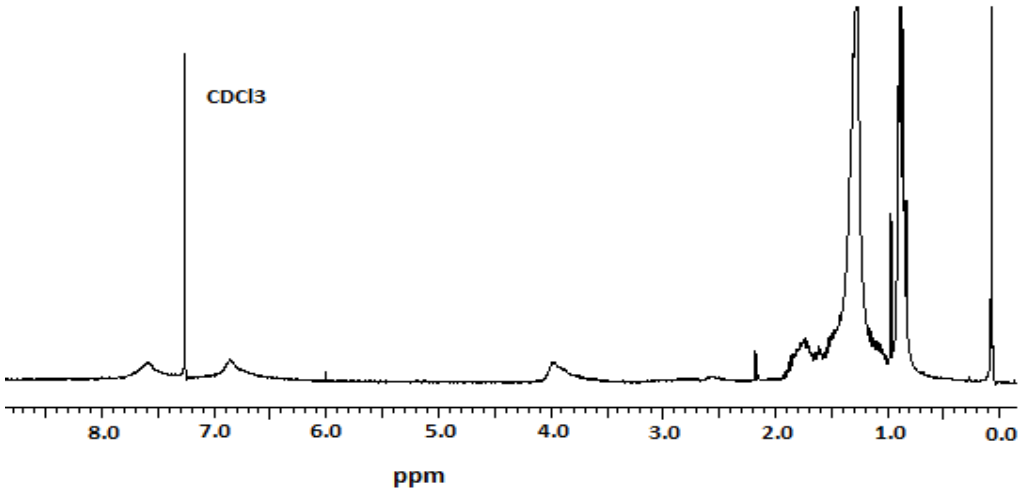

Figure 5.8. ^{1}H NMR of polymerization of an equimolar solution of the thienopyrazine and thiophene monomers.

We prepared several block copolymers using the optimized reaction conditions to explore the affect of monomer ratios and catalyst loading on the relative block lengths, Table 5.2. Using a 1:50:50 ratio of the catalyst, thiophene and thienopyrazine monomers provided a block copolymer with approximately 40 repeat units of **P3OT** and 10 repeat units of **PThPy(ArC8)** (**BCP2** and **BCP3**). The number of repeat units in the **P3OT** prepolymer was determined by ^{1}H NMR end group analysis of an aliquot of the polymerization prior to the addition of the second monomer. The integrals of the peaks for the β-protons of the two terminal thiophene rings which appear at δ 6.90 and 6.83 ppm were compared to that of the proton in the 4-position on the thiophene units in the backbone of the chain which occurs at δ 6.97 ppm, Figure 5.9 top. The length of the **PThPy(ArC8)** segment was determined by comparing the relative integral of the proton representing the peak corresponding to the protons of the thiophene backbone and that of the aryl protons on the thienopyrazine repeat units,

Table 5.2. Polymerization conditions[a] and Segment Lengths of Resulting Block Copolymers Determined by GPC and ^{1}H NMR

Block Copolymer	Polymerization of P3OT (min)	Ni(II): thiophene: Thienopyrazine	P3OT:PThPy length ratio[b,c]	P3OT:PThPy length ratio[c,d]
BCP1	60	1:25:25	23:14	19:9
BCP2	25	1:50:50	66:8	38:11
BCP3	25	1:50:50	54:11	37:8
BCP4	25	1:50:150	54:25	37:24

[a] Polymerization time after second monomer addition is 45 min in each experiment. [b]Determined by gel permeation chromatography using polystyrene standards. [c] Represents number of aryl repeat units. [d] Determined by ^{1}H NMR end group analysis.

which appear at δ 7.67 and 6.50 ppm, Figure 5.9 bottom. The oxymethylene protons on the thienopyrazine unit also give insight to the number of repeat units in the thienopyrazine segment. The oxymethylene protons on the thienopyrazine at the point of junction between the two blocks as well as the oxymethylene protons on the terminal thienopyrazine have a chemical shift at 4.0 ppm, which is higher then those along the polymer backbone (3.8 ppm).

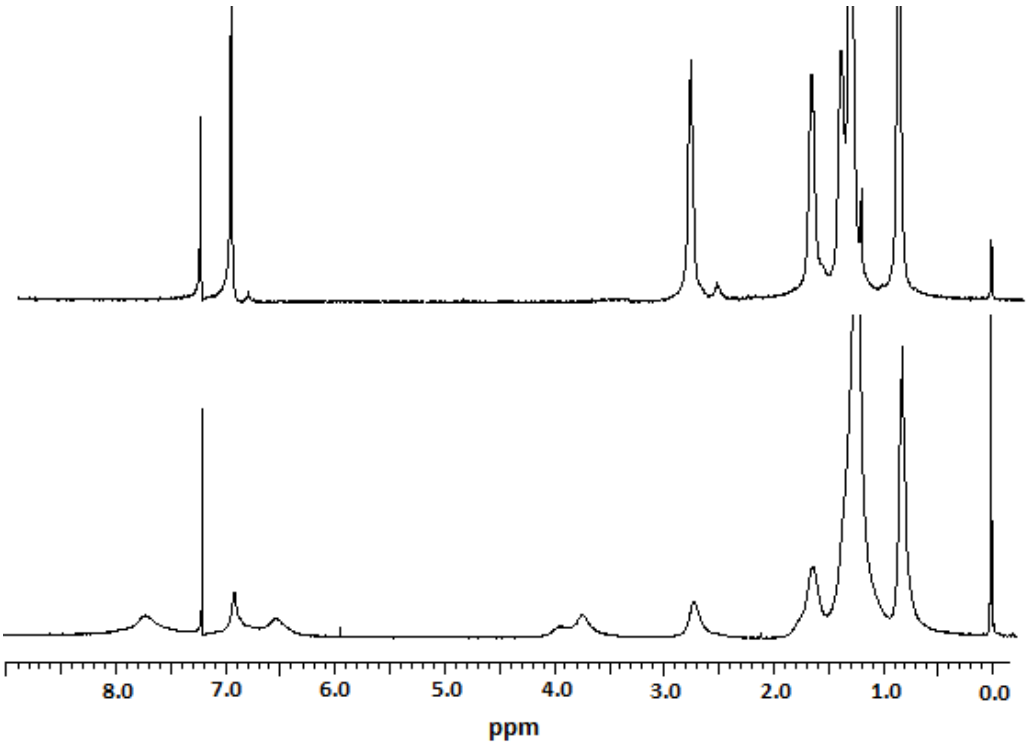

Figure 5.9. ^{1}H NMR spectra of poly(3-octylthiophene) prepolymer (top) and poly(3-octylthiophene)-*block*-poly(thieno[3,4-*b*]pyrazine), **BCP2** (bottom).

In spite of using equimolar amounts of the two types of monomer, the second (ThPy) segment of the block copolymer has fewer repeat units than the first. This is likely due to dissociation of the nickel from the polymer backbone, indicated by the

formation of low molecular weight thienopyrazine oligomers which are initiated from free nickel and are removed from the block copolymer during the purification process.

The addition of excess ligand has been shown to reduce the amount of dissociative reductive elimination in some catalyst-transfer condensation polymerizations.[18] We explored using the same polymerization conditions from above, consisting of a 1:50:50 ratio of Ni(II), thiophene and thienopyrazine, with an addition of four equivalents of the ligand 1,3-bis(diphenylphosphino)propane (dppp) prior to the polymerization of the thienopyrazine monomer. We expected the excess ligand to help eliminate the dissociation of the nickel from the backbone and thereby promote the formation of higher molecular weight polymer chains, however we found that the these reaction conditions led to the formation of a mixture of block copolymers and terminated polythiophene chains as confirmed by GPC, Figure 5.10. This suggests in this polymerization the addition of excess ligand promotes dissociation of the nickel complex from the polythiophene backbone, and the resulting in a mixture of the polythiophene homopolymer and higher molecular weight block copolymers.

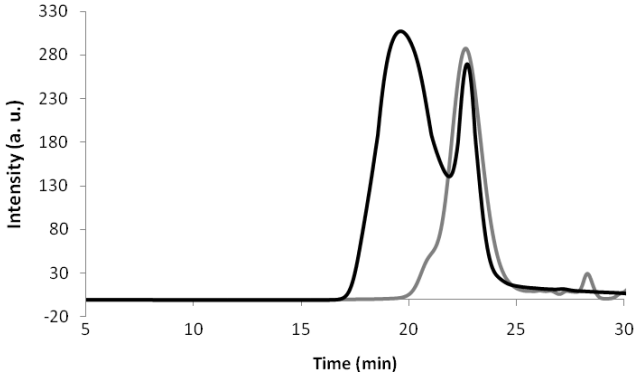

Figure 5.10. Block copolymerization of thiophene followed by thienopyrazine in the presence of excess ligand results in a mixture of P3OT and block copolymer.

We demonstrated the relationship between temperature and dissociation of the nickel catalyst from the backbone during CTCP in Chapter 4: Use of low temperatures decreases the amount of dissiciative reductive elimination during the polymerization. However, attempts to convert the polymerization of the thienopyrazine at low temperatures resulted in precipitation of low molecular weight homopolymer. Employing low temperatures in the block copolymerization did not improve the segment length of the second block.

Finally, in order to increasse the length of the second block, we explored the addition of an excess of the thienopyrazine monomer. After the formation of the prepolymer, three equivalents of the thienopyrazine monomer was added (i.e. a Ni(II):thiophene:thienopyrazine ratio of 1:50:150). The higher concentration of monomer present in the reaction mixture led to block copolymers with longer **PThPy(ArC8)** segment lengths, Table 5.2. The GPC elution curves of **BCP3** and **BCP4** are shown in Figure 5.11, where **BCP3** was synthesized using a 1:1 ratio of the thiophene and thienopyrazine monomers, and **BCP4** was prepared from a 1:3 ratio of the respective monomers.

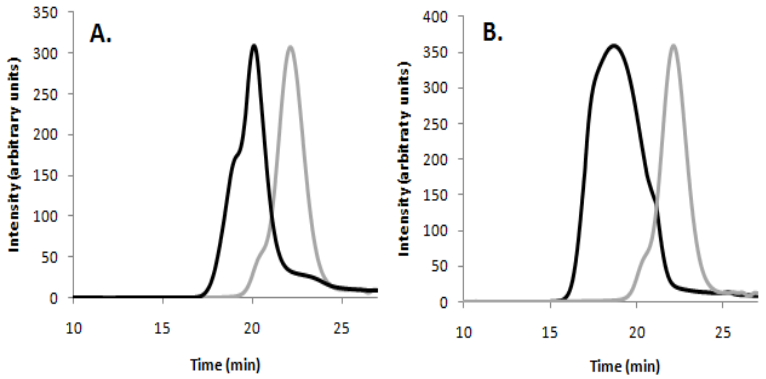

Figure 5.11. GPC elution curves of poly(3-alkylthiophene) prepolymer (gray line) and poly(3-alkylthiophene)-*block*-poly(thieno[3,4-b]pyrazine) postpolymer (black line). A, **BCP3** and B, **BCP4**.

5.4. Conclusions

The development of chain growth CTCP provides a synthetic route that affords control over polymer structure, and affords access to novel all-conjugated block copolymers. In this Chapter, we utilize this type of polymerization to prepare diblock copolymers with poly(3-alkylthiophene) (donor) and poly(thieno[3,4-b]pyrazine) (acceptor) segments. This is the first example of donor-acceptor block copolymers prepared by a one-pot condensation polymerization. We have shown that solubility of the first block is crucial for successful initiation and poropagation of the polymerization of the second monomer with transfer of the catalyst to the new growing chain end without dissociation from the chain. The success of the polymerization relied on the polymerization of the 5-bromo-2-thienylmagnesium iodide prior to the addition of the electron accepting (7-bromo-thieno[3,4-*b*]pyrazin-5-yl)magnesium bromide. Understanding the rates of monomer consumption provides important insight to optimize this process. Changing the catalyst to monomer ratios led to the formation of block copolymers with different segment lengths. These polymers could be used to study the influence of block length on the phase behavior, morphology and electronic properties of the bulk material.

5.5. References

1 . (a) *Handbook of Conducting Polymers*, 2 ed.; T. Skotheim, J. R., R. Elsenbamer, Ed. Marcel Dekker: New York, 1998. (b) Grimsdale, A. C.; Chan, K. L.; Martin, R. E.; Jokisz, P. G.; Holmes, A. B. *Chem. Rev.* **2009**, *109*, 897-1091. (c) McQuade, D. T.; Pullen, A. E.; Swager, T. M. *Chem. Rev.* **2000**, *100*, 2537-2574.

2. (a) Scherf, U.; Gutacker, A.; Koenen, N. *Acc. Chem. Res.* **2008**, *41*, 1086-1097. (b) Liang, Y.; Wang, H.; Yuan, S.; Lee, Y.; Gan, L.; Yu, L. *J. Mater. Chem.* **2007**, *17*, 2183-2194.

3. (a) Liang, Y.; Wang, H.; Yuan, S.; Lee, Y.; Gan, L.; Yu, L. *J. Mater. Chem.* **2007**, *17*, 2183–2194. (b) Lee, M.; Cho, B.-K.; Zin, W.-C. *Chem. Rev.* **2001**, *101*, 3869–3892.

4. Iovu, M. C.; Jeffries-El, M.; Zhang, R.; Kowalewski, T.; McCullough, R. D. *J. Macromol. Sci. Part A* **2006**, *43*, 1991–2000.

5. Dai, C.-A.; Yen, W.-C.; Lee, Y.-H.; Ho, C.-C.; Su, W.-F. *J. Am. Chem. Soc.* **2007**, *129*, 11036–11038.

6. Craley, C. R.; Zhang, R.; Kowalewski, T.; McCullough, R. D.; Stefan, M. C. *Macromol. Rapid Commun.* **2009**, *30*, 11–16.

7. Iovu, M. C.; Craley, R.; Jeffries-El, M.; Krankowski, A. B.; Zhang, R.; Kowalewski, T.; McCullough, R. D. *Macromolecules* **2007**, *40*, 4733–4735.

8. Bao, Z.; Chan, W. K.; Yu, L. *J. Am. Chem. Soc.* **1995**, *117*, 12426-12435.

9. Chen, T.-A.; Wu, X.; Rieke, R. D. *J. Am. Chem. Soc.* **1995**, *117,* 233-244.

10. Schluter, A. D. *J. Polym. Sci. Part A.* **2001**, *39*, 1533-1556.

11. Suzuki, Y.; Hashimoto, K.; Tajima, K. *Macromolecules* **2007**, *40*, 6521-6528.

12. Flory, P. J. *Chem. Rev.* **1946**, *39*, 137-197.

13. Zhang, Y.; Tajima, K.; Hirota, K.; Hashimoto, K. *J. Am. Chem. Soc.* **2008**, *130*, 7812-7813.

14. Ohshimizu, K.; Ueda, M. *Macromolecules* **2008**, *41*, 5289-5294.

15. Wu, P.-T.; Ren, G.; Li, C.; Mezzenga, R.; Jenekhe, S. *Macromolecules* **2009**, *42*, 2317-2320.

16. Miyakoshi, R.; Yokoyama, A.; Yokozawa, T. *Chem. Lett.* **2008**, *37*, 1022-1023.

17. Javier, A. E.; Varshney, S. R.; McCullough, R. D. *Macromolecules* **2010**, *43*, 3233-3237.

18. Yokoyama, A.; Kato, A.; Miyakoshi, R.; Yokozawa, T. *Macromolecules* **2008**, *41* 7271-7273.

19. Yokoyama, A.; Miyakoshi, R.; Yokozawa, T. *Macromolecules* **2004**, *37*, 1169-1171.

20. *Organic Photovoltaics, Mechanisms, Materials and Devices*; Sun. S.-S.; Sariciftci, N. S.; CRC Press: New York, 2005.

21. Wen, L.; Duck, B.; Dastoor, P. C.; Rasmussen, S. C. *Macromolecules* **2008**, *41*, 4576-4578.

22. Babudri, F.; Flandanese, V.; Marchese, G.; Punzi, A. *Tetrahedron Lett.* **1995**, *36*, 7305-7308.

23. Pomerantz, M.; Chaloner-Gill, B.; Harding, L. O.; Tseng, J. J.; Pomerantz, W. J. *J. Chem. Soc., Chem. Commun.* **1992**, 1672-1673.

24. Kenning, D. D.; Mitchell, K. A.; Calhoun, T. R.; Funar, M. R.; Sattler, D. J.; Rasmussen, S. C. *J. Org. Chem.* **2002**, *67*, 9073-9076.

25. Shukla, R.; Wadumethrige, S. H.; Lindeman, S. V.; Rathore, R. *Org. Lett.* **2008**, *10*, 3587-3590.

CHAPTER 6: SYNTHESIS AND CHARACTERIZATION OF POLY(5,8-QUINOXALINE ETHYNYLENE)S

6.1. Introduction

Research initiatives in the design and synthesis of novel conjugated polymers for use in organic electronic devices have resulted in a multitude of materials with a wide array of properties.[1] However, most of these are electron rich polymers with low oxidation potentials. These display p-channel semiconduction and may serve as electron donors in heterojunction devices. The electron accepting material in such devices are typically small molecules such as [6,6]-phenyl-C_{61}-butyric acid methyl ester, PCBM.[2] Employing an electron-poor polymer as the electron-accepting material in heterojunction devices could provide advantages over the use of small molecules such as better control of phase separation and less costly material processing. However, there are far fewer reports of electron poor conjugated polymers with high electron affinity than there are of electron-rich materials. One example of the use of a cyano-substituted poly(phenylene vinylene) as the electron acceptor in a bulk-heterojuction solar cell reports power conversion efficiencies of ca. 2%, indicating that other electron-poor polymers may have a role in the development of heterojunction applications.[3]

Electron accepting conjugated polymers generally contain electron withdrawing substituents such as fluorine[4] or cyano groups,[5] or they contain heteroaromatic units such as quinoline,[6] pyramidine,[7] pyridine,[8] thienopyrazine,[9] and quinoxaline[10,11] in the conjugated backbone. For example, unsubstituted poly(5,8-quinoxaline), PQ, has a high electron afffinity (E_{red} = -2.00 V versus Ag/Ag^+), and the backbone of the polymer is easily decorated with flexible side chains to afford

soluble analogs.[12] Several donor-acceptor alternating copolymers containing quinoxaline units have been reported, including those with thiophene,[13-15] fluorene[16-18] or phenylene[19] units have also been explored in efforts to prepare low band gap and electroluminescent materials.

One criteria for the preparation of low band gap conjugated polymers is the need for a structure in which the conjugated backbone can adopt a planar conformation. This increases the effective conjugation length and promotes close packing of the polymer chains, which facilitates intermolecular electronic interactions.[20] The direct connection between the heteroarenes of PQ leads to steric interactions between the neighboring quinoxaline units, thereby leading to twisting around the arene-arene bond, which impedes planarization of the conjugated backbone. In contrast, poly(arylene ethynylene)s (PAEs), with alternating aromatic and alkyne units, can adopt a planar structure that facilitates close packing of the chains in the solid state.[21] Thus we set out to explore the synthesis and electronic properties of poly(5,8-quinoxaline ethynelene)s, PQE, Figure 6.1, which consists of alternating quinoxaline and alkyne units along the conjugated backbone. This is unusual among PAEs in that the material consists exclusively of electron-accepting heteroaromatic repeat units. The properties of these polymers are compared to those of an electron rich PAE homopolymer, poly(1,4-phenylene ethynylene) (PPE),[22] and a poly(5,8-quinoxaline) (PQ), Figure 6.1.[12] A copolymer consisting of alternating electron-poor quinoxaline ethynylene and electron rich dialkoxy phenylene units (PQE-*alt*-PPE)., Figure 6.1[23] The latter is one example of a class of donor-acceptor PAE copolymers consisting of an electron rich 2,5-dialkoxy-1,4-phenylene ethynylene unit and an electron-poor heteroarylene ethynylene (e.g., benzotriazole ethynylene,[24] quinoline ethynylene,[25]and quinoxaline ethynylene [23]). The donor-

acceptor character of this class of structures has been explored extensively as an approach to prepare a conjugated polymer that possess a low band gap.

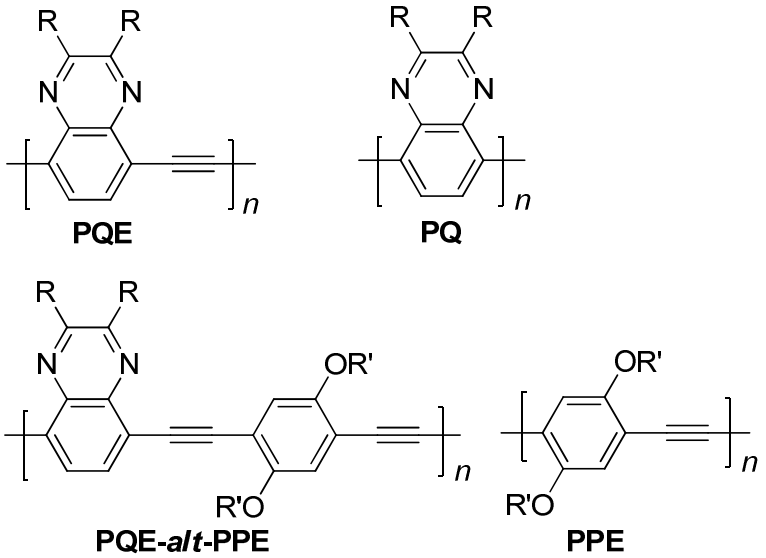

Figure 6.1. Poly(5,8-quinoxaline ethynylene)s (PQEs), poly(5,8-quinoxaline) (PQ) and poly(1,4-phenylene ethynylene) (PPE) homopolymers and alternating copolymer with phenylene and quinoxaline repeat units (PQE-*alt*-PPE) in this study.

6.2. Experimental

6.2.1. General Synthetic Methods

All starting materials were purchased from commercial sources and used without further purification. THF and Et_2O were dried over sodium benzophenone ketyl prior to distillation under argon. Column chromatography was performed on flash grade silica (32-60 Å, Sorbent Technologies, Atlanta, Georgia). Thin-layer chromatography was performed on 3×5 cm silica gel plates (0.2 mm thick, 60 F254) on an aluminum support (Sorbent Technologies). NMR analysis was performed on a Bruker DSX 400 or DSX 300 instruments using $CDCl_3$ as the solvent. Chemical shifts are reported relative to internal tetramethylsilane. ^{13}C NMR are proton decoupled. IR

analyses were performed on a Nicolet 4700 FTIR with an ATR attachment from SmartOrbit Thermoelectronic Corporation. GPC analyses were performed on a Waters 2690 Separations Module with a Waters 2410 refractive index detector at a flow rate of 1 mL/min. Ultraviolet-visible analysis was performed on a Perkin-Elmer Lambda 19 spectrophotometer, and fluorescence spectroscopy was performed on a Shimadzu RF-5301PC spectrofluorophotometer. Cyclic voltammetry experiments were performed on a BAS100B electrochemical analyzer, where thin films were cast onto an Au working electrode in a 0.1 M solution of tetrabutylammonium perchlorate in acetonitrile using a Pt auxiliary electrode and a silver wire quasi reference electrode at a scan rate of 100 mV/s. Elemental analyses were performed by Atlantic Microlab, Inc. (Norcross, GA). 4,7-Dibromobenzo[c][1,2,5]thiadiazole,[26] 1,4-bis(dodecyloxy)-2,5-diethynylbenzene and 1,4-bis(dodecyloxy)-2,5-diiodobenzene[22,27] were prepared by previously reported procedures. Synthetic prodecures and characterization of homologs **a** (R = 4-(2-ethylhexyloxy)phenyl) and **b** (R = 4-octyloxyphenyl) except for compounds **V1-2b** and **V1-3b** (R = 4-octyloxyphenyl) which are described in Chapter 4. Synthetic procedures and spectral data for **PPE(C12)** is described in Chapter 2. ^{1}H and ^{13}C NMR, IR and EI mass spectra are provided in Appendix F for all other compounds described herin.

6.2.2. Synthesis of Quinoxaline-based monomers

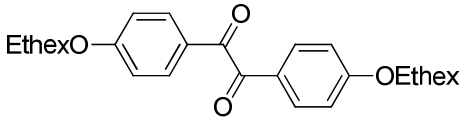

1,2-bis(4-(2-ethylhexyloxy)phenyl)ethane-1,2-dione, VI-2a. 1-bromo-2-ethylhexane (58 g 0.13 mmol) was added to a solution of 1,2-bis(4-hydroxyphenyl)ethane-1,2-dione (16 g, 68 mmol) in anhydrous DMF (250 mL) under argon. Potassium

carbonate (23 g, 169 mmol) and tetrabutylammonium bromide (10.3 g, 32.1 mmol) was added to the mixture and heated to 70° C for 48 h. The mixture was poured into H_2O (300 mL) and extracted with hexanes (3 x 100 mL). The hexane factions were combined and the solvent was removed under reduced pressure. The resulting residue was purified by column chromatography (40:60 v/v CH_2Cl_2: hexane). to afford 1,2-bis(4-(2-ethylhexyloxy)phenyl)ethane-1,2-dione **VI-2a** as a vicious yellow liquid (14.7 g, 49 %). ^{1}H NMR (300 MHz, $CHCl_3$) δ 7.92 (d, $^3J_{HH}$ = 9 Hz, 4H), 6.95 (d, $^3J_{HH}$ = 8.7 Hz, 4H), 3.91 (d, $^3J_{HH}$ = 5.7 Hz, 4H), 1.68-1.78 (m, 2H), 1.39-1.52 (m, 16H), 0.83-0.97 (m, 12H). ^{13}C NMR (75 MHz, $CDCl_3$) δ 193.56 (C=O), 164.67 (Ar C4), 132.29 (Ar C2 and C6), 125.97 (Ar C1), 114.67 (Ar C3 and C5), 70.82 (C-O), 39.16, 30.37, 28.97, 23.71, 22.60, 14.08, 11.01. IR (ATIR): 2919 (Ar C-H str.), 2852, 1655, 1593 (C=O str.), 1508, 1458, 1421, 1305, 1255, 1162, 1153 (C-O str.), 1005, 879, 836, 752, 620, 615, 509 cm^{-1}.

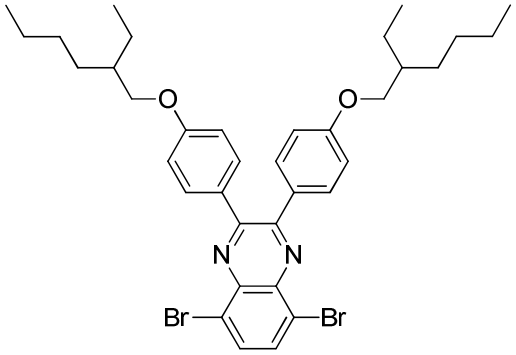

5,8-Dibromo-2,3-bis(4-(2-ethylhexyloxy)phenyl)quinoxaline, V1-3a.

Sodium borohydride (6.7 g, 180 mmol) was added in six equal portions, ten minutes apart, to a solution of 4,7-dibromobenzo[*c*][1,2,5]thiadiazole (8.9 g, 30 mmol) and $CoCl_2 \cdot 6H_2O$ (0.1 g, 0.4 mmol) in ethanol (200 mL) and stirred for an additional 30 min. The solvent was removed under reduced pressure and the residue was taken up in CH_2Cl_2 (100 mL) and the solution was washed with H_2O (2 x 50 mL), dried over $MgSO_4$ and the solvent was removed under reduced pressure to afford diamine **VI-1**

that was used without further purification. The crude 3,6-dibromobenzene-1,2-diamine (4.1 g, 15 mmol) was added to a solution of 1,2-bis(4-(2-ethylhexyloxy)phenyl)ethane-1,2-dione (6.9 g, 15 mmol) in acetic acid (200 mL) and the mixture was heated to reflux for 72 h under argon. The mixture was poured into H_2O (800 mL) and the resulting mixture was neutralized with a 10% solution of aqueous NaOH and then extracted with CH_2Cl_2 (3 x 500 mL). The organic extracts were combined and the solvent was removed under reduced pressure. The resulting residue was purified by column chromatography (40:60 v/v CH_2Cl_2:hexanes) to afford the dibromo-quinoxaline monomer **VI-3a** as a bright yellow viscous liquid (6.7 g, 65 %): ^{1}H NMR (300 MHz, $CHCl_3$) δ 7.84 (s, 2H, quinoxaline C-H), 7.66 (d, $^3J_{HH}$ = 9 Hz, 4H, Ph C2-H), 6.89 (d, $^3J_{HH}$ = 8.7 Hz, 4H, Ph C3-H), 3.88 (d, $^3J_{HH}$ = 6 Hz, 4H, -OCH_2-), 1.70-1.76 (m, 2H), 1.26-1.52 (m, 16H), 0.86-0.98 (m, 12H). ^{13}C NMR (75 MHz, $CDCl_3$) δ 160.69 (Ph C4), 153.57 (quinoxaline C2 and C3), 132.43 (quinoxaline C6 and C7), 131.60 (Ph C2), 130.24 (Ph C1), 123.40 (quinoxaline C5 and C8), 114.39 (Ph C3), 70.55 (C-O), 39.29, 30.47, 29.06, 23.81, 23.03, 14.08, 11.09. IR (ATIR): 2916 (Ar C-H str.), 1244, 1169 (C-O str), 1603 (C=N str.), 1478, 1379 (C-C str.), 538 (C-Br str.) 1510, 1331, 1288, 1009, 984, 899, 829, 731, 654, 611 cm^{-1}. HRMS *calc.* for $C_{36}H_{44}N_2O_2Br_2$ = 694.1770, *obs.* = 694.1746, Δ = 3.5 ppm. Elemental Analysis: Theoretical: C, 62.07%; H, 6.37%; N, 4.02%. Found: C, 62.16%; H, 6.40%; N, 4.04%.

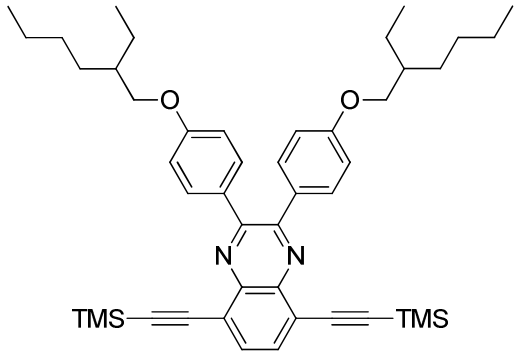

2,3-bis(4-(2-Ethylhexyloxy)phenyl)-5,8-bis((trimethylsilyl)ethynyl) quinoxaline, VI-4a. A mixture of dibromoquinoxaline **VI-3a** (6.6 g, 9.5 mmol) in THF (20 mL) and triethylamine (10 mL) was degassed by two freeze-pump-thaw cycles. $Pd(PPh_3)_2Cl_2$ (0.64 g, 0.91 mmol) and CuI (0.27 g, 1.4 mmol) were added to the solution followed by tetramethylsilyl acetylene (1.9 g, 20 mmol) and the mixture was stirred at 50 °C for 24 h. H_2O (1 mL) was added and the solvent was removed under reduced pressure. The resulting residue was taken up in CH_2Cl_2 (80 mL) and the solution was washed with H_2O (150 mL). The solvent from the organic extracts was removed under reduced pressure and the resulting residue was purified by column chromatography (30:70 v/v CH_2Cl_2: hexanes) to afford the TMS-protected monomer **VI-4a** as a yellow solid (4.7 g, 67%): mp = 118.6-119 °C. ^{1}H NMR (300 MHz, $CHCl_3$) δ 7.75 (s, 2H, quinoxaline C-H), 7.70 (d, $^3J_{HH}$ = 8.7 Hz, 4H, Ph C2-H), 6.86 (d, $^3J_{HH}$ = 8.7 Hz, 4H, Ph C3-H), 3.87 (d, $^3J_{HH}$ = 5.7 Hz, 4H, -OCH_2-), 1.68-1.75 (m, 2H), 1.28- 1.52 (m, 16H), 0.88- 0.96 (m, 12H), 0.35 (s, 18H). ^{13}C NMR (75 MHz, $CDCl_3$): δ 160.52 (Ph C4), 152.36 (quinoxaline C2 and C3), 140.67 (quinoxaline C1 and C4), 132.54 (quinoxaline C6 and C7), 131.56 (Ph C2), 131.00 (Ph C1), 123.04 (quinoxaline C5 and C8), 114.16 (Ph C3), 103.18 (C≡C-TMS), 101.48 (C≡C-TMS), 70.58 (C-O), 39.45, 30.50, 29.09, 23.83, 23.04, 14.10, 11.12, 0.01. IR (ATIR): 2918 (Ar C-H str.), 2148 (C≡C str.), 1244, 1176 (C-O str.), 1600 (C=N str.), 1478, 1379 (C-C str.), 542 (C-Br str.) 1512, 1460, 1063, 1014, 831, 756, 627 cm^{-1}. HRMS *calc.* for

$C_{46}H_{62}N_2O_2Si_2$ = 730.4350, *obs.* = 730.4360, Δ = 1.4 ppm. Elemental Analysis: Theoretical: C, 75.56%; H, 8.55%; N, 3.83%. Found: C, 75.55%; H, 8.45%; N, 3.87%.

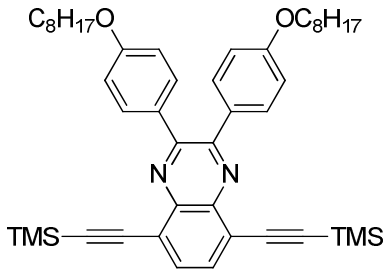

2,3-bis(4-(octyloxy)phenyl)-5,8-bis((trimethylsilyl)ethynyl)quinoxaline, V1-4b. $Pd(PPh_3)Cl_2$ (0.2 g, 0.3 mmol) and CuI (0.06 g, 0.31 mmol) were added to a solution of dibromo-quinoxaline **V1-3b** (2.18 g, 3.1 mmol) in THF (12 mL) and triethylamine (4 mL) and degassed by two freeze-pump-thaw cycles. Trimethylsilyl acetylene (0.92 mL, 6.5 mmol) was added to the mixture and the solution was heated at 50 °C for 24 h. The mixture was poured into H_2O (100 mL) and extracted with CH_2Cl_2 (2 x 50 mL). The organic extracts were combined and the solvent was removed under reduced pressure. The residue was purified by column chromotography (30:70 v/v CH_2Cl_2:hexanes) followed by recrystallization from isopropanol to afford the protected quinoxaline monomer **V1-4b** as a yellow solid (1.78 g, 77%): mp = 105-106 °C. ^{1}H NMR (300 MHz, $CDCl_3$) δ 7.76 (s, 2H, quinoxaline C-H), 7.70 (d, $^3J_{HH}$ = 8.7 Hz, 4H, Ph C2-H), 6.85 (d, $^3J_{HH}$ = 8.7 Hz, 4H, Ph C3-H), 3.98 (t, $^3J_{HH}$ = 6.6 Hz, 4H, -OCH_2-), 1.75-1.82 (m, 4H), 1.26-1.49 (m, 20H), 0.89 (t, $^3J_{HH}$ = 6.6 Hz, 6H), 0.35 (s, 18H). ^{13}C NMR (75 MHz, $CDCl_3$) δ 160.24 (Ph C4), 152.36 (quinoxaline C2 and C3), 140.68 (quinoxaline C1 and C4), 132.54 (quinoxaline C6 and C7), 131.58 (Ph C2), 131.05, 123.04, 122.20, 114.09 (Ph C3), 103.21, 68.03 (C-O), 31.81, 29.34, 39.22, 26.03, 22.67, 14.10, 0.01 (one missing

signal due to coincident CH_2 peaks). IR (ATIR): 2915 (Ar C-H str.), 2848, 2146, 1602, 1509, 1467, 1374, 1261, 1243 (C-O str.), 1176, 1041, 831, 754, 626, 546.

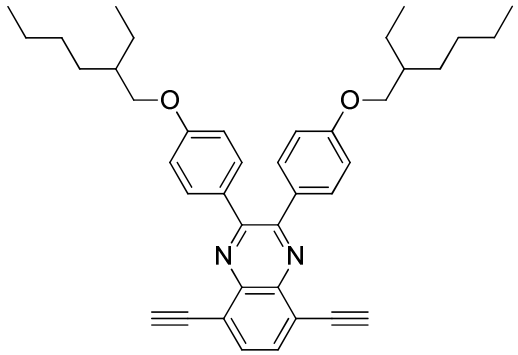

2,3-bis(4-(2-ethylhexyloxy)phenyl)-5,8-diethynylquinoxaline, VI-5a. A solution of tetra-*n*-butylammonium fluoride (1 M in THF, 6 mL, 6 mmol) was added to a solution of **VI-4a** (2.0 g, 2.7 mmol) in THF (16 mL) under argon. The mixture was stirred at room temperature for 45 min and H_2O (50 mL) was added. The mixture was extracted with CH_2Cl_2 (2 x 30mL), the organic extracts were combined and the solvent was removed under reduced pressure. The residue was purified by column chromatography (40:70 v/v CH_2Cl_2: hexanes) to afford the diethynyl-quinoxaline monomer **VI-5a** as an orange viscous liquid (1.18 g, 73%). ^{1}H NMR (300 MHz, $CHCl_3$) δ 7.83 (s, 2H, quinoxaline C-H), 7.62 (d, $^3J_{HH}$ = 8.7 Hz, 4H, Ph C2-H), 6.87 (d, $^3J_{HH}$ = 9 Hz, 4H, Ph C3-H), 3.87 (d, $^3J_{HH}$ = 6 Hz, 4H, -OCH_2-), 3.61 (s, 2H), 1.70-1.78 (m, 2H), 1.26-1.55 (m, 16H), 0.88-0.98 (m, 12H). ^{13}C NMR (75 MHz, $CDCl_3$) δ 160.51 (Ph C4), 153.33 (quinoxaline C2 and C3), 140.96 (quinoxaline C1 and C4), 133.20 (quinoxaline C6 and C7), 131.57 (Ph C2), 130.91 (Ph C1), 122.71 (quinoxaline C5 and C8), 114.36 (Ph C3), 85.00 (C≡C-H), 80.18 (C≡C-H), 70.56 (C-O), 39.29, 30.48, 29.06, 23.81, 23.04, 14.09, 11.1. HRMS *calc.* for $C_{40}H_{46}N_2O_2$ = 586.3559, *obs.* = 586.3565 Δ = 1.0 ppm. IR (ATIR): 3236 (C≡C-H str.) 2918 (Ar C-H str.), 2148 (C≡C str.), 1244, 1176 (C-O str.), 1600 (C=N str.), 1478, 1379 (C-C str.),

542 (C-Br str.) 1512, 1460, 1063, 1014, 831, 756, 627 cm^{-1}. Elemental Analysis: Theoretical: C, 81.87%; H, 7.90%; N, 4.77%. Found: C, 82.01%; H, 7.88%; N, 4.84%.

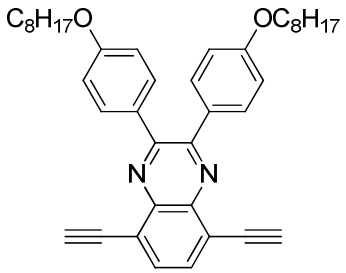

2,3-bis(4-(octyloxy)phenyl)-5,8-diethynylquinoxaline, VI-5b. A solution of tetra-*n*-butylammonium fluoride (1M in THF, 3 mL, 3 mmol) was added to a solution of protected quinoxaline **VI-4b** (1.00g, 1.37 mmol) in THF (11 mL). The solution was stirred at room temperature for 40 min and quenched with H_2O (1 mL). The solvent was removed and H_2O was added (50 mL) and extracted with CH_2Cl_2 (2 x 50 mL), the organic extracts were combined and the solvent was removed under reduced pressure. The residue was purified by column chromatography (50:50 v/v CH_2Cl_2:hexanes) to afford diethynyl-quinoxaline **VI-5b** as a yellow solid (0.68 g, 85%): mp = 94-96 °C. ^{1}H NMR (300 MHz, $CDCl_3$) δ 7.83 (s, 2H, quinoxaline C-H), 7.62 (d, $^3J_{HH}$ = 9 Hz, 4H, Ph C2-H), 6.86 (d, $^3J_{HH}$ = 9 Hz, 4H, Ph C3-H), 3.98 (t, $^3J_{HH}$ = 6.6 Hz, 4H, O-CH_2-), 3.61 (s, 2H, C≡C-H), 1.68-1.83 (m, 4H), 1.29-1.46 (m, 20H), 0.88 (t, $^3J_{HH}$ = 6.6 Hz, 6H). ^{13}C NMR (75 MHz, $CDCl_3$) δ 160.13 (Ph C4), 153.16 (quinoxaline C2 and C3), 140.86 (quinoxaline C1 and C4), 133.10 (quinoxaline C6 and C7), 131.53 (Ph C2), 130.89 (Ph C1), 122.64 (quinoxaline C5 and C8), 114.15 (Ph C3), 84.99 (C≡C-H), 80.10 (C≡C-H), 67.91 (C-O), 31.74, 31.52, 29.29, 29.11, 25.96, 22.58, 14.02. IR (ATIR): 3267 (C≡C-H str.), 2916 (Ar C-H str.), 2848, 2144 (C≡C str.), 1603, 1510, 1467, 1375, 1292, 1257, 1243 (C-O str.), 1174, 1022, 831, 755, 627, 538.

6.2.3. Synthesis of Polymers

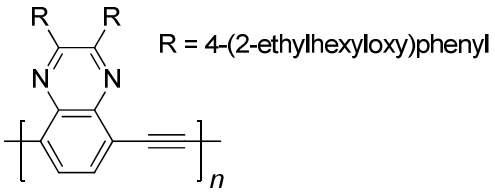

Poly(5,8-(2,3-bis(4(2-ethylhexyloxy)phenyl)quinoxaline ethynylene), PQE(EH). A solution of dibromo-quinoxaline **VI-3a** (1.0 g, 1.8 mmol) and diethynyl-quinoxaline **VI-5a** (0.84 g, 1.8 mmol) in THF (25 mL) was degassed by two freeze-pump-thaw cycles. Diisopropylamine (5.0 mL, 35 mmol), CuI (55 mg, 0.29 mmol), and $Pd(PPh_3)_4$ (0.40 g, 0.35 mmol) were added and the solution was and heated at 45 °C for 24 h. The mixture was poured into methanol (200 mL) and the resulting precipitate was isolated by filteration. The solid was subjected to sequential extraction with acetone, hexane and chloroform in a Soxhlet extractor. The solvent was removed from the chloroform fraction under reduced pressure afforded the quinoxaline polymer **PQE(EH)** as a red solid (0.842 g, 90%). ^{1}H NMR (300 MHz, $CHCl_3$) δ ^{1}H NMR (300 MHz, $CHCl_3$) δ 7.78-7.67 (m, 4H), 7.40-7.37 (m, 8H), 6.80-6.7 (m, 8H), 3.94-3.68 (m, 8H), 1.26-1.55 (m, 36H), 0.95-0.84 (m, 24H). IR (ATIR): 2954 (Ar C-H str.), 1255, 1165 (C-O str), 1371 (C-C str.), 2848, 1599, 1509, 1254, 1003, 999, 787, 685, 498 cm^{-1}. GPC (THF, UV-vis detector) M_n = 19 kg/mol, PDI = 2.1. Elemental Analysis: Theoretical: C, 75.73%; H, 7.46%, N, 4.71%. Found: C, 75.19%; H, 7.24%; N, 4.05%.

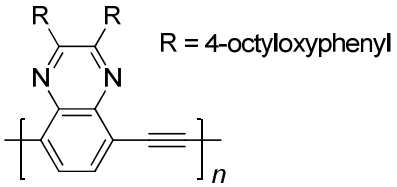

R = 4-octyloxyphenyl

Poly(5,8-(2,3-bis(4-octyloxyphenyl)quinoxaline ethynylene), PQE(C8). A solution of dibromo-quinoxaline **VI-3b** (1.2 g, 1.7 mmol) and diethynyl-quinoxaline **VI-5b** (1.01 g, 1.7 mmol) in THF (20 mL) was degassed by two freeze-pump-thaw cycles. Diisopropylamine (5 mL), CuI (110 mg, 58 mmol), and $Pd(PPh_3)_4$ (0.80 g, 0.70 mmol) were added and the solution was and heated at 45 °C for 24 h. The solution was poured into methanol (200 mL) and the resulting precipitate was isolated by filteration. The precipitated red polymer, **PQE(C8)**, was insoluble in common organic solvents such as chloroform, xylenes, 1,4-dichlorobenzene and thus not characterized further (1.9 g, 95%).

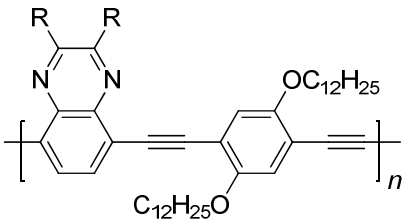

R = 4-(2-ethylhexyloxy)phenyl

Poly(5,8-(2,3-bis(4(2-ethylhexyloxy)phenyl)quinoxaline-*alt*-(2,5-didodecyloxy)-1,4-phenylene ethynylene), PQE(EH)-*alt*-PPE(C12). A solution of diethynyl-quinoxaline **VI-5a** (1.2 g, 2.0 mmol) and 1,4-bis(dodecyloxy)-2,5-diiodobenzene (1.3 g, 2.0 mmol) in THF (20 mL) was degassed by two freeze-pump-thaw cycles. Diisopropylamine (5 mL, 35 mmol), CuI (70 mg, 0.37 mmol), and $Pd(PPh_3)_4$ (0.40 g, 0.37 mmol) were added and the solution was heated at 45 °C for 24 h. The solution was poured into methanol (200 mL) and the resulting precipitate was isolated by filteration. The solid was subjected to sequential extraction with

acetone, hexane and chloroform in a Soxhlet extractor. The solvent was removed from the chloroform fraction under reduced pressure afforded the alternating quinoxaline and dialkoxy copolymer **PQE(EH)-*alt*-PPE(C12)** as a red solid (96 mg, 5%). The remaining polymer was a red solid (1.34 g, 70%), and insoluble in common organic solvents thus was not characterized further. ^{1}H NMR (300 MHz, $CHCl_3$) δ 7.75-7.63 (2H), 7.5-7.4 (4H), 7.41-7.35 (4H) 6.98-6.83 (2H), 3.9-3.88 (8H), 1.38-1.21 (62H), 0.93-0.81 (18H). IR (ATIR): 2910, 2908, 2841 (Ar C-H str.), 1254 (C-O str), 1038 (C-N) 1363 (C-C str.), 1593, 995, 785, 689 cm^{-1}. GPC (THF, UV-vis detector) M_n = 23 kg/mol, PDI = 2.1. Elemental Analysis: Theoretical: C, 78.63 %; H, 9.28 %; N, 2.74 %. Found: C, 79.14 %; H, 9.01 %; N, 2.95 %.

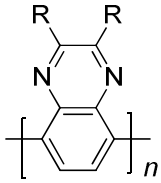

R = 4-(2-ethylhexyloxy)phenyl

Poly(2,3-bis(4-(2-ethylhexyl)oxyphenyl)quinoxaline-5,8-diyl), PQ(EH). In an argon filled glove-box, $Ni(COD)_2$ (0.71 g, 2.6 mmol) was added to a Schlenk flask containing a solution of dibromide **VI-4a** (1.5 g, 2.2 mmol), 2,2'-bipyridine (0.44 g, 2.8 mmol) and 1,5-cyclooctadiene (1 mL, 8 mmol) in anhydrous *N*,*N*-dimethyformamide (25 mL). The mixture was stirred at 60 °C for 48 h, and then poured into MeOH (100 mL). The solution was filtered and the resulting gray precipitate was dissolved in $CHCl_3$ (50 mL) and the solution was stirred with 10% aqueous HCl (20 mL) for 30 min. The organic layer was separated and stirred with saturated aqueous NaCl (20 mL) for 30 min. The organic layer was separated and the polymer was precipitated by pouring the solution into acetone (200 mL). The solution was filtered and **PQ(EH)** was obtained as a yellow solid. ^{1}H NMR (300 MHz, $CDCl_3$) δ 8.32 (br s, 2H, quinoxaline C-H), 7.34 (b, 4H, phenyl C-H), 6.59 (b, 4H, phenyl C-

H) 3.64 (b, 4H, -OCH_2-), 1.56-1.67 (m, 2H), 1.38-1.24 (m, H), 0.87 (b, 12H). IR (ATIR): 2927, 2856, 1604, 1511, 1467, 1384, 1342, 1294, 1243, 1172, 1027, 977, 831, 736, 665, 592, 540 cm^{-1}. GPC (THF, UV-vis detector) 4.28 kDa, PDI = 1.93.

6.3. Results and Discussion

6.3.1. Monomer Synthesis

The poly(5,8-quinoxaline ethynylene)s in this study were prepared by a palladium-catalyzed condensation polymerizations of a 5,8-dibromoquinoxaline and a similarly substituted 5,8-diethynylquinoxaline monomer, Figure 6.2. Each monomer was substituted with either 4-octyloxyphenyl or 4-(2-ethylhexyloxy)phenyl side chains in the 2- and 3-positions of each quinoxaline ring. The 5,8-dibromoquinoxalines were prepared according to modified published procedures.[28] Dibromobenzothiadiazole was reduced with sodium borohydride to afford diamine **VI-1**, which was used without purification in a subsequent condensation with diketones **VI-2a** or **VI-2b** to give the 5,8-dibromoquinoxaline monomers **VI-3a** and **VI-3b**, respectively, Figure 6.2. Sonogashira coupling of trimethylsilylacetylene and the 5,8-dibromoquinoxalines **VI-3** afforded the corresponding TMS-protected 5,8-diethynylquinoxalines, **VI-4**. Subsequent desilylation with tetra-*n*-butylammonium fluoride (TBAF) afforded the 5,8-diethynylquinoxaline monomers **VI-5**.

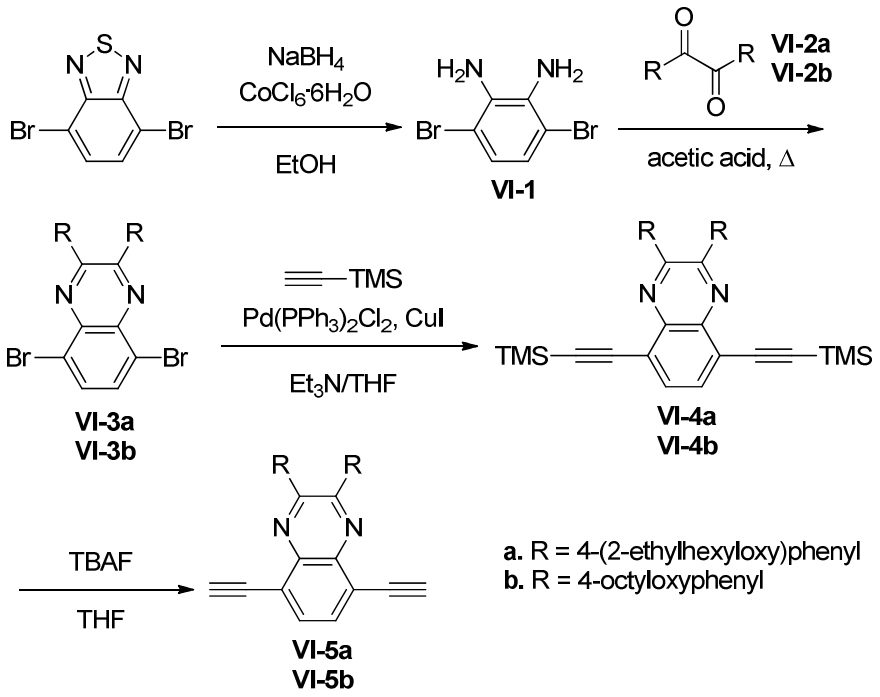

Figure 6.2. Synthesis of dibromoquinoxaline (**VI-3**) and dialkyne quinoxaline (**VI-5**) monomers.

6.3.2. Synthesis and Characterization of Quinoxaline-Based PPEs

Palladium-catalyzed coupling of 5,8-dibromoquinoxalines **VI-3** and 5,8-diethynylquinoxalines **VI-5** afforded the poly(5,8-quinoxaline ethynylene)s (PQE), Figure 6.3. Poly(5,8-quinoxaline ethynylene) with 4-(2-ethylhexyloxy)phenyl side chains, **PQE(EH)**, was precipitated from MeOH and the precipitate was purified by successive extractions with acetone, hexanes and chloroform in a Soxhlet extractor. The acetone and hexanes fractions removed catalyst and low molecular weight oligomers. The material extracted into chloroform contained **PQE(EH)** with an M_n = 19 kg/mol and PDI = 2.1 (determined by gel permeation chromatography). The remaining polymer in the Soxhlet thimble was insoluble in common organic solvents. Poly(5,8-quinoxaline ethynylene) with 4-octyloxyphenyl side chains, **PQE(C8)**, was insoluble in common organic solvents and was not further characterized.

The chloroform fraction of **PQE(EH)** was characterized by ^{1}H NMR and IR spectroscopy (see Appendix F for spectra). Unlike poly(5,8-quinoxaline vinylenes), which undergo degradation in a matter of minutes in light and air,[10] the poly(quinoxaline ethynylene)s in this study are stable in light and air (observed over a number of weeks).

The alternating donor-acceptor copolymer **PQE(EH)-*alt*-PPE(C12)** was synthesized by Sonogashira coupling of diethynyl quinoxaline monomer **VI-5a** and 1,4-bis(dodecyloxy)-2,5-diiodobenzene, Figure 6.3.[23] Successive extractions with acetone and hexanes in a Soxhlet extractor removed catalyst and unreacted monomers. The remaining red solid was only partially soluble in hot organic solvents such as chloroform, xylenes and 1,1,2,2-tetrachloroethane. Only the chloroform soluble portion of the polymer was further characterized. Poly(2,5-didodecyloxy-1,4-phenylene ethynylene), **PPE(C12)** was synthesized by polymerization of the di(dodecyloxy) substituted diiodo- and diethynylbenzene monomers, Figure 6.3.[22] Poly(2,3-(4-(2-ethylhexyl)oxyphenyl)quinoxaline-5,8-diyl) (**PQ(EH)**) were prepared by the condensation polymerization of 5,8-dibromoquinoxaline **VI-3a** using Yamamoto coupling conditions, Figure 6.3.[12]

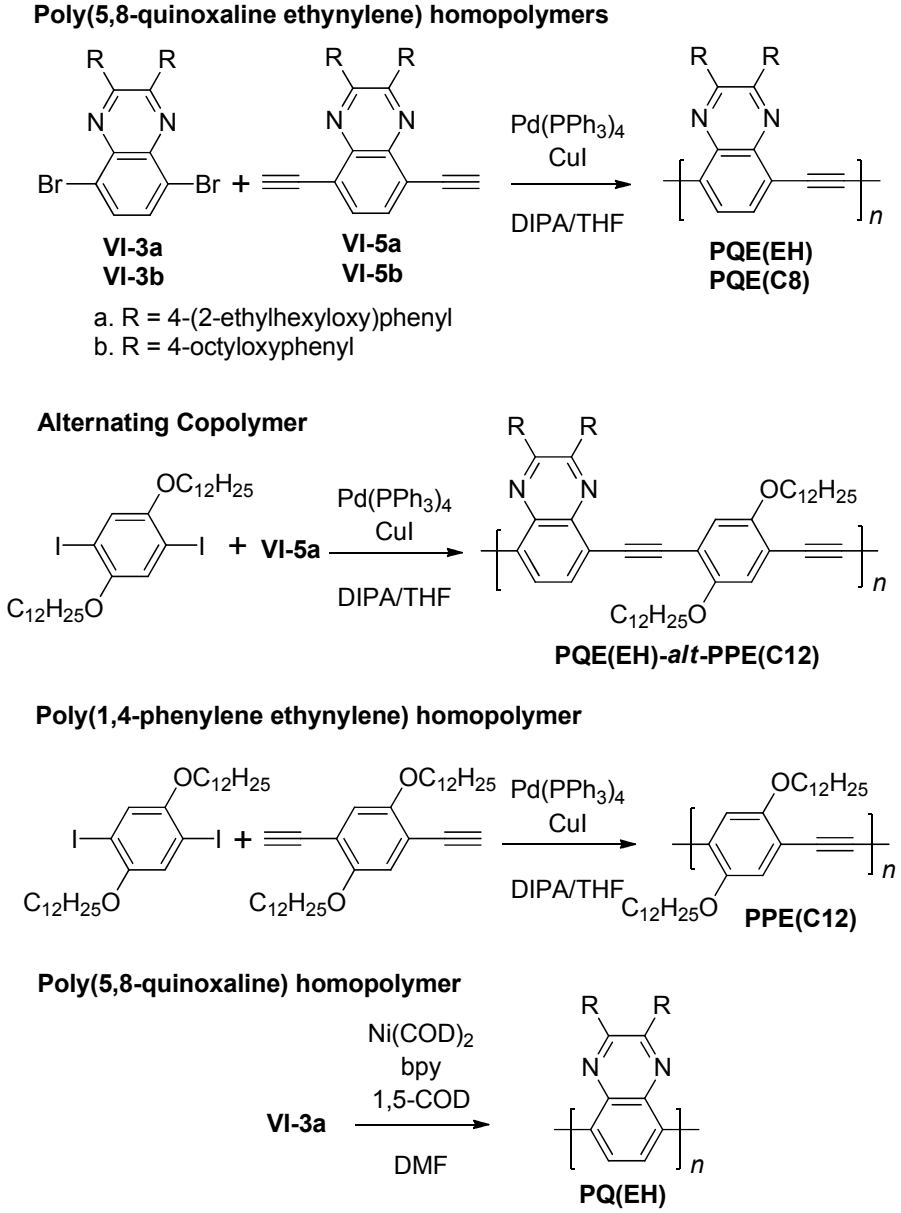

Figure 6.3. Synthesis of quinoxaline homopolymers, alternating copolymer, and PPE.

6.3.3. Optical Properties

The absorption spectra of solutions of **PPE(C12)**, **PQ(EH)** and the quinoxaline based PPEs, **PQE(EH)** and **PQE(EH)-*alt*-PPE(C12)** (the chloroform soluble portion) were obtained in chloroform at a concentration of 50 μg/mL, Figure 6.4. Poly(5,8-quinoxaline) **PQ(EH)** has an absorption maxima at 390 nm, which is

consistent with the previously reported value for this polymer.[6] Poly(5,8-quinoxaline ethynylene) **PQE(EH)** has a significantly red-shifted and broader absorption, with two absorption maxima, at 422 and 505 nm. The large red-shift of the absorption maximum and the absorption edge (550 nm) of **PQE(EH)** compared to **PQ(EH)** is consistent with the greater conjugation of the former as a result of a more planar structure arising from separation of the quinoxaline units by the alkyne units. **PQE(EH)** is also significantly red-shifted compared to the dialkoxy PPE, **PPE(C12)**, which has an absorption maxima at 447 nm. The absorption spectra of the alternating quinoxaline-dialkoxyphenylene PPE, **PQE(EH)-*alt*-PPE(C12)**, is also very broad, and slightly blue shifted with respect to **PQE(EH)**.

The fluorescence spectra of the polymers were also obtained, Figure 6.4. In solution, poly(quinoxaline ethynylene) **PQE(EH)** has an emission at 554 nm which is red-shifted with respect to the corresponding polyquinoxaline **PQ(EH)** (498 nm). This is consistent with a more planar structure arising from separation of the quinoxaline units by the alkyne units. Both quinoxaline-based PPEs in this study, **PQE(EH)** and the alternating donor-acceptor copolymer **PQE(EH)-*alt*-PPE(C12)**, have much lower fluorescence intensity than both the dialkoxy PPE, **PPE(C12)**, and the poly(5,8-quinoxaline) homopolymer **PQ(EH)** which may indicate aggregation of the conjugated polymer chains.[29]

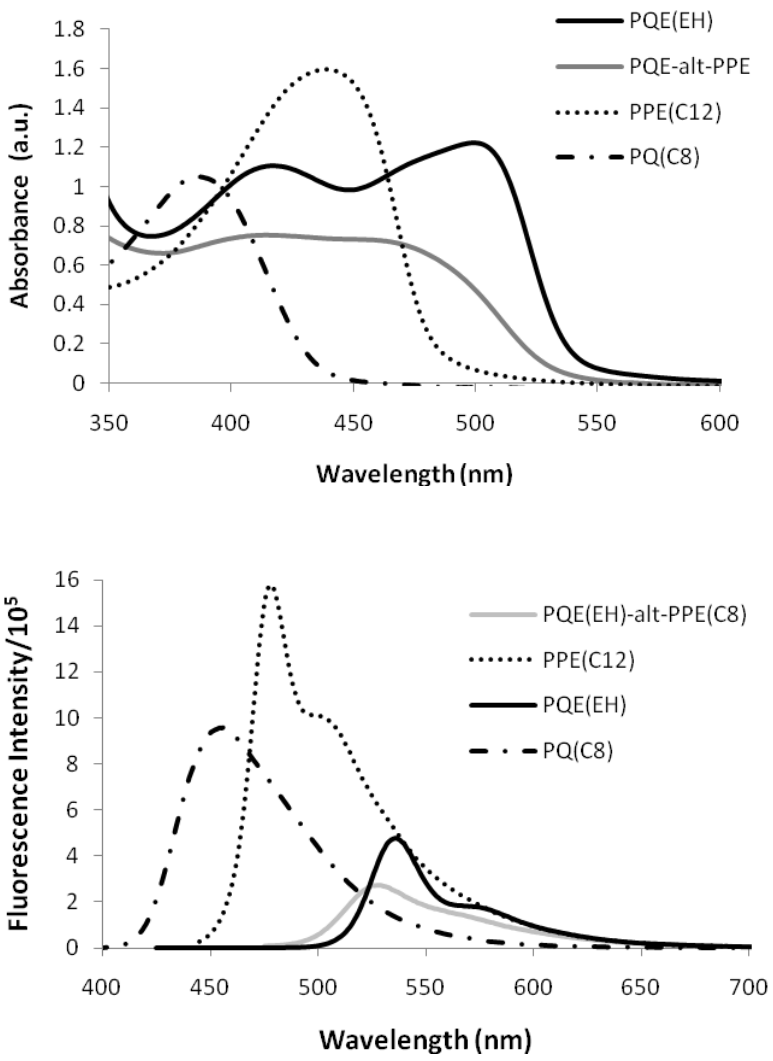

Figure 6.4. UV-vis absorption spectra (top) and fluorescence spectra (bottom) of solutions of **PQE(EH)** (black line), **PQ(EH)** (dashed line), **PQE(EH)-*alt*-PPE(C12)** (gray line) and **PPE(C12)** (dotted line). Solutions in chloroform at a concentration of 50 μg/mL.

The solid state absorption spectra of films of the polymers were obtained by spin casting solutions of the polymers in chloroform (20 mg/mL) onto quartz slides, Figure 6.5. The absorption maxima of the polymers and the optical band gaps are given in Table 6.1. All of the conjugated polymers in this study have red-shifted

absorption maxima in comparison to the solution spectra as a result of the interactions of the polymer chains in the solid state, which can be attributed to aggregation of the chains. Films of poly(5,8-quinoxaline ethynylene) **PQE(EH)** have two absorption maxima, at 406 nm and 516 nm. In common with the spectra of solutions of these polymers, these are significantly red-shifted with respect to the absorption maxima of polyquinoxaline **PQ(EH)**. The optical bandgap of **PQE(EH)**, determined from the absorption onset, is 2.25 eV, which is significantly less than that of **PQ(EH)** (2.73 eV).

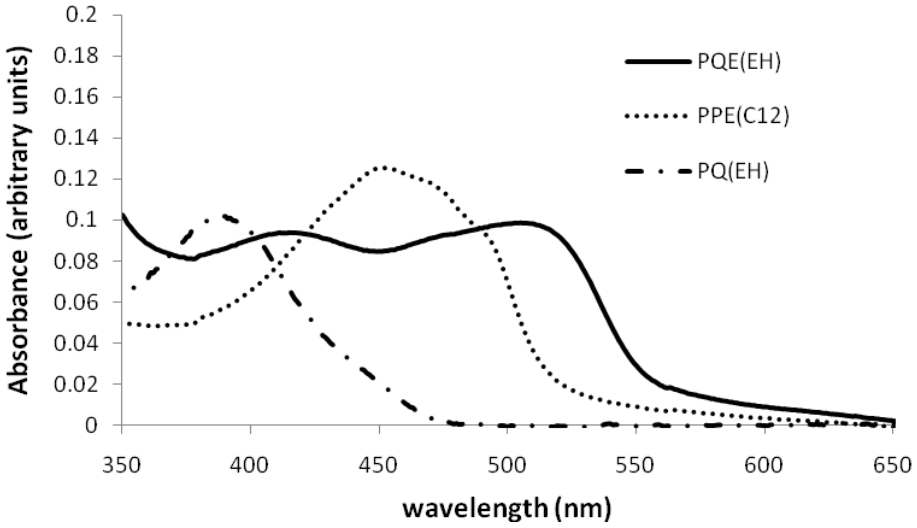

Figure 6.5. Solid-state UV-vis absorption spectra of poly(5,8-quinoxaline ethynyleene) **PQE(EH)** (solid line), poly(5,8-quinoxaline) **PQ(EH)** (dashed line), and poly(1,4-phenylene ethynylene) **PPE(C12)** (dotted line).

This is consistent with a more conjugated, planar structure that results from the incorporation of alternating ethynylene units in the conjugated backbone which separates the quinoxaline units and relieves steric interactions between arlyene units. Films suitable for determining the solid state spectra of the alternating donor-acceptor

copolymer could not be prepared due to the low solubility of the polymer. However a previously reported alternating quinoxaline ethynylene-phenylene copolymer has a previously reported bandgap of 2.30 eV.[30] The poly(quinoxaline ethynylene) homopolymer **PQE(EH)** has a lower bandgap than the alternating copolymer, which is in contrast to the decrease in the bandgap of PPEs relying on the incorporation of other alternating electron deficient and electron rich arenes in the backbone, as previously suggested.[27] The PQE homopolymers have lower bandgaps than other previously reported alternating donor-acceptor PAEs as well, Table 6.1.

Table 6.1. Optical Properties of the Quinoxaline-Based and Dialkoxy PPE Polymers and Copolymers

	solution ($CHCl_3$)		thin films		
	λ_{max}^{abs} (nm)	λ_{max}^{em} (nm)	λ_{max}^{abs} (nm)	λ_{max}^{em} (nm)	E_g^{opt} (eV)
PQE(EH)	422, 505	531	406, 516	554	2.25
PQ(EH)	390	451	395	498	2.73
PPE(C12)	447	477	467	563	2.38
phenylene-*alt*-quinoxaline	br[a]	br[a]	493[b]	558[b]	2.30[b]
phenylene-*alt*-benzotriazole [c]	445	500	463	560	2.36
phenylene-*alt*-quinoline [d]	430	560	412	605	2.30

[a] Broad absorption, see Figure 4. [b] Alternating copolymer containing phenylene and quinoxaline units, see reference 23. [c] Alternating copolymer containing phenylene and benzotriazole units, see reference 24. [d] Alternating copolymer containing phenylene and quinonline units, see reference 25.

6.3.4. Cyclic-Voltammetry

Cyclic voltammograms of the polymers were collected by drop casting chloroform solutions of the polymers (15mg/mL) onto an Au working electrode. Poly(5,8-quinoxaline) **PQ(EH)** exhibits a reduction peak at -2.10 V vs Ag quasi reference electrode, and a re-oxidation potential at -1.72 V vs Ag wire, Figure 6.6, which is consistent with previously reported values for similarly substituted poly(5,8-quinoxaline)s.[12] The poly(5,8-quinoxaline ethynylene)s have higher electron affinity than the corresponding **PQ**, with **PQE(EH)** displaying a reduction wave with a peak potential of -1.27 V and a re-oxidation peak at -1.19 V. The redox behavior remains the same on repeated cycling of the potential. There are no observable oxidation peaks at positive potentials for either polymer. The poly(5,8-quinoxaline ethynylene)s also have higher electron affinity than the alternating quinoxaline and dialkoxy PQE-*alt*-PPEs, which has reduction potentials of -1.54 V vs Ag wire.[23]

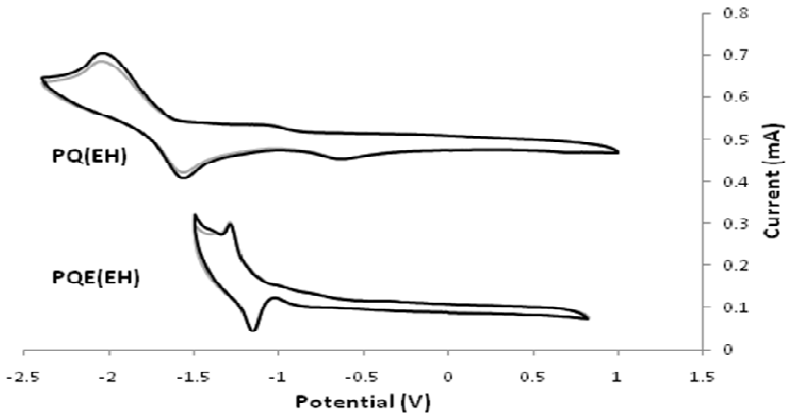

Figure 6.6. Cyclic voltammograms of films of poly(5,8-quinoxaline) **PQ(EH)** (top) and poly(5,8-quinoxaline ethynylene) **PQE(EH)** (bottom) on Au immersed in a 0.1 M solution of tetrabutylammonium perchlorate in acetonitrile (100 mV/s sweep rate, potentials reported against a Ag wire quasi reference electrode) . The black curve represents the first potential cycle, the gray represents the second.

6.4. Conclusions

In conclusion, we have described the preparation of a new class of electron accepting polymers, poly(5,8-quinoxaline ethynylene)s, PQEs, consisting of alternating quinoxaline and alkyne segments in the polymer backbone. This is the first example of the broad class of poly(arylene ethynylene)s consisting of electron accepting heteroaromatic repeat units. These materials have good stability in light and air and are much more soluble than alternating quinoxaline ethynylene and phenylene copolymers, PQE-*alt*-PPE. In comparison to poly(5,8-quinoxaline)s (PQ), the poly(5,8-quinoxaline ethynylene)s have red-shifted optical absorptions corresponding to a lower band gap as a result of the planarization of the backbone by incorporating the alkyne unit to relieve steric interactions between the quinoxaline units. These materials are susceptible to reduction (E_{red} = -1.27 V vs Ag/Ag^{+}) and have a higher electron affinity than corresponding poly(5,8-quinoxaline)s. Accordingly, these materials may be useful as an electron accepting material for a variety of applications. For example, poly(quinoxaline ethynylene)s are better matched with the solar emission spectrum then dialkoxy PPEs, and exhibit fluorescence quenching, which may be an advantage for applications such as photovoltaic cells, where emission is a source of loss of power conversion efficiency.[31] The exploration of PAE homopolymers that incorporate electron poor heteroarenes, as well as copolymers, offers new opportunities to further tailor the electronic structure and properties of conjugated polymers to serve as electron accepting materials

6.5. References

1. *Handbook of Conducting Polymers*; 2 ed.; T. Skotheim, J. R., R. Elsenbamer, Ed.; Marcel Dekker: New York, 1998.

2. Günes, S.; Neugebauer, H.; Sariciftci, N. S. *Chem. Rev.* **2007**, *107*, 1324-13338.

3. Granström, M.; Petritsch, K.; Arias, A. C.; Lux, A.; Andersson, M. R.; Friend, R. H. *Nature* **1998**, *395*, 257-260.

4. Jin, Y.; Kim, K.; Park, S. H.; Song, S.; Kim, J.; Jung, J.; Lee, K.; Suh, H. *Macromolecules* **2007**, *40*, 6799-6806.

5. Greenham, N. C.; Moratti, S. C.; Bradley, D. D. C.; Friend, R. H.; Holmes, A. B. *Nature* **1993**, *365*, 628-630.

6. Saito, N.; Kanbara, T.; Nakamura, Y.; Yamamoto, T.; Kubota, K. *Macromolecules* **1994**, *27*, 756-761.

7. Kanbara, T.; Kushida, T.; Saito, N.; Kuwajima, I.; Kubota, K.; Yamamoto, T. *Chem. Lett.* **1992**, 21, 583-586.

8. Yamamoto, T.; Maruyama, T.; Zhou, Z.; Ito, T.; Fukuda, T.; Yomeda, Y.; Begum, F.; Ikeda, T.; Sasaki, S.; Takezoe, H.; Fukuda, A.; Kubota,; K. *J. Am. Chem. Soc.* **1994**, *116*, 4832-4845.

9. Wen, L.; Duck, B. C.; Dastoor, P. C.; Rasmussen, S. C. *Macromolecules* **2008**, *41*, 4576.

10. Jonforsen, M.; Johansson, T.; Inganäs, O.; Andersson, M. R. *Macromolecules* **2002**, *35*, 1638-1643.

11. Saito, N.; Kanbara, T.; Kushida, T.; Kubota, K.; Yamamoto, T. *Chem.Lett.* **1993**, *22*, 1775-1778.

12. Yamamoto, T.; Sugiyama, K.; Kushida, T.; Inoue, T.; Kanbara, T. *J. Am. Chem. Soc.* **1996**, *118*, 3930-3937.

13. Zhang, G.; Fu, Y.; Zhang, Q.; Xie, Z. *Polymer* **2010**, *51*, 2312-2319.

14. Lee, B.-L.; Yamamoto, T. *Macromolecules* **1999**, *32*, 1375-1382.

15. Peng, Q.; Xu, J.; Zheng, W. *J. Poly. Sci. Part A* **2009**, *47*, 3399-3408.

16. Kulkarni, A.; Zhu, Y.; Jenekhe, S. A. *Macromolecules* **2005**, *38*, 1553-1563.

17. Lee, P.-I.; Hsu, S. L.-C.; Lin, P. *Macromolecules* **2010**, *43*, 8051-8057.

18. Xu, E.; Zhong, H.; Lai, H.; Zeng, D.; Zhang, J.; Zhu, W.; Fang, Q. *Macromol. Chem. Phys.* **2010**, *211*, 651-656.

19. Liu, C.-L.; Tsai, J.-H.; Lee, W.-Y.; Chen, W.-C.; Jenekhe, S. A. *Macromolecules* **2008**, *41*, 6952-6959.

20. Ohkita, H.; Cook, S.; Astuti, Y.; Duffy, W.; Tierney, S.; Zhang, W.; Heeney, M.; McCulloch, I.; Nelson, J.; Bradley, D. D. C.; Durrant, J. R. *J. Am. Chem. Soc.* **2008**, *130*, 3030-3042.

21. Bunz, U. H. F. *Chem. Rev.* **2000**, *100*, 1605-1644.

22. Moroni, M.; Le Moigne, J.; Luzzati, S. *Macromolecules* **1994**, *27*, 562-571.

23. Bangcuyo, C. G.; Ellsworth, J. M.; Evans, U.; Myrick, M. L.; Bunz, U. H. F. *Macromolecules* **2003**, *36*, 546-548.

24 . Tanimoto, A; Yamamoto, T. *Adv. Synth. Catal.* **2004**, *346*, 1818-1823.

25 . Jégou, G.; Jenekhe, S. A. *Macromolecules* **2001**, *34*, 7926-7928.

26. Neto, B. A. D.; Lopes, A. S. A.; Edeling, G.; Gonçalves, R. S.; Costa, V. E. U.; Quina, F. H.; Dupont, J. *Tetrahedron* **2005**, *61*, 10975-10982.

27. Nambiar, R.; Woody, K. B.; Ochocki, J. D.; Brizius, G. L.; Collard, D. M., *Macromolecules* **2009**, *42*, 43-51.

28. Tsami, A.; Bunnagel, T. W.; Farrell, T.; Scharber, M.; Choulis, S. A.; Brabec, C. J.; Scherf, U. *J. Mater. Chem.* **2007**, *17*, 1353-1355.

29 . Halkyard, C. E.; Rampey, M. E.; Kloppenburg, L.; Studer-Martinez, S. L.; Bunz, U. H. F. *Macromolecules* **1998**, *31*, 8655-8659.

30 . Zhang, L.; Zhang, Q. Y.; Yan, H.; Zhang, J.; Gu, J.; Zhang, H.; Guo, F. *Syn. Met.* **2009**, *159*, 2038-2042.

31. Bredas, J.-L.; Norton, J. E.; Cornil, J.; Coropceanu, V., *Accs. Chem. Res.* **2009**, *42*, 1691-1699.

CHAPTER 7: CONCLUSIONS AND OUTLOOK

The potential to use conjugated polymers as the semiconductor in devices such as photovoltaic cells and field effect transistors creates a need to understand the relationships between the structure of materials and their properties. The design and synthesis of new materials which self-organize into ordered nanostructures creates opportunities to establish and exploit relationships between electronic properties and morphology or molecular packing. The research presented in this thesis details progress in the development of synthetic routes which provide access to new classes of conjugated polymers that contain either dissimilar side chains that segregate or dissimilar conjugated blocks which phase separate.

7.1. Regioregular Poly(1,4-Phenylene Ethynylene)s

Variations of the side chains on the backbone of a conjugated polymer provide opportunities to tailor the molecular assembly and electronic properties of the material. The placement of side chains relative to one another can greatly influence the bulk properties of the polymer. Asymmetrically disubstituted PPEs prepared using traditional synthetic methods have irregular placement of side chains on the conjugated backbone. In Chapter 2, we described the first synthetic route to regioregular asymmetrically substituted PPEs by polymerization of an asymmetrically substituted 2,5-dialkoxy-4-iodophenylacetylenes.[1] Characterization of these materials revealed that the effect of regioregularity on the properties of the asymmetrically substituted dialkoxy PPEs is greatest when there is a large difference in the side chain length.

Regioregular side chain placement becomes even more important in conjugated polymers when the side chains are amphiphilic. In Chapter 3, we described a novel class of amphiphilic PPEs bearing a combination of a semifluoroalkoxy and an alkoxy side chain on each phenyl ring.[2] Both regioregular and regiorandom analogs were synthesized and characterized. While it was expected that amphiphilic side chains placement would afford a further level of control over the molecular packing and orientation of the conjugated polymer chains, the combination of side chains on the PPEs impeded crystallization. This is in contrast to the highly ordered and oriented solid phases formed by alkyl/semifluoroalkyl substituted poly(bithiophene)s.[3] The difference in the behavior of these classes of polymers may arise from the extent to which the side chains of dialkoxy-PPEs interdigitate. Segregation of the dissimilar side chains of the amphiphilic PPEs disrupts this interdigitation and thereby interferes with crystallization.

These studies provide insight to the importance of the identity of the side chains in PPEs. In a separate study, the Collard research group prepared amphiphilic PPEs with hydrophilic alkoxy and hydrophobic tri(ethylene oxide) (-$(OCH_2CH_2)_3OCH_3$), or PEG, side chains on each phenyl repeat unit, Figure 7.1.[4] Unlike the semifluoroalkoxy/alkoxy PPEs described above, these materials have a highly ordered, bilayer lamellar structure arising from the segregation of hydrophobic and hydrophilic to form a Janus-like chain. This study suggests the possibility that if the individual side chains do not have dissimilar segments (i.e., fluoroalkyl versus semifluoroalkyl), interdigidation does not impede crystallization.

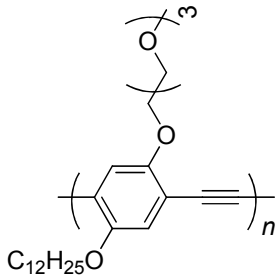

Figure 7.1. Amphiphilic PPEs with hydrophilic alkoxy and hydrophobic tri(ethylene oxide) (-$(OCH_2CH_2)_3OCH_3$) side chains on each phenyl repeat unit.[4]

From the results of Chapters 2 and 3, it can be concluded that regioregularity influences both the solution and bulk properties of an asymmetrically substituted PPE. As a regiorandom substitution pattern can be avoided by the use of an appropriately substituted A-B type monomer, this synthetic route should be considered when synthesizing any asymmetrically substituted PPE.

The current understanding of the influence on the electronic properties resulting from unsymmetrical side chain substitution of regioregular PPEs could be further explored. Amphiphilic structures that give rise to highly ordered materials may have good charge transport properties due to close packing in the solid state. Mobility measurements would provide insight into the potential utility of these polymers for device applications such as field effect transistors. The synthesis of PPEs with amphiphilic side chains which do not disrupt interdigitation, such as the PEG/alkoxy PPEs described above, could provide highly ordered materials for these types of studies. It is possible that the substitution of each phenyl ring of the PPE with both a fully fluorinated and an alkyl side chain may also provide polymers that are highly ordered and also hydrophobic, which is ideal for electronic devices. However, it is likely that these types of materials may have low solubility in common organic

solvents. This problem may be circumvented by using fluorinated solvents for processing.

Another avenue which may be considered is the synthesis of PPEs with asymmetrically substituted arenes bearing both a bulky non-crystallizing and a linear crystallizing side chain. Side chains with different steric requirements may promote the formation of new molecular assemblies, such as a cylindrical nanostructure. It is also possible that regioregular substitution of PPEs with a hydrophobic and hydrophilic side chain could have interesting properties. Hydrophilic side chains allow for PPEs to be processed by techniques such as Langmuir-Blodgett, providing self-organized polymer films with uniform thickness.[5] These materials may be advantageous in applications such as OLEDs, where maintaining control of the emission yield and obtaining polarized light are advantageous.

7.2. Preparation of Block Copolymers from Telechelic Poly(3-alkylthiophene)

Conjugated block copolymers can provide access to interesting new morphologies as a result of phase separation of the conjugated blocks. In this thesis, we have explored new synthetic routes to donor-acceptor block copolymers that phase separate into electron rich and electron poor domains and may be advantageous in organic electronic devices such as bulk heterojunction solar cells. In Chapter 4 we established new synthetic routes to a mono-functional, telechelic poly(3-octylthiophene) where the single bromine end group can be used as a functional handle in subsequent coupling reactions.[6] We chose to couple the monofunctional PAT to the electron accepting polymer poly(5,8-quinoxaline), resulting in a new class of D-A-D triblock copolymers with poly(3-octylthiophene) donor and poly(5,8-quinoxaline) acceptor blocks. Characterization of the D-A-D triblock copolymers in

this study revealed efficient fluorescence quenching of the polymers in the solid state, consistent with the occurrence of electron transfer, which is ideal behavior for solar cells. However, initial tests on these materials in photovoltaic devices fabricated from the block copolymers sandwiched between the transparent anode (ITO/PEDOT:PSS) and cathode (Ag) were unresponsive. It is possible that using higher molecular weight analogs of the block copolymers, or using different processing conditions would provide functional device.

The synthetic methods established in this study could be applied toward the synthesis of many different types of conjugated block copolymers. For example, the telechelic, monofunctional PAT could be coupled to any appropriately substituted electron accepting polymer, providing access to new classes of donor-acceptor block copolymers, Figure 7.2. Polymers that are terminated in functional groups such as alkynes,[7] vinyls,[8] stannanes,[9] boronates,[10] and phosphonantes[11] are all candidates for subsequent coupling to the telechelic PAT.

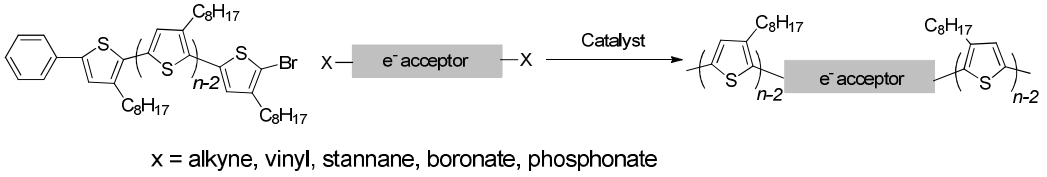

Figure 7.2. Telechelic PAT coupled to an appropriately substituted electron accepting polymer to provide D-A-D triblock copolymers.

One interesting electron accepting polymer that could be coupled to telechelic PAT is a cyano derivative of poly(p-phenylene vinylene), MEH-CN-PPV, Figure 7.3.[12] This conjugated polymer has been successfully incorporated as the electron accepting material in the active layer of a photovoltaic device.[13] Thus, this material may also be useful as the acceptor in a donor-acceptor block copolymer.

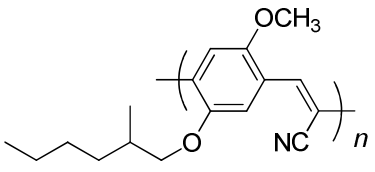

MEH-CN-PPV

Figure 7.3. A cyano derivative of poly(p-phenylene vinylene), MEH-CN-PPV.[13]

Telechelic PAT could also be used to study the differences between block copolymers where the conjugated blocks are directly linked, and block copolymers which have insulating aliphatic spacers separating the conjugated segments, Figure 7.4. It is possible that the direct linkage between the donor and acceptor segments of a block copolymer may decrease the efficiency of a photovoltaic device, as charge carriers may easily recombine at the same interface. It has been proposed that introducing an aliphatic spacer between the conjugated blocks would reduce this problem, while still allowing nanoscale phase separation.[14] However, to our knowledge there are no studies which directly compare materials where the conjugated segments of the block copolymer are equivalent and the block copolymer chains only differ in the presence of an aliphatic spacer between the segments.

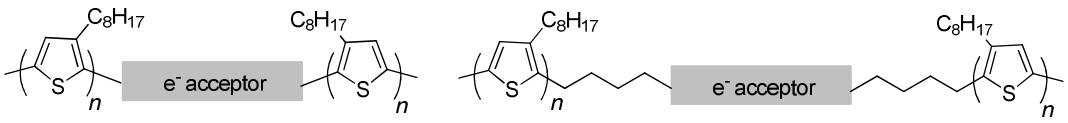

Figure 7.4. D-A-D triblock copolymers, with direct linkage of the conjugated blocks (left) and an aliphatic spacer between conjugated blocks (right).

The telechelic PAT described in Chapter 4 could be modified to contain a functionalized aliphatic chain, which could be coupled in a subsequent reaction to the

electron accepting polymer. For example, a palladium catalyzed Heck reaction could be used to couple 1-(4-bromobutyl)-4-vinylbenzene to the bromine-terminated poly(3-octylthiophene), resulting in a telechelic poly(3-alkylthiophene) with a functionalized aliphatic end-group, Figure 7.5.

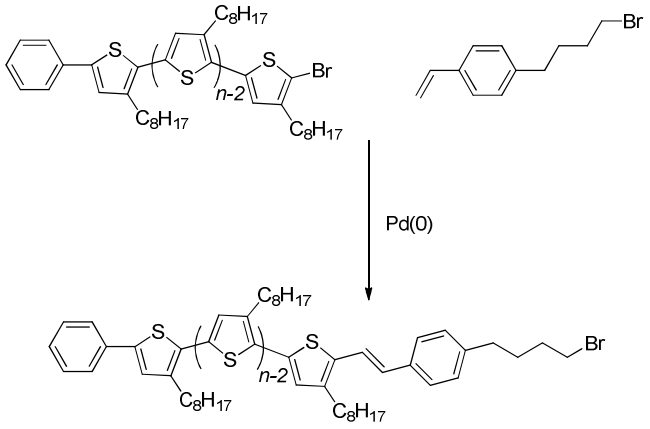

Figure 7.5. Proposed synthesis of telechelic poly(3-alkylthiophene) with a functionalized aliphatic end-group.

7.3. One-Pot Polymerization of Donor-Acceptor Block Copolymers

The synthetic methods described in Chapter 4 provide access to interesting new conjugated block copolymers. However there are some disadvantages associated with the synthetic methods used to prepare these polymers. The individual polymer blocks have to be separately synthesized and purified, and may require post-polymerization modifications. If the subsequent coupling reaction does not go to completion, or if there is a stoichiometric imbalance of the two polymers in the reaction mixture, there will be unreacted homopolymer impurities which will be difficult to separate from the block copolymers. In Chapter 5, we explore using a one-pot, chain growth polymerization to prepare donor-acceptor block copolymers. In this polymerization, the first block is grown from an initiator, only reacting with the monomer at the active end group, and a second monomer is added to the

polymerization mixture to give the second block. While there have been a few examples of this type of polymerization previously reported, these reports were restricted to block copolymers containing electron donating thiophene and phenylene monomer units.[15-19] We have reported the first example of a donor-acceptor diblock copolymer prepared using this method. We have shown that the segment lengths of the block copolymer can be controlled by varying the ratio between the initiator and monomers.

As this synthetic method provides easy access to diblock copolymers that only vary in the lengths of the respective segments, future studies could include studying the influence of block length on the phase behavior and morphology of the materials. These materials could also be incorporated as the active layer in bulk-heterojunction solar cells. The band gaps of thienopyrazine can be modified by the substitution of the monomer unit with different functional groups,[20] so it may be possible to tune the energy levels of the polymers to optimize charge transfer from the electron donating poly(3-alkylthiophene) to the poly(thienopyrazine) acceptor.

7.4. Electron-Accepting Conjugated Polymers

One limitation to the study of donor-acceptor block copolymers is the availability of only a few electron accepting polymers. Most conjugated polymers have low electron affinity and are electron donating.[21] The synthesis of new electron accepting polymers provides opportunities to explore the utility of these materials in device applications. In Chapter 4 we described the incorporation of poly(5,8-quinoxaline) as the electron accepting material in conjugated triblock copolymers. Photovoltaic devices fabricated from block copolymers which incorporated poly(5,8-quinioxaline) as the electron accepting material in photovoltaic devices fabricated

from the block copolymers sandwiched between the transparent anode (ITO/PEDOT:PSS) and cathode (Ag) were unresponsive. One possible explanation is poor mobility of the semiconducting conjugated materials, which can lead to charge trapping and recombination.[22] While poly(5,8-quinoxaline) is a known electron acceptor, steric interactions between the quinoxaline units causes distortion of the backbone from planarity, which may be detrimental to the charge transport properties of the material. In Chapter 6, we report a new class of electron accepting quinoxaline-based conjugated polymer, poly(5,8-quinoxaline ethynylene)s where incorporating an alkyne between the quinoxaline units allows for planarization of the conjugated backbone.[23] In comparison to poly(5,8-quinoxaline)s, the poly(5,8-quinoxaline ethynylene)s have red-shifted optical absorptions and lower band gaps, consistent with planarization of the conjugated backbone. The poly(5,8-quinoxaline ethynylene) in this study had reduction potential of -1.27 V vs Ag/Ag^+, corresponding to a higher electron affinity than similarly substituted poly(5,8-quinoxaline) (E_{red} = -2.01 V vs Ag/Ag^+), indicating that poly(5,8-quinoxaline ethynylene)s are good candidates for use as electron accepting semiconductors.

Further characterization of the PQEs is needed to determine the utility of these materials in organic electronic devices. For example, mobility measurements of the conjugated polymers would provide insight to the charge transport properties of the material. These materials could be used as an electron acceptor in the active layer of a device by blending the polymers with an electron donating material or incorporating the polymers into D-A-D triblock copolymers. Poly(5,8-quinoxaline ethynylene) with terminal alkyne units could be synthesized by using a slight excess of the 5,8-diethynylquinoxaline monomer, Figure 7.6. A subsequent coupling reaction with the monofunctional PAT described in Chapter 4 would provide D-A-D triblock

copolymers with a poly(3-octylthiophene) donor segment and poly(5,8-quinoxaline ethynylene) acceptor segment.

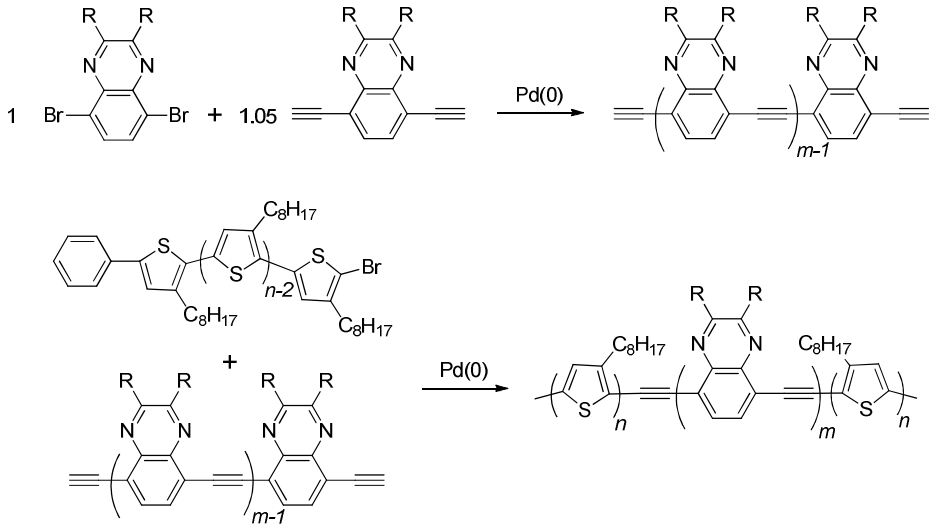

Figure 7.6. Proposed synthesis of D-A-D triblock copolymers with a poly(3-octylthiophene) donor segment and a poly(5,8-quinoxaline ethynylene) acceptor segment.

7.5. References

1. Nambiar, R.; Woody, K. B.; Ochocki, J. D.; Brizius, G. L.; Collard, D. M. *Macromolecules* **2009**, *42*, 43-51.

2. Woody, K. B.; Nambiar, R.; Brizius, G. L.; Collard, D. M. *Macromolecules* **2009**, *42*, 8102-8111.

3. Wang, B.; Watt, S.; Hong, M.; Domercq, B.; Sun, R.; Kippelen, B.; Collard, D. M. M*acromolecules* **2008**, *41*, 5156-5165.

4. R. Nambiar, Ph.D. Dissertation, Georgia Institute of Technology, 2009

5. Arias-Marin, E.; Moigne, J. L.; Guillon, D.; Geffroy, B. *Macromolecules* **2003**, *36*, 3570-3579.

6. Woody, K. B.; Leever, B. J.; Durstock, M. F.; Collard, D.M. *submitted to Macromolecules*.

7. Bunz, U. H. F. *Chem. Rev.* **2000**, *100*, 1605-1644.

8. Yin, L.; Liebscher, J. *Chem. Rev.* **2007**, *107*, 133-173.

9. Bao, Z.; Chan, W. K.; Yu, L. *J. Am. Chem. Soc.* **1995**, *117*, 12426-12435.

10. Schlüter, A. D. *J. Polym. Sci. Part A.* **2001**, *39*, 1533-1556.

11. Suzuki, Y.; Hashimoto, K.; Tajima, K. *Macromolecules* **2007**, *40*, 6521-6528.

12. Baigent, D. R.; Greenham, N. C.; Grüner, J.; Marks, R. N.; Friend, R. H.; Moratti, S. C.; Holmes, A. B. *Syn. Met.* **1994**, *67*, 3-10.

13. Granström, M.; Petritsch, K.; Arias, A. C.; Lux, A.; Andersson, M. R.; Friend, R. H. *Nature* **1998**, *395*, 257-260

14. Zhang, C.; Choi, S.; Haliburton, J.; Cleveland, T.; Li, R.; Sun, S.-S.; Ledbetter, A.; Bonner, C. E. *Macromolecules* **2006**, *39*, 4317-4326.

15. Zhang, Y.; Tajima, K.; Hirota, K.; Hashimoto, K. *J. Am. Chem. Soc.* **2008**, *130*, 7812-7813.

16. Yokoyama, A.; Kato, A.; Miyakoshi, R.; Yokozawa, T. *Macromolecules* **2008**, *41* 7271-7273.

17. Miyakoshi, R.; Yokoyama, A.; Yokozawa, T. *Chem. Lett.* **2008**, *37*, 1022-1023.

18. Wu, P.-T.; Ren, G.; Li, C.; Mezzenga, R.; Jenekhe, S. *Macromolecules* **2009**, *42*, 2317-2320.

19. Ohshimizu, K.; Ueda, M. *Macromolecules* **2008**, *41*, 5289-5294.

20. Wen, L.; Nietfeld, J. P.; Amb, C. M.; Rasmussen, S. C. *J. Org. Chem.* **2008***, 73,* 8529-8536.

21. *Handbook of Conducting Polymers*; 2 ed.; T. Skotheim, J. R., R. Elsenbamer, Ed.; Marcel Dekker: New York, 1998.

22. Brédas, J.-L.; Norton, J. E.; Cornil, J.; Coropceanu, V. *Acc. Chem. Res.* **2009**, *42*, 1691-1699.

23. Woody, K. B.; Henry, E. M.; Collard, D. M. *submitted to Macromolecules.*

APPENDIX A: ^{1}H AND ^{13}C NMR, IR AND MASS SPECTRA OF MONOMERS AND POLYMERS DESCRIBED IN CHAPTER 2

^{1}H NMR spectra were collected on a Varian Mercury Vx 300 MHz instrument using $CDCl_3$ as a solvent. ^{13} C NMR spectra were obtained at 75.5 MHz. IR analyses were performed on a Nicolet 4700 FTIR with an ATR attachment from SmartOrbit Thermoelectronic Corporation.

4-Dodecyloxy-3-iodophenol

A. ^{1}H NMR

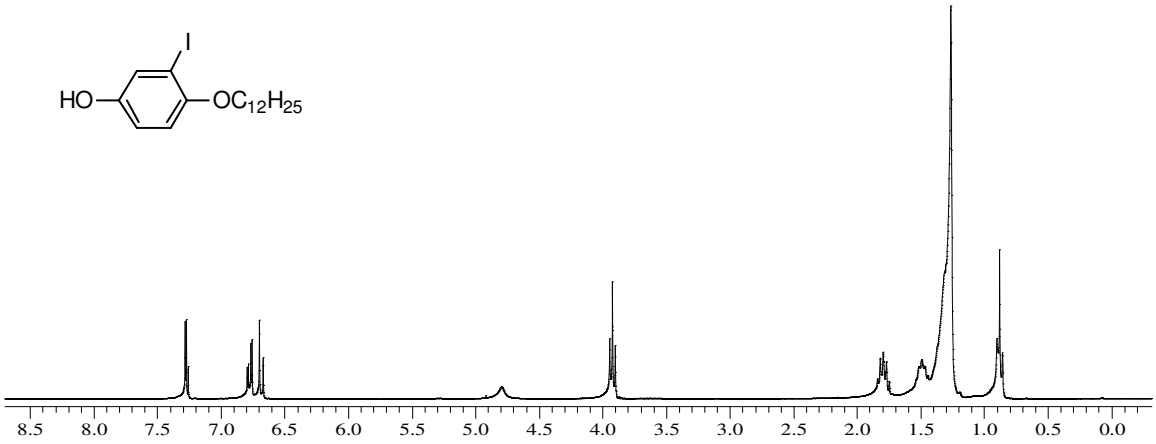

B. ^{13}C NMR

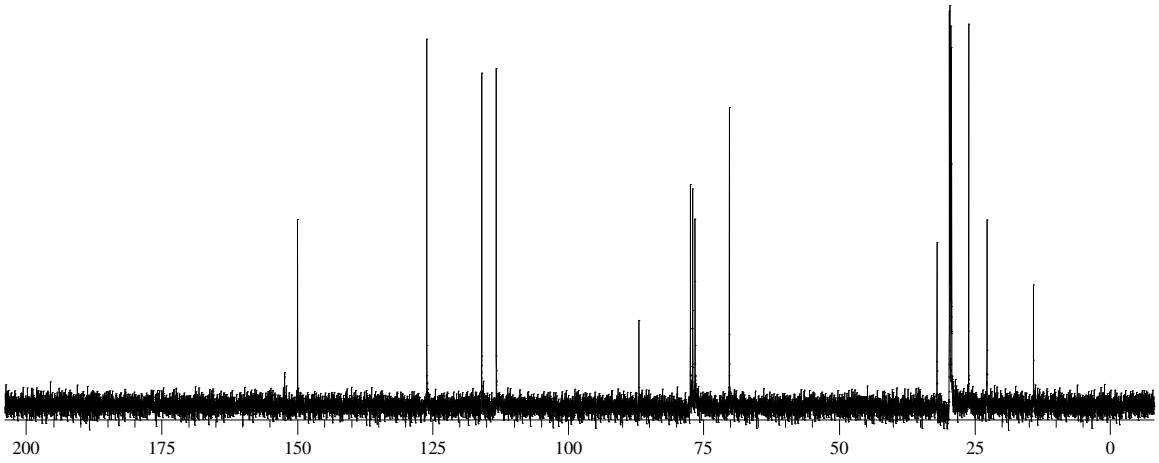

C. IR spectrum

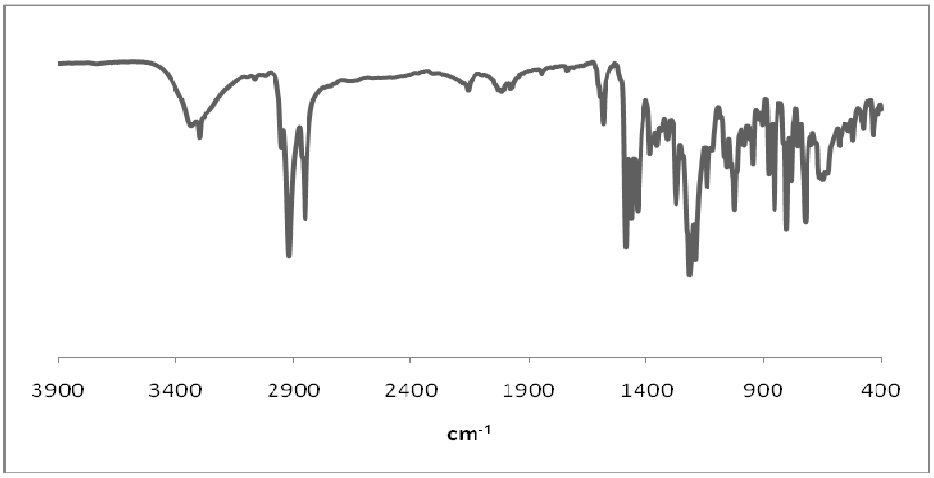

D. EI mass spectrum

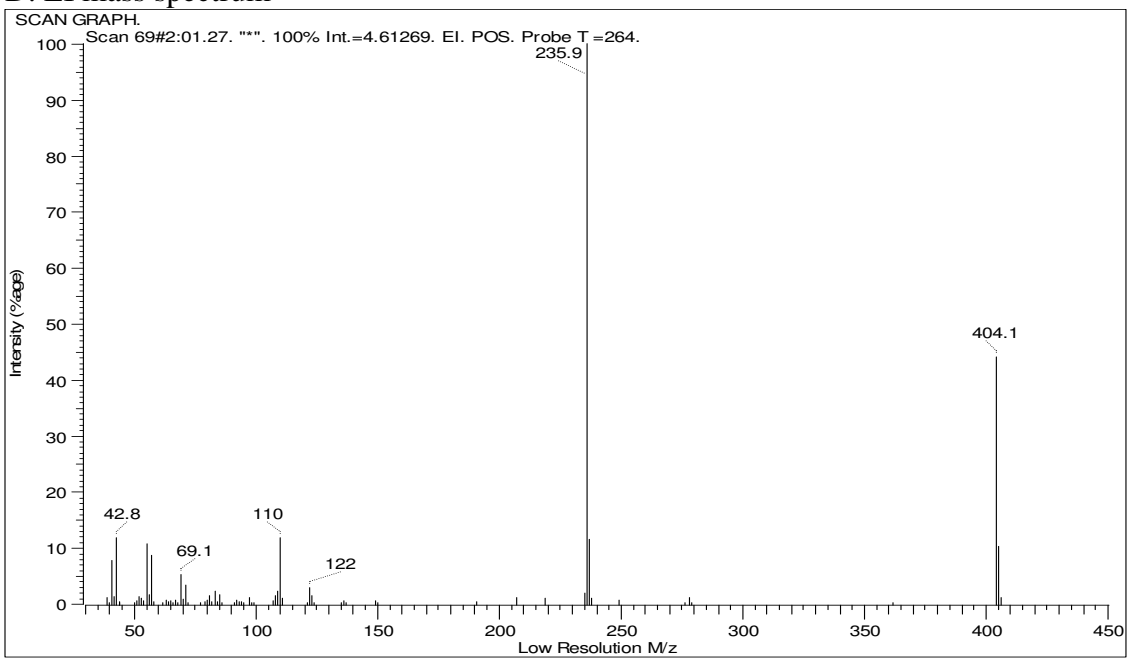

Figure A.1. ^{1}H NMR, ^{13}C NMR, IR spectrum and EI mass spectrum for 4-dodecyloxy-3-iodophenol, **II-1**.

1-(Dodecyloxy)-2-iodo-4(hexyloxy)benzene

A. ^{1}H NMR

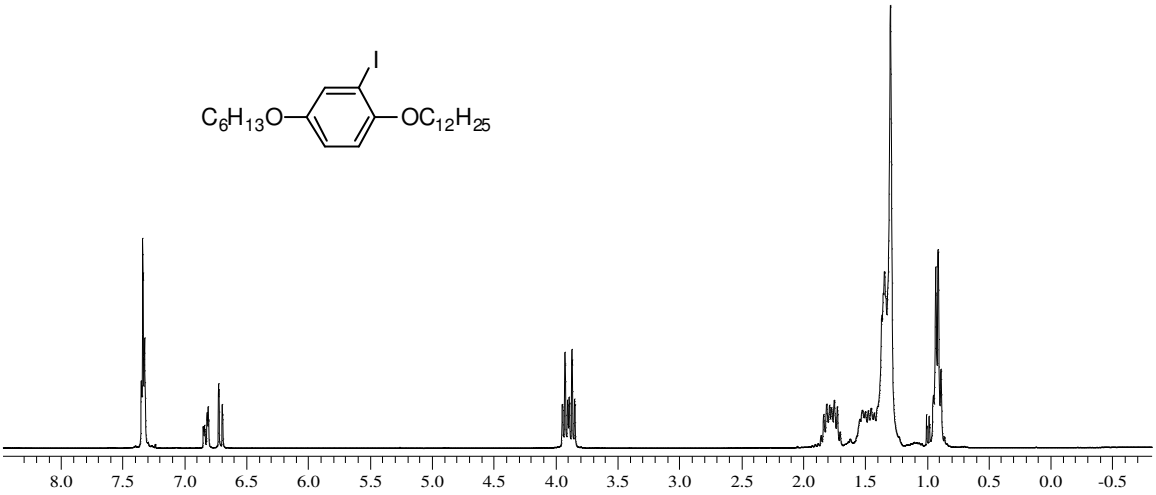

B. ^{13}C NMR

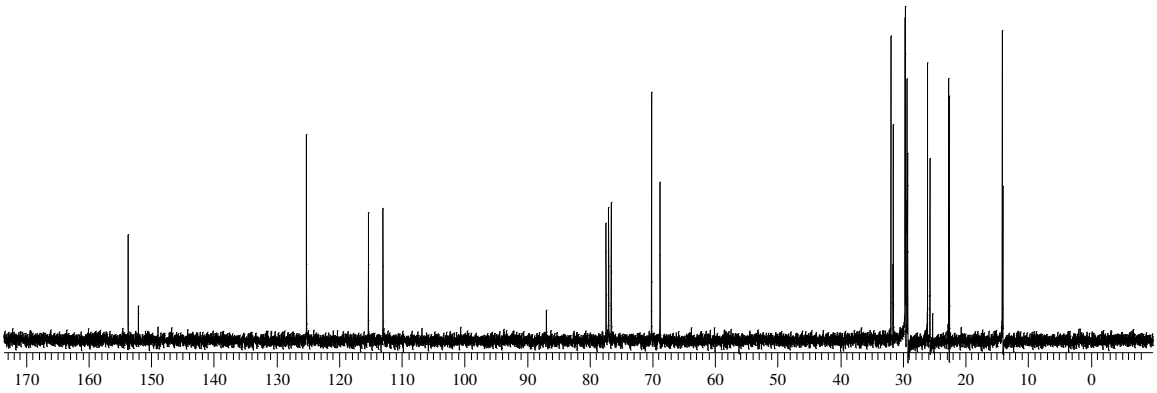

C. IR spectrum

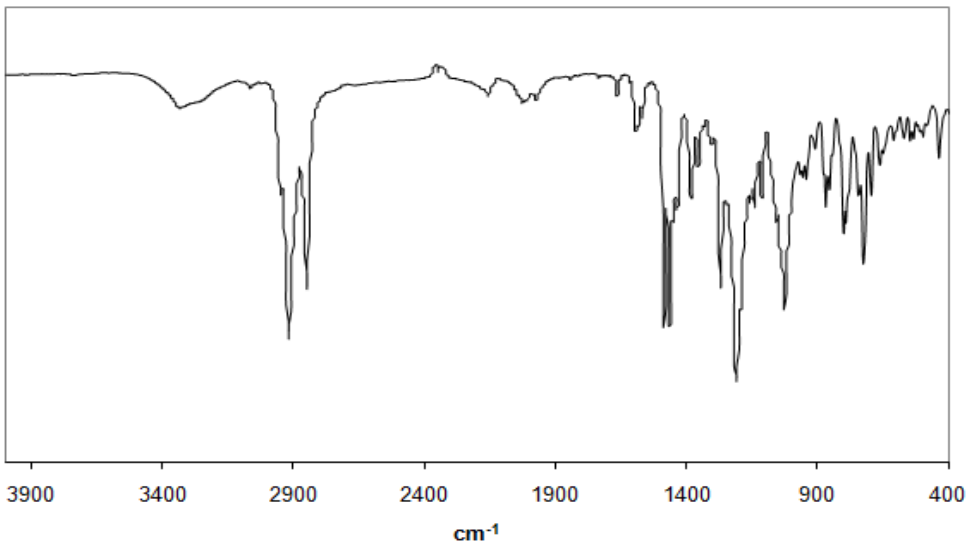

D. EI mass spectrum

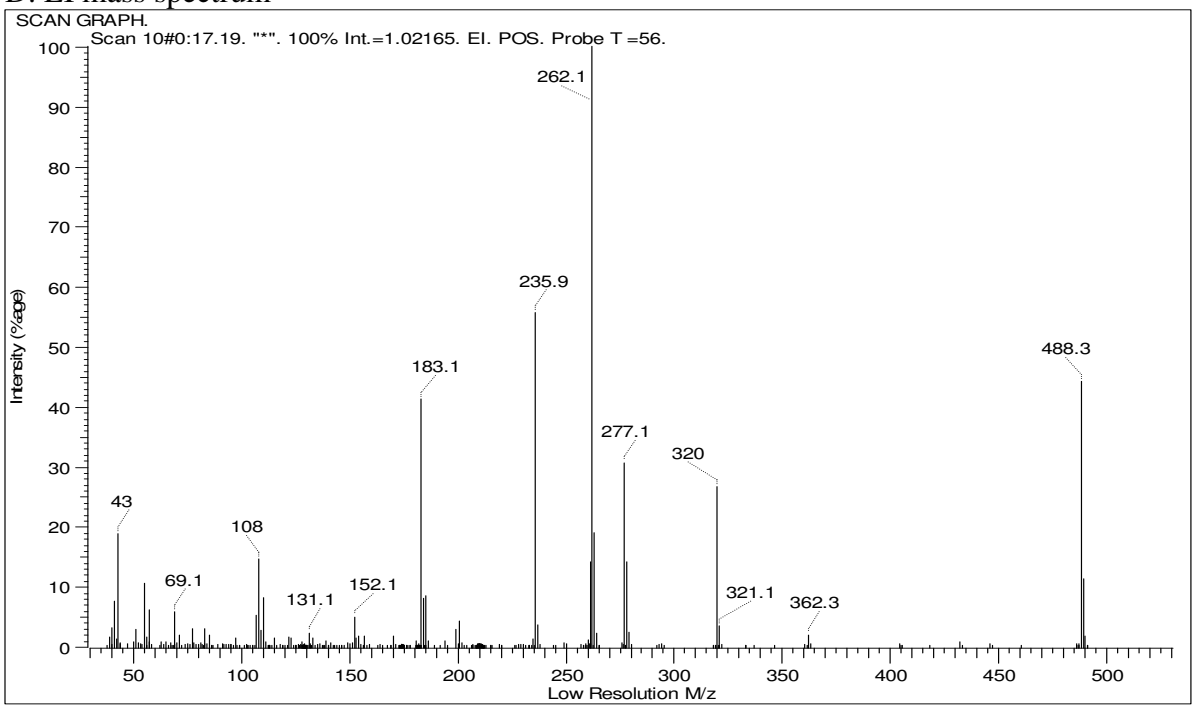

Figure A.2. ^{1}H NMR, ^{13}C NMR, IR spectrum and EI mass spectrum for 1-(dodecyloxy)-2-iodo-4(hexyloxy)benzene, **II-2**.

5-(Dodecyloxy)-4-iodo-2-(hexyloxy)benzaldehyde

A. ^{1}H NMR

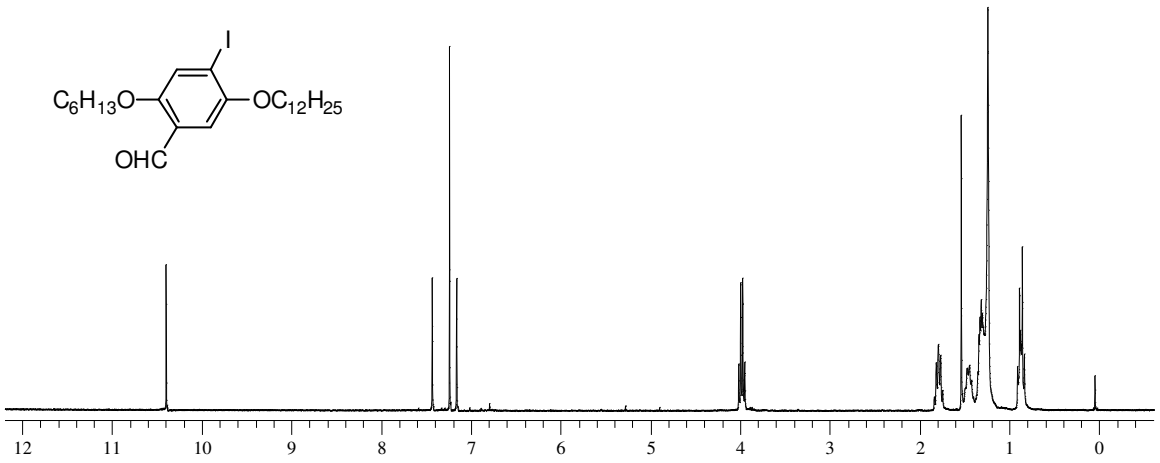

B. ^{13}C NMR

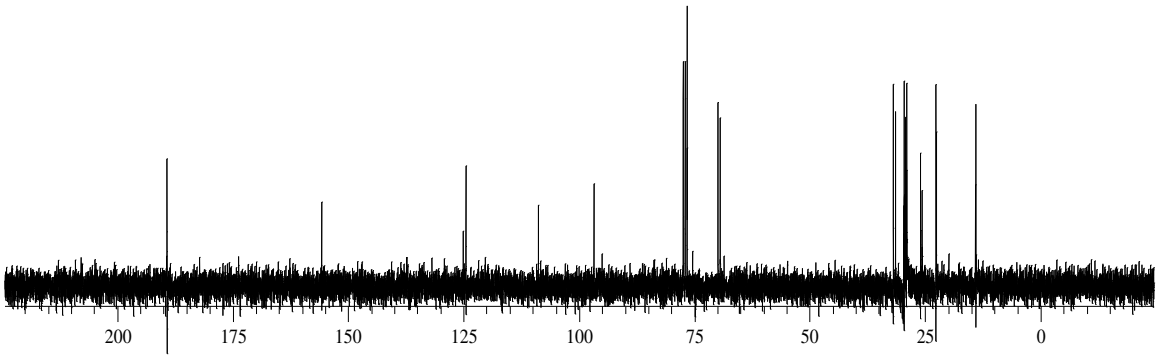

C. IR spectrum

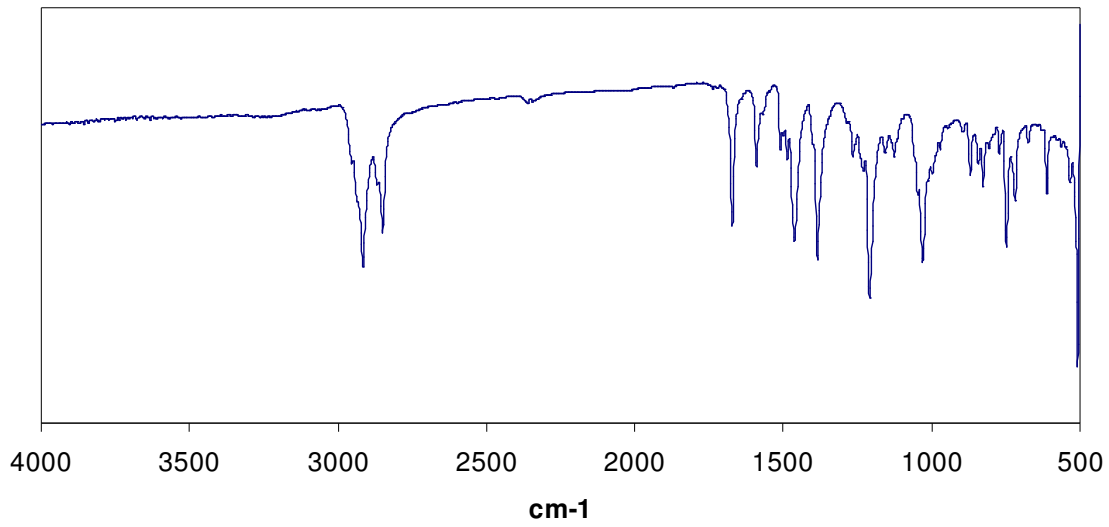

D. EI mass spectrum

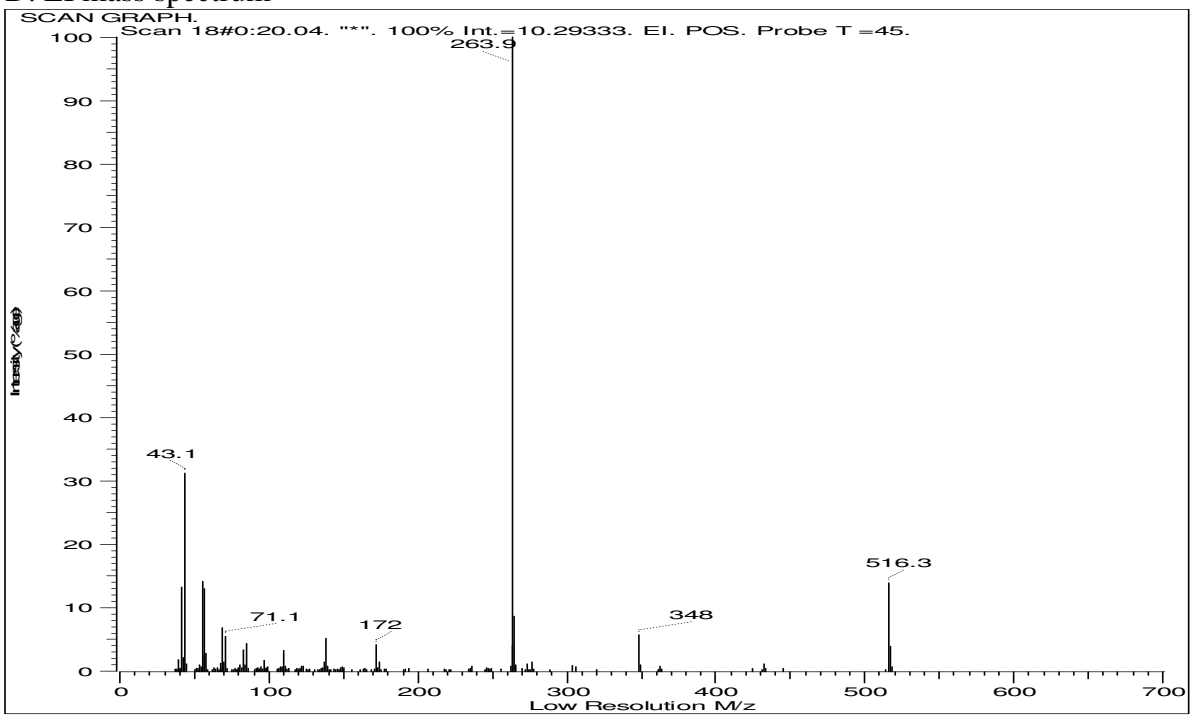

Figure A.3. ^{1}H NMR, ^{13}C NMR, IR spectrum and EI mass spectrum for 5-(dodecyloxy)-4-iodo-2-(hexyloxy)benzaldehyde, **II-3**.

1-(Dodecyloxy)-5-ethynyl-2-iodo-4-(hexyloxy)benzene

A. ^{1}H NMR

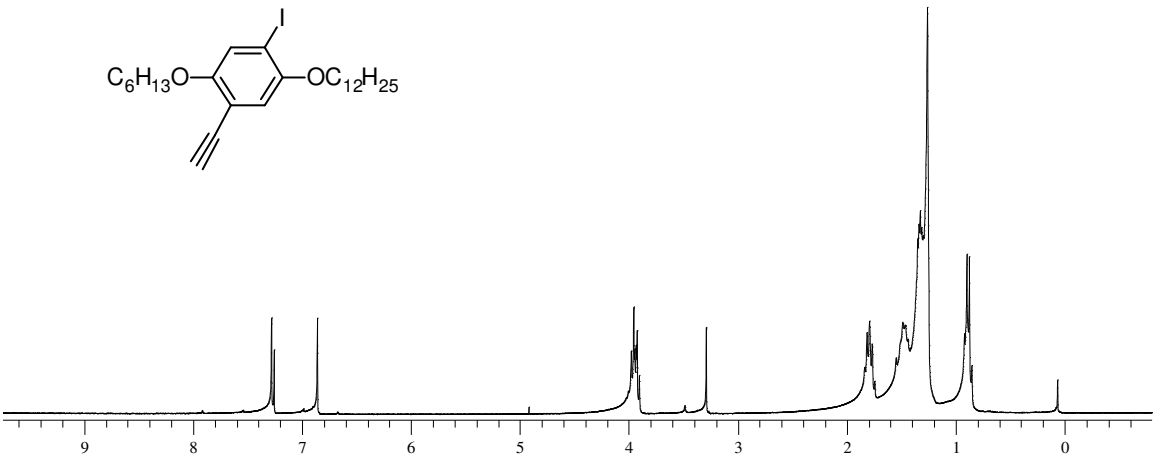

B. ^{13}C NMR

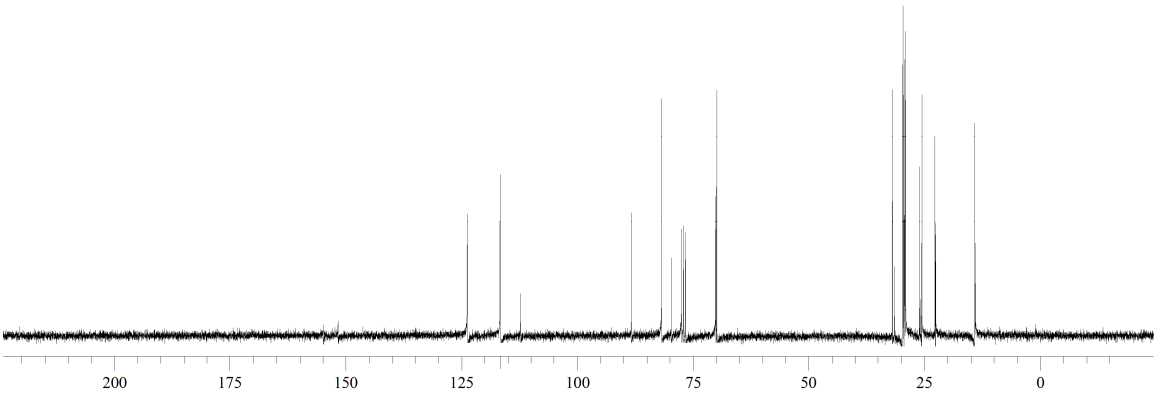

C. IR spectrum

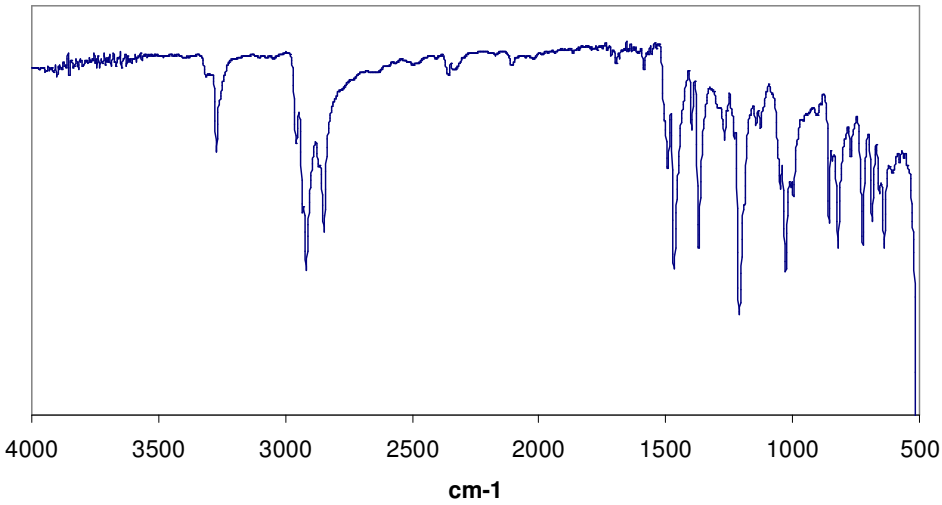

D. EI mass spectrum

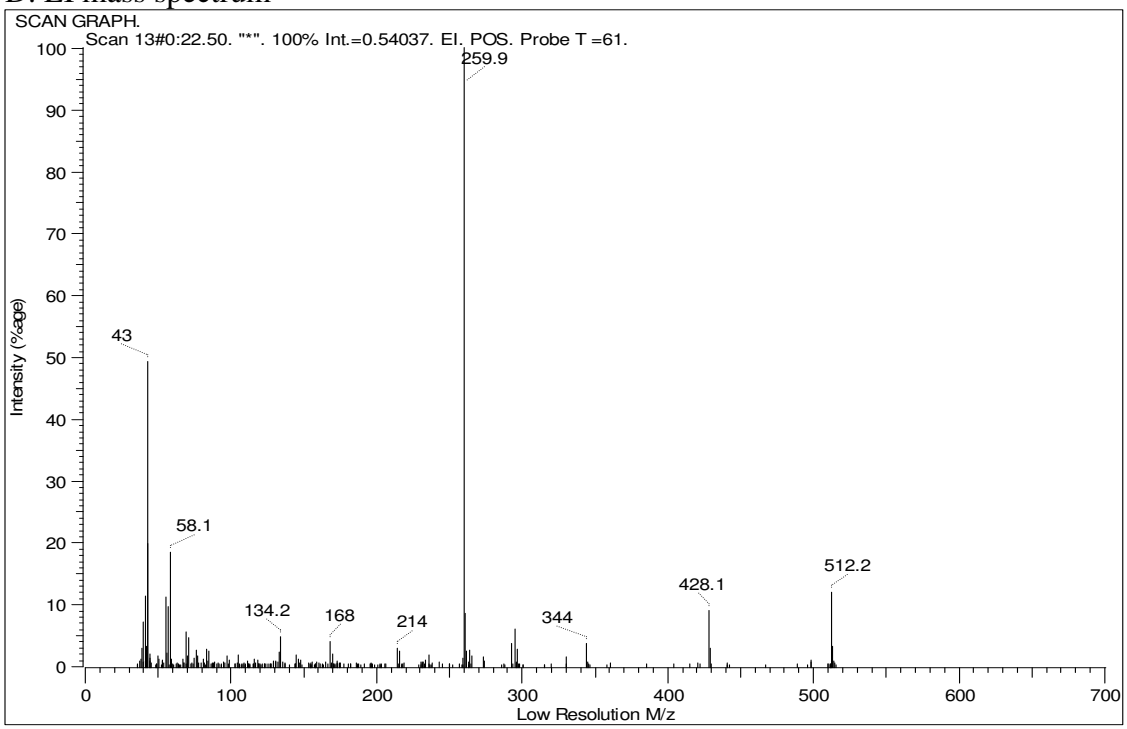

Figure A.4. ^{1}H NMR, ^{13}C NMR, IR spectrum and EI mass spectrum for 1-(dodecyloxy)-5-ethynyl-2-iodo-4-(hexyloxy)benzene, **II-4**.

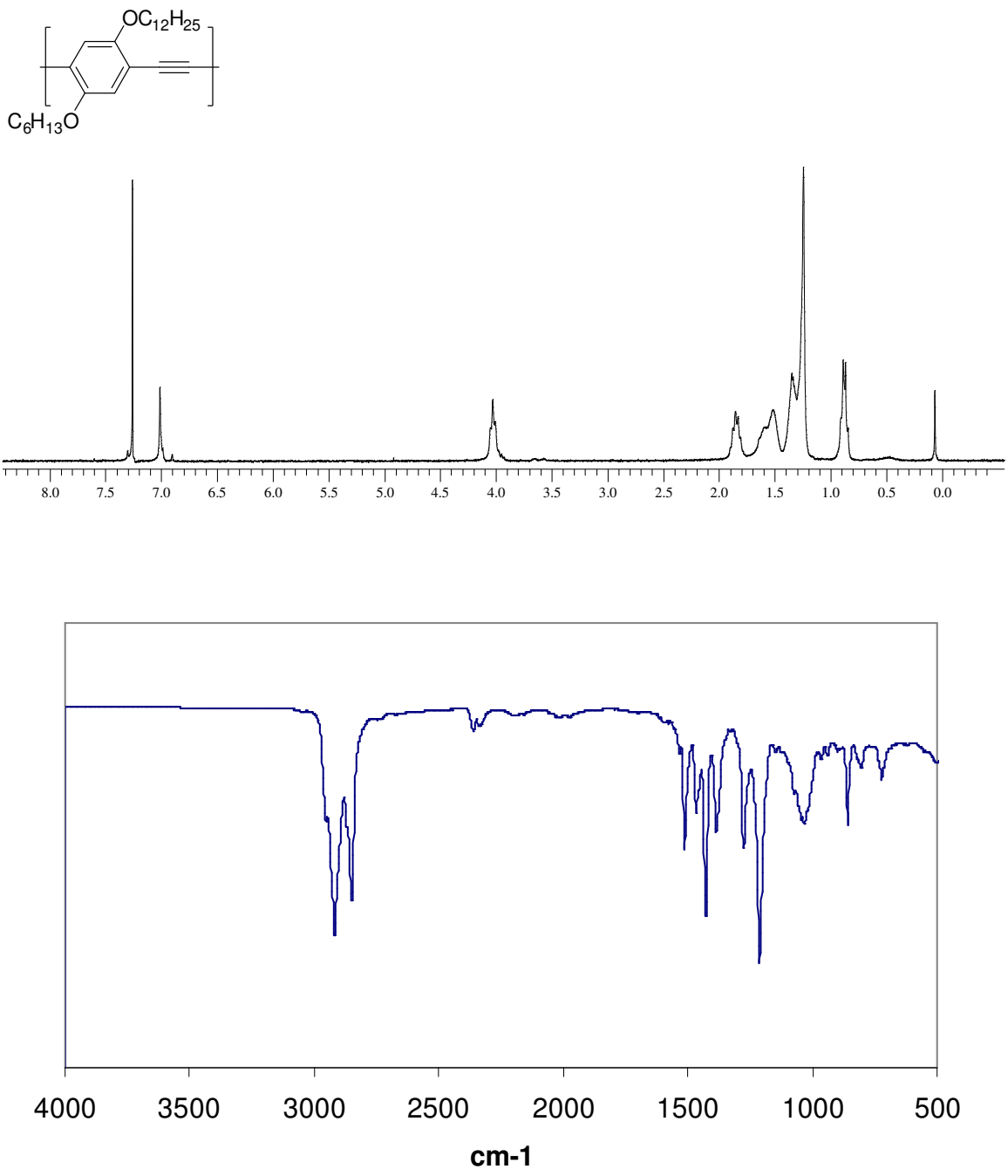

Figure A.5. ^{1}H NMR (top) and IR (bottom) for **RgPPE(6/12)**.

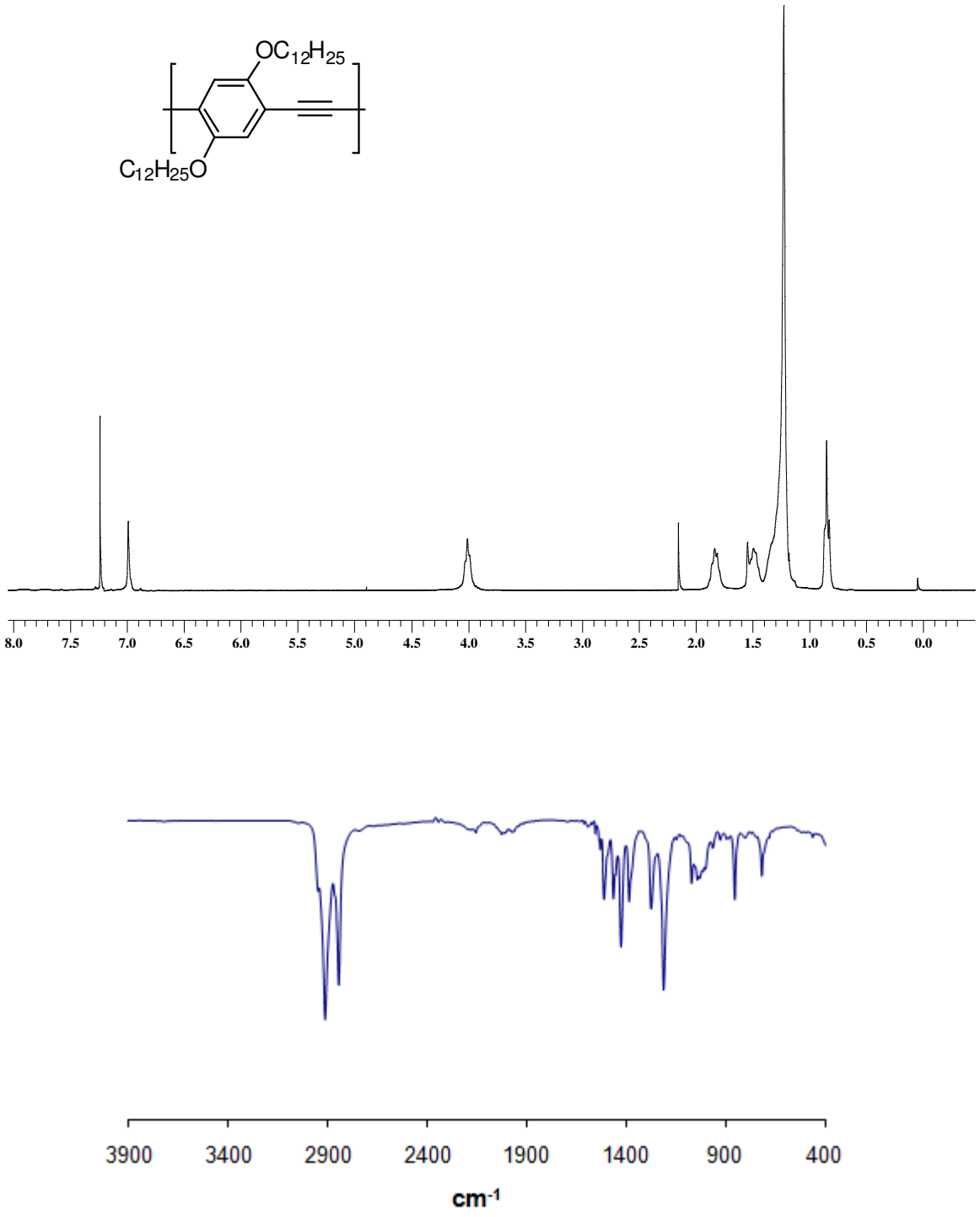

Figure A.6. ^{1}H NMR (top) and IR (bottom) for **PPE(C12)**.

APPENDIX B: ^{1}H AND ^{13}C NMR, IR SPECTRA, AND EI MASS SPECTRA OF MONOMERS AND POLYMERS DESCRIBED IN CHAPTER 3

^{1}H NMR spectra were collected on a Varian Mercury Vx 300 MHz instrument using $CDCl_3$ as a solvent. ^{13} C NMR spectra were obtained at 75.5 MHz. IR analyses were performed on a Nicolet 4700 FTIR with an ATR attachment from SmartOrbit Thermoelectronic Corporation.

7,7,8,8,9,9,10,10,11,11,12,12,12-Tridecafluoro-5-iodododecan-1-ol

A. ^{1}H NMR

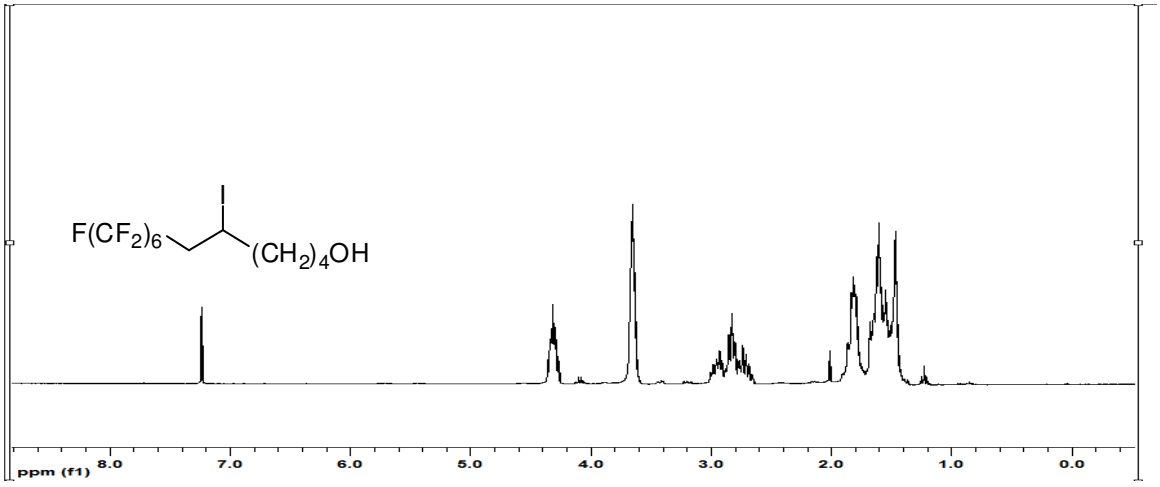

B. ^{13}C NMR

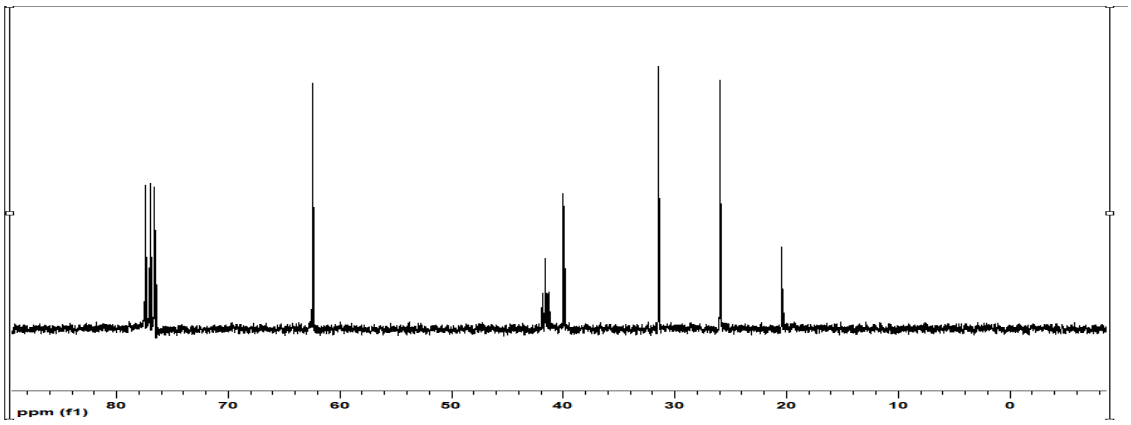

C. IR spectrum

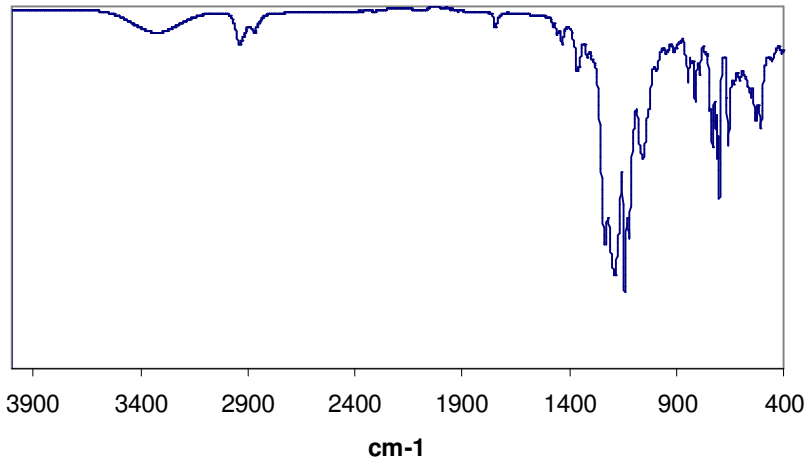

Figure B.1 ^{1}H NMR, ^{13}C NMR, and IR spectrum of 7,7,8,8,9,9,10,10,11,11,12,12,12-tridecafluoro-5-iododododecan-1-ol, **III-1a**.

9,9,10,10,11,11,12,12,12-Nonafluoro-7-iodododecan-1-ol

A. ^{1}H NMR

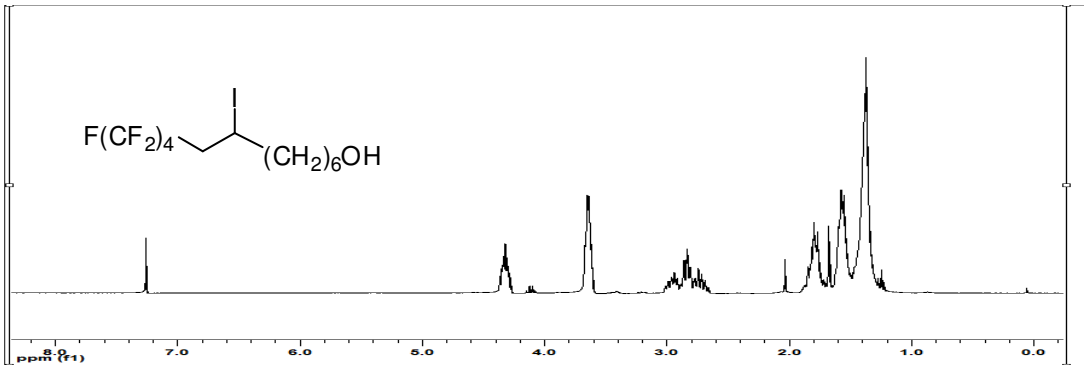

B. ^{13}C NMR

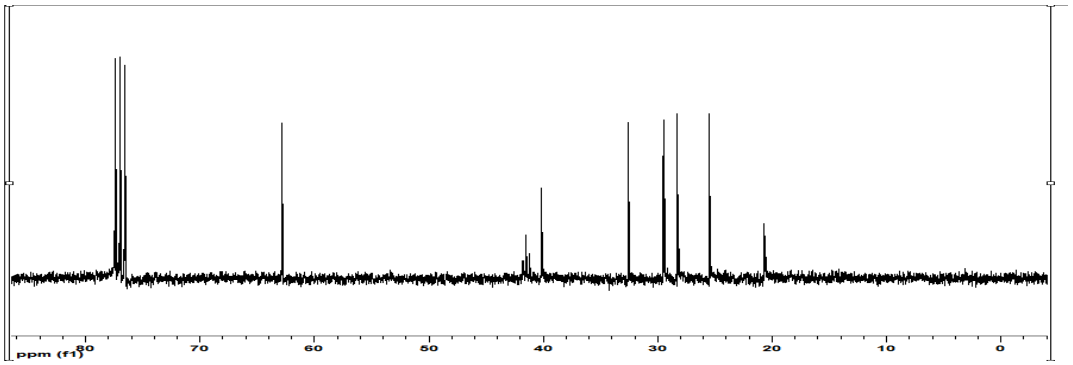

C. IR spectrum

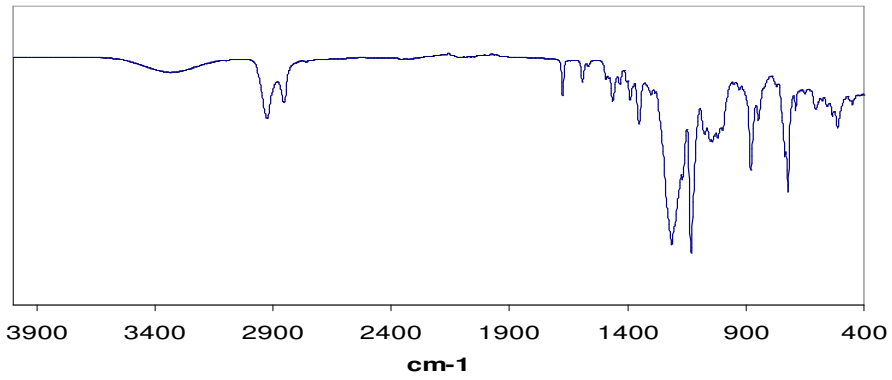

Figure B.2 ^{1}H NMR, ^{13}C NMR, and IR spectrum of 9,9,10,10,11,11,12,12,12-nonafluoro-7-iodododecan-1-ol, **III-1b**.

11,11,12,12,12-Pentafluoro-9-iodododecan-1-ol

A. ^{1}H NMR

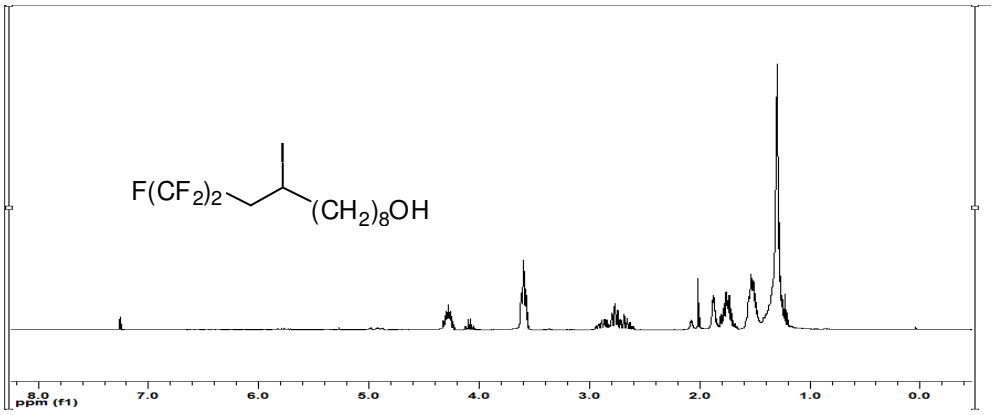

B. ^{13}C NMR

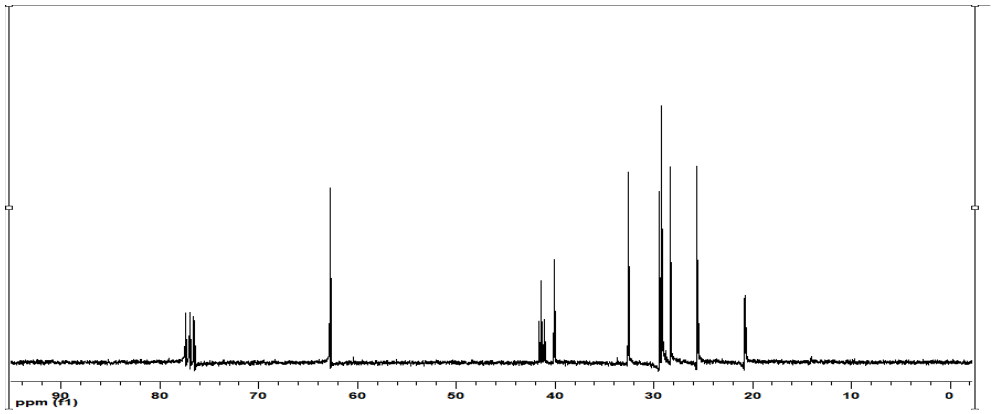

C. IR spectrum

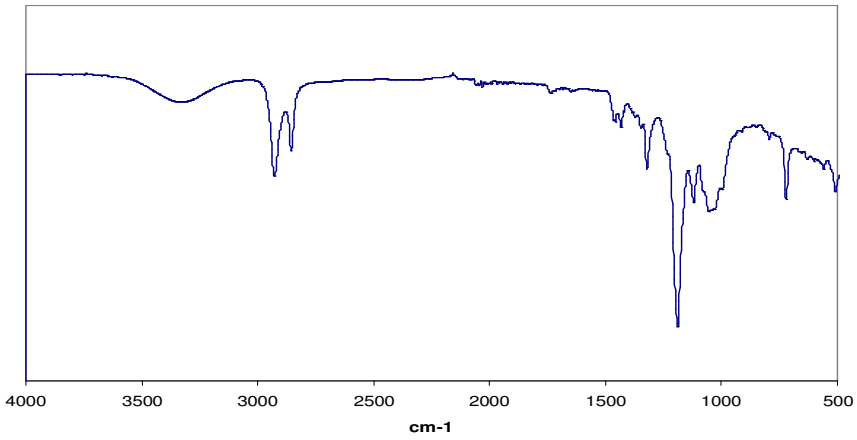

Figure B.3 ^{1}H NMR, ^{13}C NMR, and IR spectrum of 11,11,12,12,12-pentafluoro-9-iodododecan-1-ol, **III-1c**.

7,7,8,8,9,9,10,10,11,11,12,12,12-Tridecafluorododododecan-1-ol

A. ^{1}H NMR

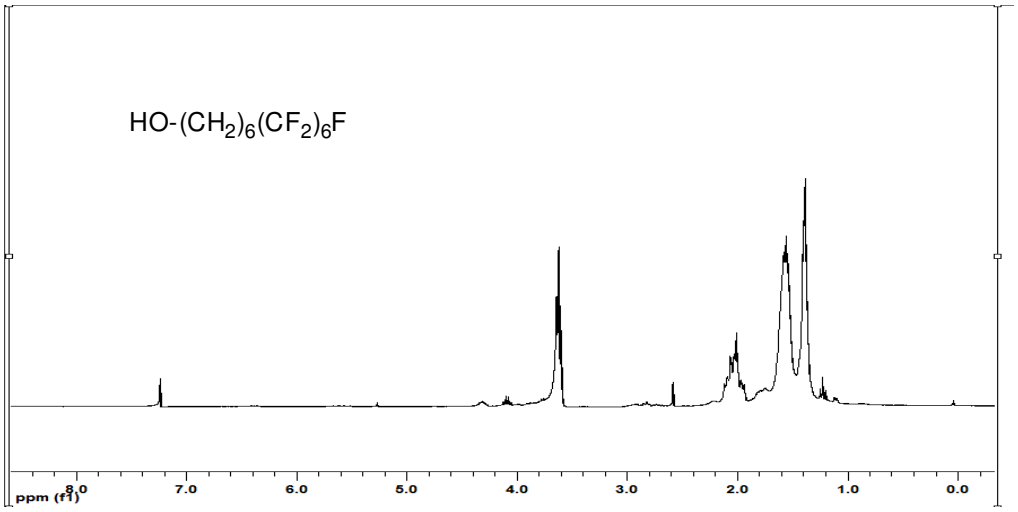

B. ^{13}C NMR

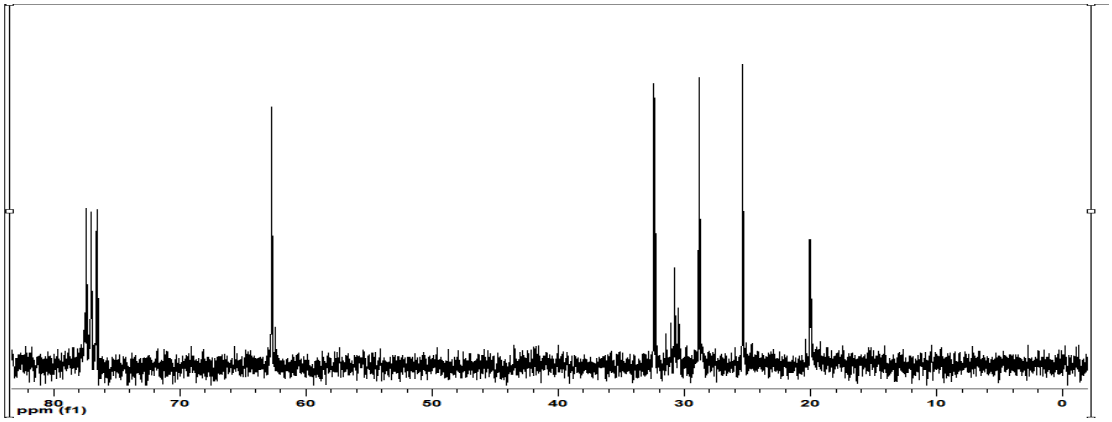

C. IR spectrum

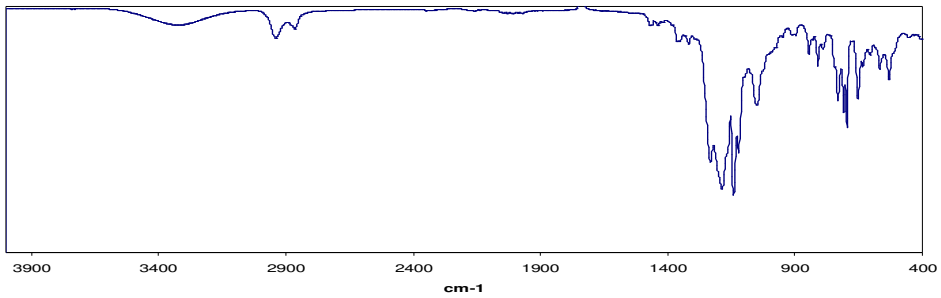

Figure B.4 ^{1}H NMR, ^{13}C NMR and IR spectrum of 7,7,8,8,9,9,10,10,11,11,12,12,12-tridecafluorododododecan-1-ol, **III-2a**.

9,9,10,10,11,11,12,12,12-Nonafluorododecan-1-ol

A. ^{1}H NMR

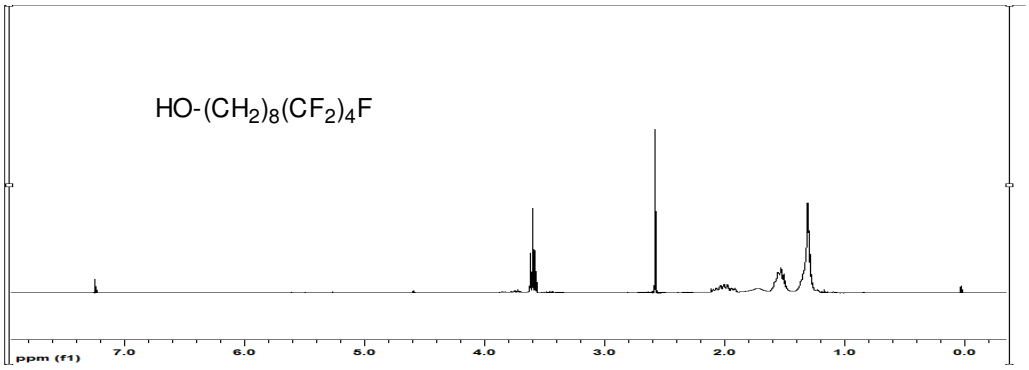

B. ^{13}C NMR

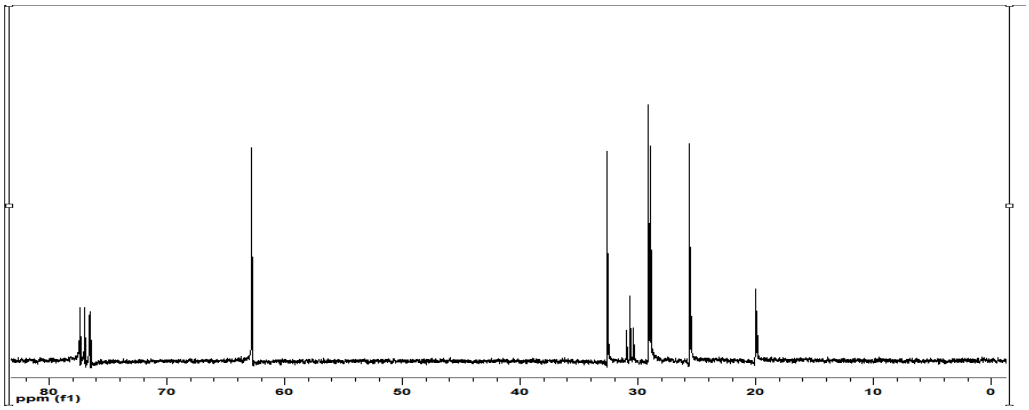

C. IR spectrum

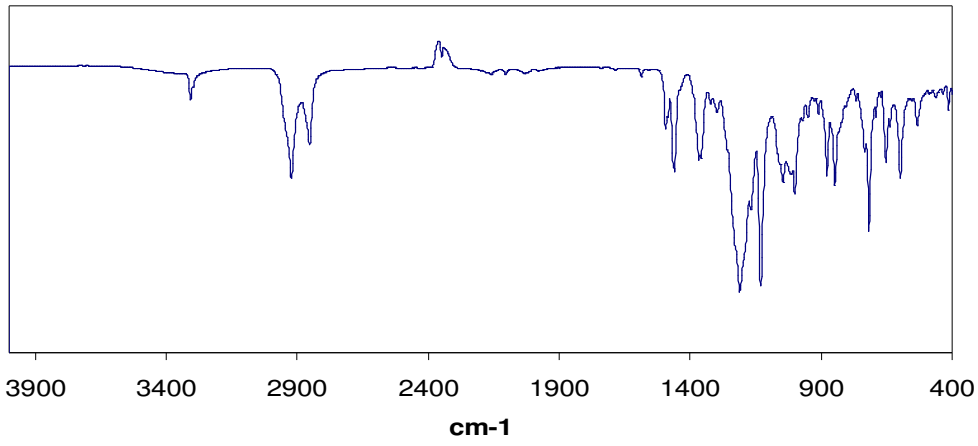

Figure B.5 ^{1}H NMR, ^{13}C NMR and IR spectrum, of 9,9,10,10,11,11,12,12,12-nonafluorododecan-1-ol, **III-2b**.

11,11,12,12,12-Pentafluorododecan-1-ol

A. ^{1}H NMR

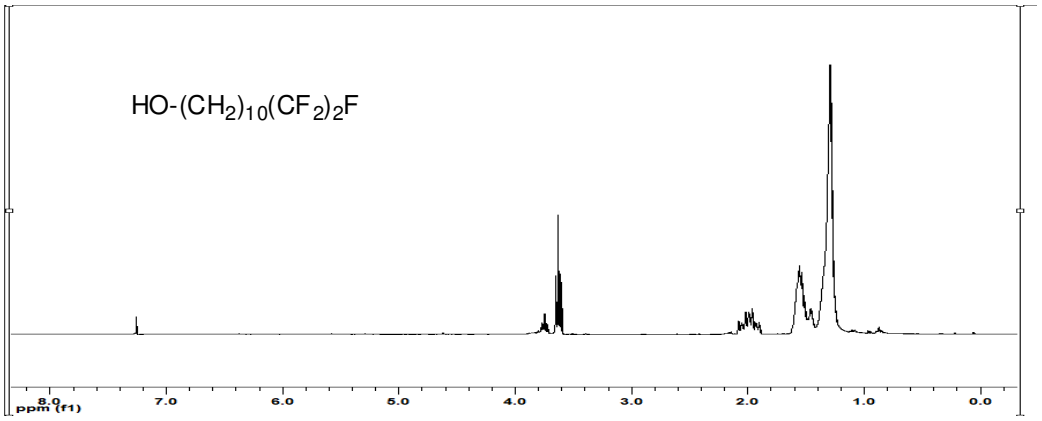

B. ^{13}C NMR

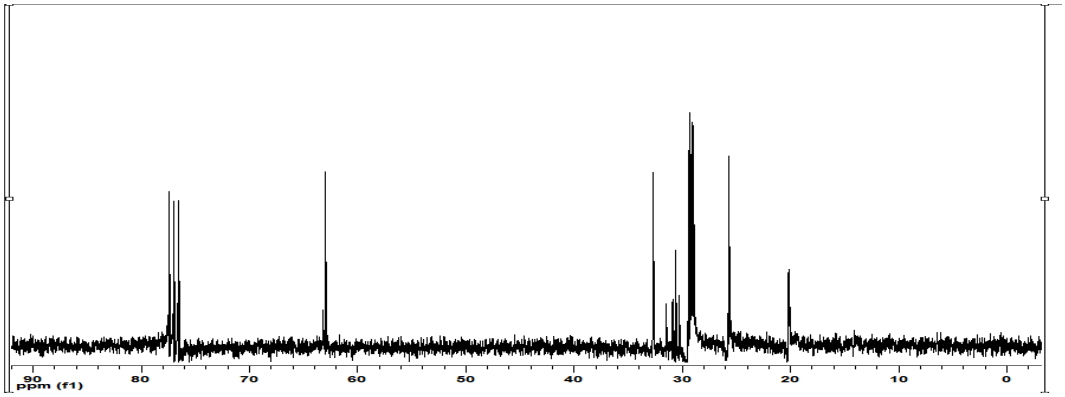

C. IR spectrum

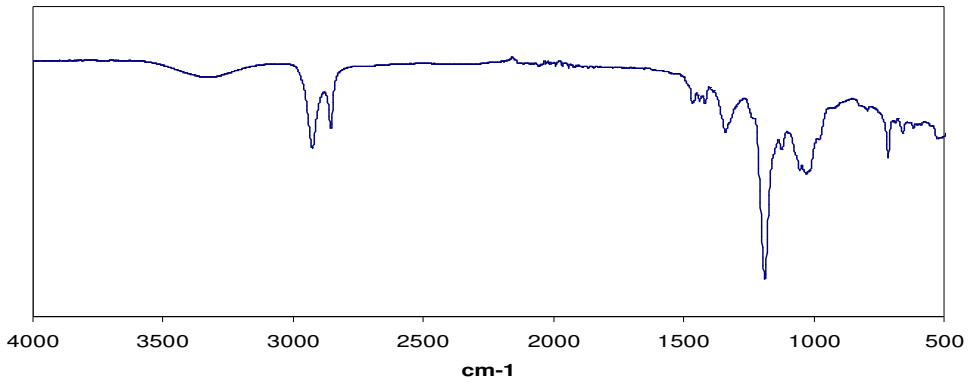

Figure B.6 ^{1}H NMR, ^{13}C NMR and IR spectrum of 11,11,12,12,12-pentafluorododecan-1-ol, **III-2c**.

1-(Dodecyloxy)-4-(7,7,8,8,9,9,10,10,11,11,12,12,12-tridecafluorododecyloxy)benzene

A. ^{1}H NMR

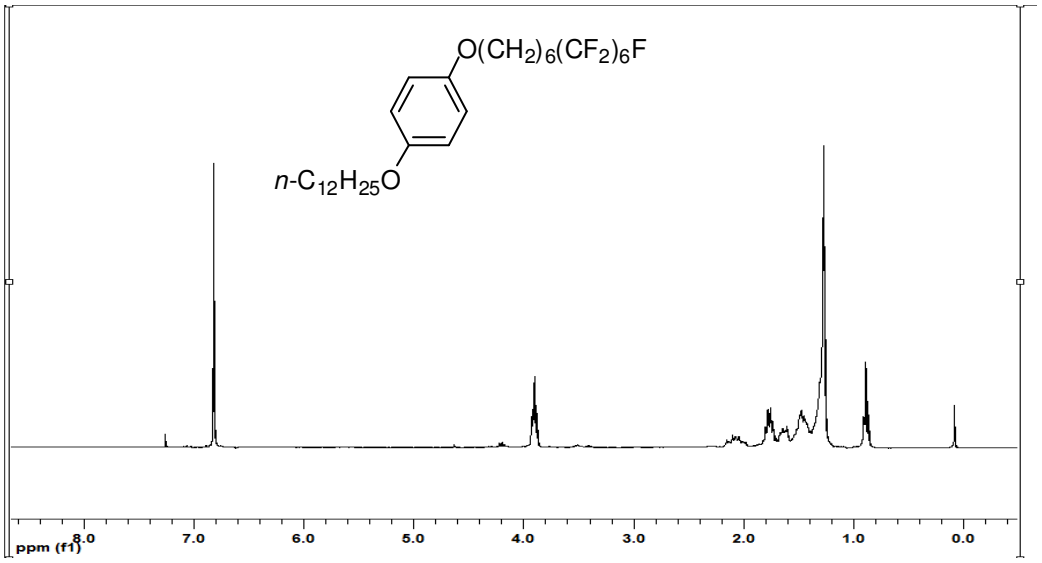

B. ^{13}C NMR

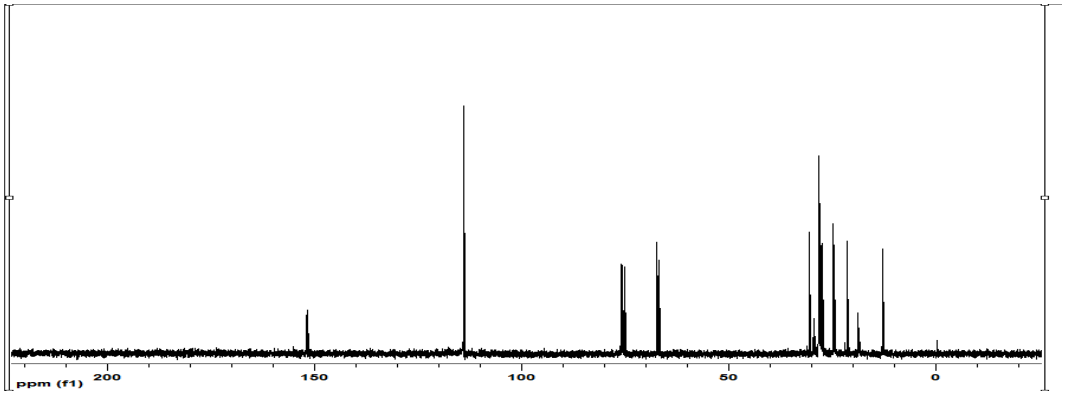

C. IR spectrum

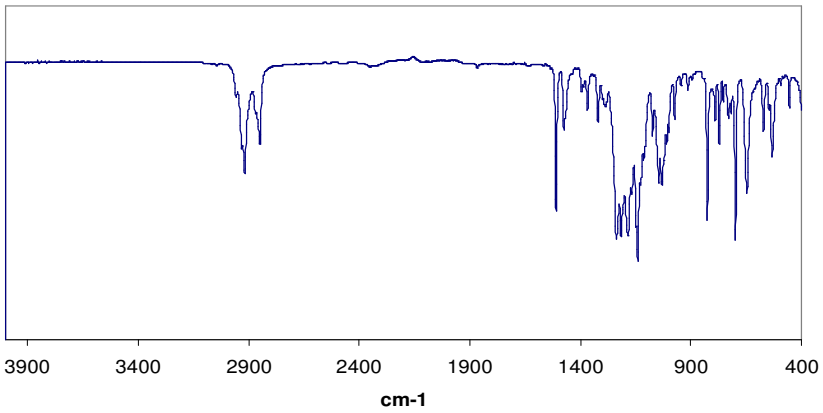

D. EI mass spectrum

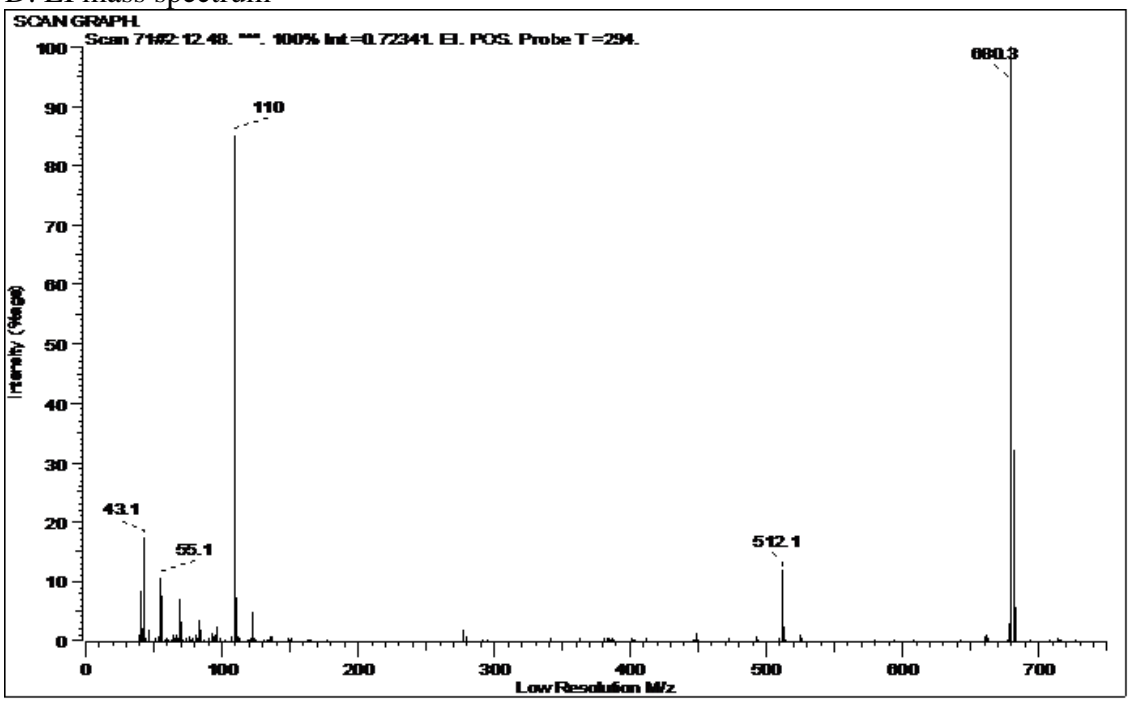

Figure B.7 ^{1}H NMR, ^{13}C NMR, IR spectrum and EI mass spectrum of 1-(dodecyloxy)-4-(7,7,8,8,9,9,10,10,11,11,12,12,12-tridecafluorododecyloxy)benzene, **III-3**.

1-(Dodecyloxy)-4-(9,9,10,10,11,11,12,12,12-nonafluorododecyloxy)benzene

A. ^{1}H NMR

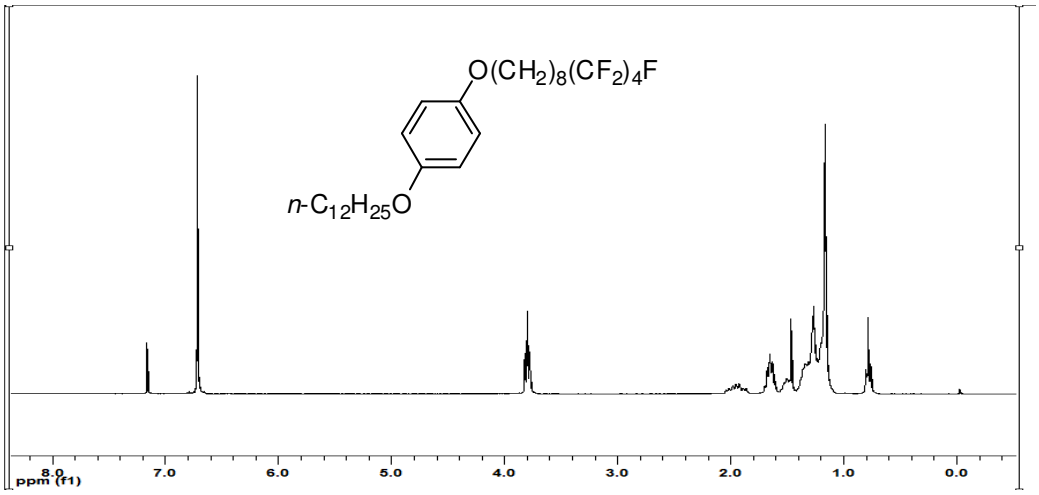

B. ^{13}C NMR

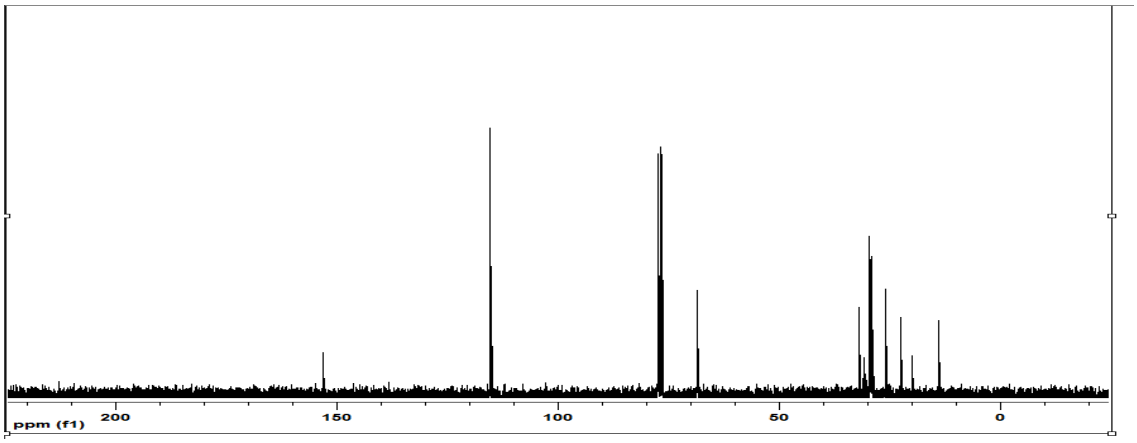

C. IR spectrum

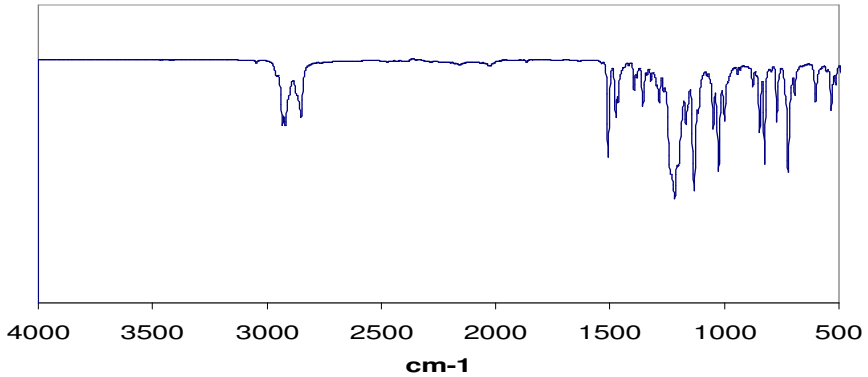

D. EI mass spectrum

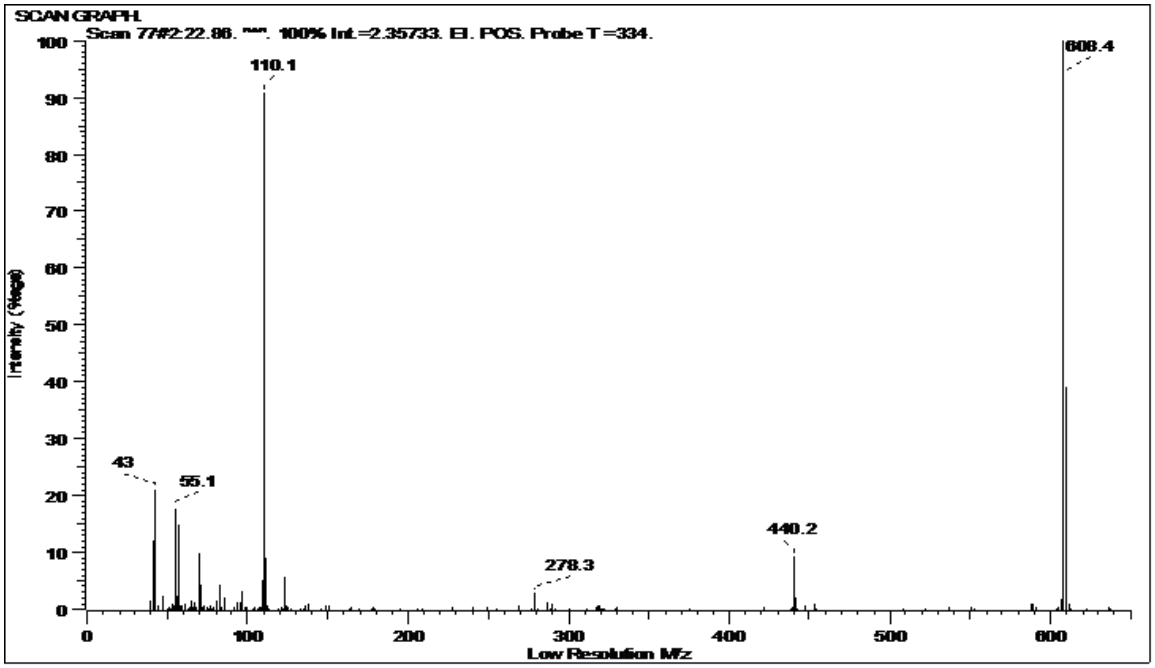

Figure B.8 ^{1}H NMR, ^{13}C NMR, IR spectrum and EI mass spectrum of 1-(dodecyloxy)-4-(9,9,10,10,11,11,12,12,12-nonafluorododecyloxy)benzene, **III-3b**.

1-(Dodecyloxy)-2,5-diiodo-4-(7,7,8,8,9,9,10,10,11,11,12,12,12-tridecafluorododecyloxy)benzene

A. ^{1}H NMR

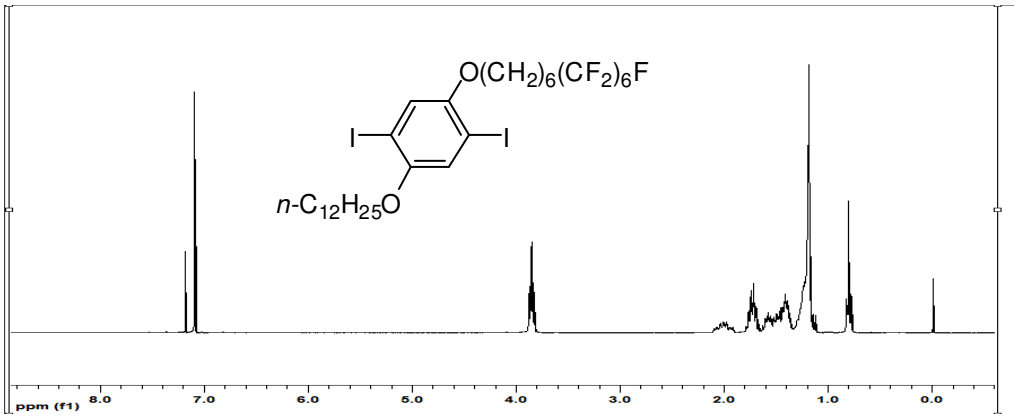

B. ^{13}C NMR

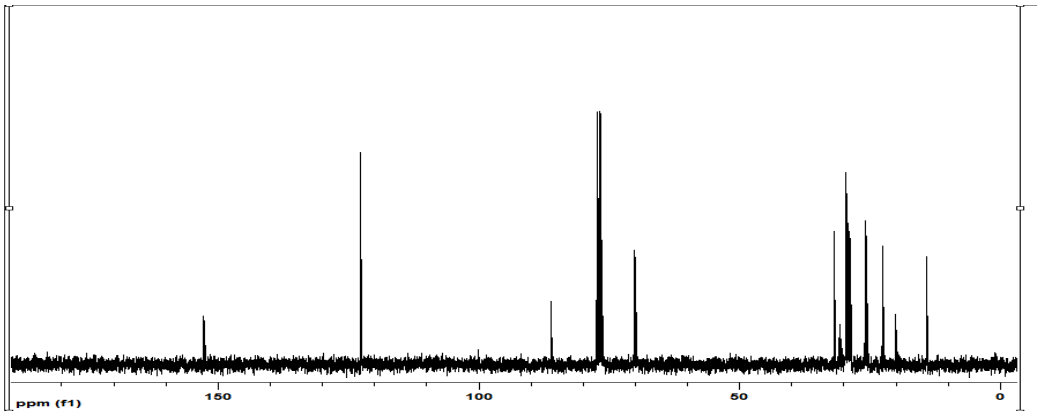

C. IR spectrum

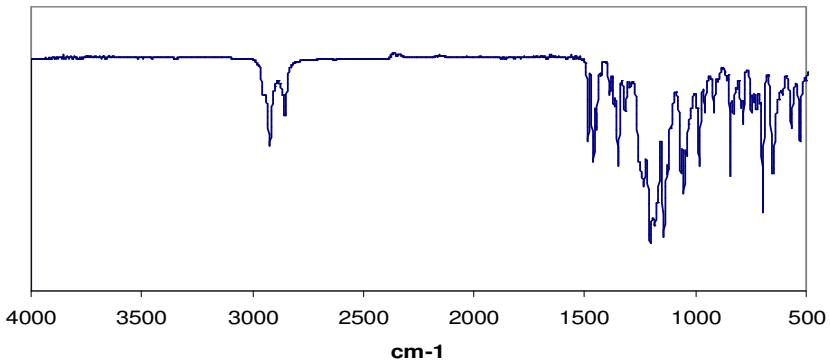

D. EI mass spectrum

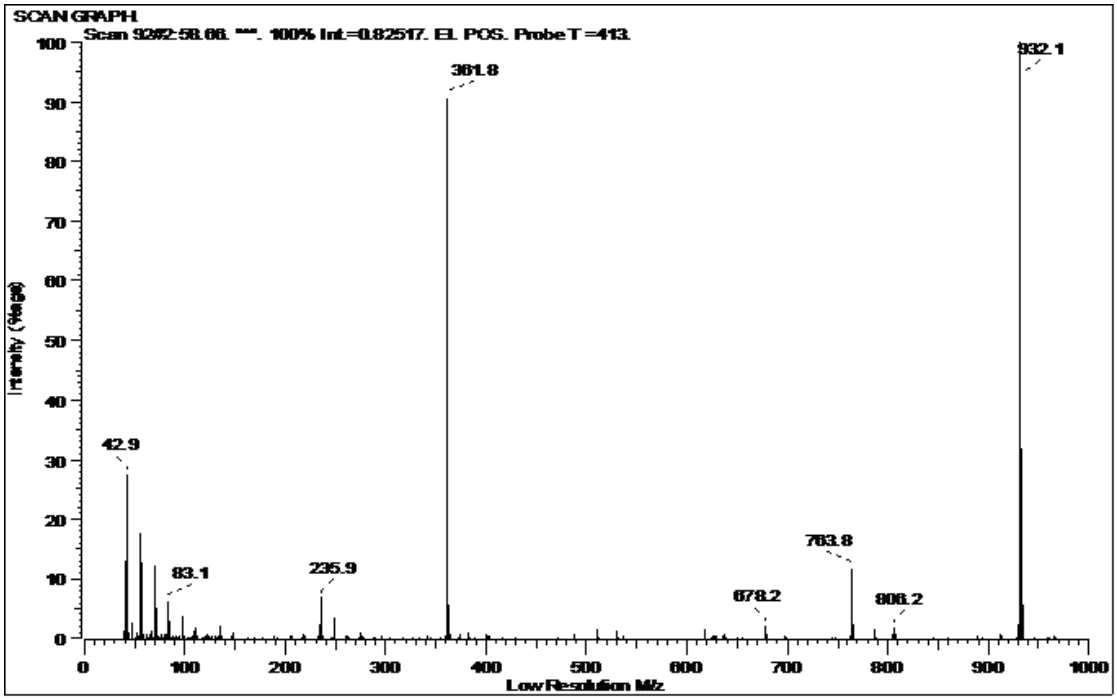

Figure B.9 ^{1}H NMR, ^{13}C NMR, IR spectrum and EI mass spectrum of 1-(dodecyloxy)-2,5-diiodo-4-(7,7,8,8,9,9,10,10,11,11,12,12,12-tridecafluorododecyloxy)benzene, **III-4a**.

1-(Dodecyloxy)-2,5-diiodo-4-(9,9,10,10,11,11,12,12,12-nonafluorododecyloxy)benzene

A. ^{1}H NMR

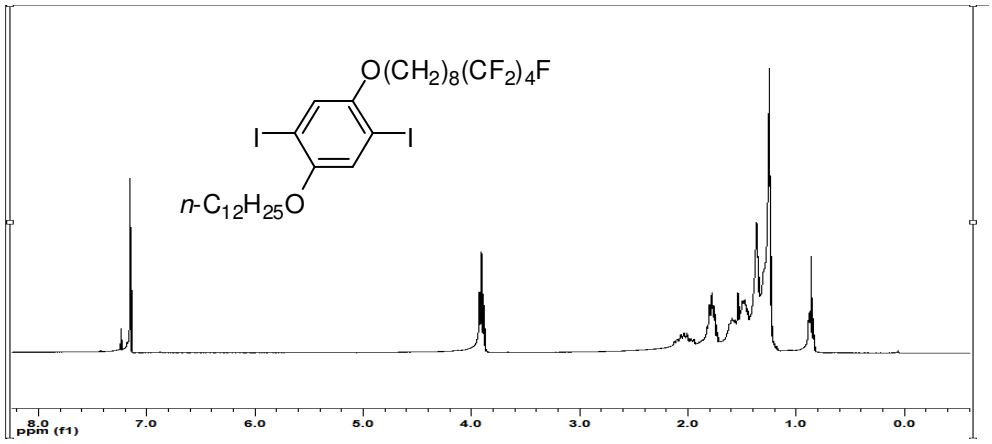

B. ^{13}C NMR

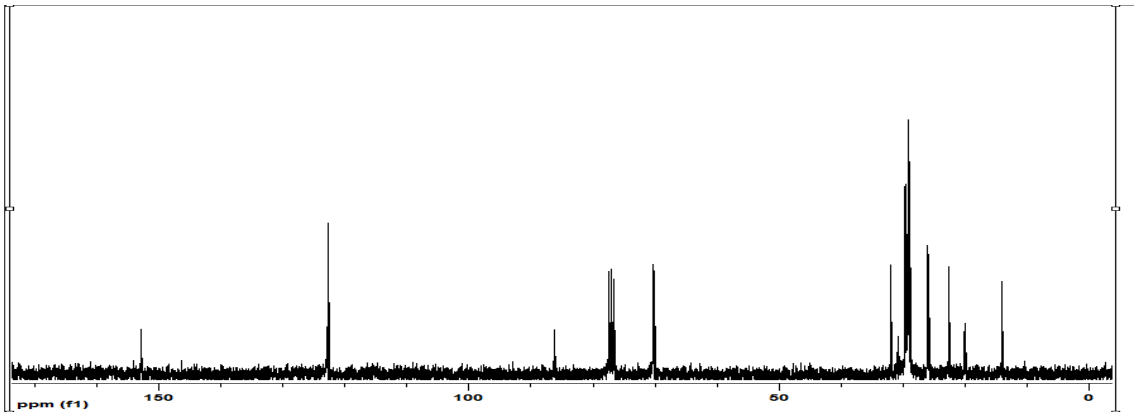

C. IR spectrum

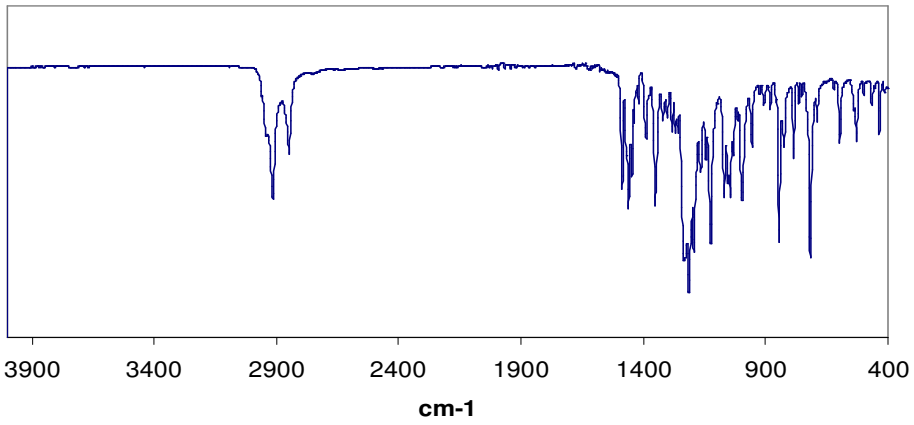

D. EI mass spectrum

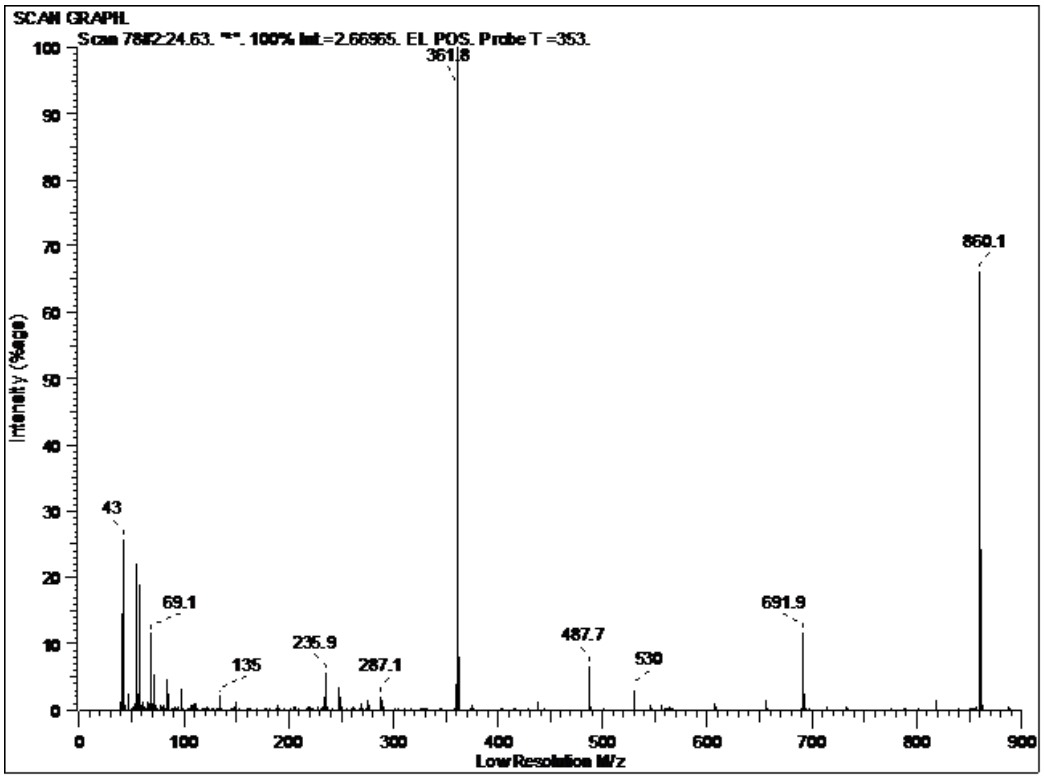

Figure B.10 ^{1}H NMR, ^{13}C NMR, IR spectrum and EI mass spectrum of 1-(dodecyloxy)-2,5-diiodo-4-(9,9,10,10,11,11,12,12,12-nonafluorododecyloxy)benzene, **III-4b**.

1-(Dodecyloxy)-2,5-diethynyl-4-(7,7,8,8,9,9,10,10,11,11,12,12,12-tridecafluorododecyloxy)benzene

A. ^{1}H NMR

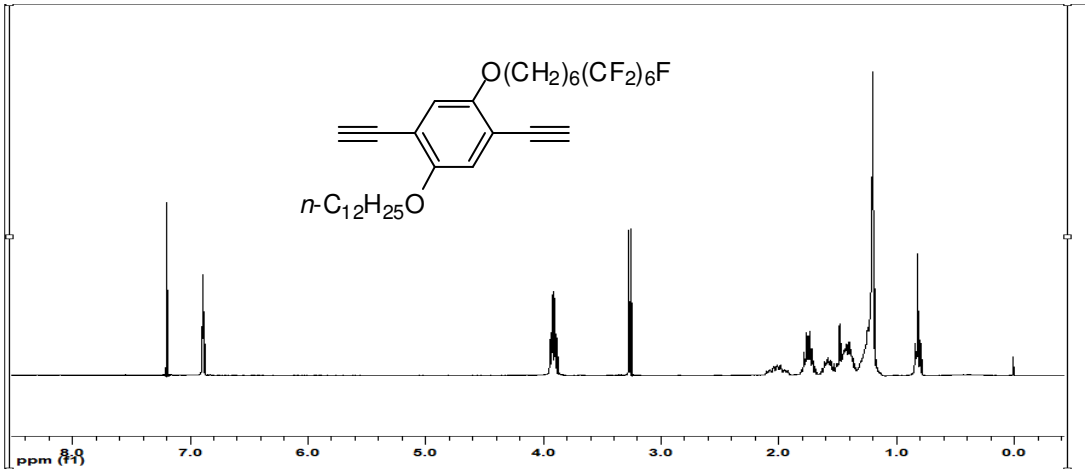

B. ^{13}C NMR

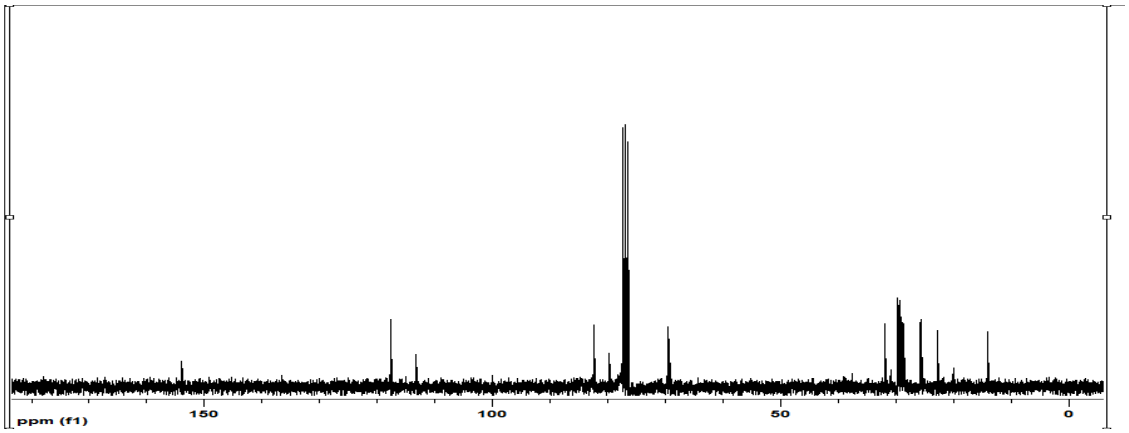

C. IR spectrum

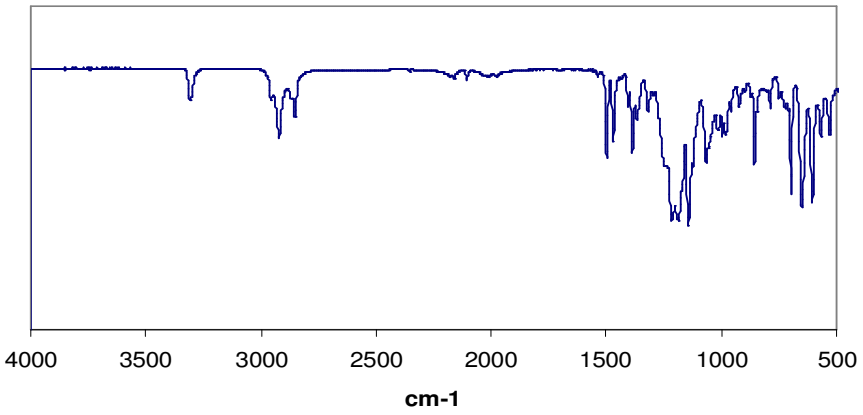

D. EI mass spectrum

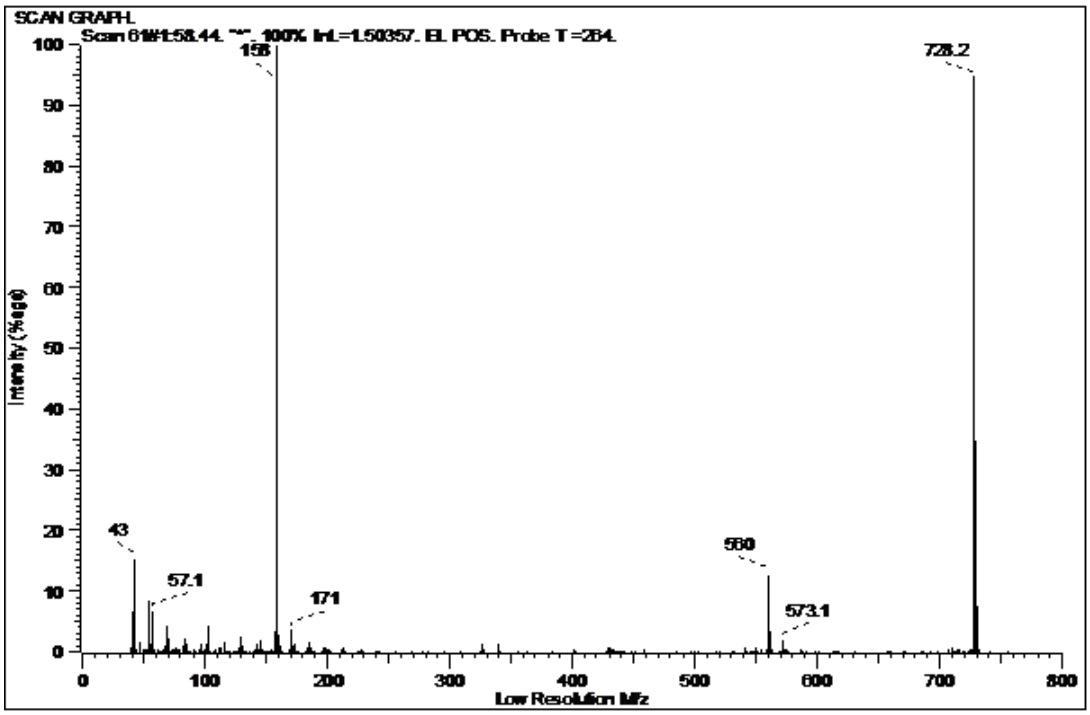

Figure B.11 ^{1}H NMR, ^{13}C NMR, IR spectrum and EI mass spectrum of 1-(dodecyloxy)-2,5-diethynyl-4-(7,7,8,8,9,9,10,10,11,11,12,12,12-tridecafluorododecyloxy)benzene, **III-6a**.

1-(Dodecyloxy)-2,5-diethynyl-4-(9,9,10,10,11,11,12,12,12-nonafluorododecyloxy)benzene

A. ^{1}H NMR

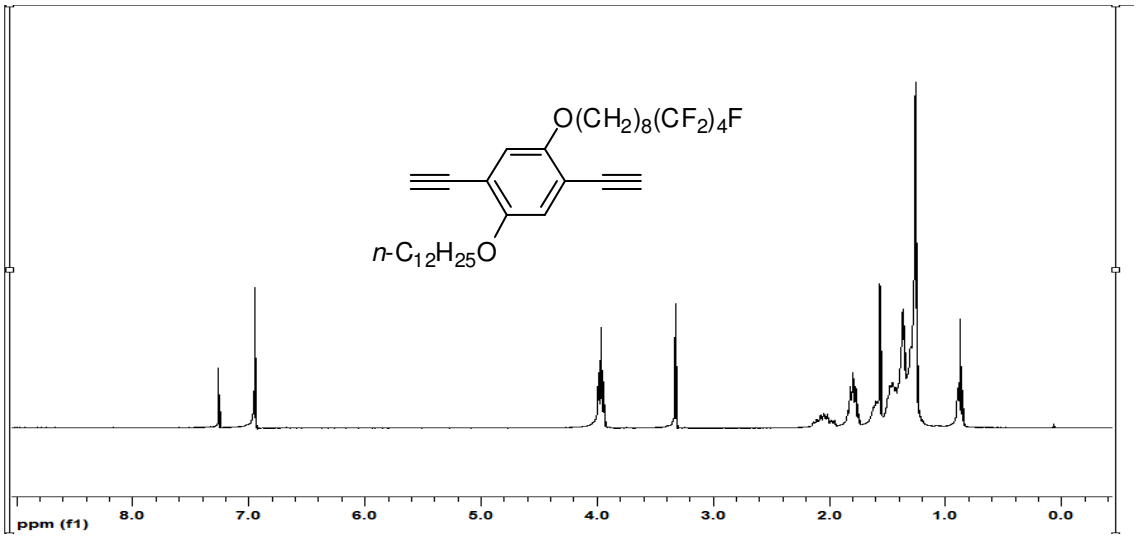

B. ^{13}C NMR

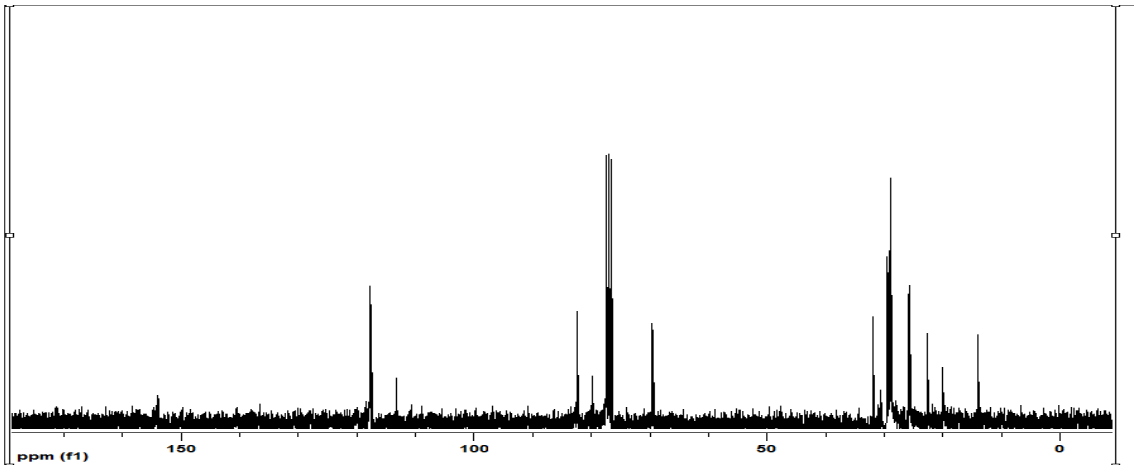

C. IR spectrum

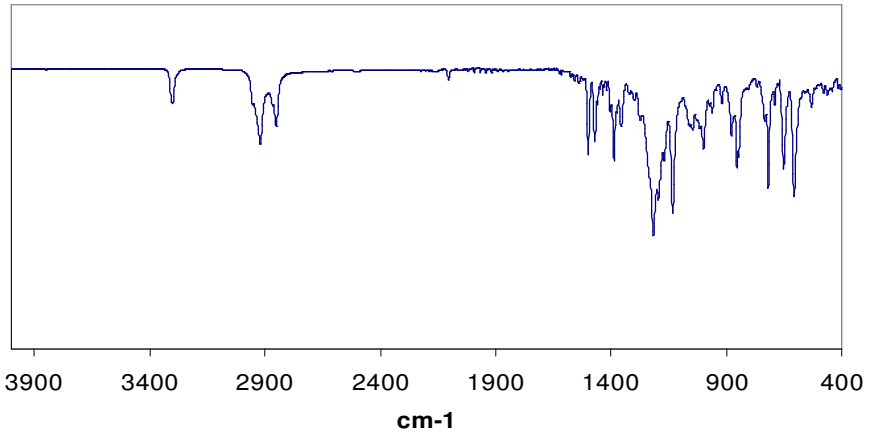

D. EI mass spectrum

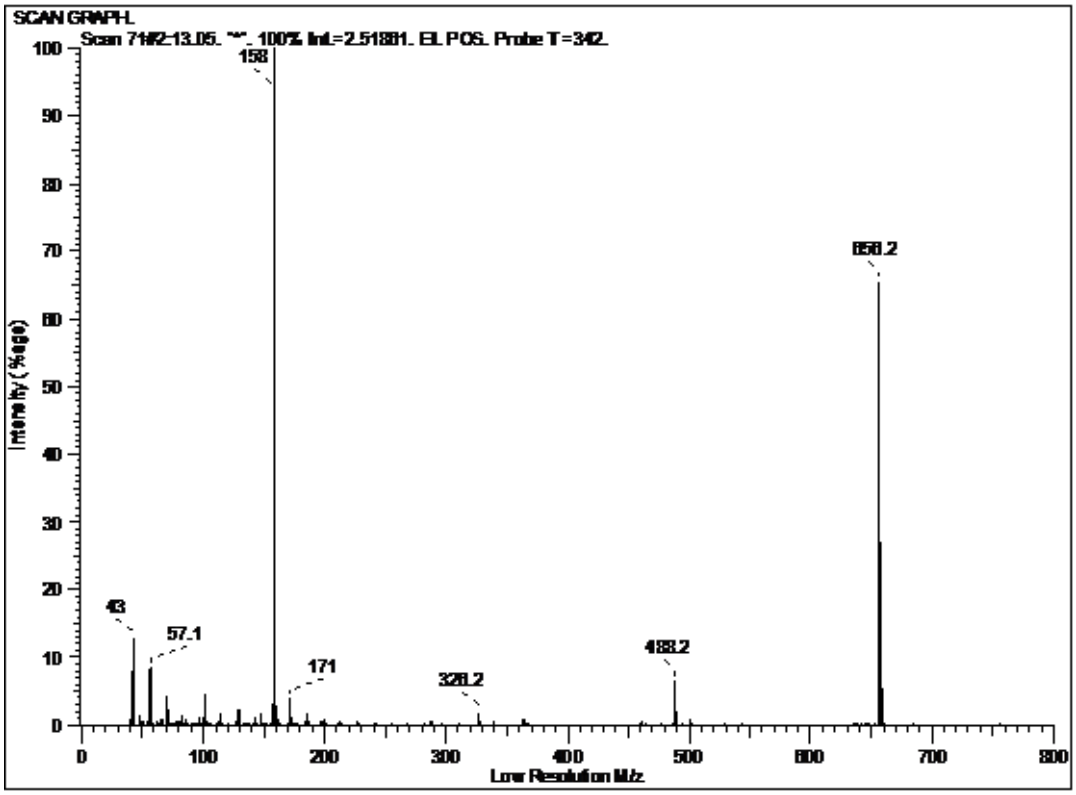

Figure B.12 ^{1}H NMR, ^{13}C NMR, IR spectrum and EI mass spectrum of 1-(dodecyloxy)-2,5-diethynyl-4-(9,9,10,10,11,11,12,12,12-nonafluorododecyloxy)benzene, **III-6b**.

4-(7,7,8,8,9,9,10,10,11,11,12,12,12-Tridecafluorododecyloxy)-1-(dodecyloxy)-2-iodobenzene

A. ^{1}H NMR

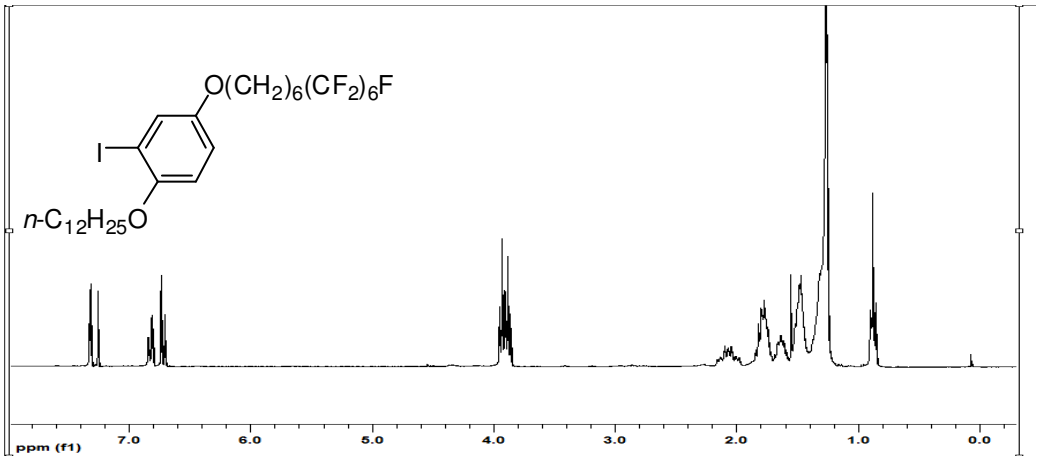

B. ^{13}C NMR

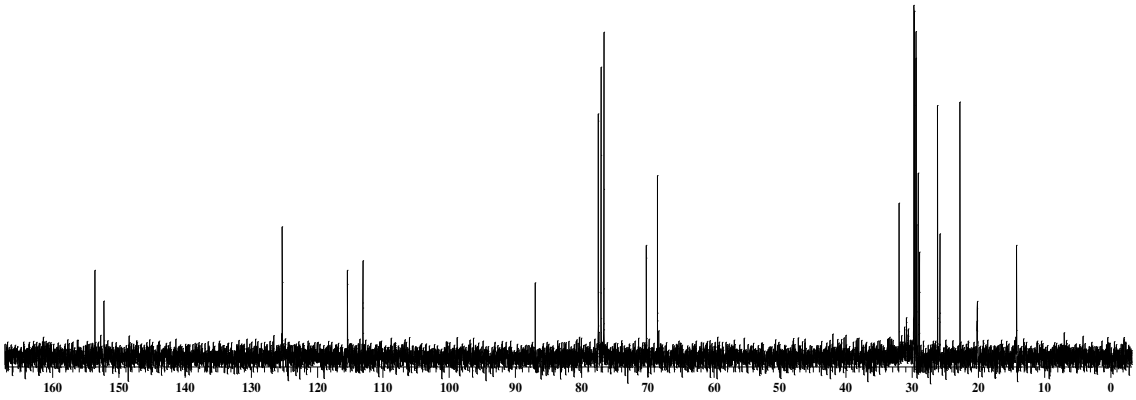

C. IR spectrum

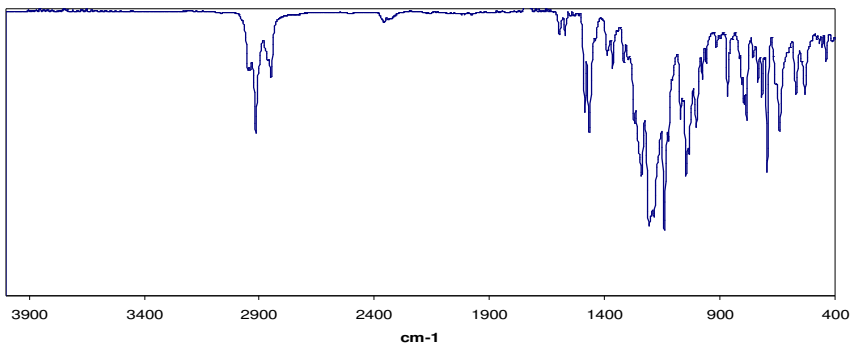

D. EI mass spectrum

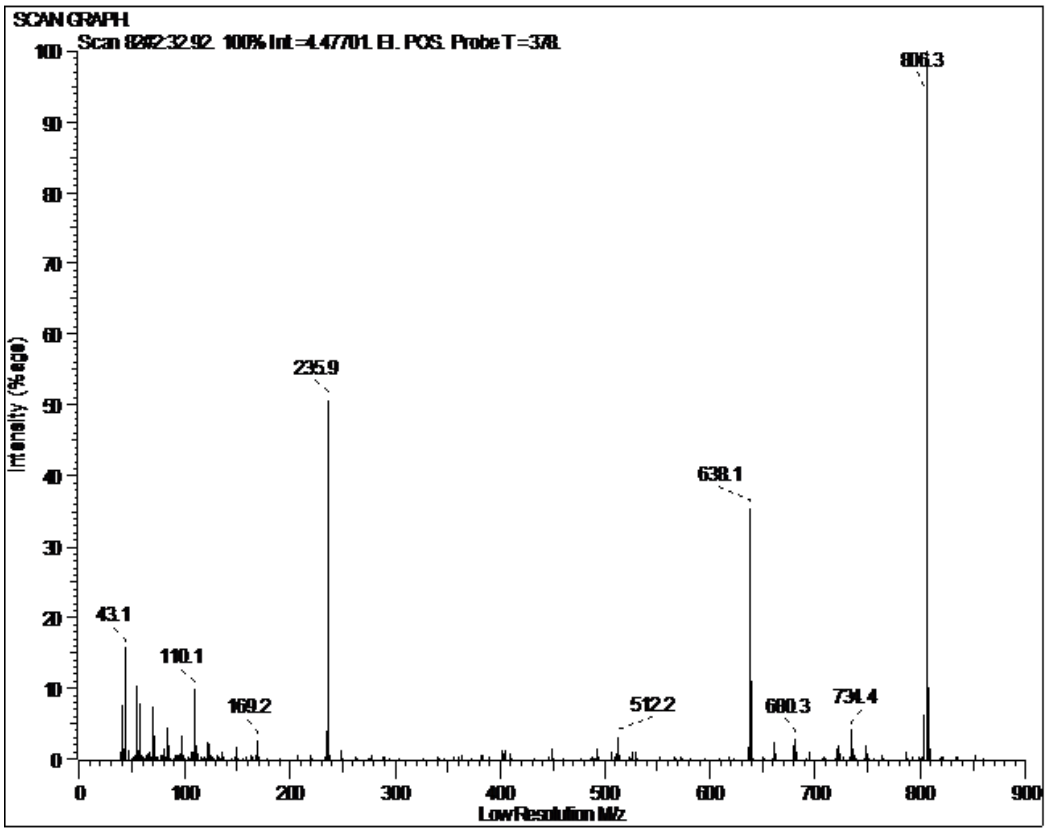

Figure B.13 ^{1}H NMR, ^{13}C NMR, IR spectrum and EI mass spectrum of 4-(7,7,8,8,9,9,10,10,11,11,12,12,12-tridecafluorododecyloxy)-1-(dodecyloxy)-2-iodobenzene, **III-7a**.

1-(Iodecyloxy)-5-iodo-4-(9,9,10,10,11,11,12,12,12-nonafluorododecyloxy)benzene

A. ^{1}H NMR

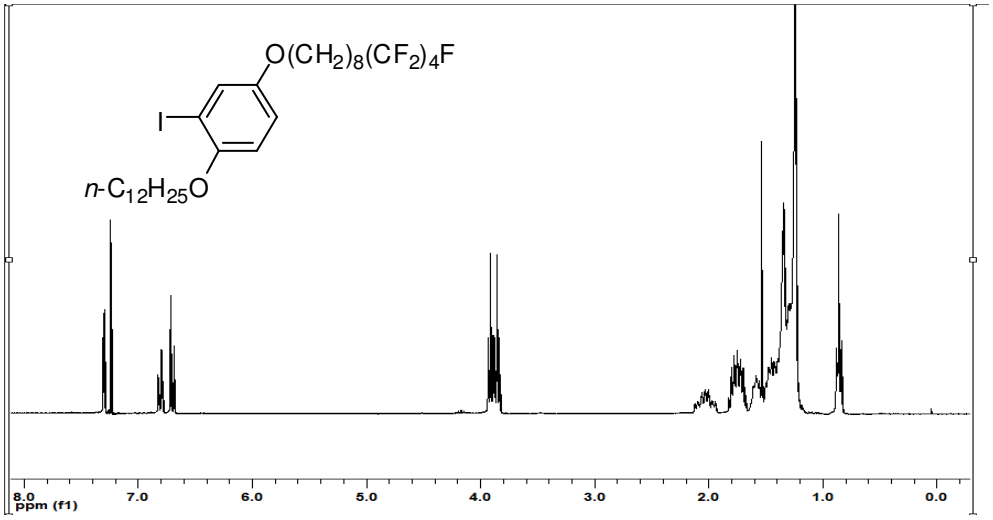

B. ^{13}C NMR

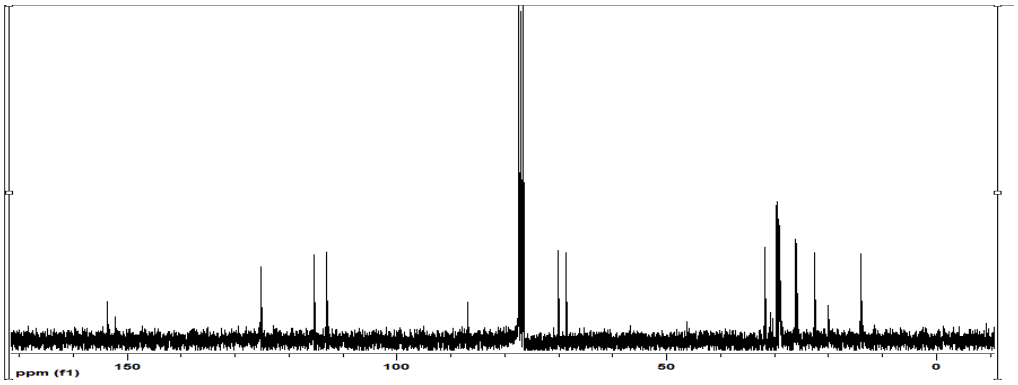

C. IR spectrum

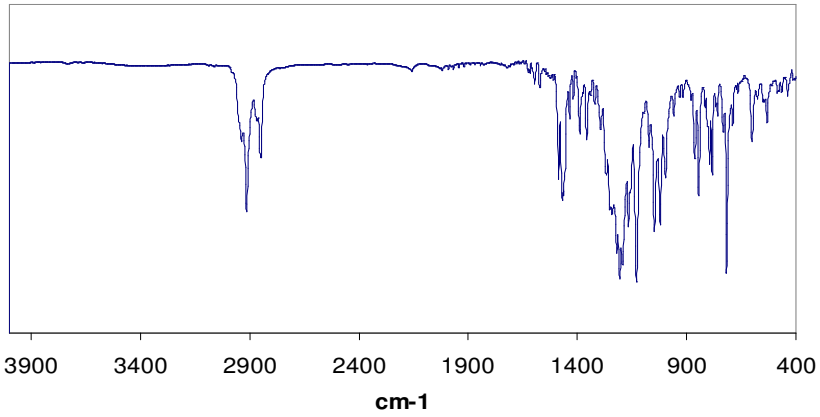

D. EI mass spectrum

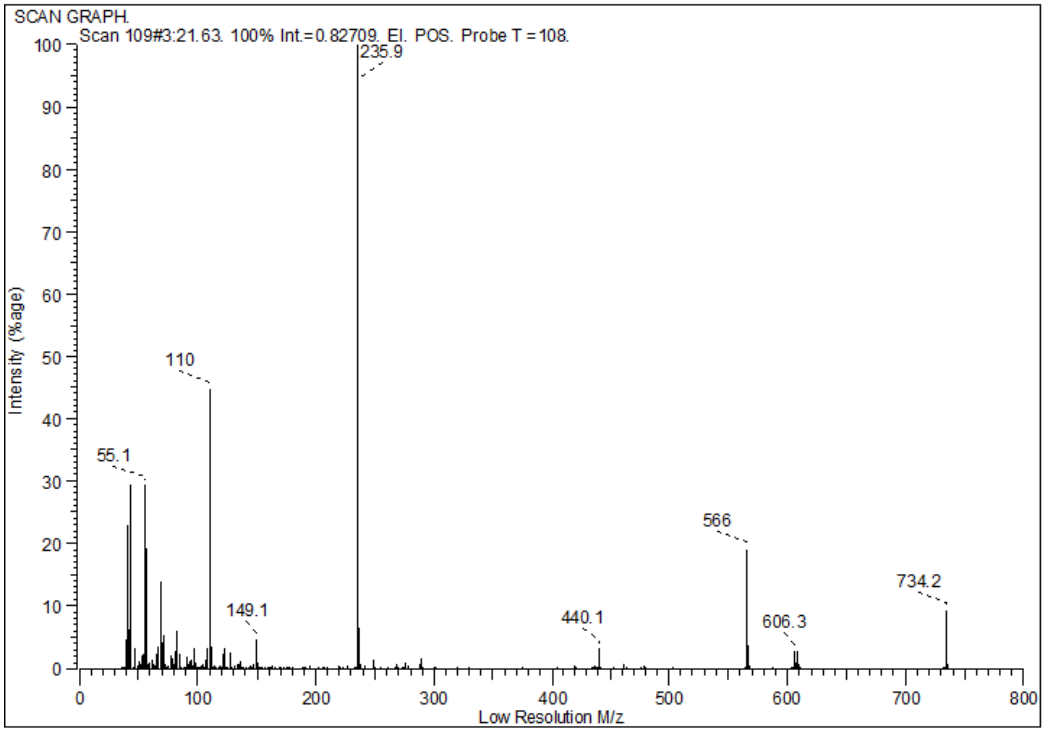

Figure B.14 ^{1}H NMR, ^{13}C NMR, IR spectrum and EI mass spectrum of 1-(iodecyloxy)-5-iodo-4-(9,9,10,10,11,11,12,12,12-nonafluorododecyloxy)benzene, **III-7b**.

4-(11,11,12,12,12-Pentafluorododecyloxy)-1-(dodecyloxy)-2-iodobenzene

A. ^{1}H NMR

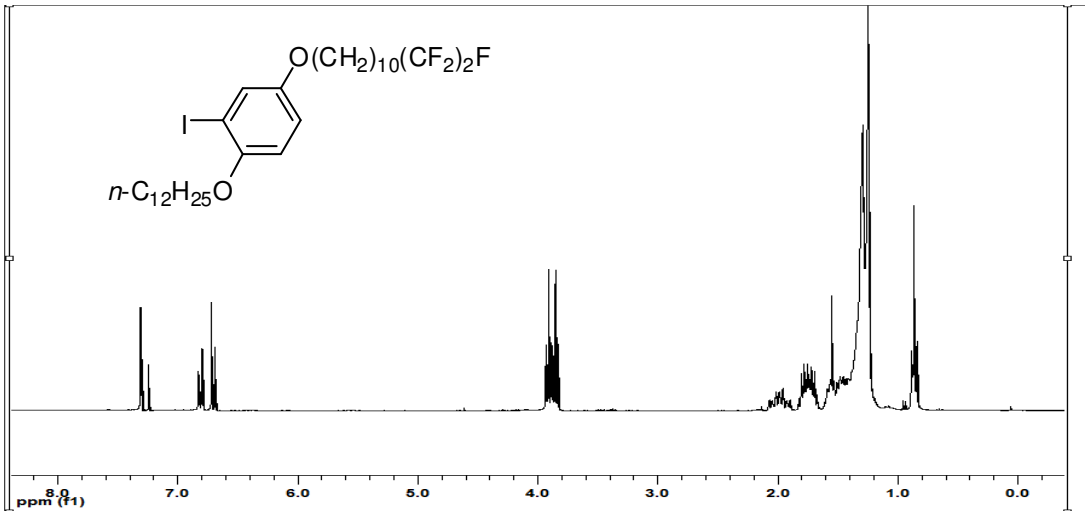

B. ^{13}C NMR

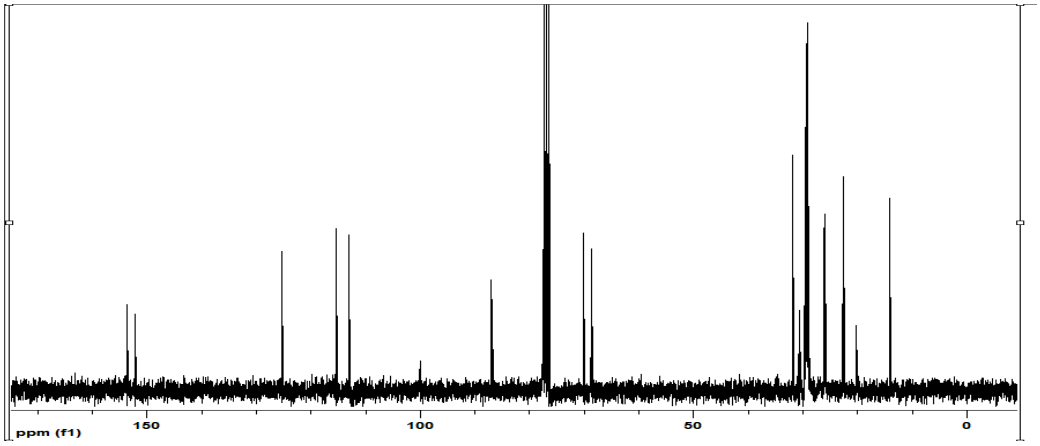

C. IR spectrum

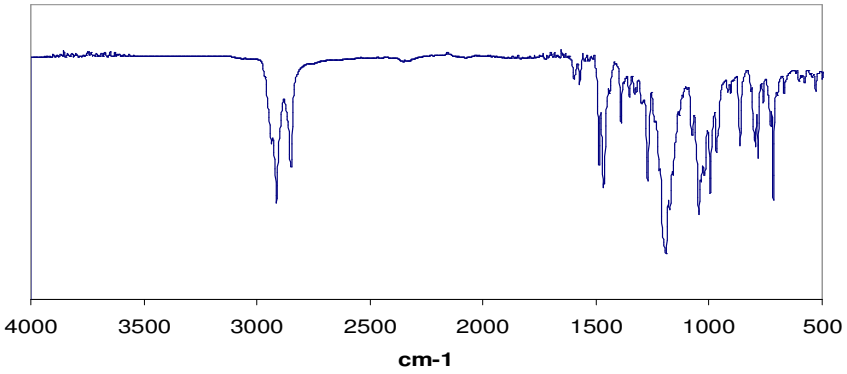

D. EI mass spectrum

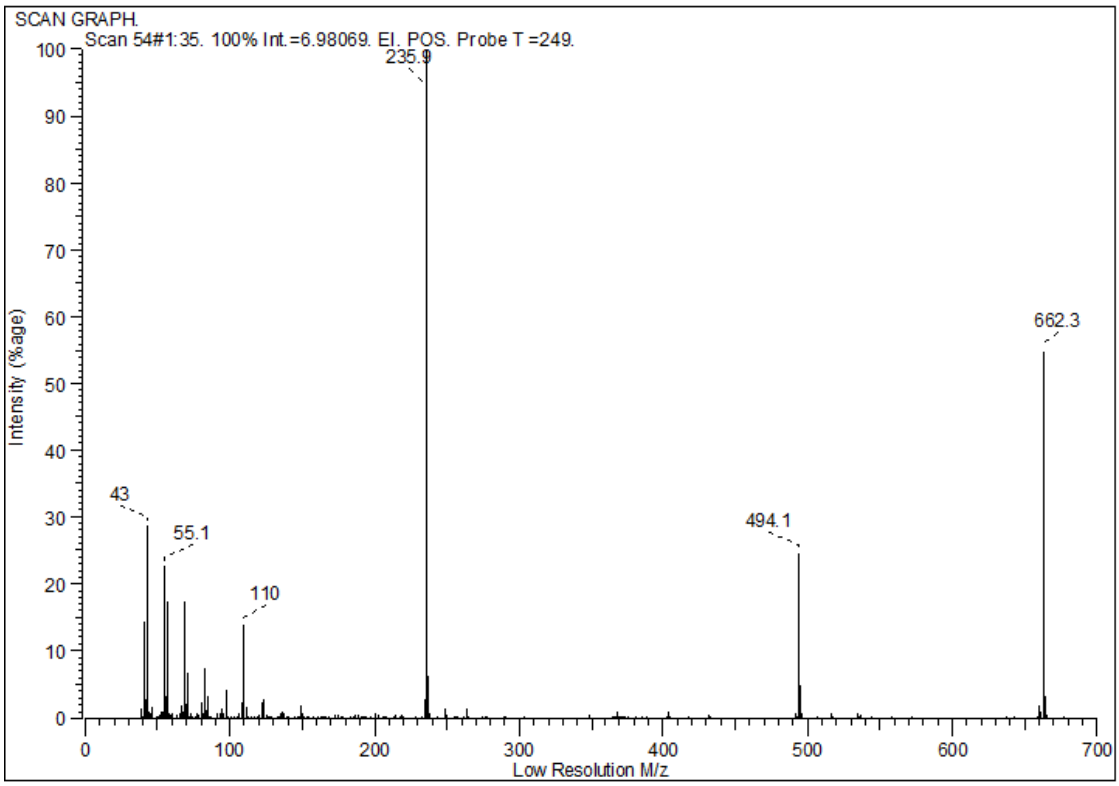

Figure B.15 ^{1}H NMR, ^{13}C NMR, IR spectrum and EI mass spectrum of 4-(11,11,12,12,12-pentafluorododecyloxy)-1-(dodecyloxy)-2-iodobenzene, **III-7c**.

2-(7,7,8,8,9,9,10,10,11,11,12,12,12-Tridecafluorododecyloxy)-5-(dodecyloxy)-4-iodobenzaldehyde

A. ^{1}H NMR

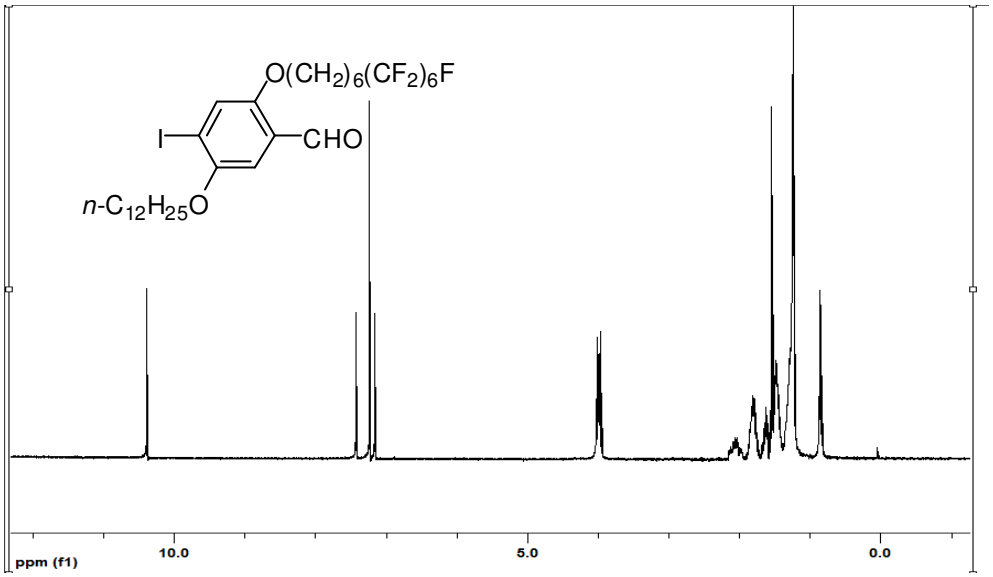

B. ^{13}C NMR

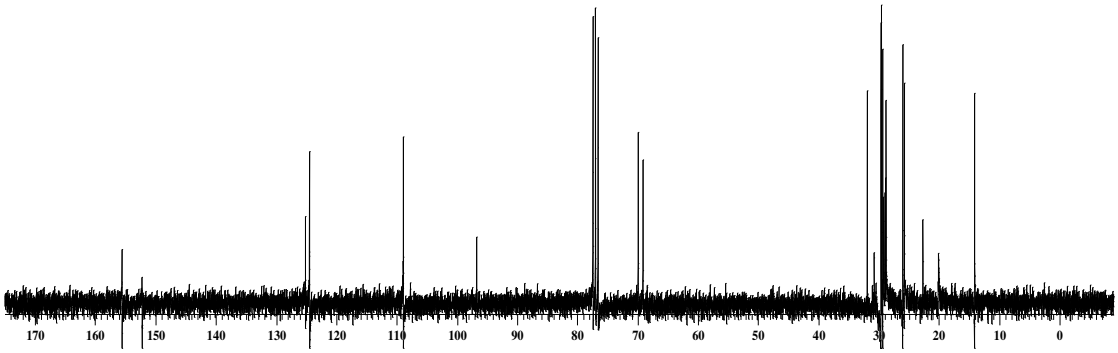

C. IR spectrum

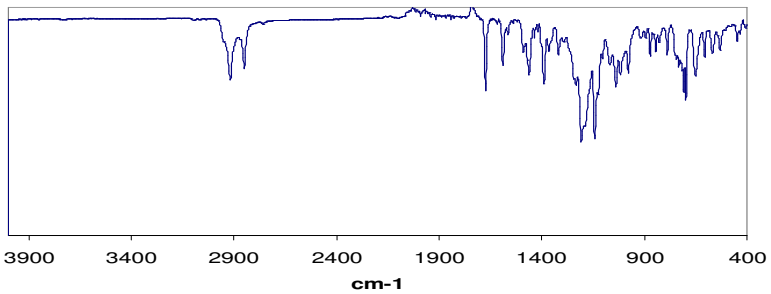

D. EI mass spectrum

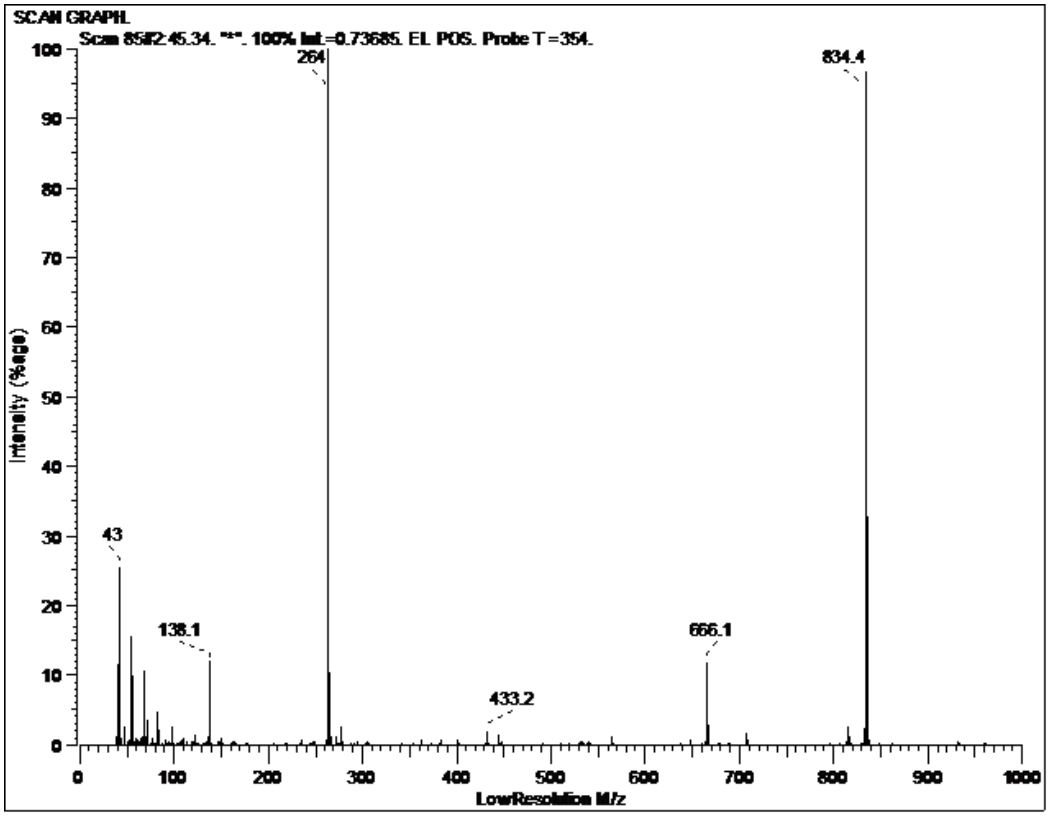

Figure B.16 ^{1}H NMR, ^{13}C NMR, IR spectrum and EI mass spectrum of 2-(7,7,8,8,9,9,10,10,11,11,12,12,12-tridecafluorododecyloxy)-5-(dodecyloxy)-4-iodobenzaldehyde, **III-8a**.

5-(Dodecyloxy)-4-iodo-2-(9,9,10,10,11,11,12,12,12-nonafluorododecyloxy)benzaldehyde

A. ^{1}H NMR

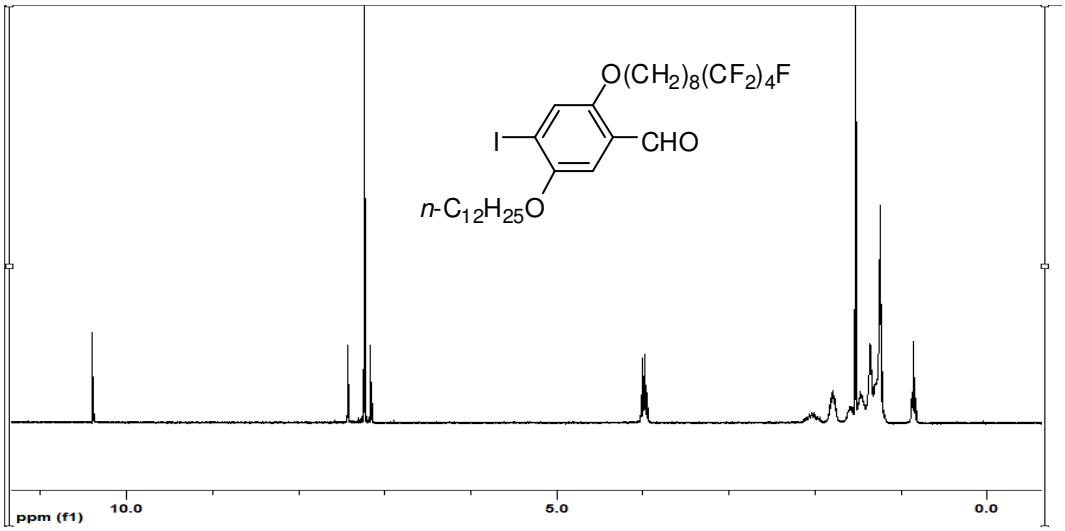

B. ^{13}C NMR

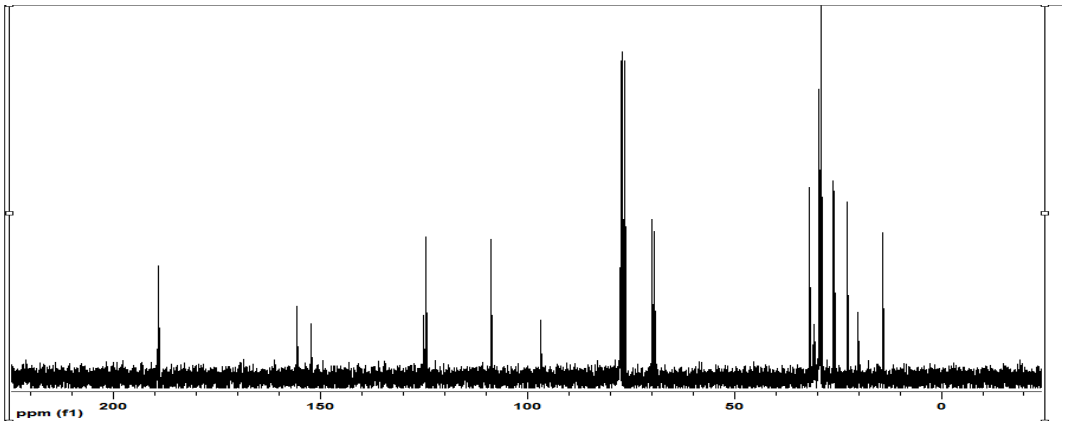

C. IR spectrum

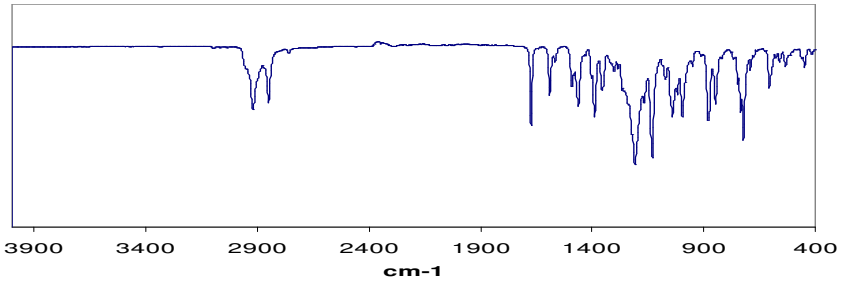

D. EI mass spectrum

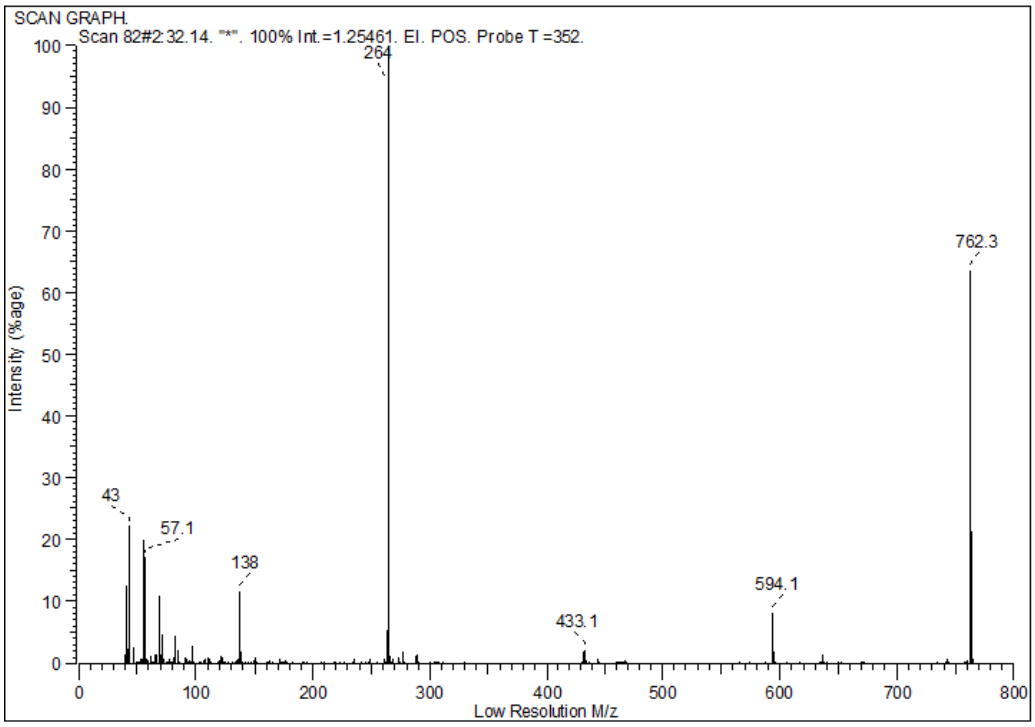

Figure B.17 ^{1}H NMR, ^{13}C NMR, IR spectrum and EI mass spectrum of 5-(dodecyloxy)-4-iodo-2-(9,9,10,10,11,11,12,12,12-nonafluorododecyloxy)benzaldehyde, **III-8b**.

2-(11,11,12,12,12-Pentafluorododecyloxy)-5-(dodecyloxy)-4-iodobenzaldehyde

A. ^{1}H NMR

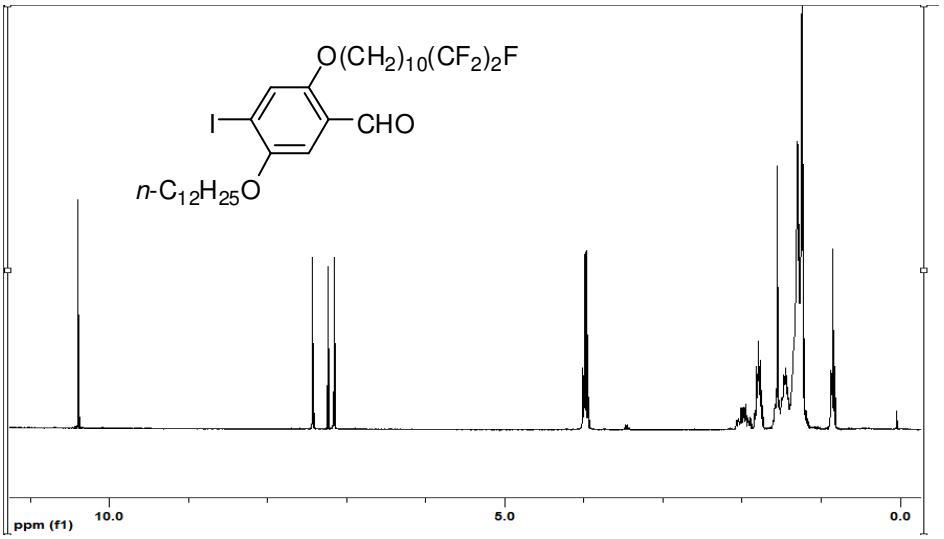

B. ^{13}C NMR

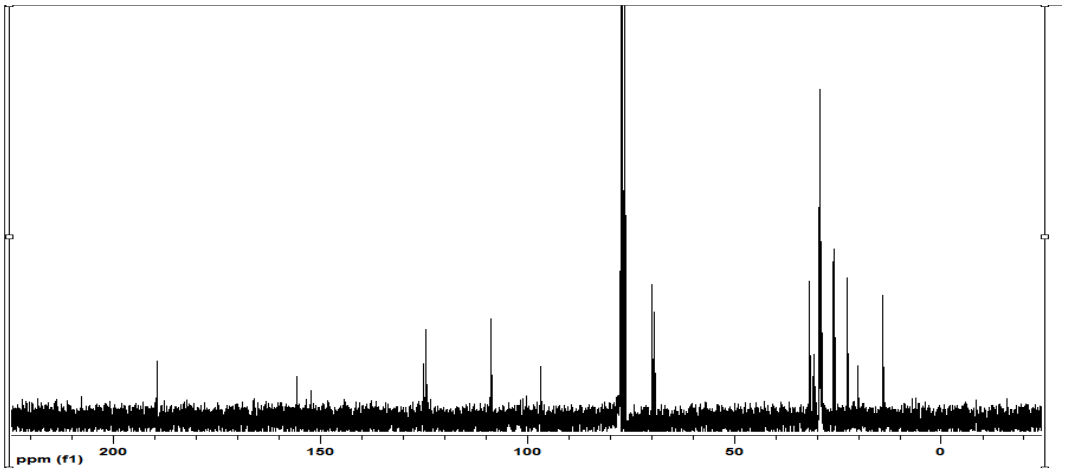

C. IR spectrum

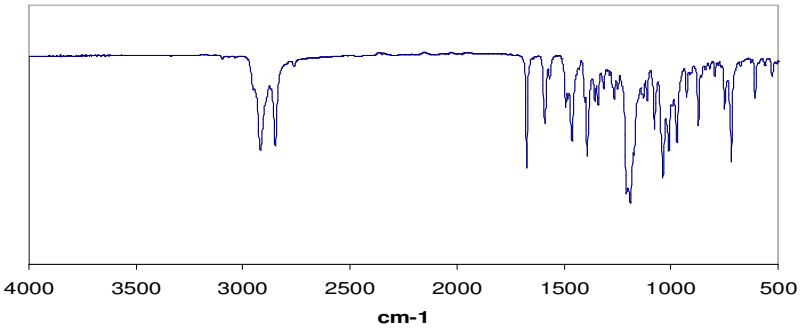

D. EI mass spectrum

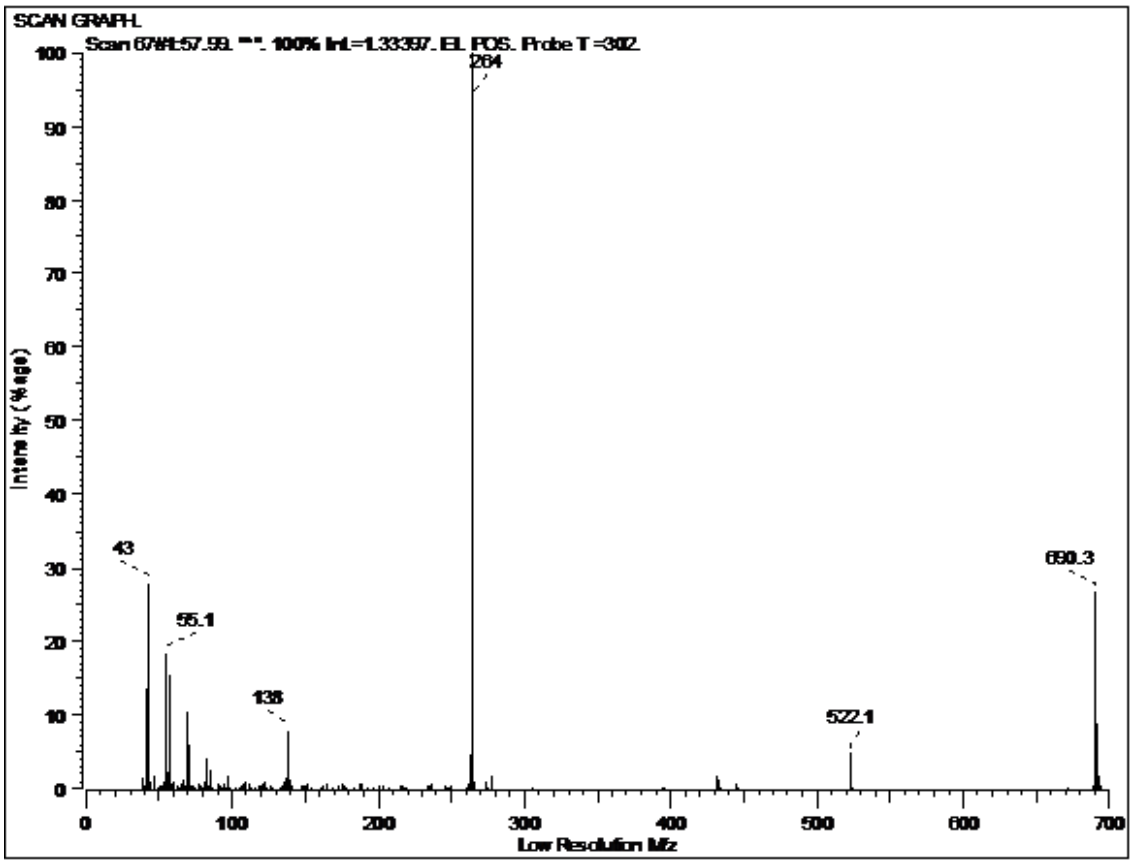

Figure B.18 ^{1}H NMR, ^{13}C NMR, IR spectrum and EI mass spectrum of 2-(11,11,12,12,12-pentafluorododecyloxy)-5-(dodecyloxy)-4-iodobenzaldehyde, **III-8c**.

1-(7,7,8,8,9,9,10,10,11,11,12,12,12-Tridecafluorododecyloxy)-4-(dodecyloxy)-2-ethynyl-5-iodobenzene

A. ^{1}H NMR

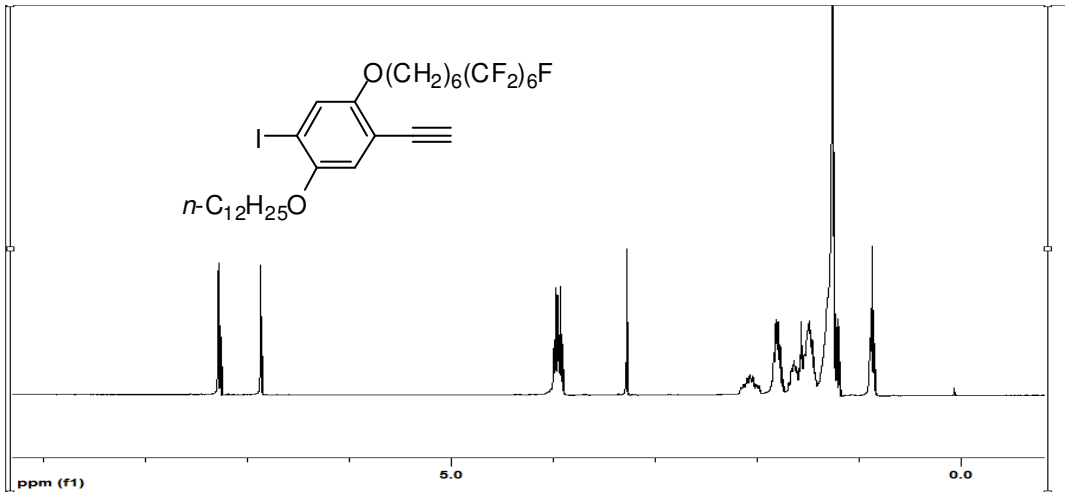

B. ^{13}C NMR

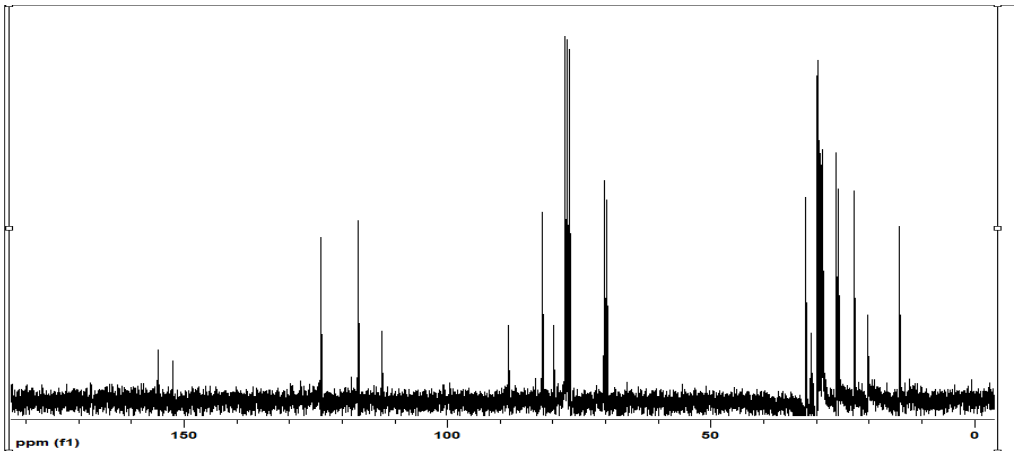

C. IR spectrum

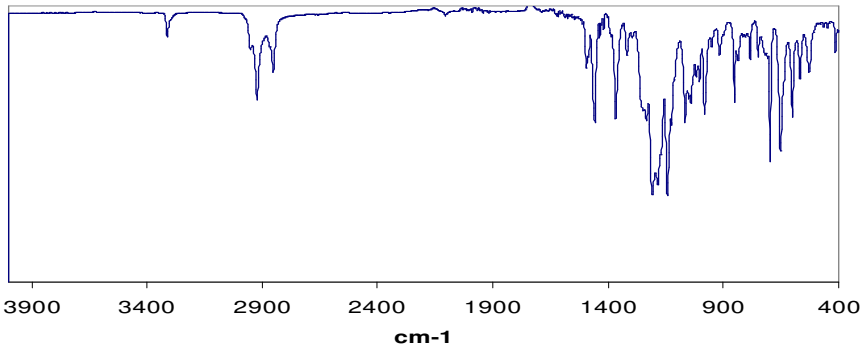

D. EI mass spectrum

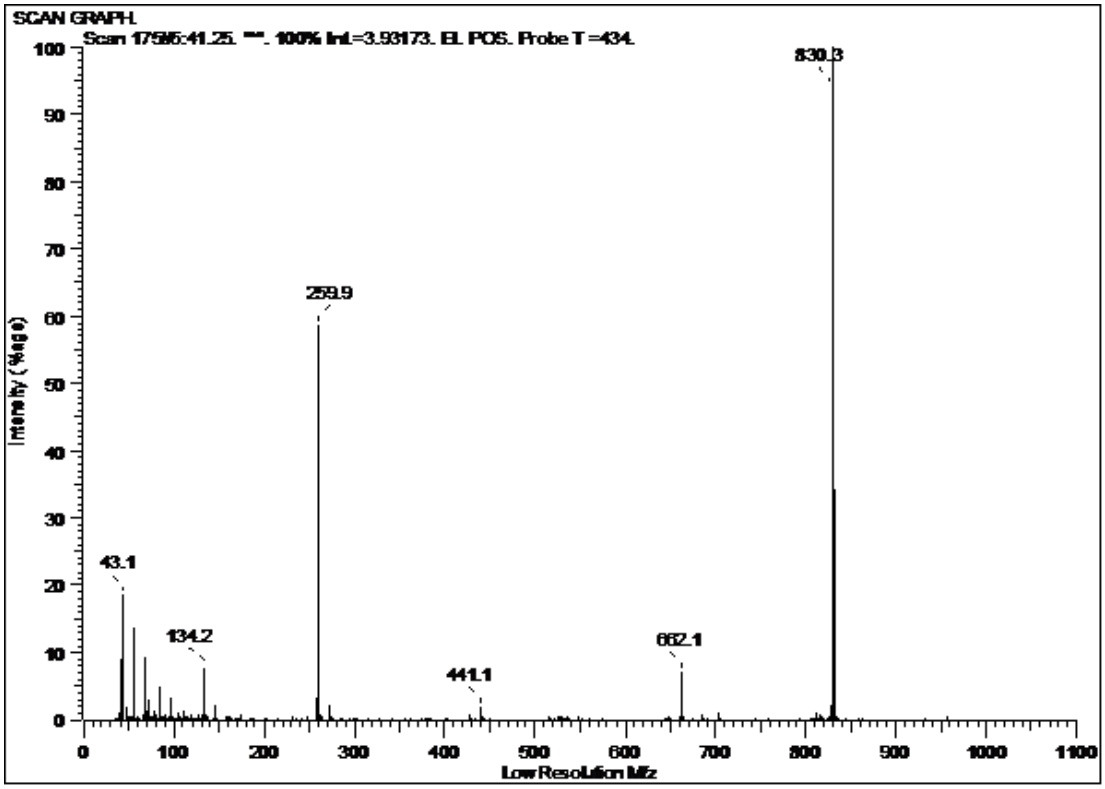

Figure B.19 ^{1}H NMR, ^{13}C NMR, IR spectrum and EI mass spectrum of 1-(7,7,8,8,9,9,10,10,11,11,12,12,12-tridecafluorododecyloxy)-4-(dodecyloxy)-2-ethynyl-5-iodobenzene, **III-9a**.

1-(Dodecyloxy)-5-ethynyl-2-iodo-4-(9,9,10,10,11,11,12,12,12-nonafluorododecyloxy)benzene

A. ^{1}H NMR

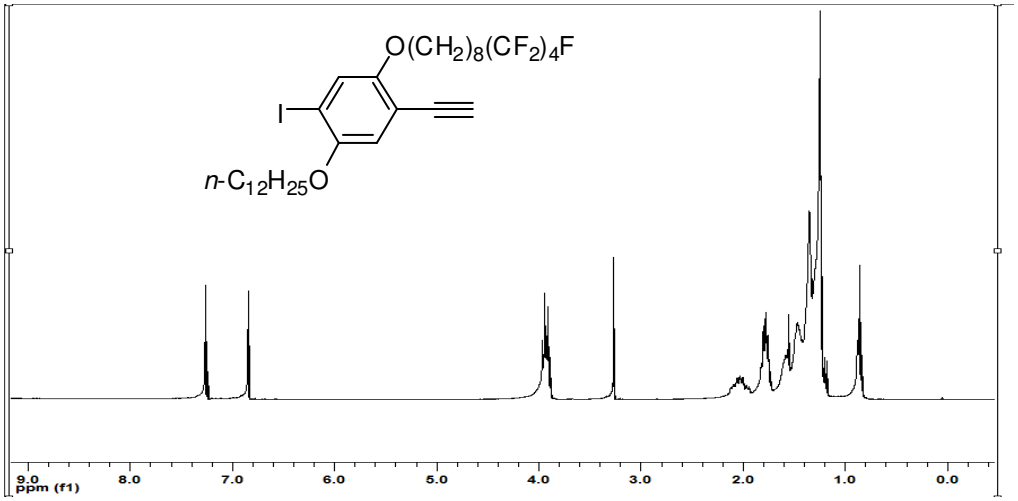

B. ^{13}C NMR

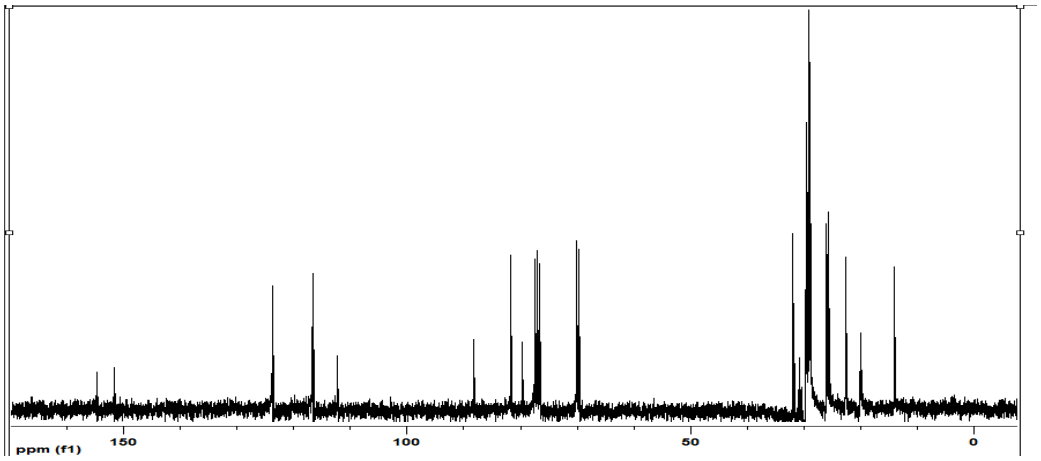

C. IR spectrum

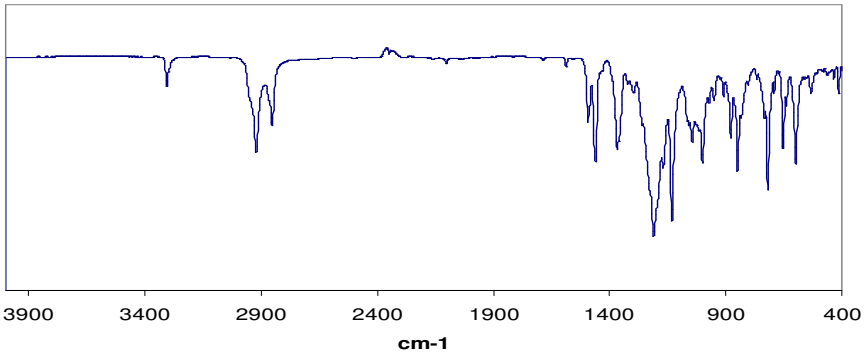

D. EI mass spectrum

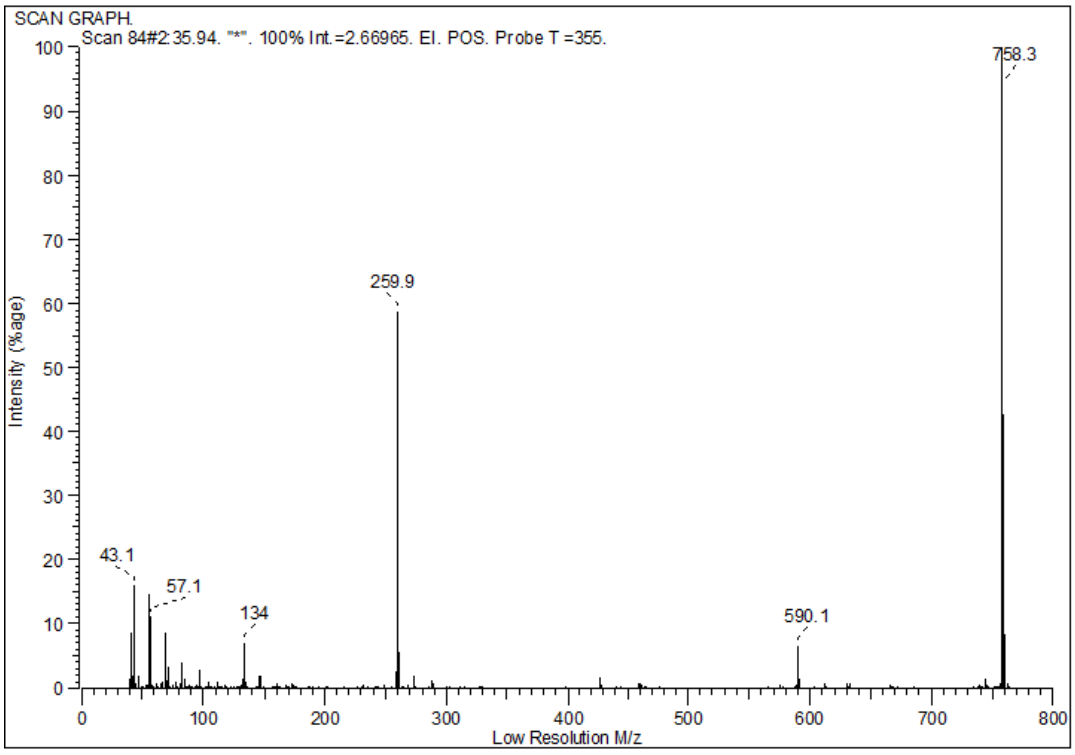

Figure B.20 ^{1}H NMR, ^{13}C NMR, IR spectrum and EI mass spectrum of 1-(dodecyloxy)-5-ethynyl-2-iodo-4-(9,9,10,10,11,11,12,12,12-nonafluorododecyloxy)benzene, **III-9b**.

1-(11,11,12,12,12-Pentafluorododecyloxy)-4-(dodecyloxy)-2-ethynyl-5-iodobenzene

A. ^{1}H NMR

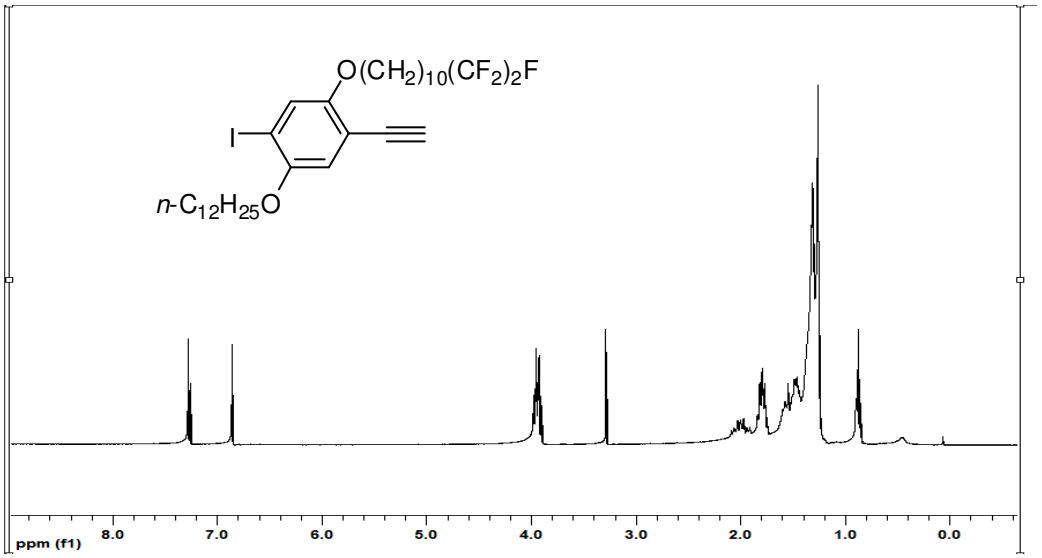

B. ^{13}C NMR

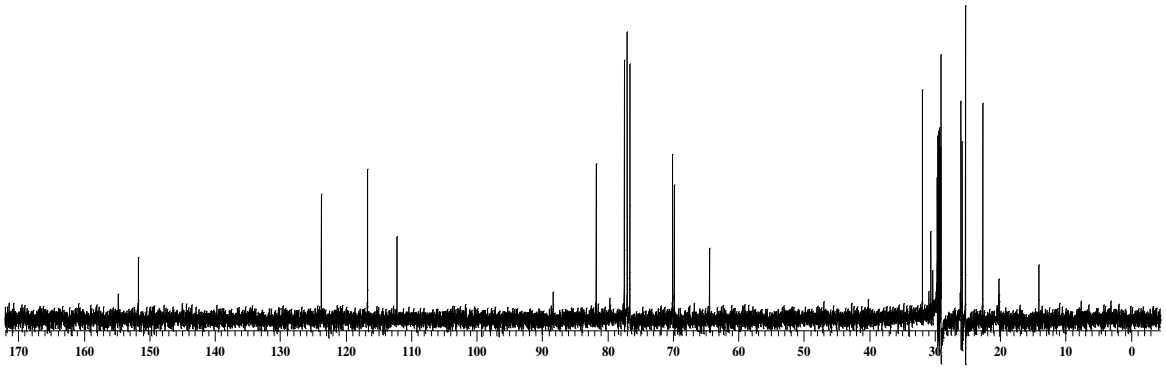

C. IR spectrum

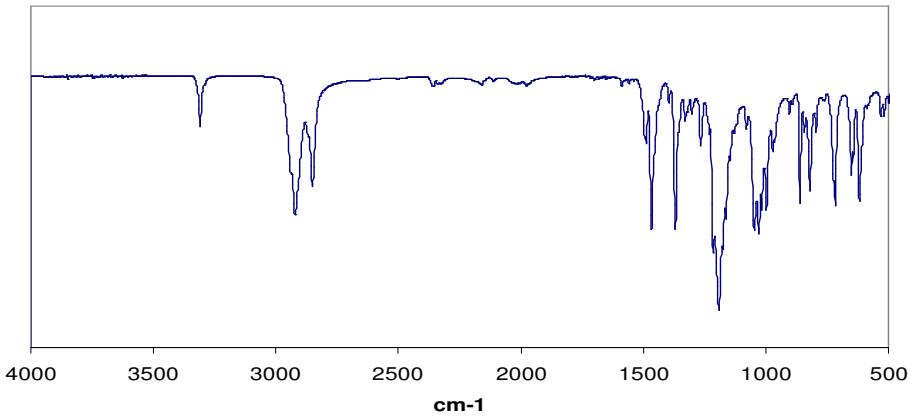

D. EI mass spectrum

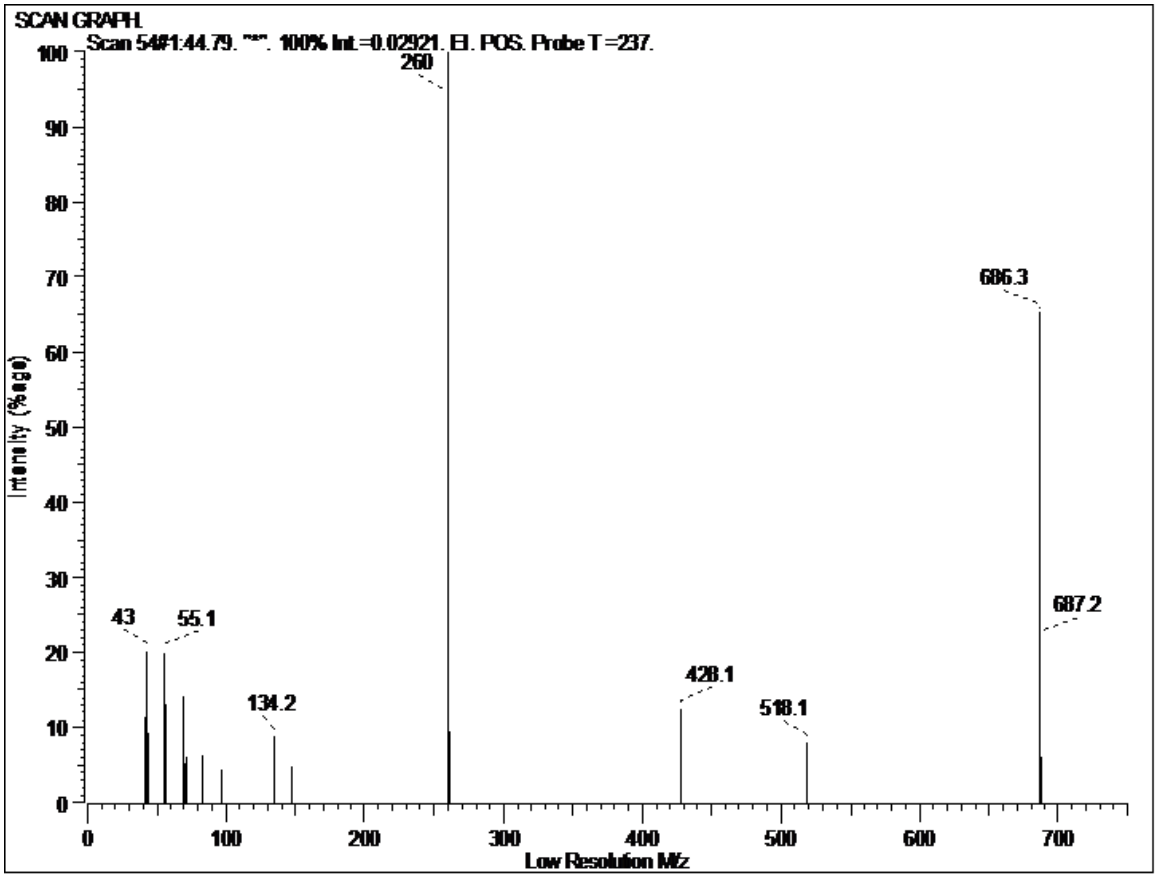

Figure B.21 ^{1}H NMR, ^{13}C NMR, IR spectrum and EI mass spectrum of 1-(11,11,12,12,12-pentafluorododecyloxy)-4-(dodecyloxy)-2-ethynyl-5-iodobenzene, **III-9c**.

A. ^{1}H NMR spectrum

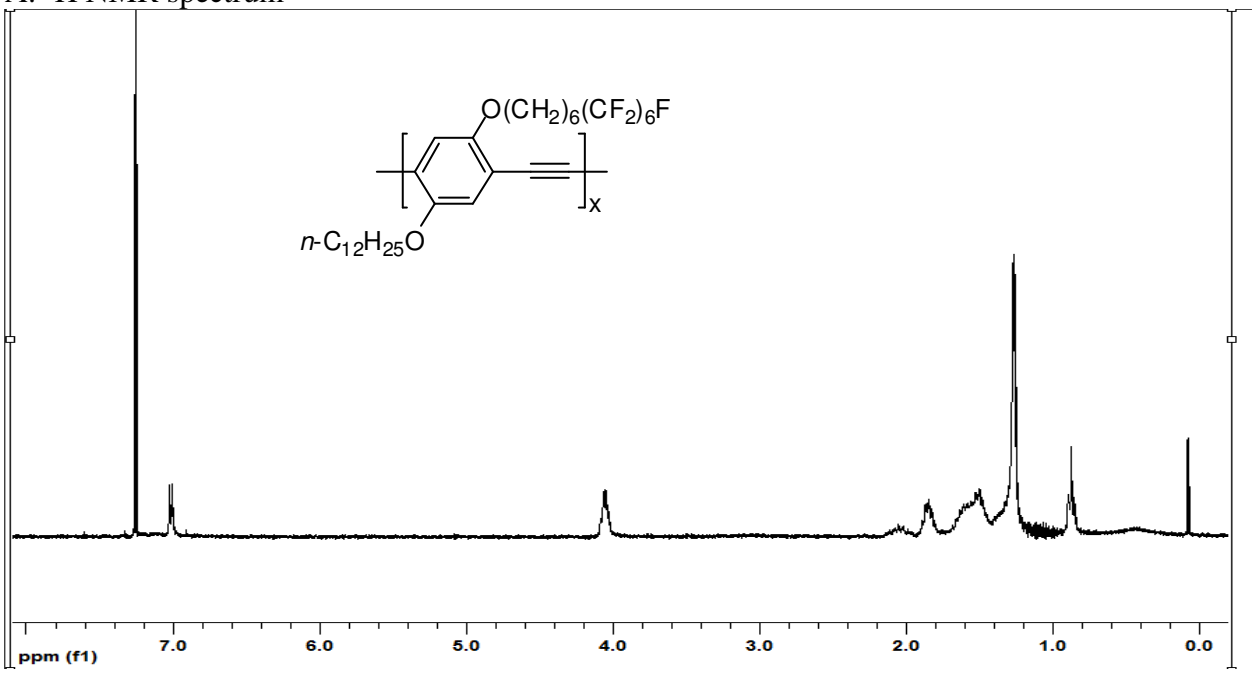

B. IR spectrum

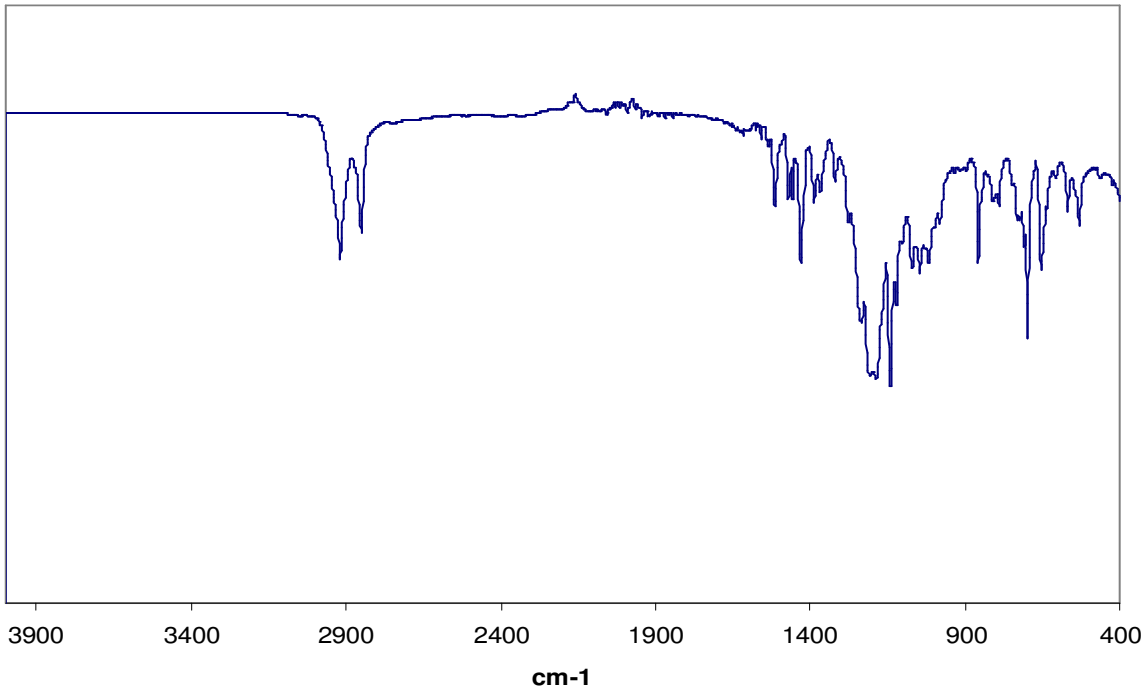

Figure B.22 ^{1}H NMR and IR spectrum for **RgPPE(6,6/12)**.

A. ^{1}H NMR

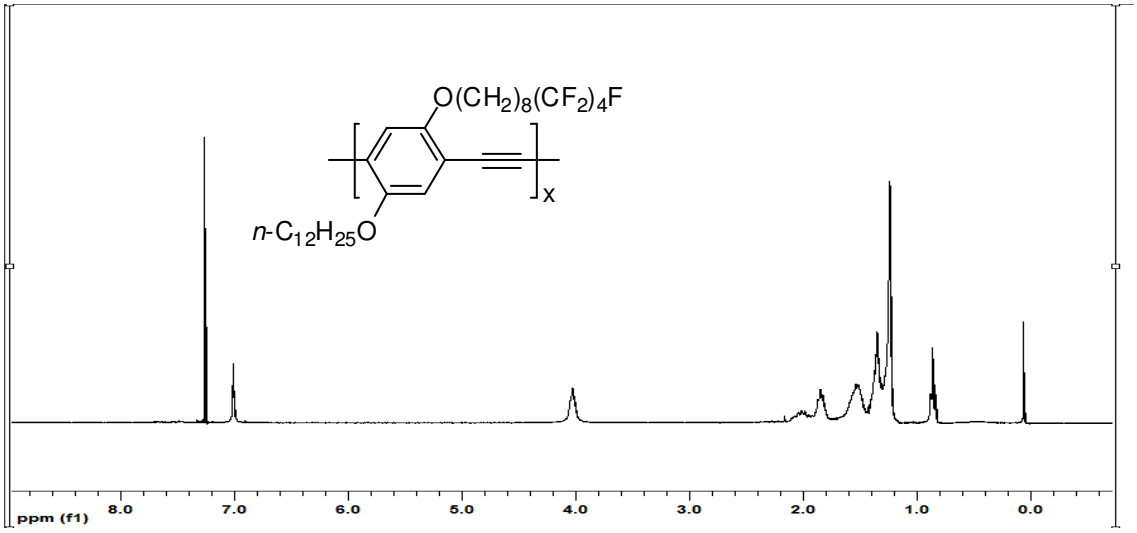

B. ^{13}C NMR

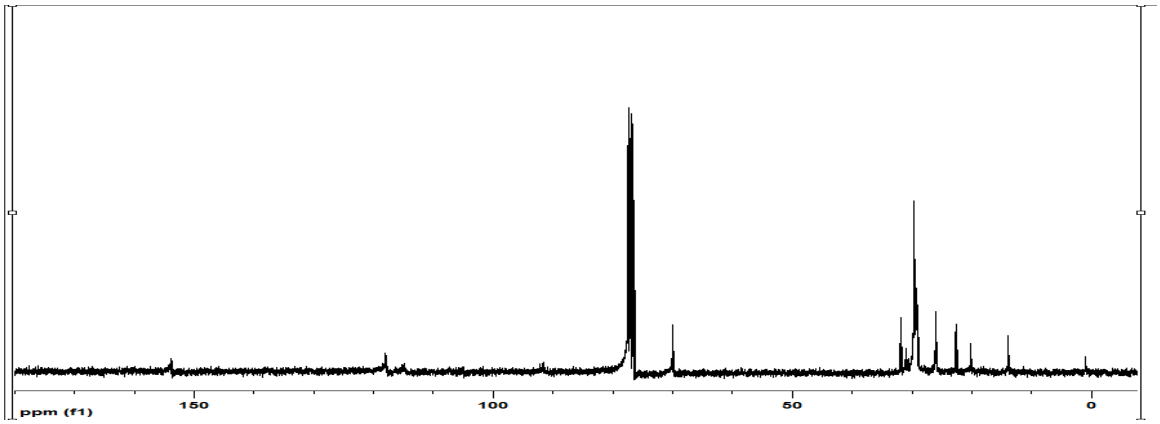

C. IR spectrum

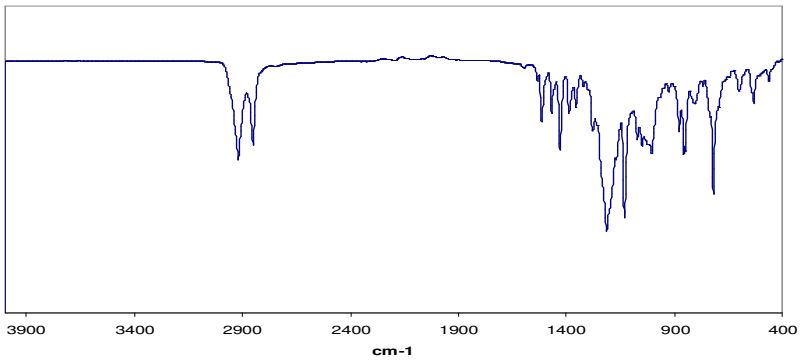

Figure B.23 ^{1}H NMR, ^{13}C NMR and IR for **RgPPE(8,4/12).**

A. ^{1}H NMR

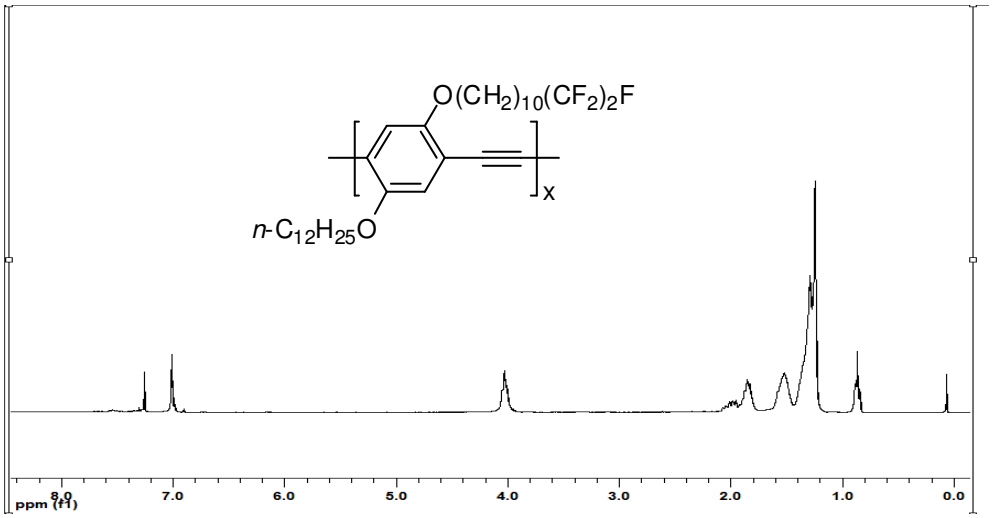

B. ^{13}C NMR

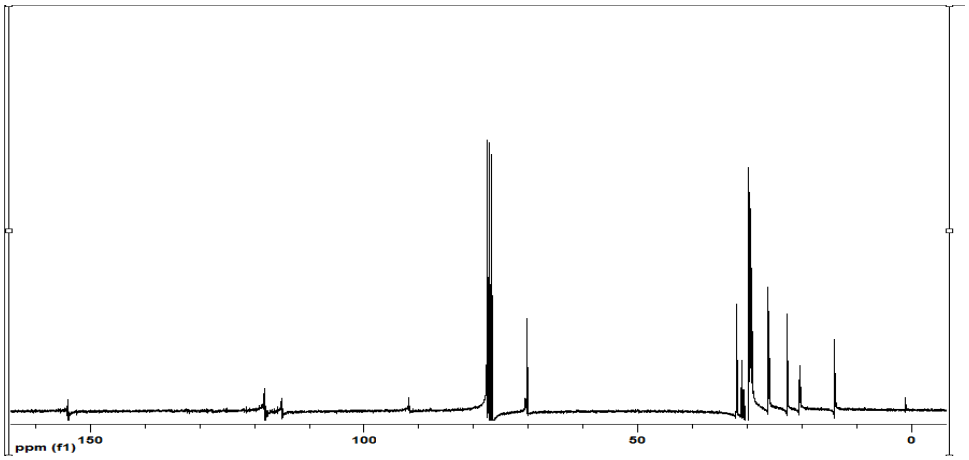

C. IR spectrum

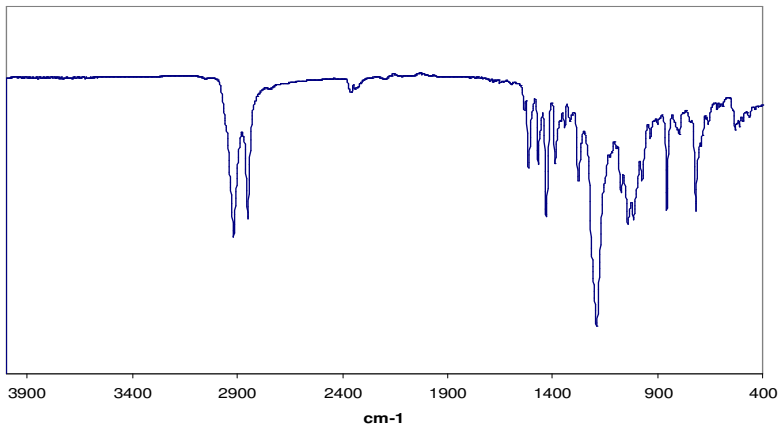

Figure B.24. ^{1}H NMR, ^{13}C NMR and IR spectrum for **RgPPE(10,2/12)**.

A. ^{1}H NMR

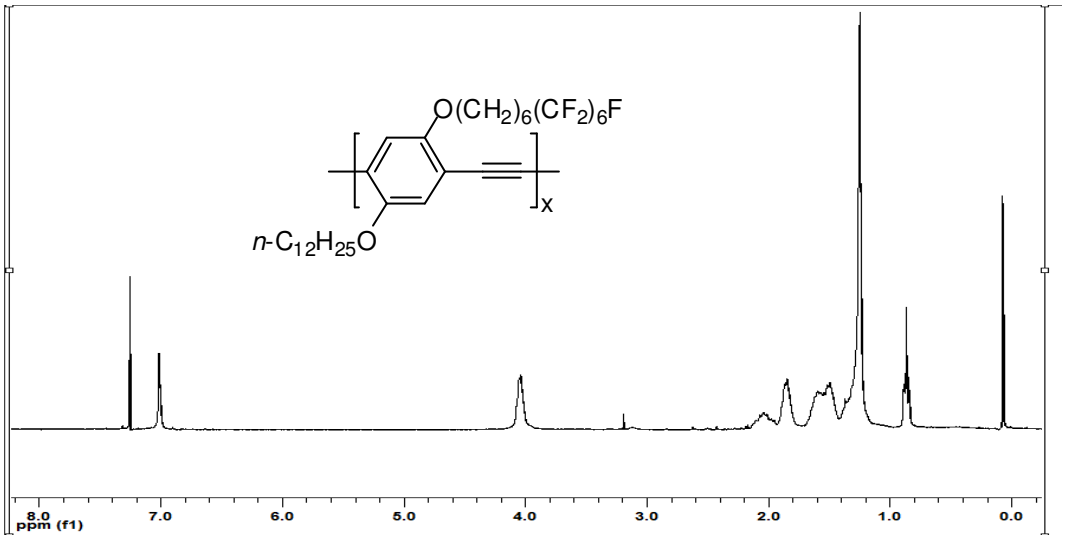

B. ^{13}C NMR

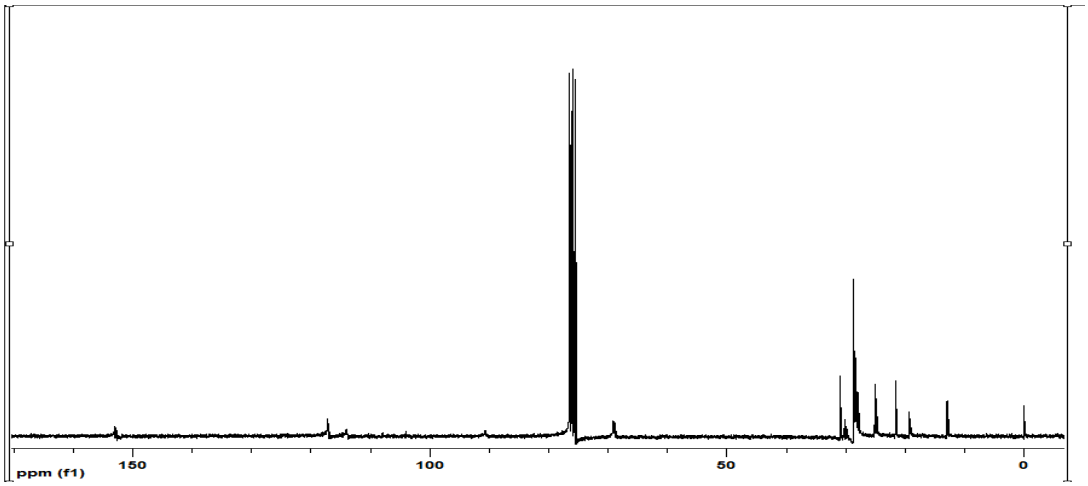

C. IR spectrum

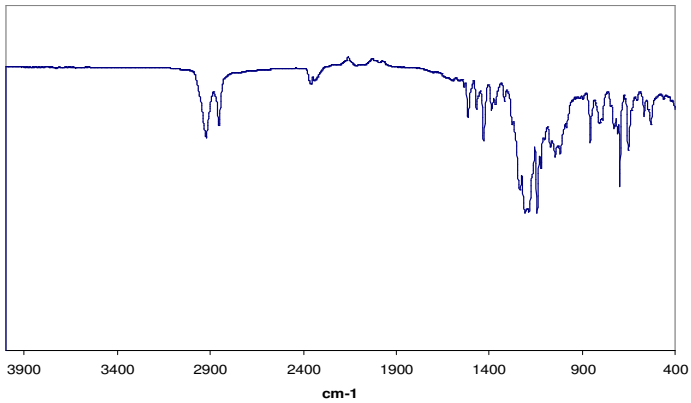

Figure B.25. ^{1}H NMR, ^{13}C NMR and IR spectrum for **RnPPE(6,6/12)**.

A. ^{1}H NMR

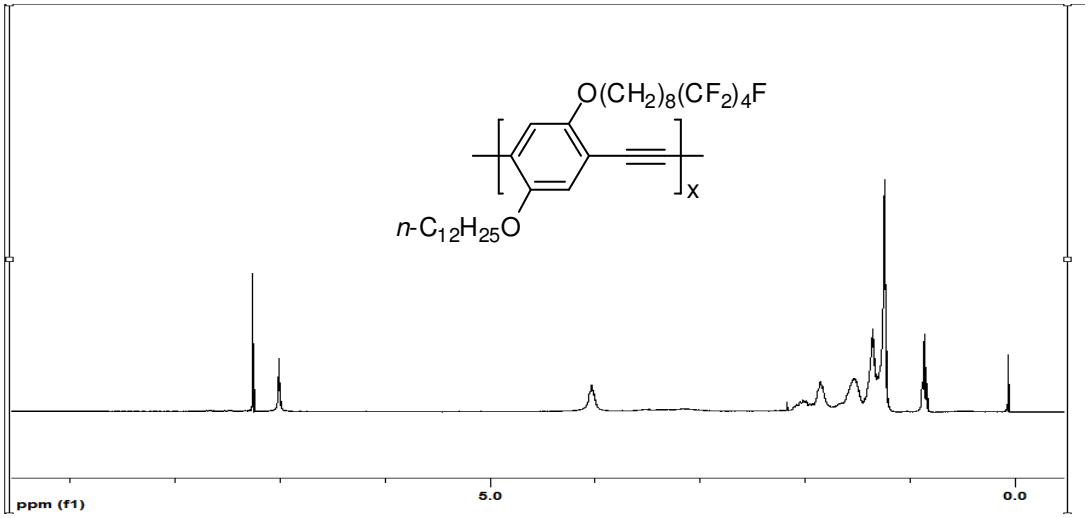

B. ^{13}C NMR

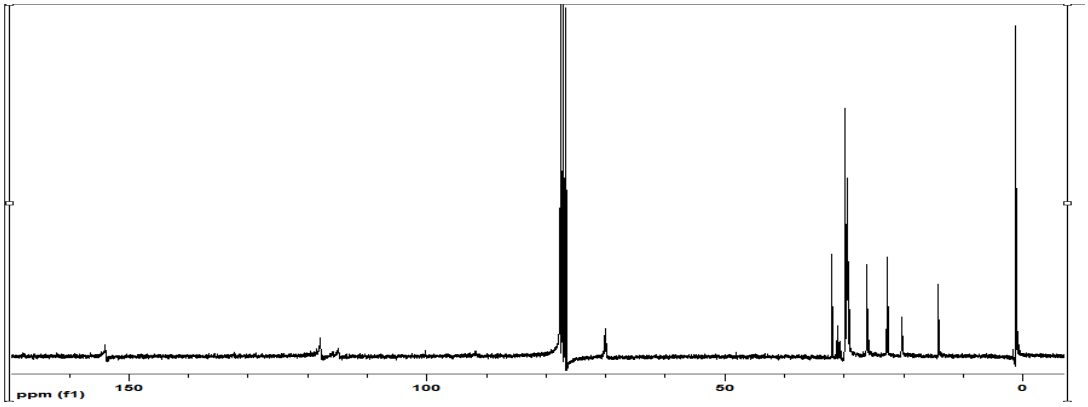

C. IR spectrum

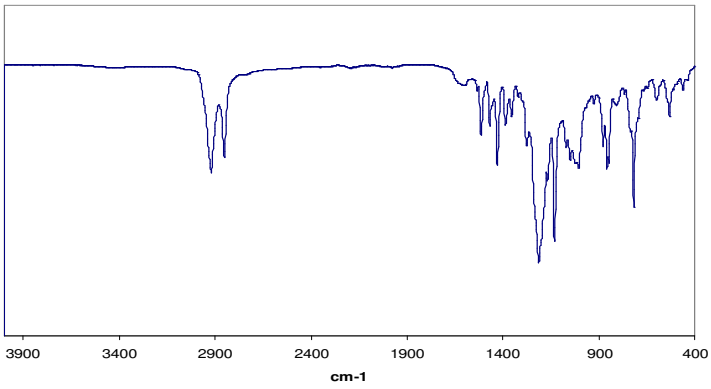

Figure B.26. ^{1}H NMR, ^{13}C NMR and IR spectrum for **RnPPE(8,4/12)**.

APPENDIX C: MODIFICATION OF SILCON SUBSTRATES DESCRIBED IN CHAPTER 3

Silicon wafers were first cleaned by a treatment in piranha solution (25% H_2O_2, 75% H_2SO_4, 10 min, room temperature), followed by washing with distilled water and then acetone. The slides were dried at 125ºC for 24 h. Slides modified with a hydrocarbon were prepared by stirring the silicon wafers in dodecyldimethylchlorosilane (0.3 M in anhydrous pentane) under argon, Figure S1. After 2 h the slides were removed and washed with water and acetone.

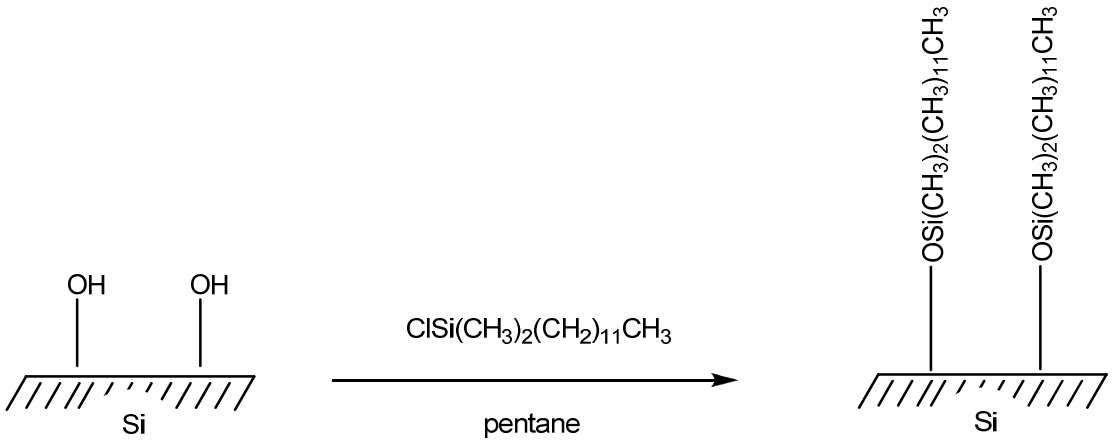

Figure C.1. Modification of silicon substrates with hydrocarbon.

In order to add a fluorocarbon chain to the surface, the appropriate monochlorosilane had to first be synthesized, Figure C.2.

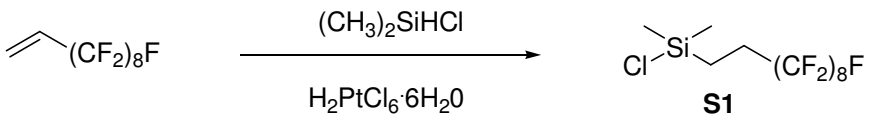

Figure C.2. Synthesis of fluorocarbon silane used to modify silicon substrates.

Chloro(3,3,4,4,5,5,6,6,7,7,8,8,9,9,10,10,10-heptadecafluorodecyl)dimethylsilane (**S1**) was prepared as follows: In a dry round bottom flask under argon added (perfluorooctyl)ethylene (2.5 g, 5.6 mmol) and dimethylchlorosilane (1.22 mL, 11.2 mmol) and a trace of chloroplatinic acid hexahydrate. The mixture was stirred overnight at room temperature. Slides modified with a fluorocarbon were prepared by immersing slides in **S1** (0.5 M in anhydrous pentane) under argon. After stirring two hours at room temperature, removed slides and washed with water and acetone.

APPENDIX D: ^{1}H AND ^{13}C NMR, IR AND MASS SPECTRA OF MONOMERS AND POLYMERS DESCRIBED IN CHAPTER 4

^{1}H NMR spectra were collected on a Varian Mercury Vx 300 MHz instrument using $CDCl_3$ as a solvent. ^{13} C NMR spectra were obtained at 75.5 MHz. IR analyses were performed on a Nicolet 4700 FTIR with an ATR attachment from SmartOrbit Thermoelectronic Corporation.

1,2-Bis(4-(octyloxy)phenyl)ethane-1,2-dione

A. ^{1}H NMR

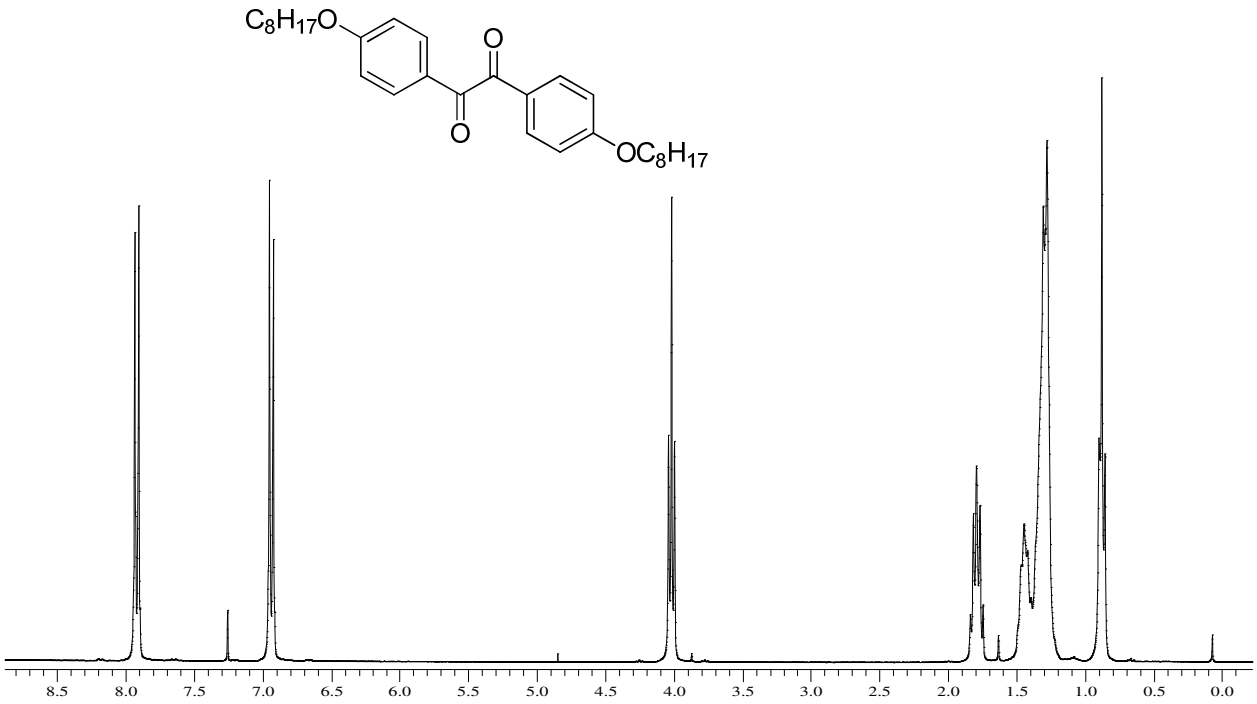

B. ^{13}C NMR

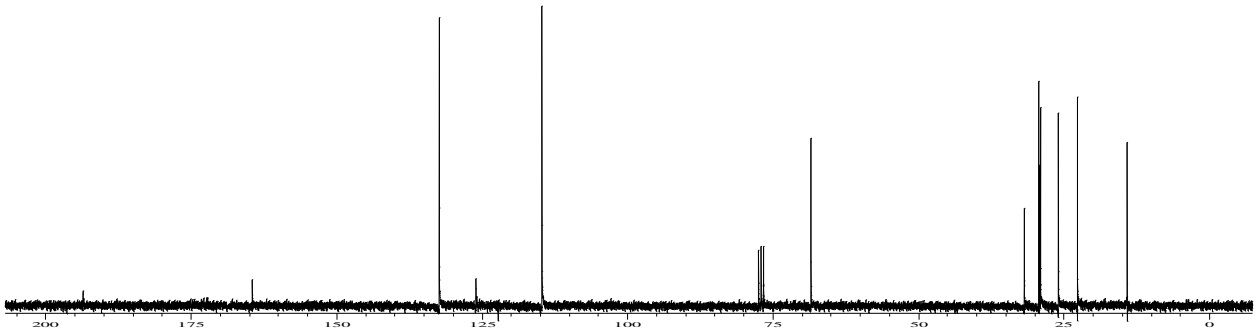

C. IR spectrum

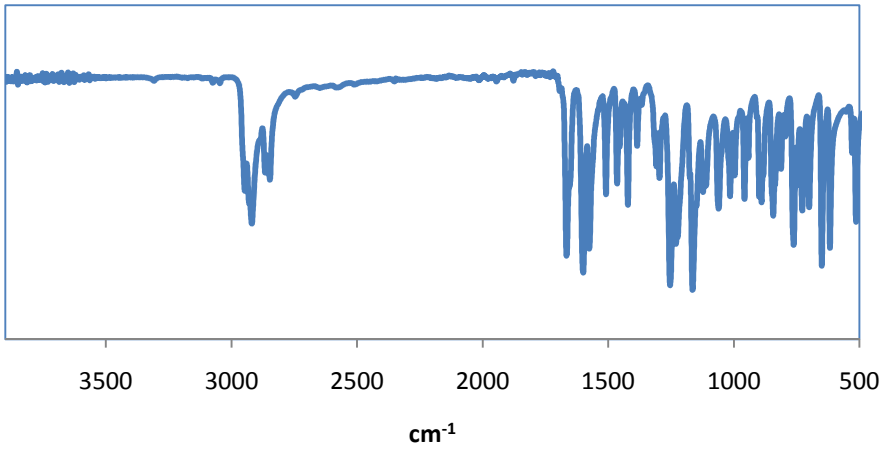

D. EI mass spectrum

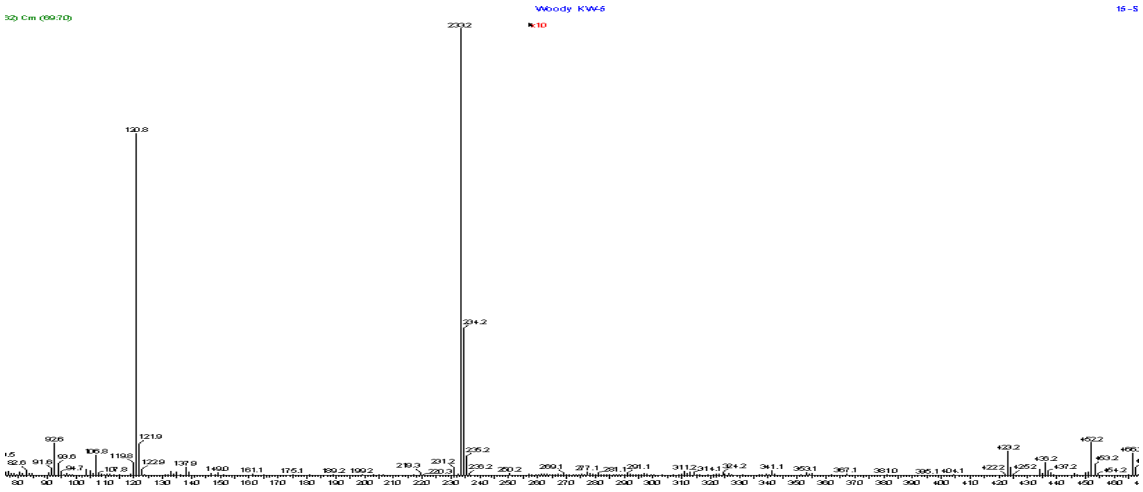

Figure D.1. ^{1}H NMR, ^{13}C NMR, IR spectrum and EI mass spectrum for 1,2-bis(4-(octyloxy)phenyl)ethane-1,2-dione, **IV-3a**.

5,10-Diethyltetradecane-7,8-dione

A. ^{1}H NMR

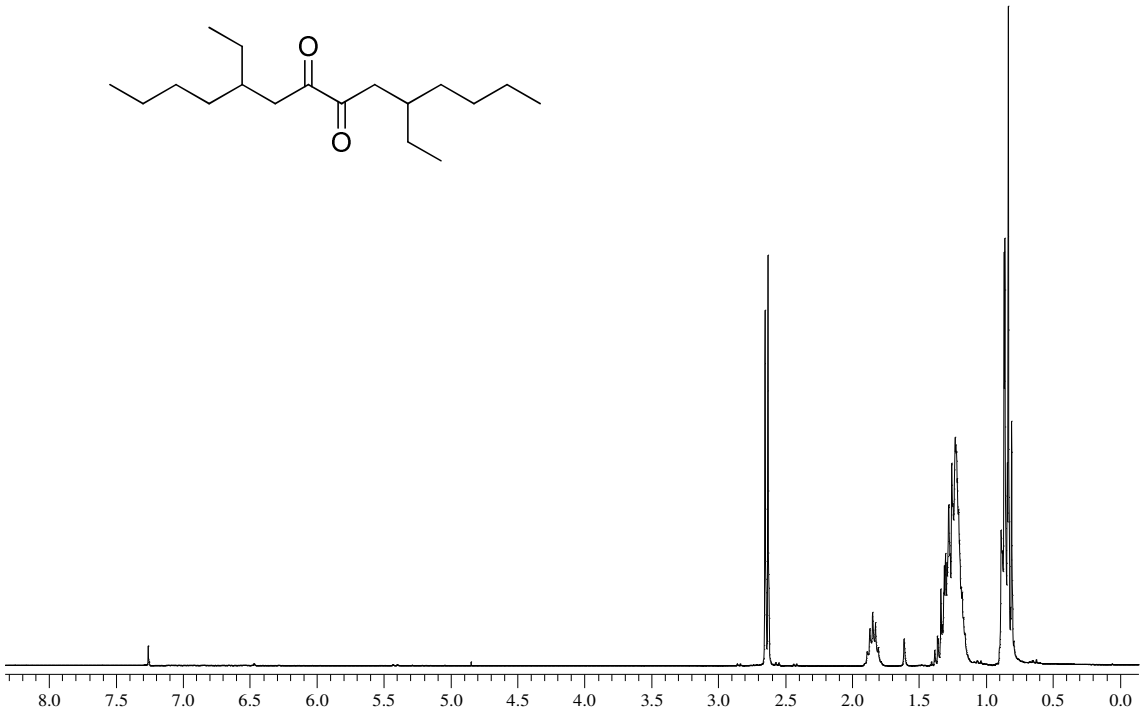

B. ^{13}C NMR

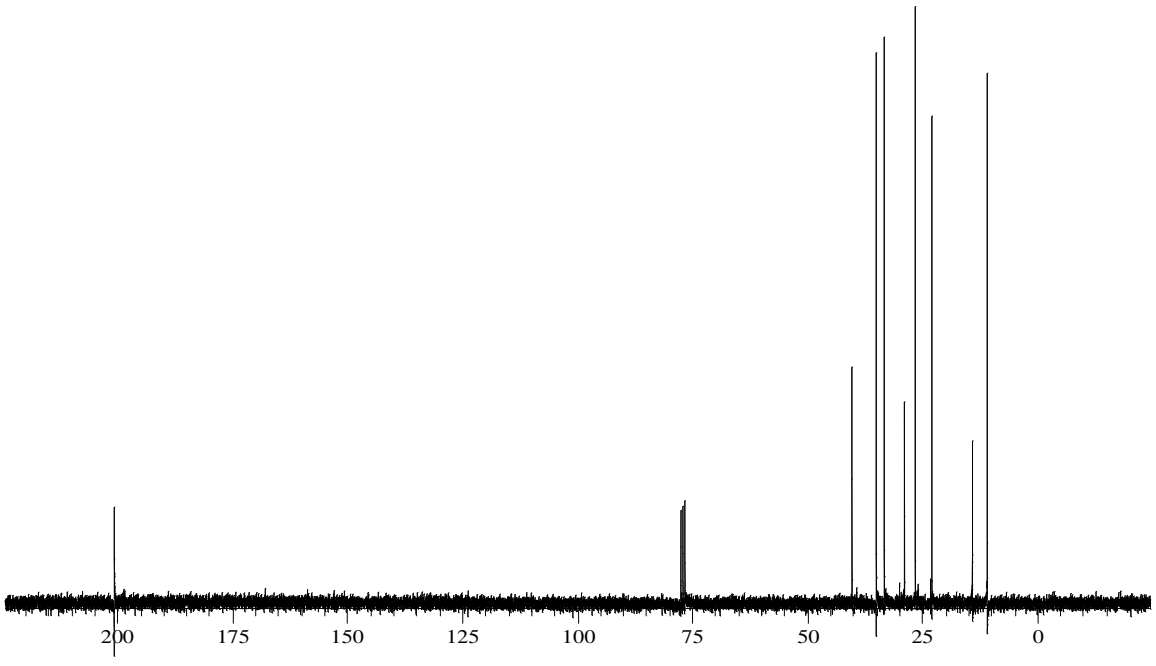

C. IR spectrum

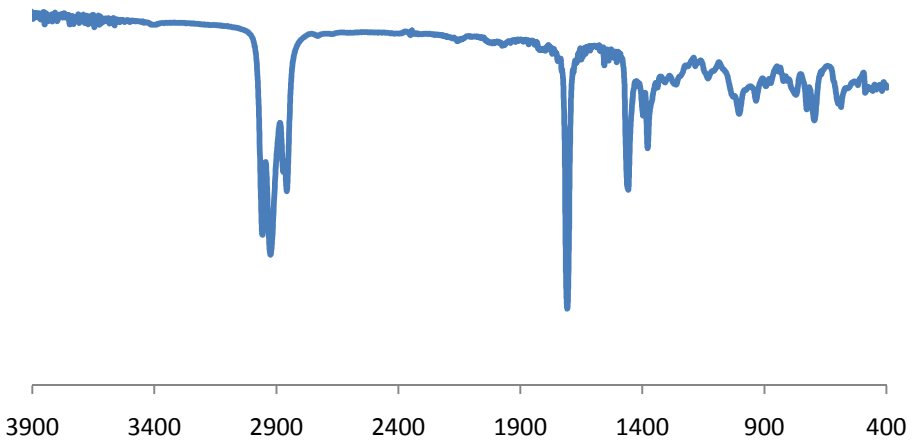

Figure D.2. ^{1}H NMR, ^{13}C NMR and IR spectrum for 5,10-diethyltetradecane-7,8-dione **IV-3b**.

5,8-Dibromo-2,3-bis(4-(octyloxy)phenyl)quinoxaline

A. ^{1}H NMR

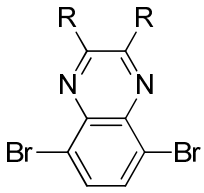

R = 4-octyloxyphenyl

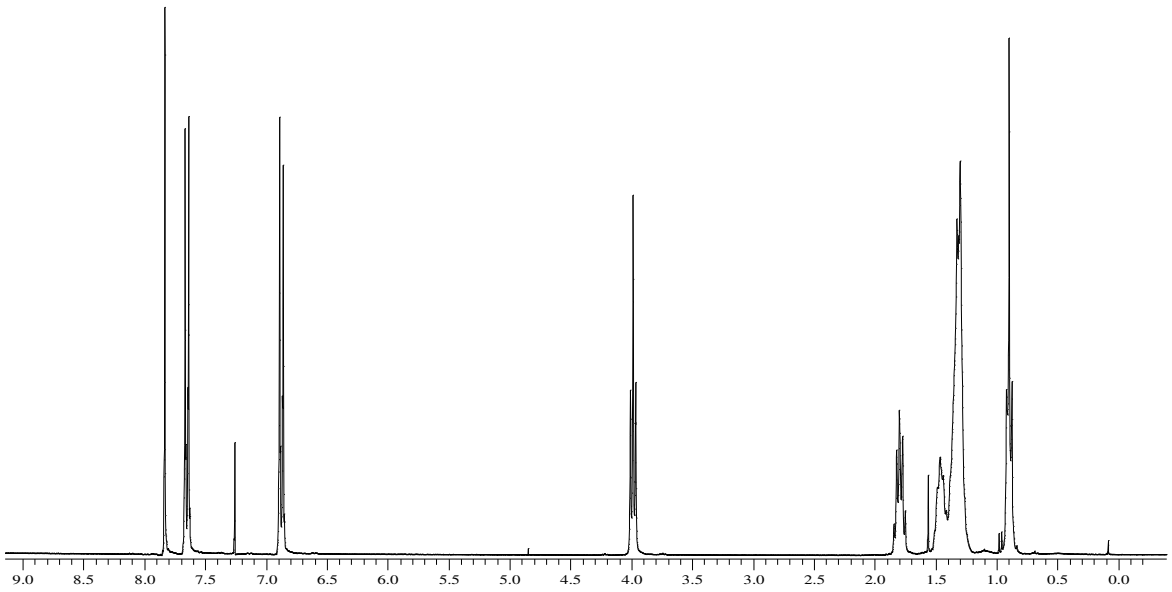

B. ^{13}C NMR

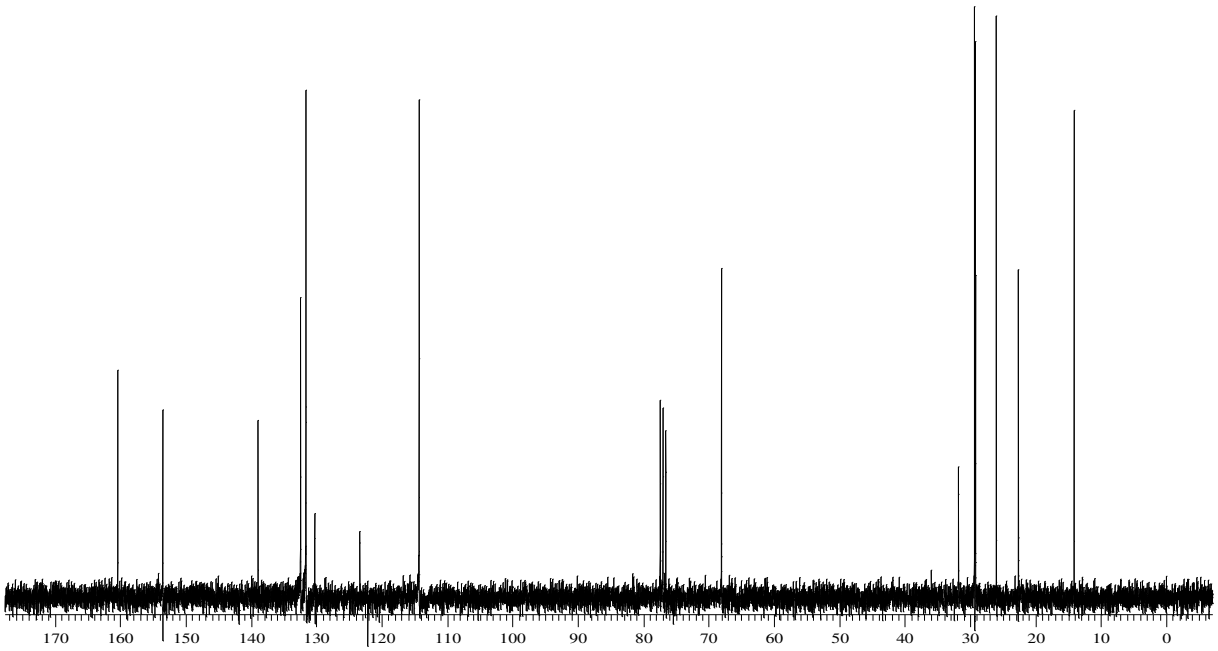

C. IR spectrum

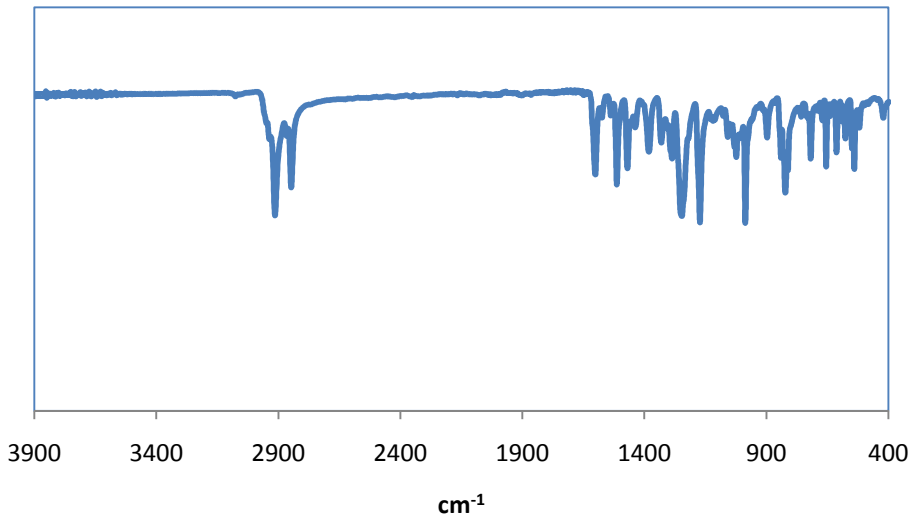

D. EI mass spectrum

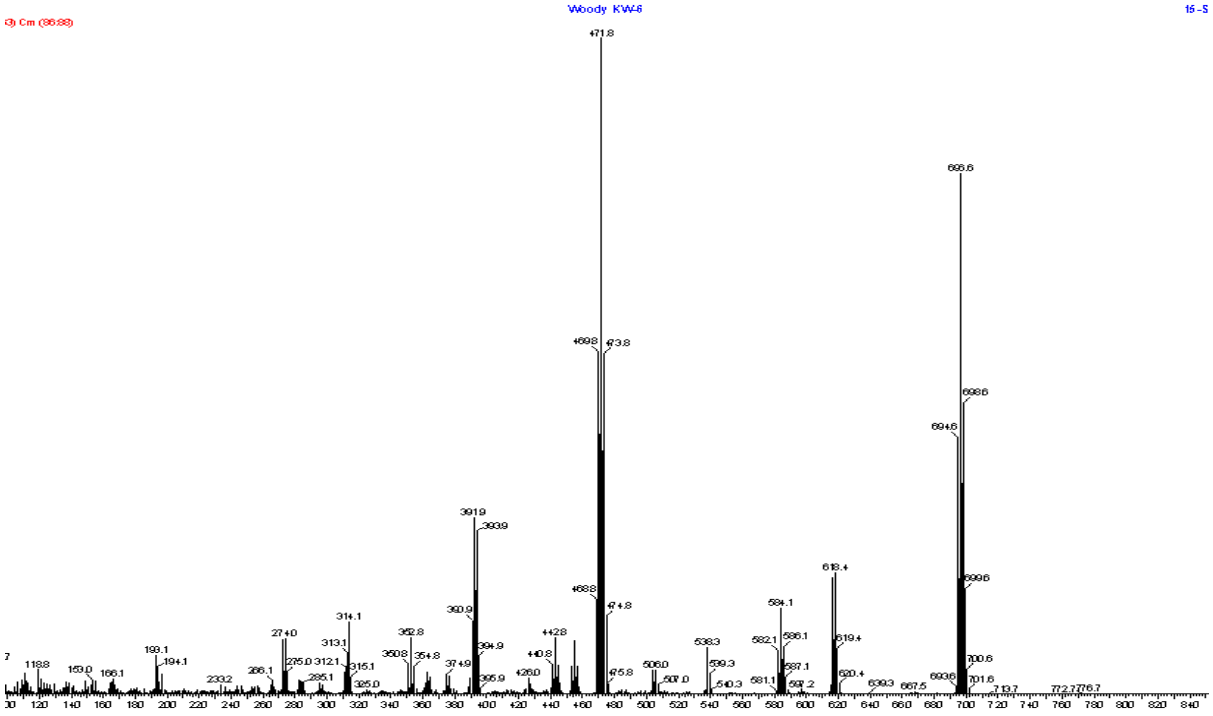

Figure D.3. ^{1}H NMR, ^{13}C NMR, IR spectrum and EI mass spectrum for 5,8-dibromo-2,3-bis(4-(octyloxy)phenyl)quinoxaline, **IV-4a**.

5,8-Dibromo-2,3-bis(2-ethylhexyl)quinoxaline

A. ^{1}H NMR

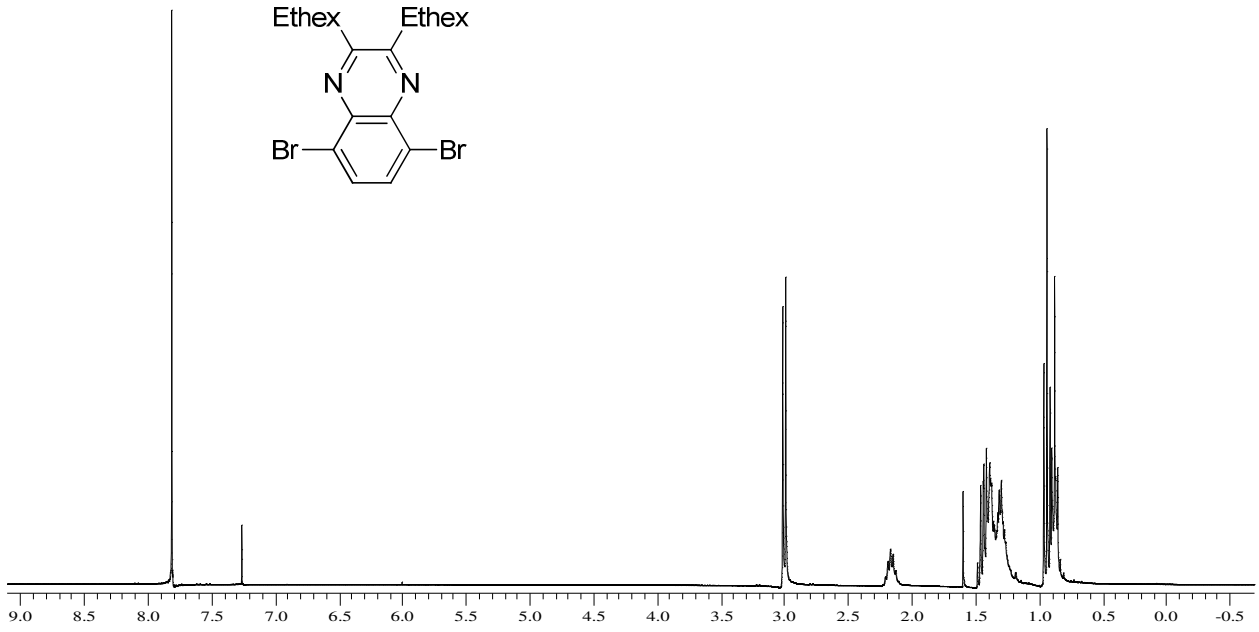

B. ^{13}C NMR

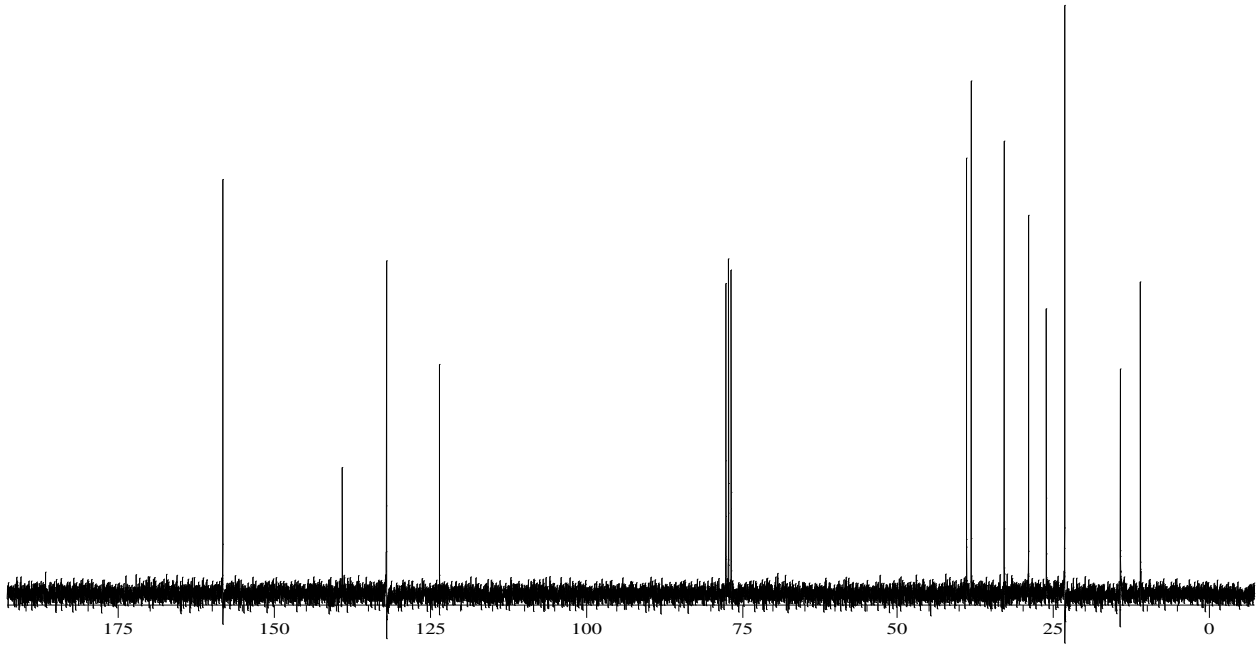

C. IR spectrum

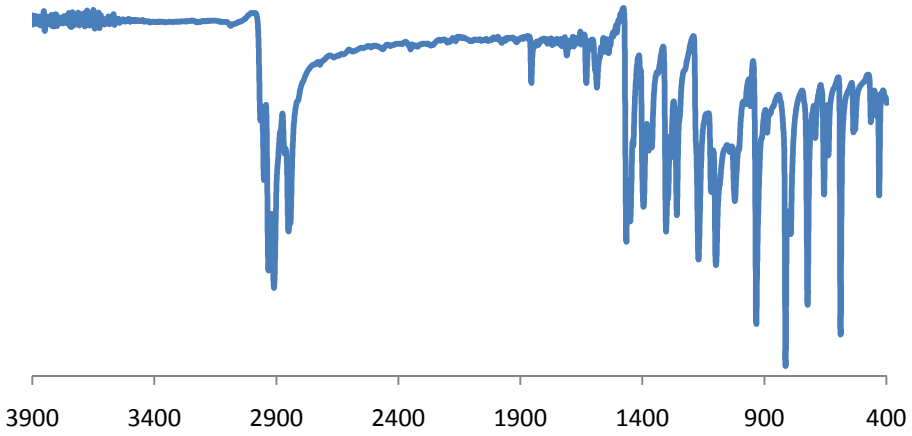

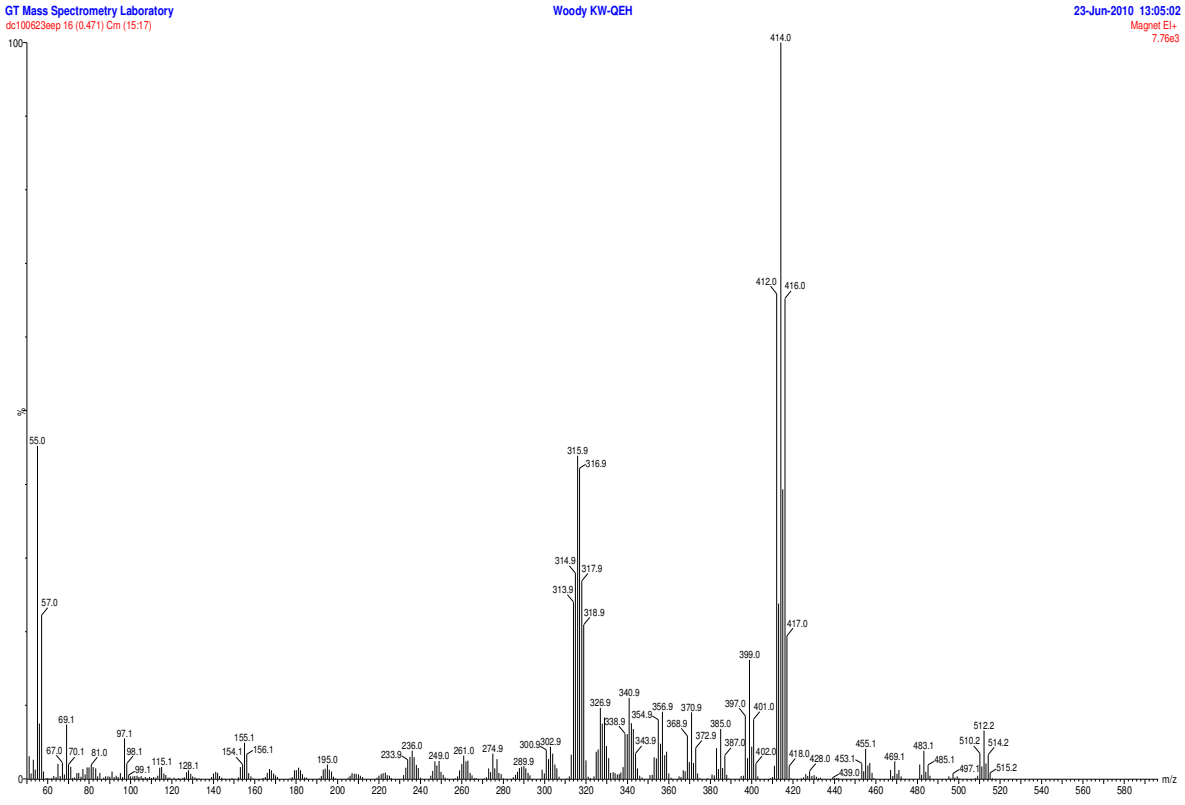

Figure D.4. ^{1}H NMR, ^{13}C NMR, IR spectrum and EI mass spectrum for 5,8-dibromo-2,3-bis(2-ethylhexyl)quinoxaline, **IV-4b**.

2,3-Bis(4-(octyloxy)phenyl)-5,8-bis(4,4,5,5-tetramethyl-1,3,2-dioxaborolan-2-yl)quinoxaline

A. ^{1}H NMR

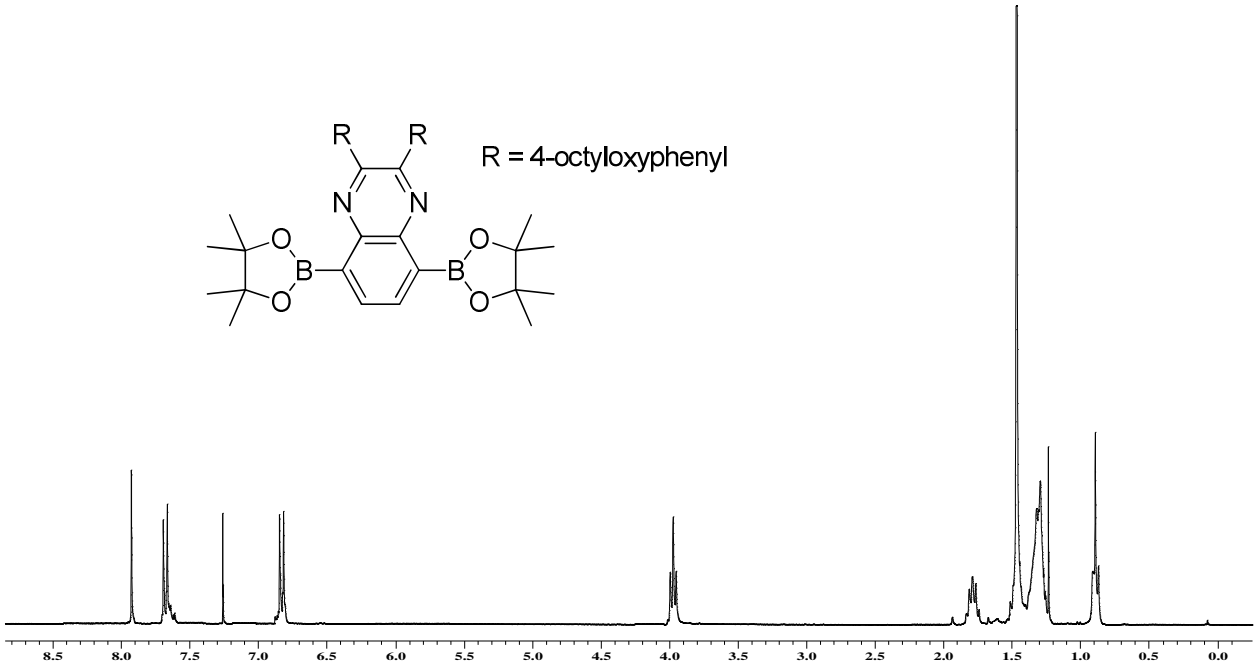

B. ^{13}C NMR

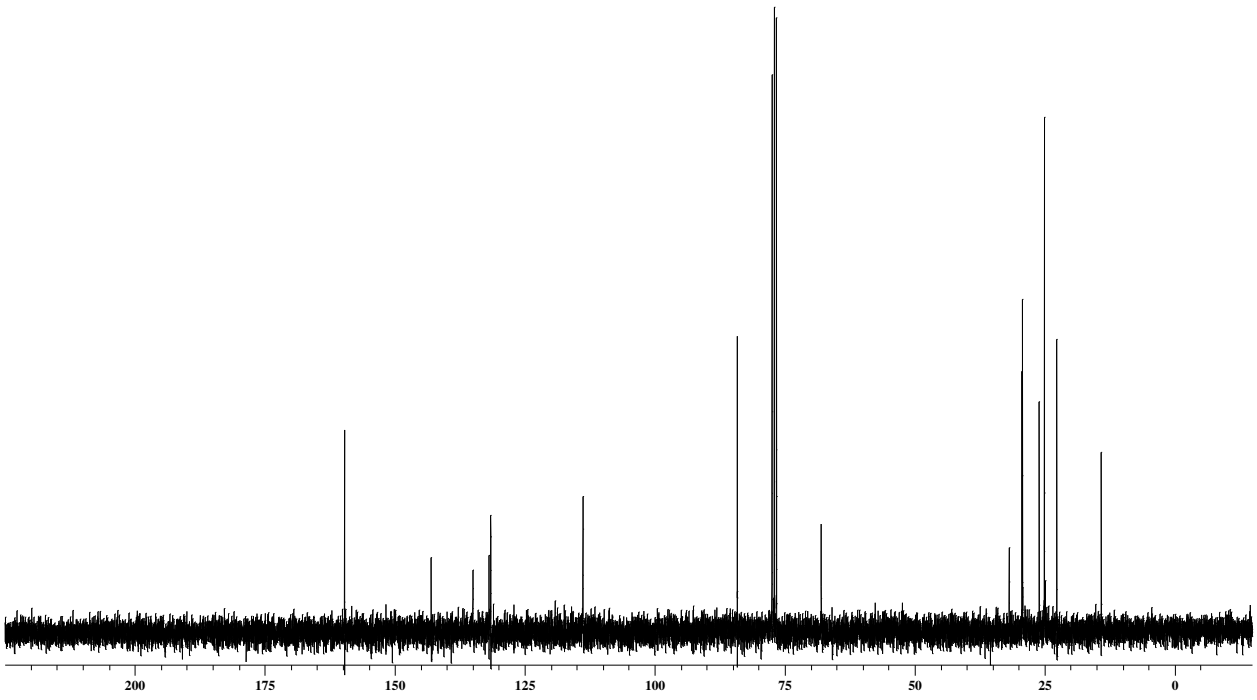

C. IR spectrum

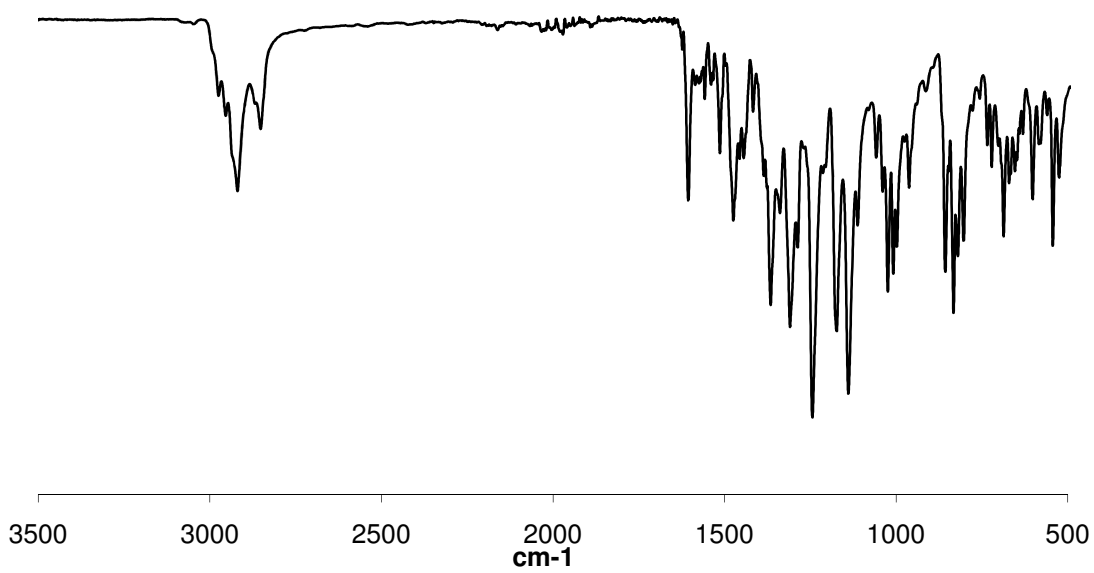

Figure D.5. ^{1}H NMR, ^{13}C NMR and IR spectrum for 2,3-bis(4-(octyloxy)phenyl)-5,8-bis(4,4,5,5-tetramethyl-1,3,2-dioxaborolan-2-yl)quinoxaline, **IV-7**.

2,3-Bis(4-(octyloxy)phenyl)-5,8-bis(3-octylthiophen-2-yl)quinoxaline

A. ^{1}H NMR

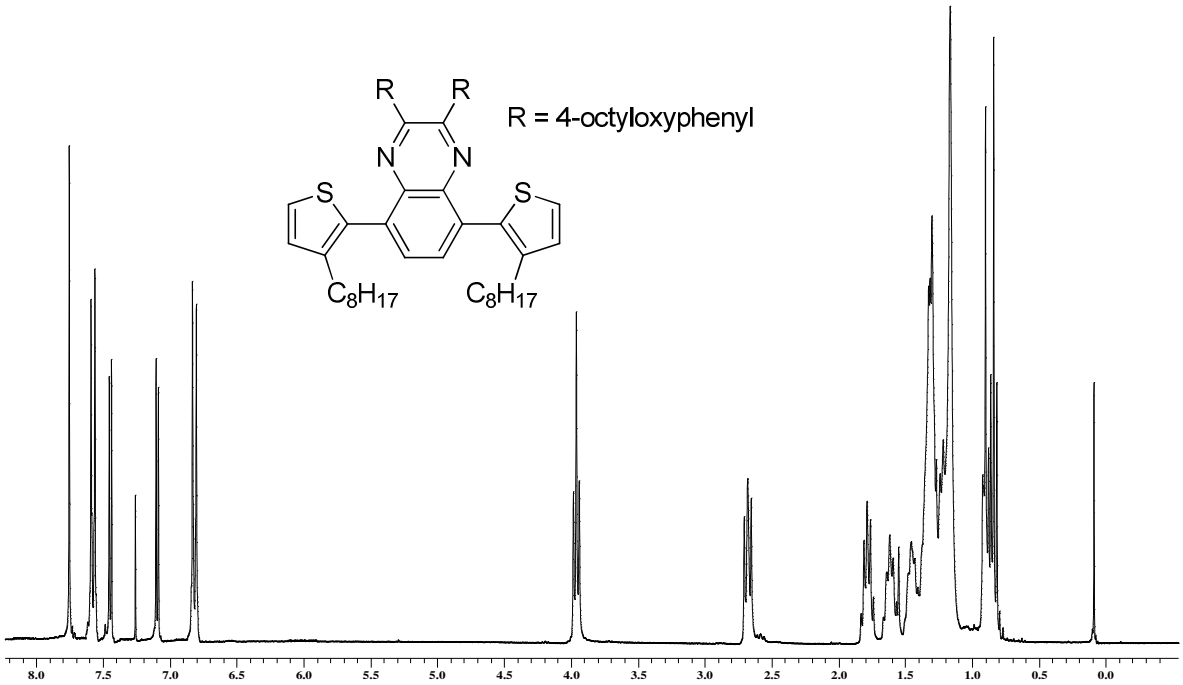

B. ^{13}C NMR

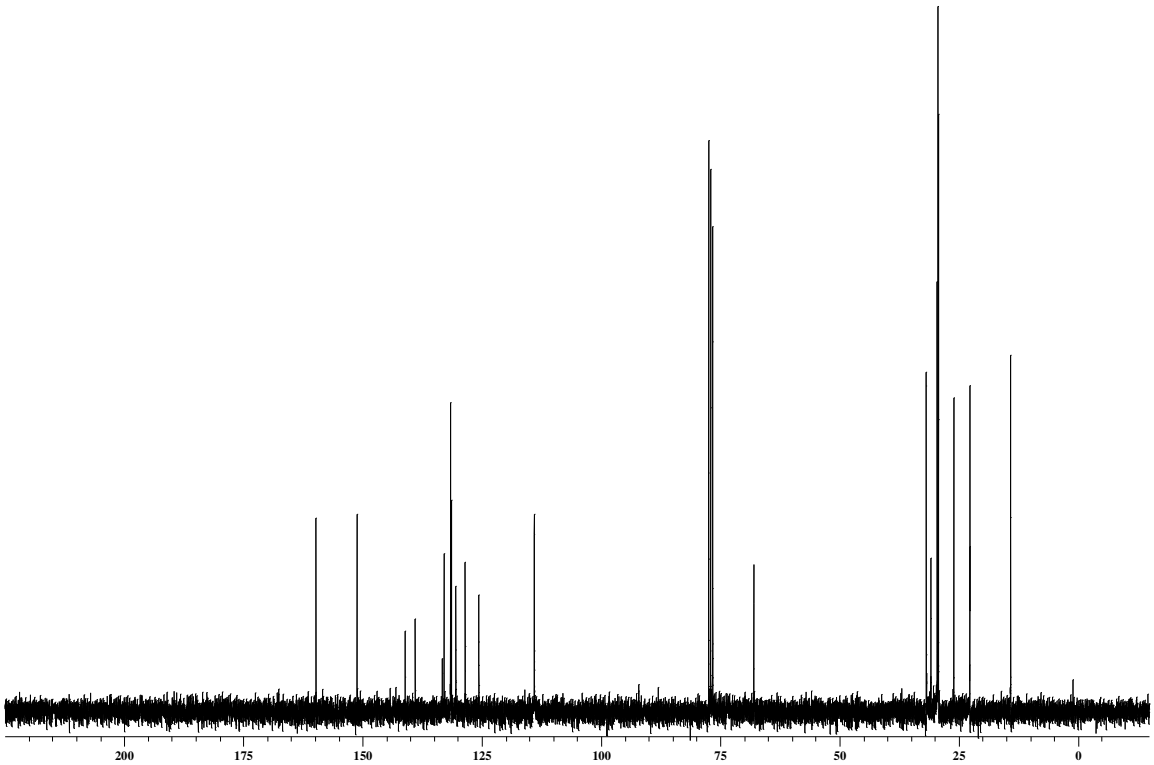

C. IR spectrum

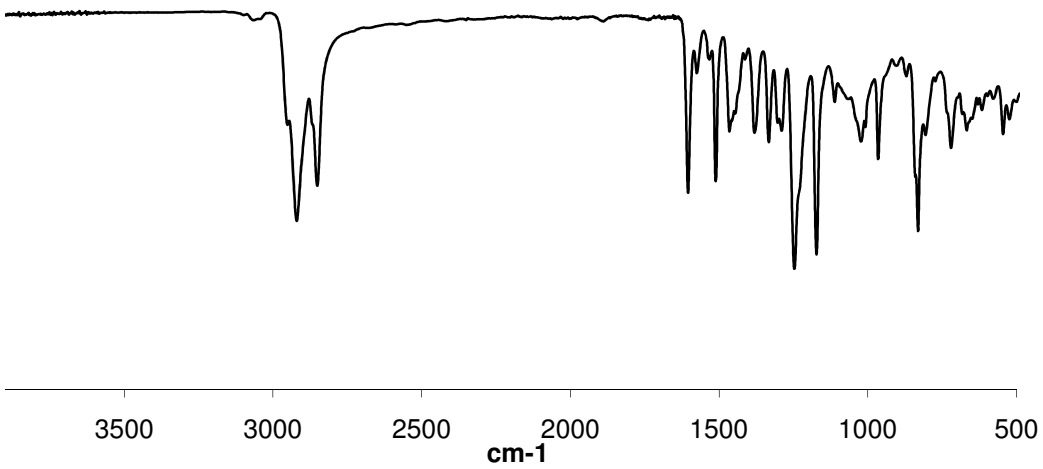

Figure D.6. ^{1}H NMR, ^{13}C NMR and IR spectrum for 2,3-bis(4-(octyloxy)phenyl)-5,8-bis(3-octylthiophen-2-yl)quinoxaline, **IV-8**.

A. ^{1}H NMR

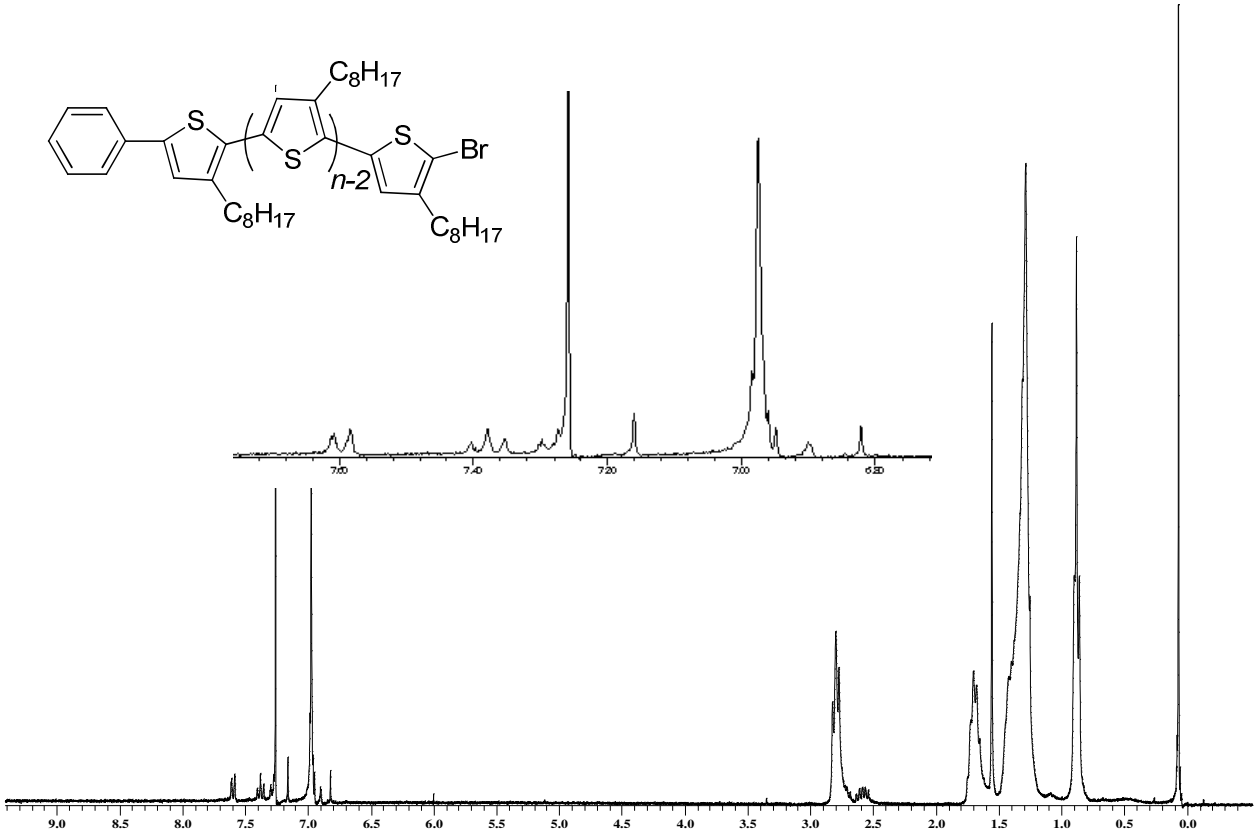

B. ^{13}C NMR

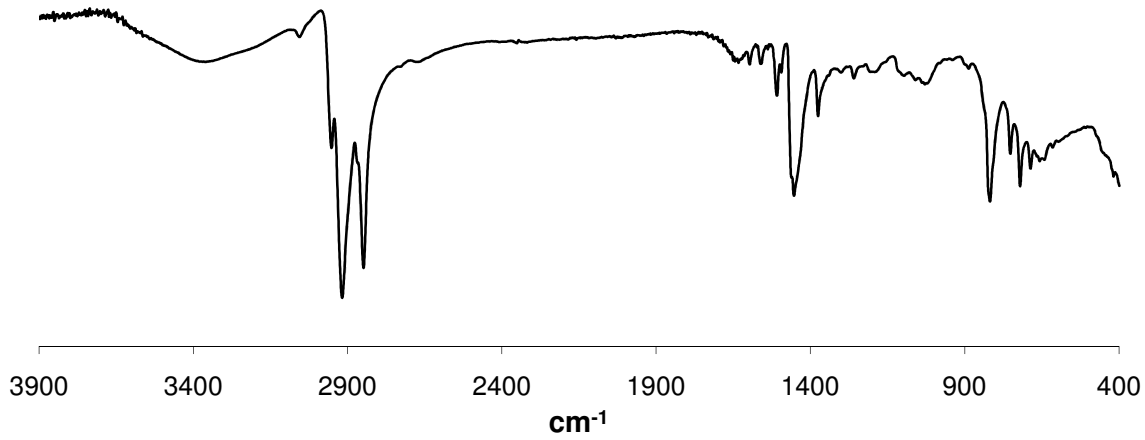

Figure D.7. ^{1}H NMR and IR spectrum of phenyl-initiated poly(3-octylthiophene), **Ph-P3OT-Br**.

A. ^{1}H NMR

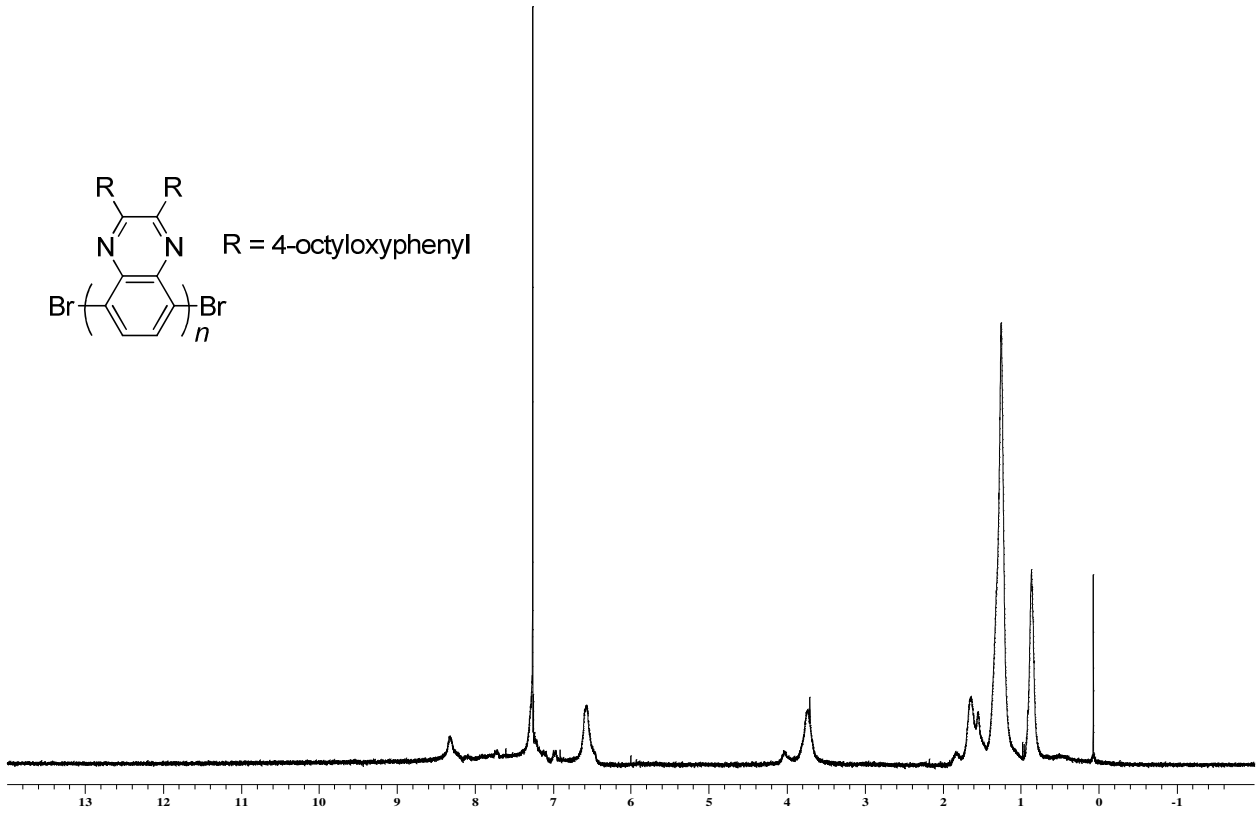

B. ^{13}C NMR

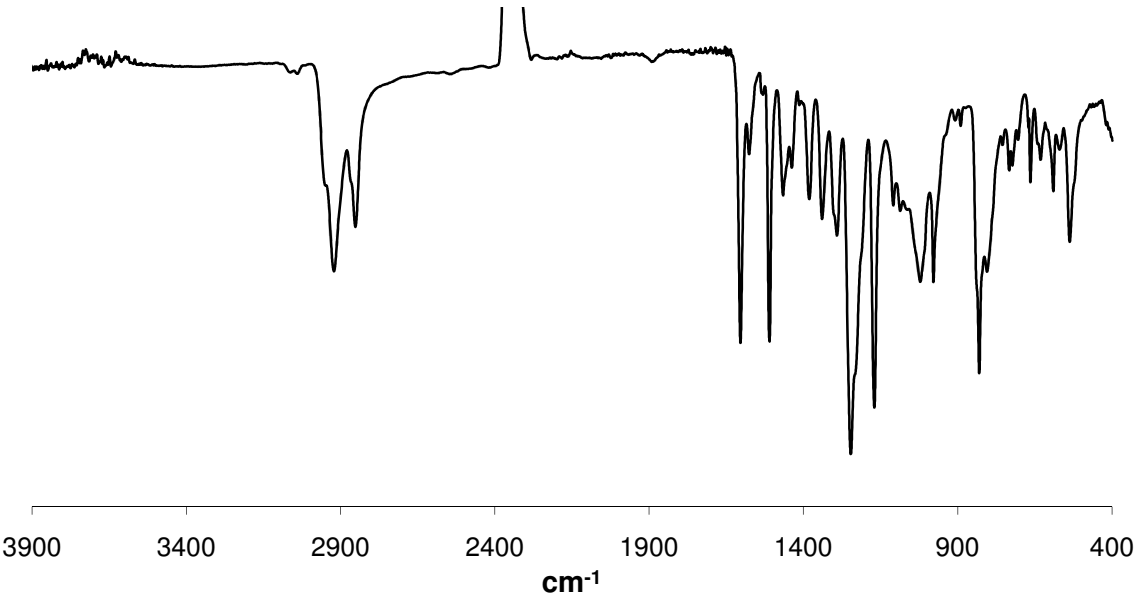

Figure D.8. ^{1}H NMR and IR spectrum and of poly(2,3-(4-octyloxyphenyl)quinoxaline-5,8-diyl), **PQ(C8)Br$_2$**.

A. ^{1}H NMR

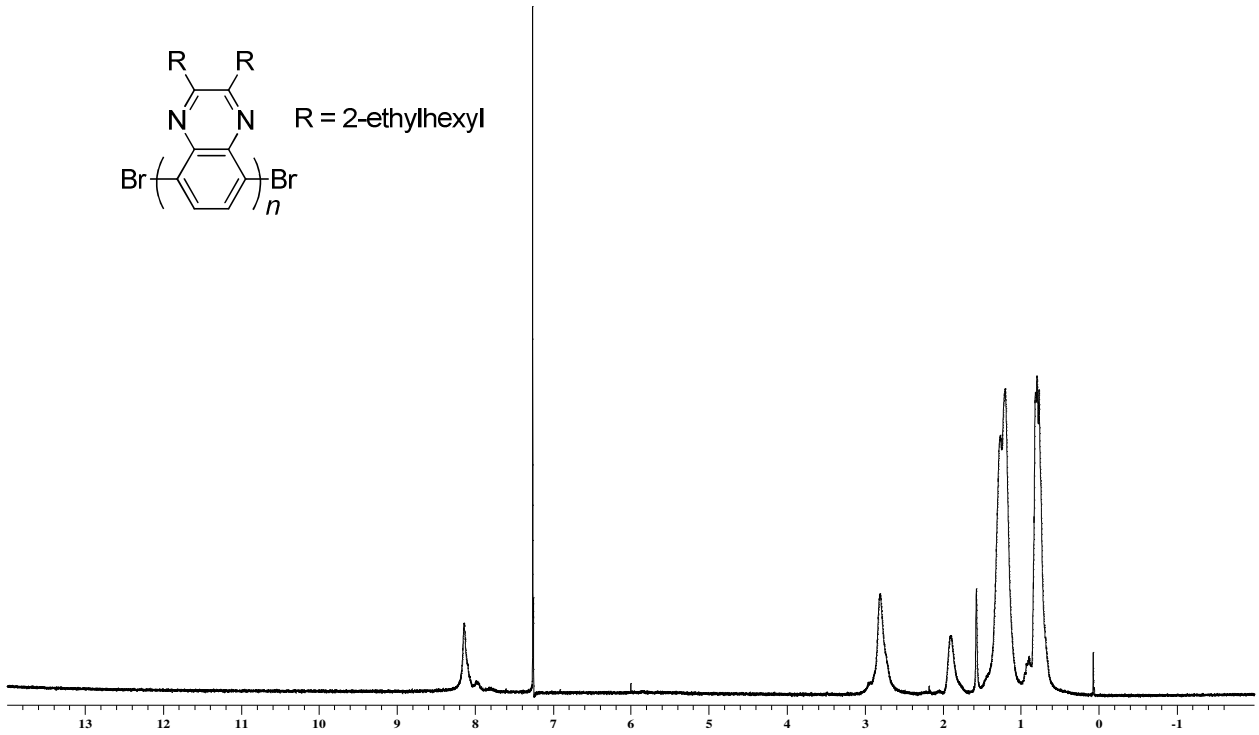

B. ^{13}C NMR

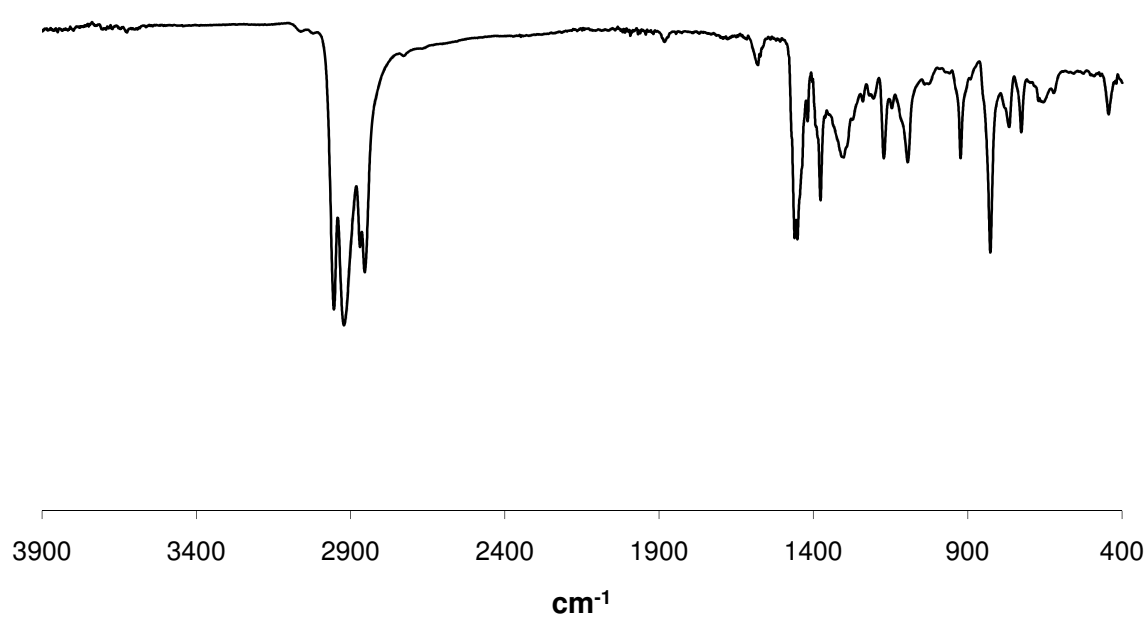

Figure D.9. ^{1}H NMR and IR spectrum and of poly(2,3-(2-ethylhexyl)quinoxaline-5,8-diyl), **PQ(EH)Br$_2$**.

A. ^{1}H NMR

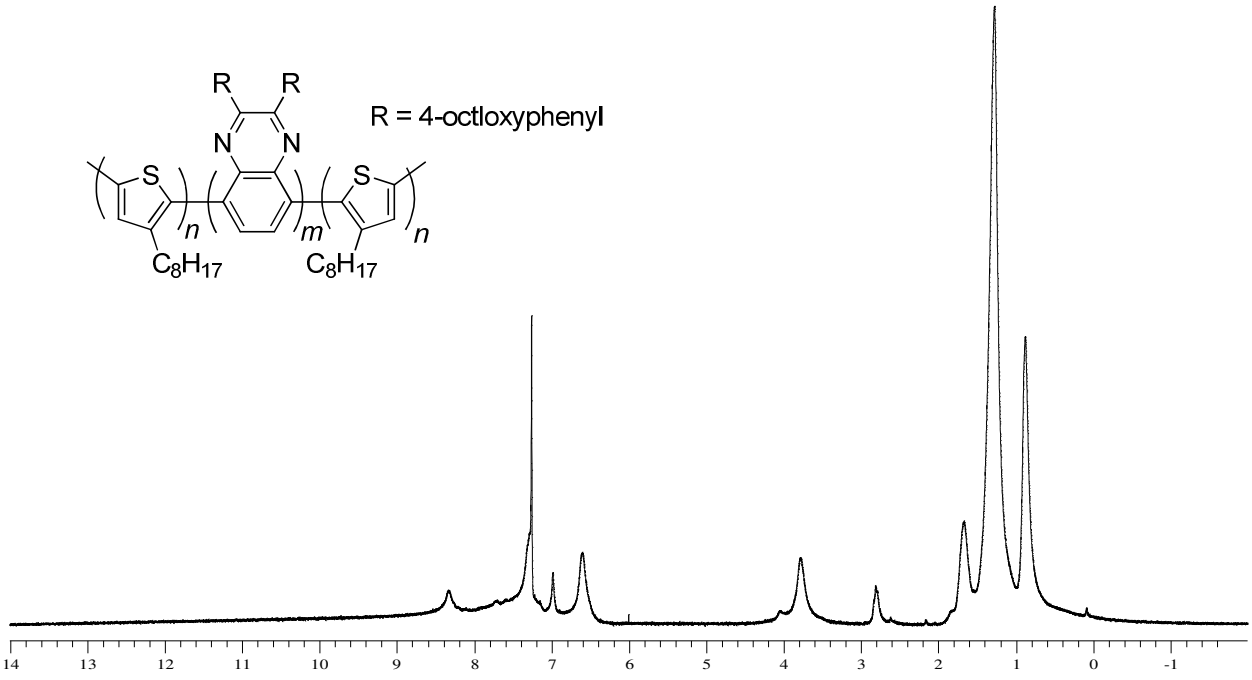

B. ^{13}C NMR

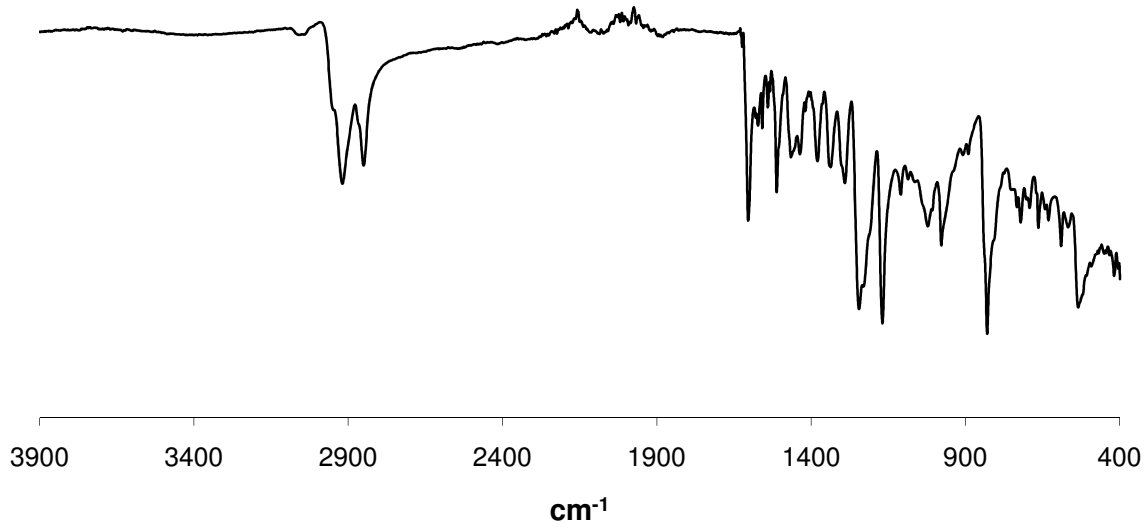

Figure D.10. ^{1}H NMR and IR spectrum and of ABA triblock copolymer **P3OT-PQ(C8)-P3OT**.

A. ^{1}H NMR

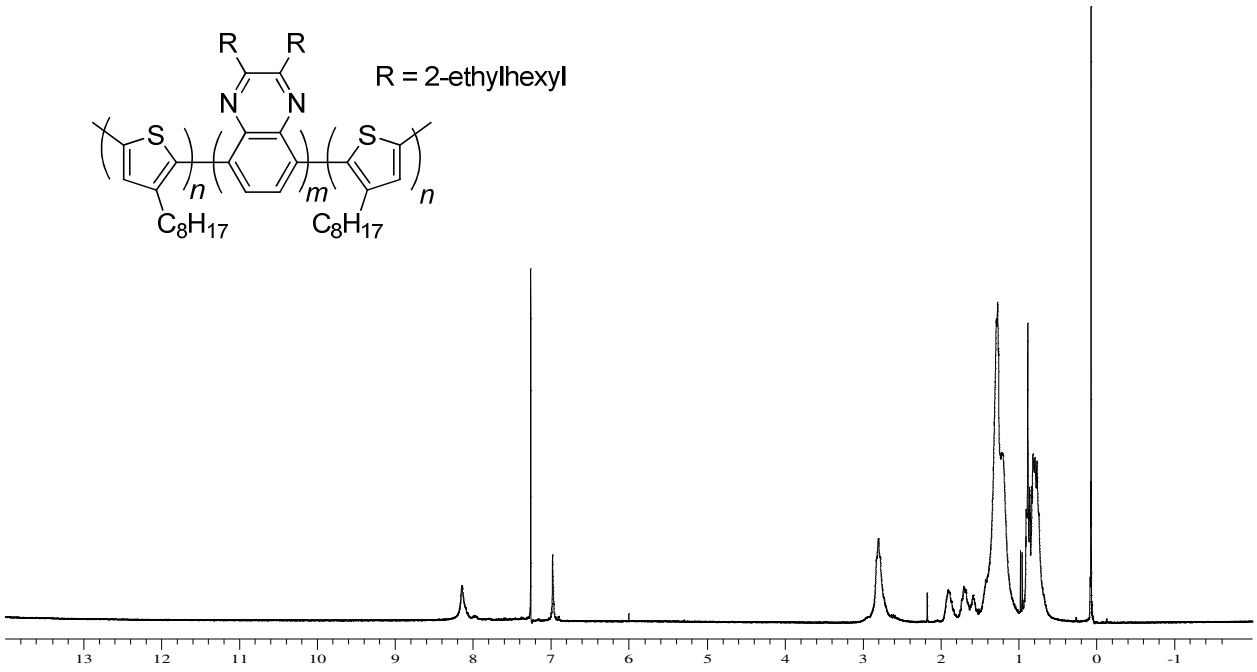

B. ^{13}C NMR

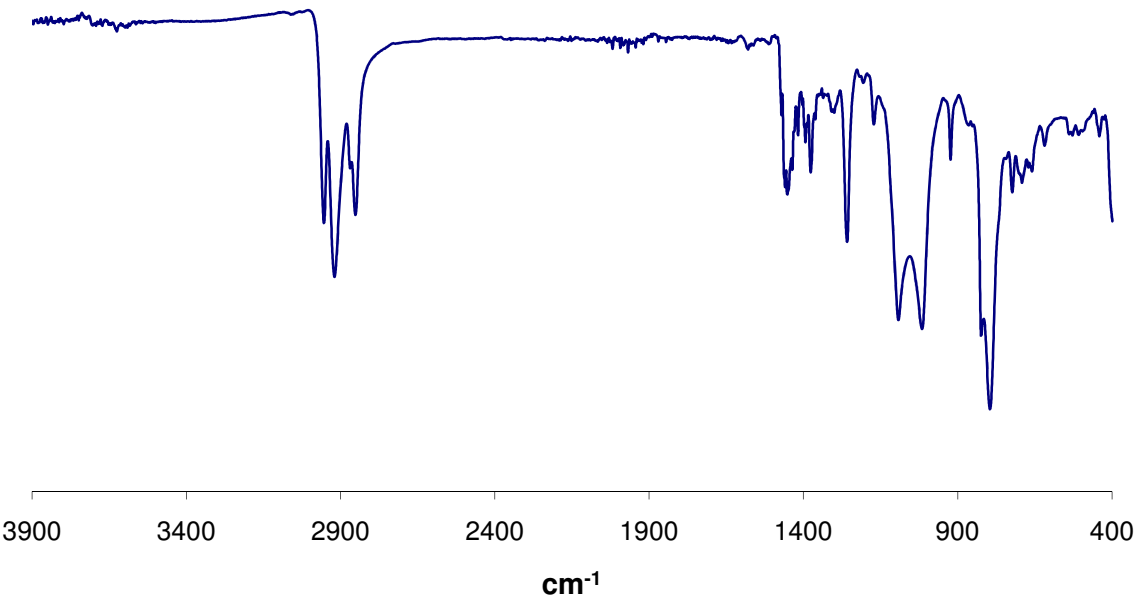

Figure D.11. ^{1}H NMR and IR spectrum and of ABA triblock copolymer **P3OT-PQ(EH)-P3OT**.

APPENDIX E: ^{1}H AND ^{13}C NMR, IR AND MASS SPECTRA OF MONOMERS AND POLYMERS DESCRIBED IN CHAPTER 5

^{1}H NMR spectra were collected on a Varian Mercury Vx 300 MHz instrument using $CDCl_3$ as a solvent. ^{13} C NMR spectra were obtained at 75.5 MHz. IR analyses were performed on a Nicolet 4700 FTIR with an ATR attachment from SmartOrbit Thermoelectronic Corporation.

Tetradecane-7,8-dione

A. ^{1}H NMR

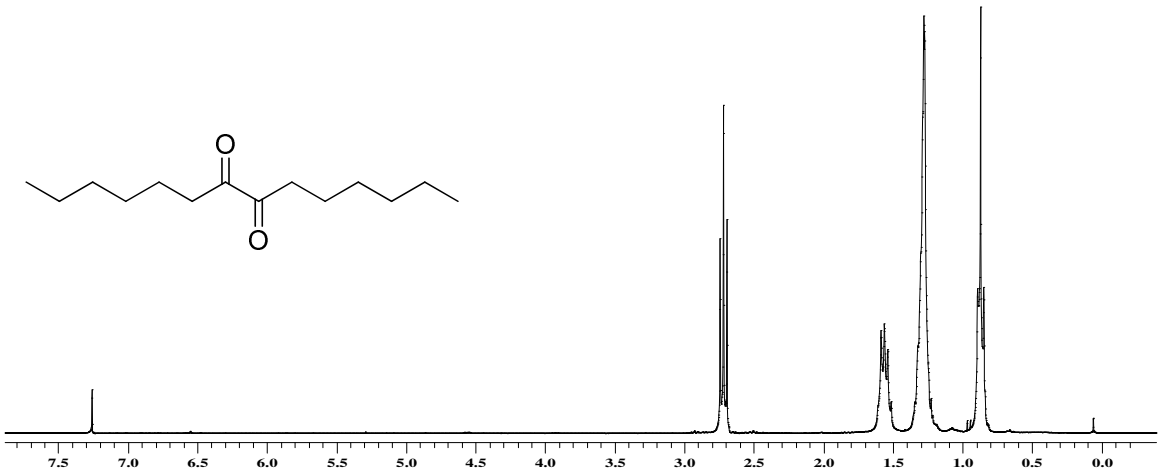

B. ^{13}C NMR

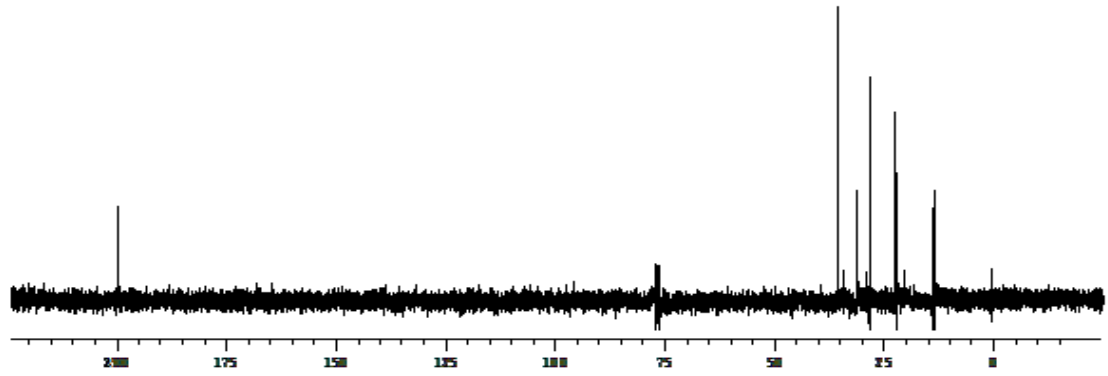

C. IR spectrum

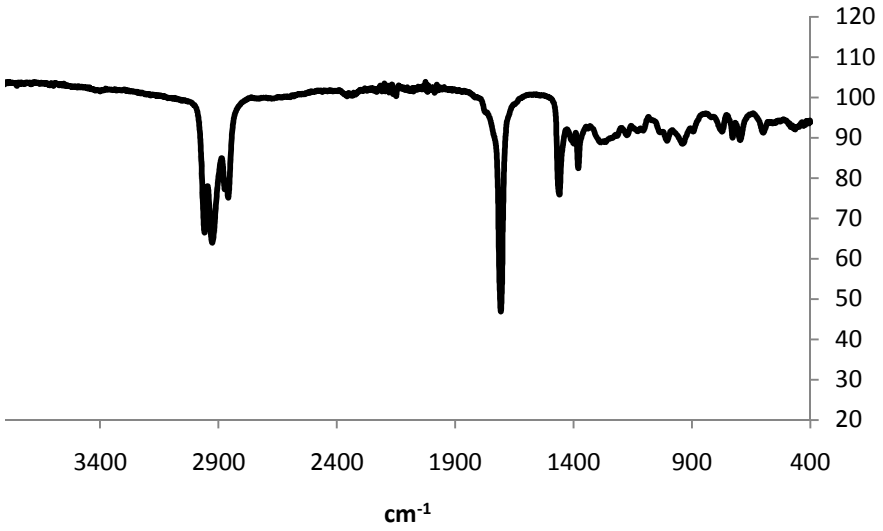

D. EI mass spectrum

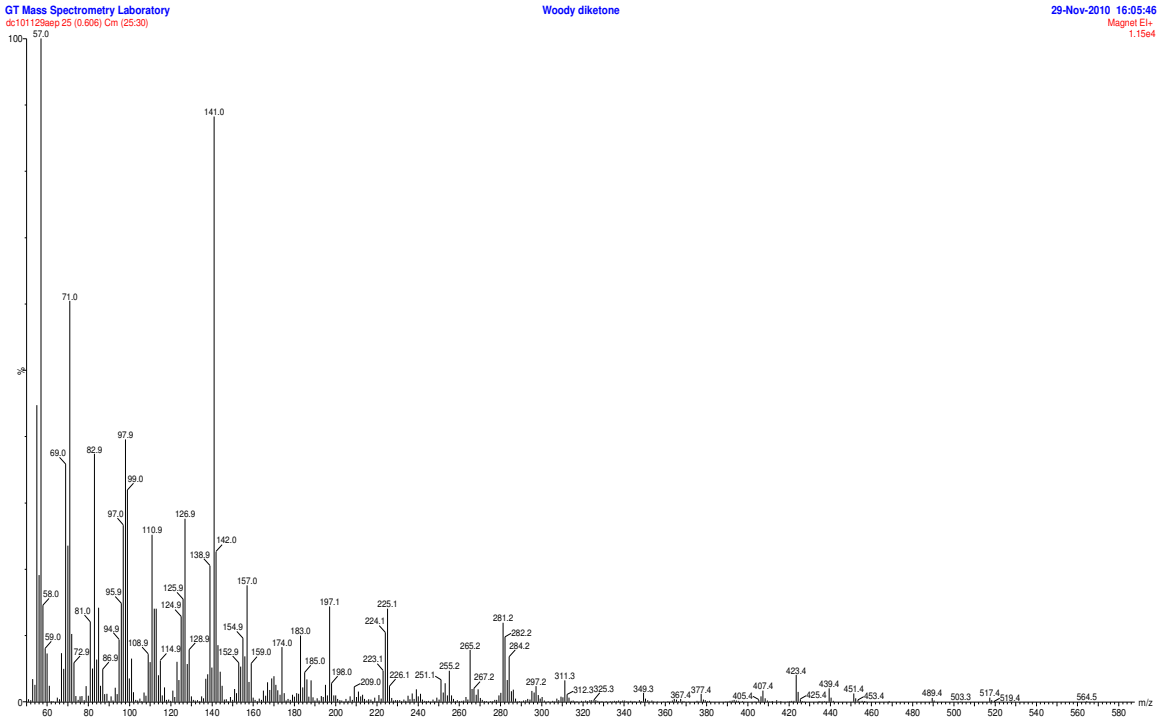

Figure E.1. ^{1}H NMR, ^{13}C NMR, IR spectrum and EI mass spectrum for tetradecane-7,8-dione, **V-1a**.

2,5-Dibromo-3,4-dinitrothiophene

A. ^{13}C NMR

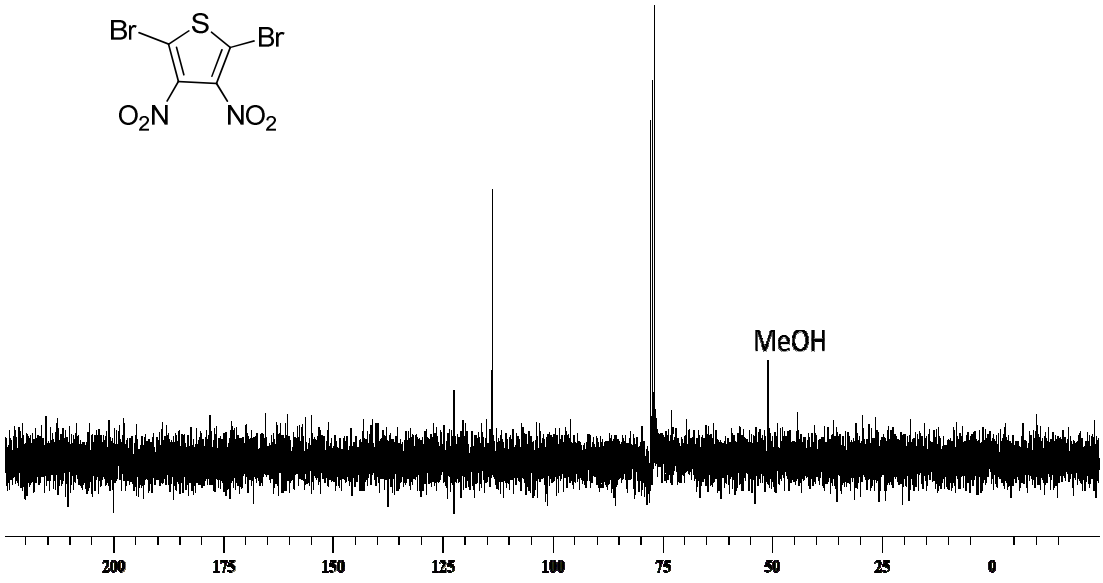

B. IR spectrum

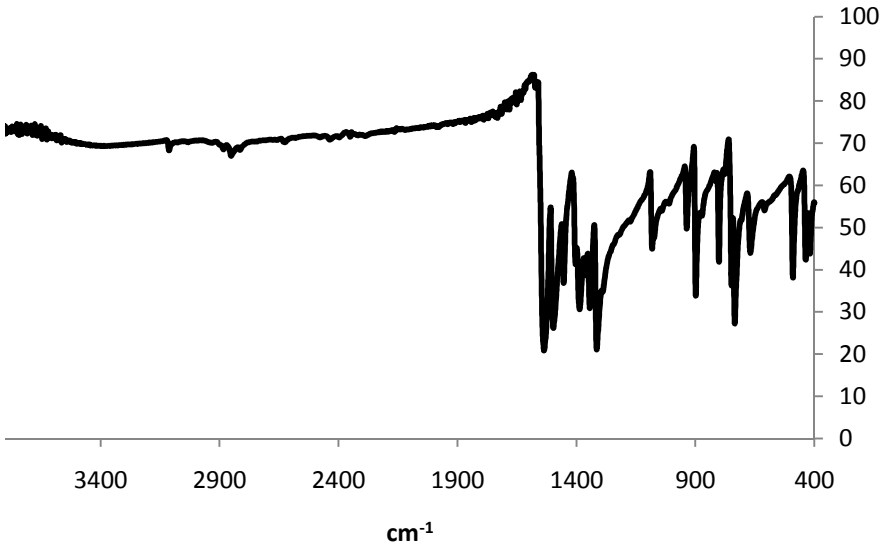

C. EI mass spectrum

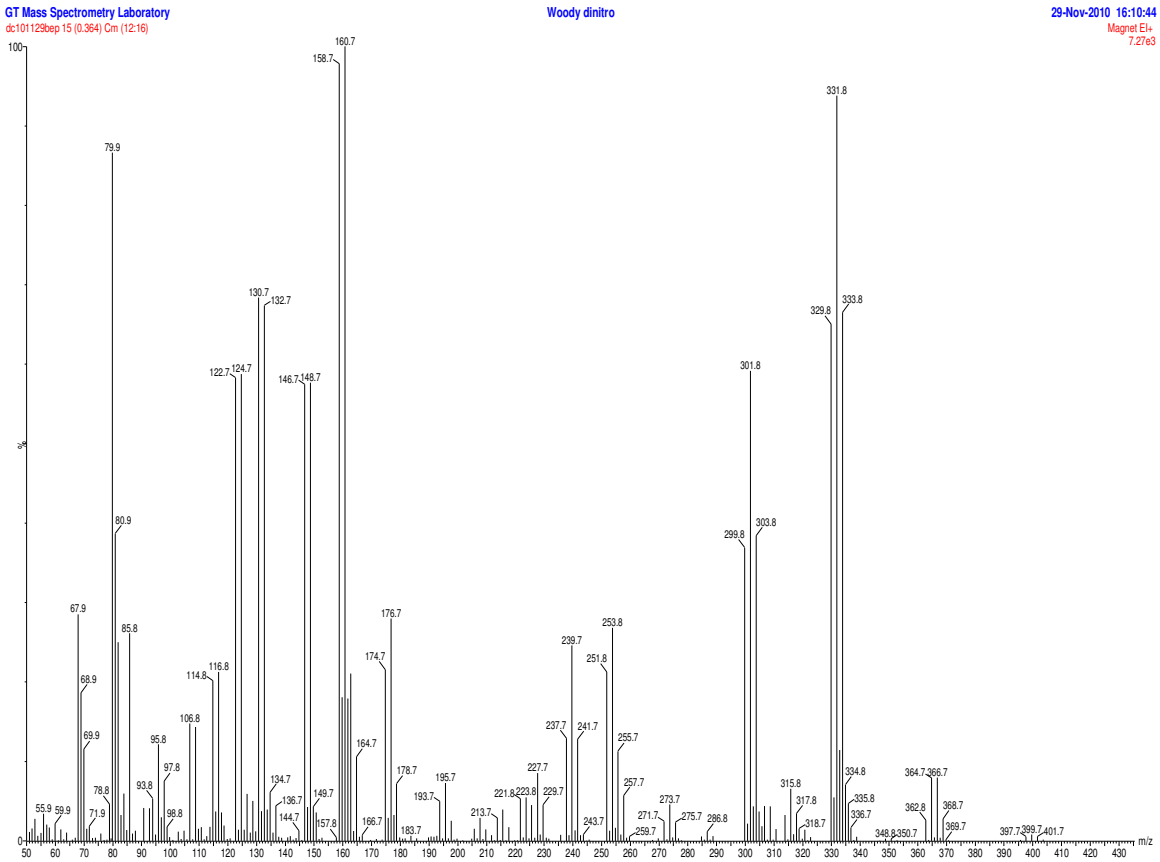

Figure E.2. ^{13}C NMR, IR spectrum and EI mass spectrum of 2,5-dibromo-3,4-dinitrothiophene, **V-2**.

2,3-Dihexylthieno[3,4-b]pyrazine

A. ^{1}H NMR

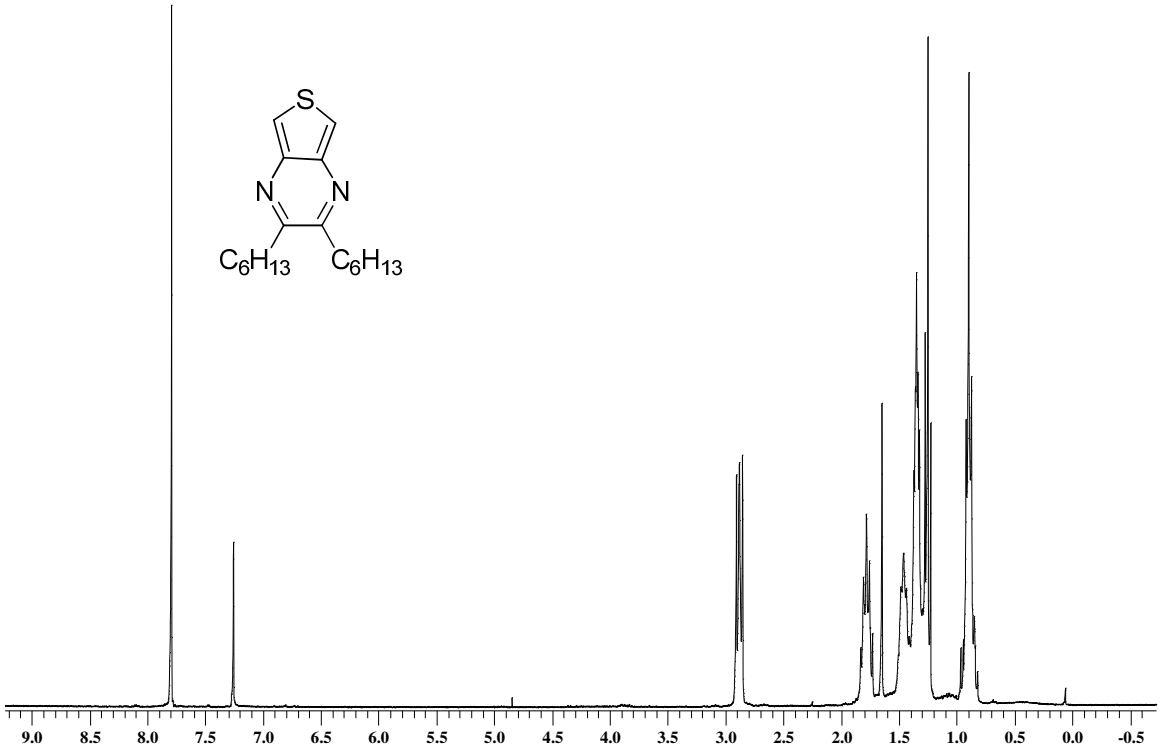

B. ^{13}C NMR

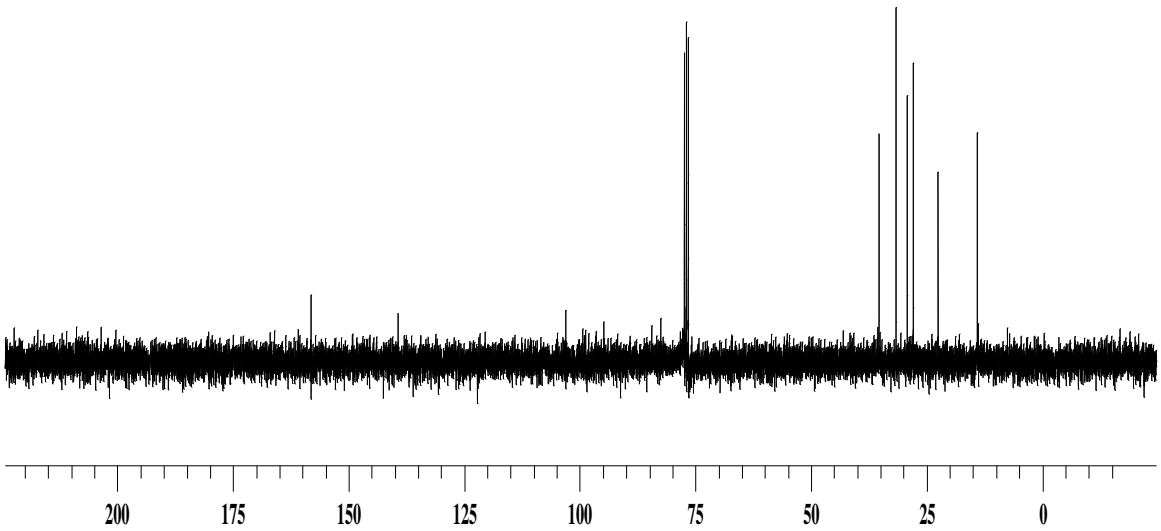

Figure E.3. ^{1}H NMR and ^{13}C NMR for 2,3-dihexylthieno[3,4-b]pyrazine, **V-3a**.

2,3-Bis(4-(octyloxy)phenyl)thieno[3,4-b]pyrazine

A. ^{1}H NMR

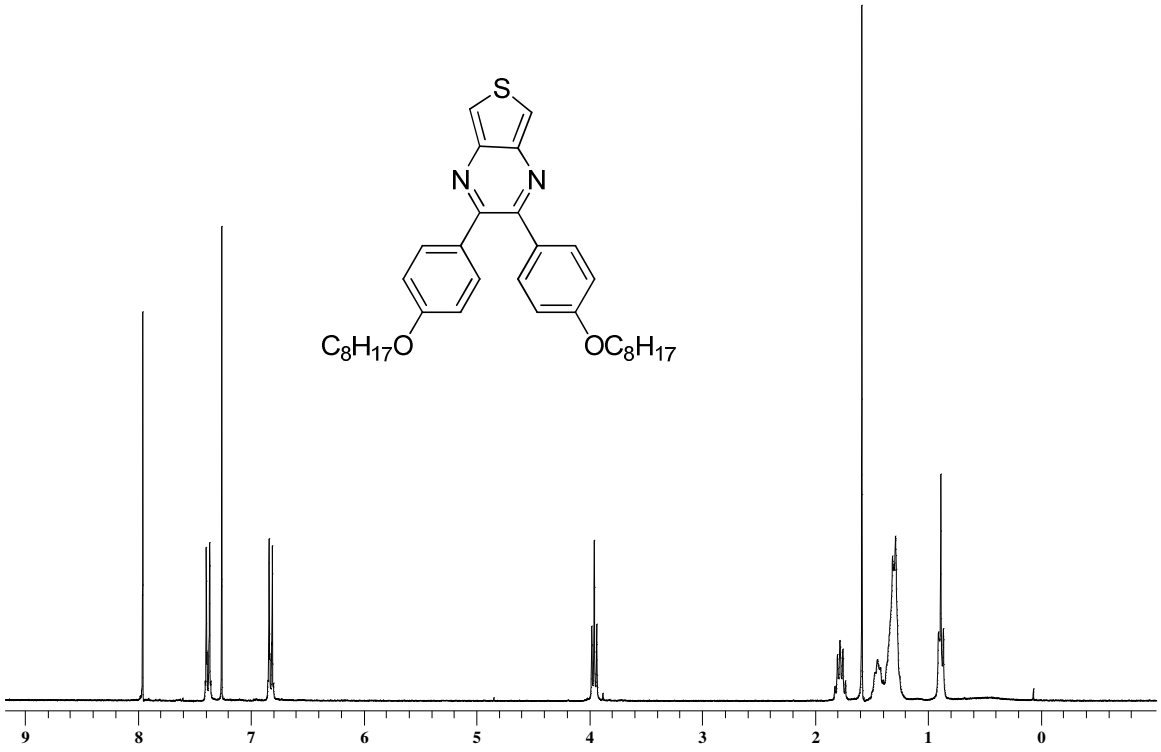

B. ^{13}C NMR

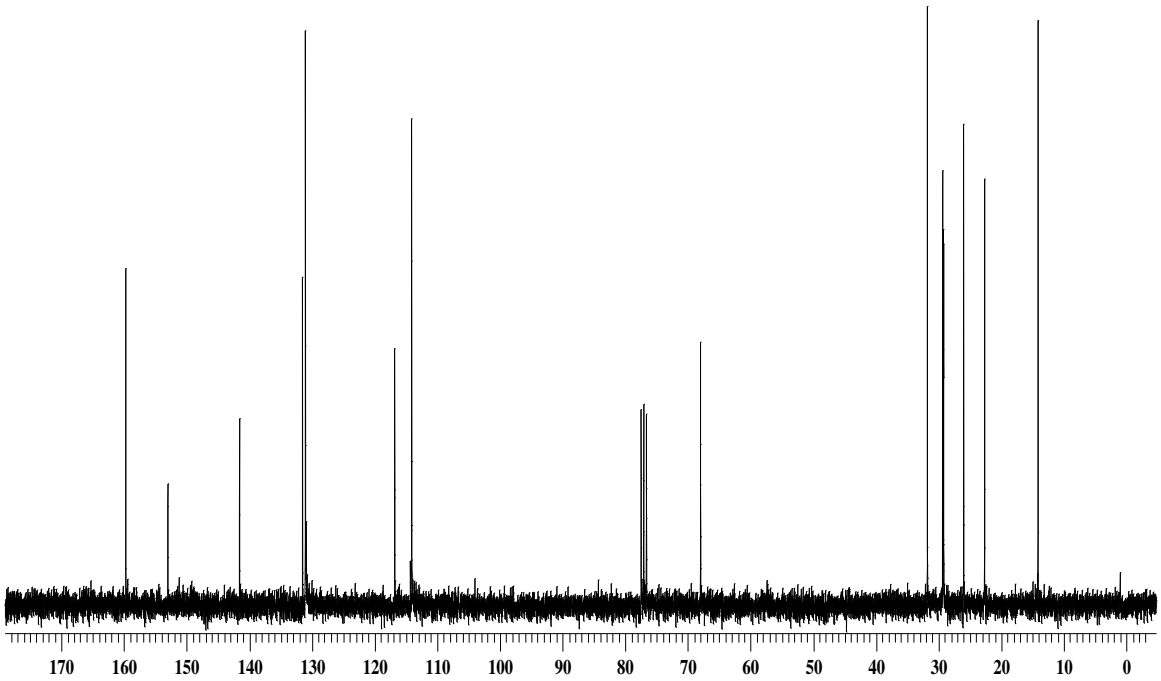

C. IR spectrum

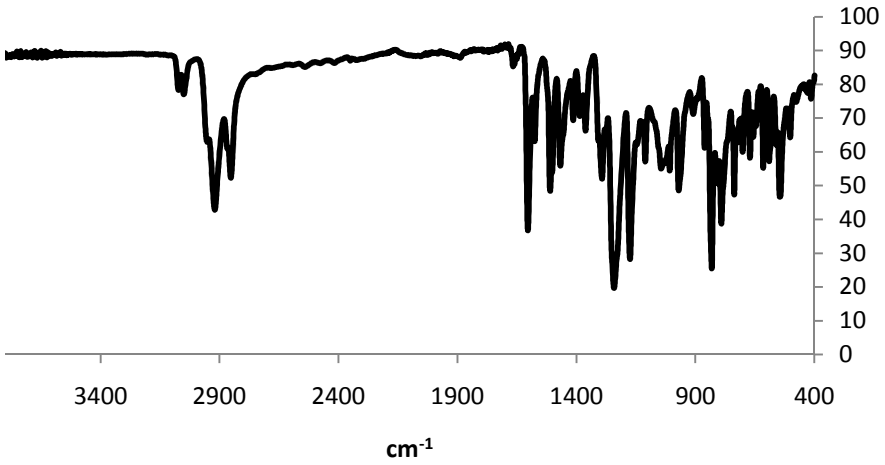

D. Mass spectrum

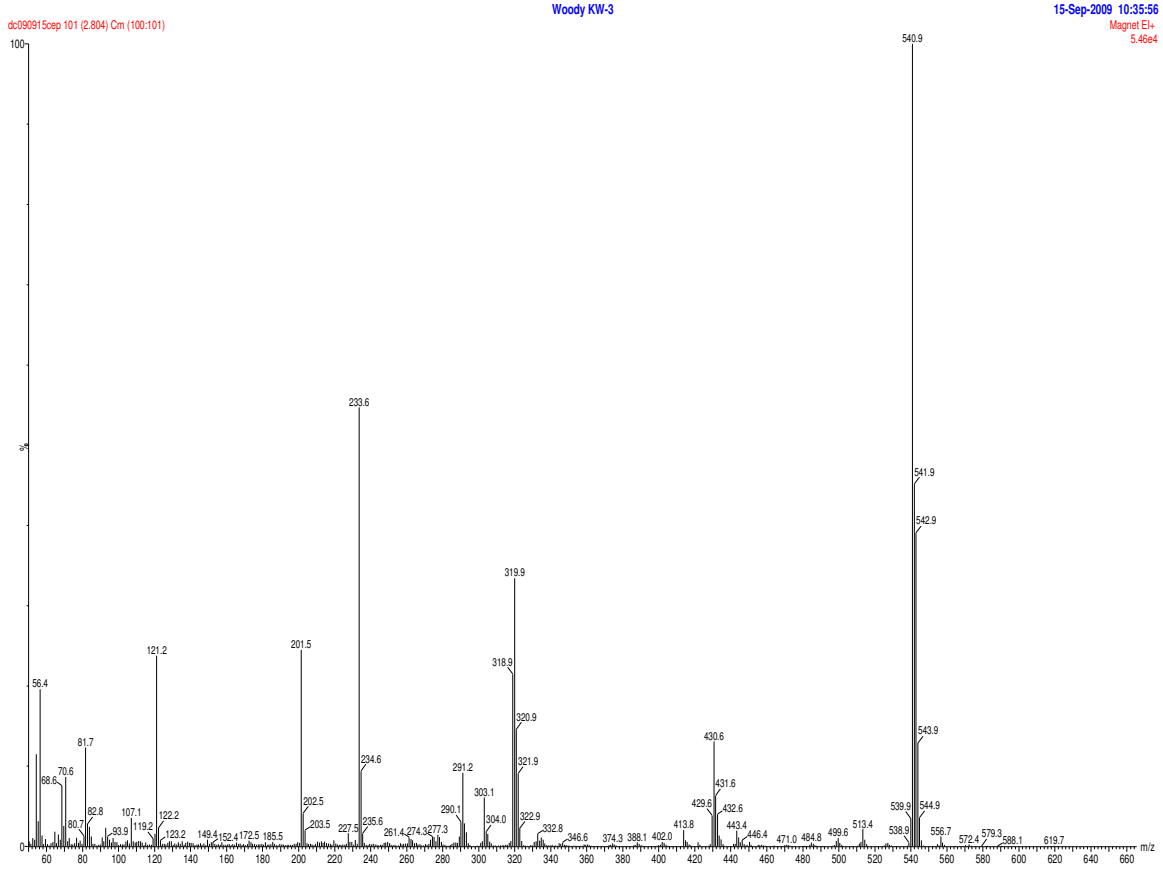

Figure E.4. ^{1}H NMR, ^{13}C NMR, IR spectrum and mass spectrum for 2,3-bis(4-(octyloxy)phenyl)thieno[3,4-b]pyrazine, **V-3b**.

5,7-Dibromo-2,3-dihexylthieno[3,4-b]pyrazine

A. ^{1}H NMR

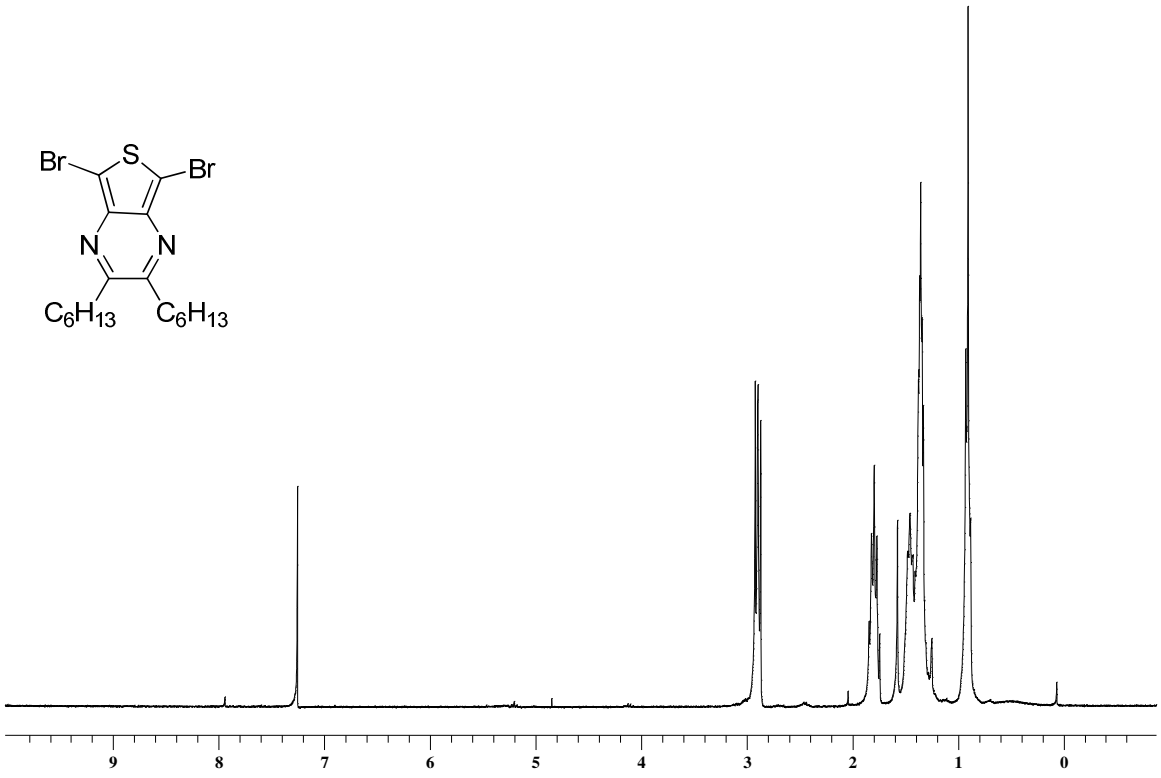

B. ^{13}C NMR

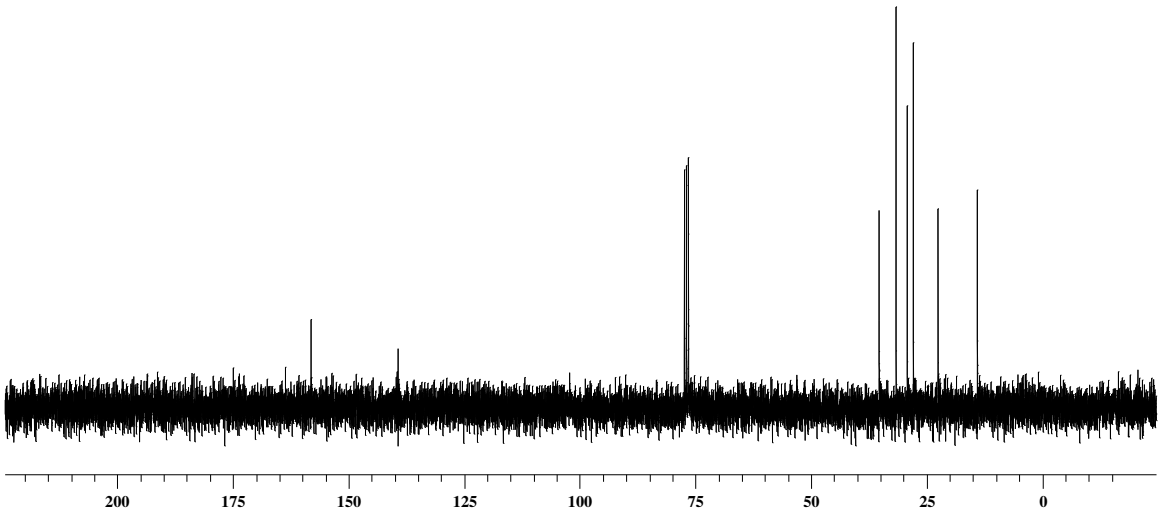

Figure E.5. ^{1}H NMR and ^{13}C NMR for 5,7-dibromo-2,3-dihexylthieno[3,4-b]pyrazine, **V-4a**.

5,7-Dibromo-2,3-bis(4-(octyloxy)phenyl)thieno[3,4-b]pyrazine

A. ^{1}H NMR

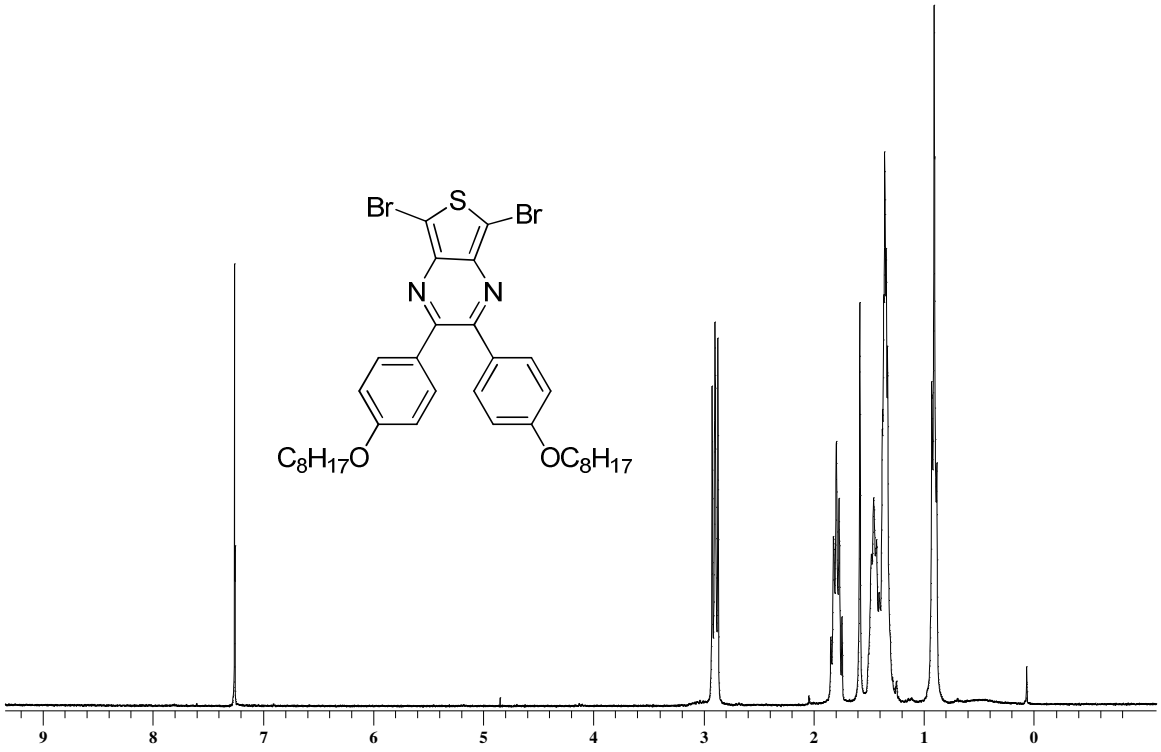

B. ^{13}C NMR

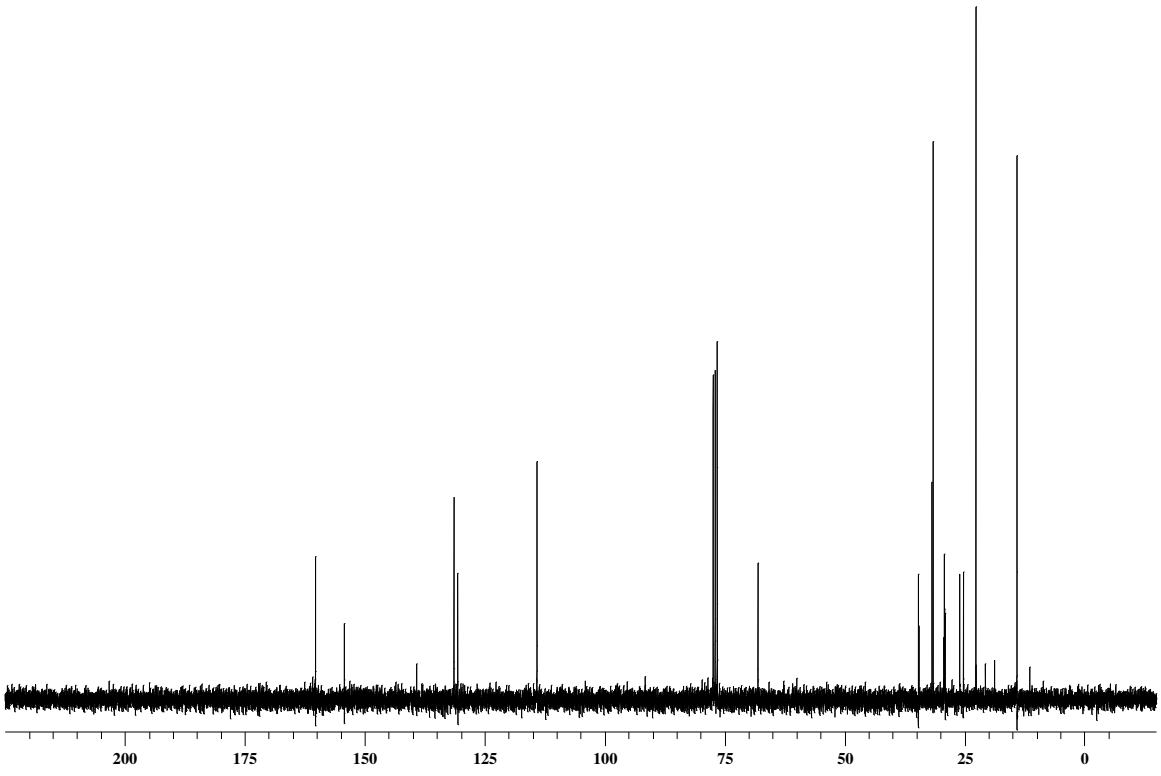

C. IR spectrum

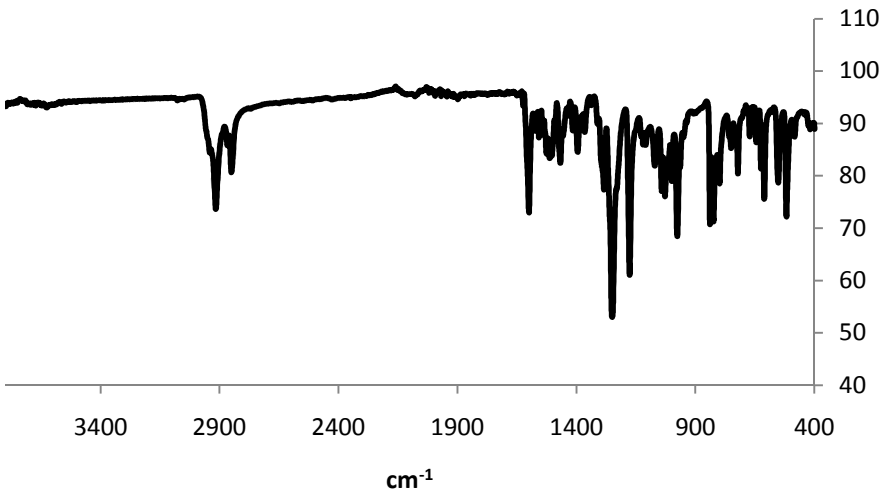

D. Mass spectrum

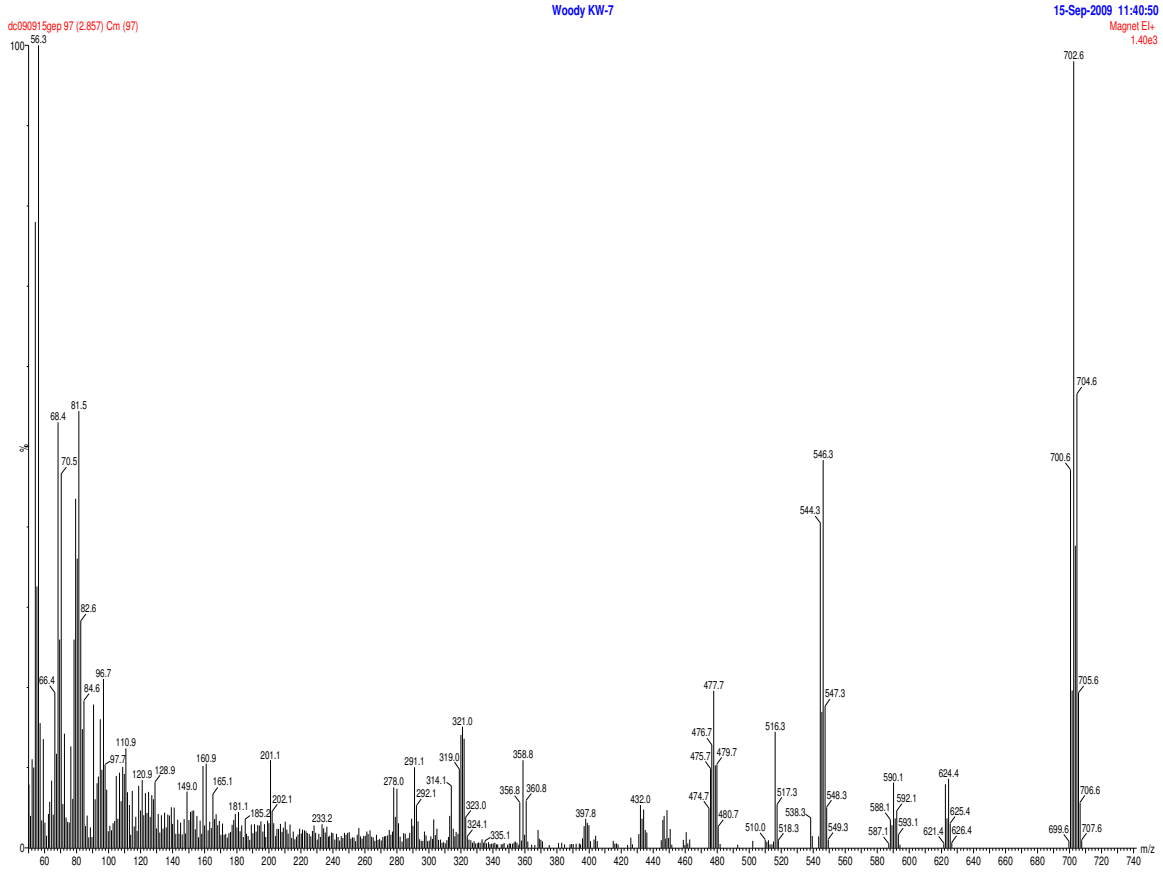

Figure E.6. ^{1}H NMR, ^{13}C NMR, IR spectrum and EI mass spectrum for 5,7-dibromo-2,3-bis(4-(octyloxy)phenyl)thieno[3,4-b]pyrazine, **V-4b**.

Poly(3-octylthiophene)

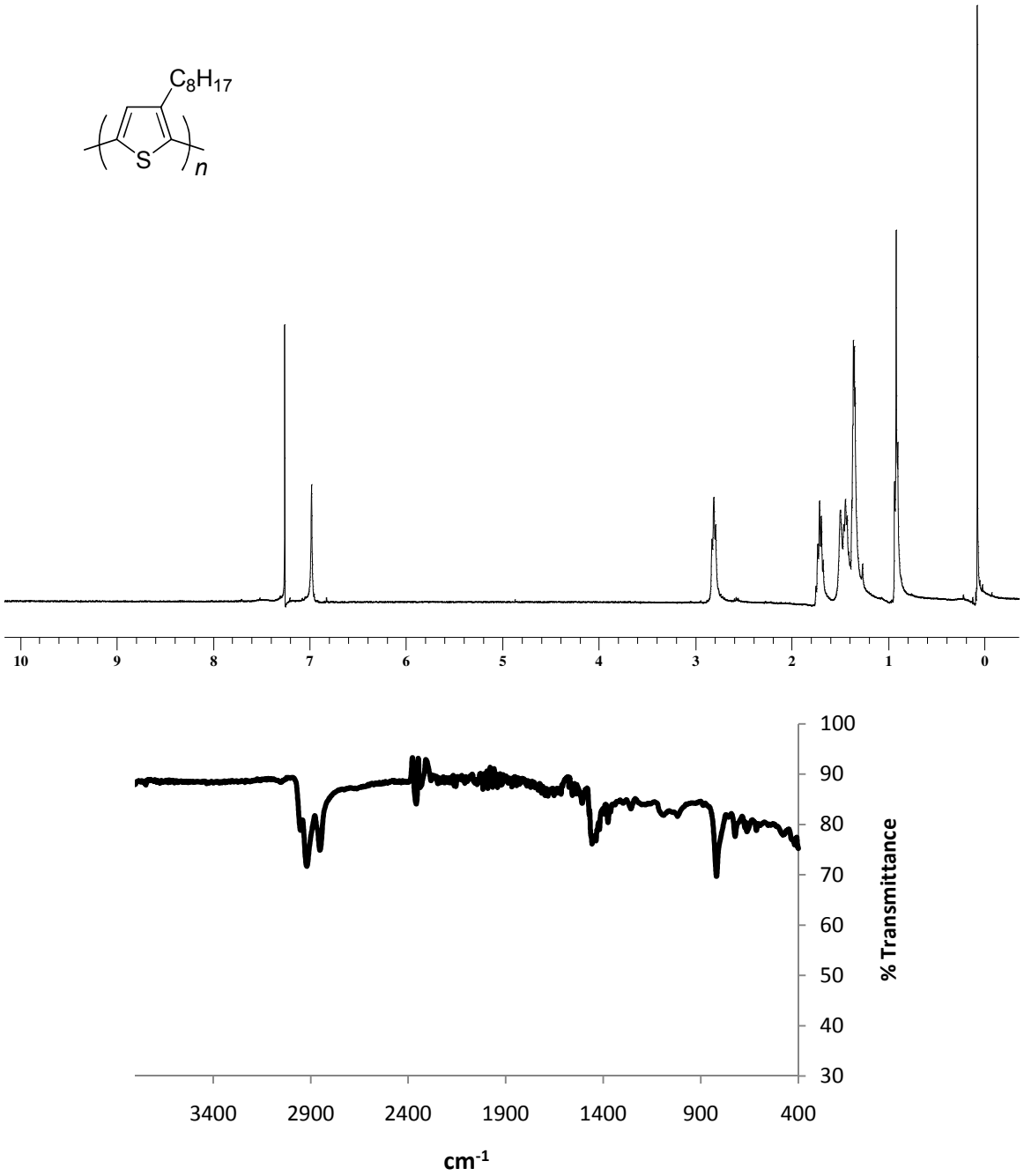

Figure E.7. ^{1}H NMR and IR spectrum for poly(3-octylthiophene), **P3OT**.

Poly(2,3-dihexylthieno[3,4-b]pyrazine)

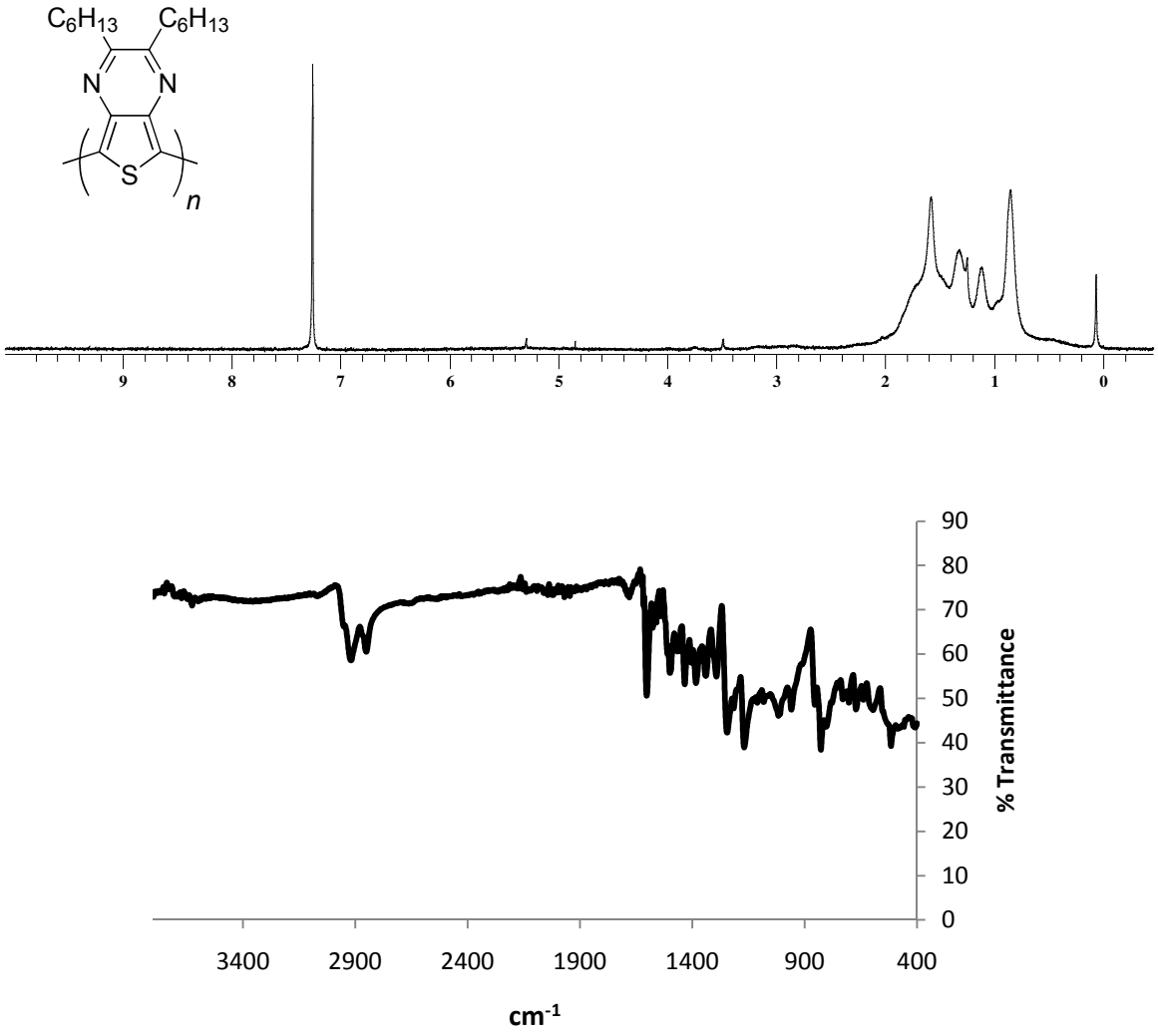

Figure E.8. [1]H NMR and IR spectrum for poly(2,3-dihexylthieno[3,4-b]pyrazine), **PThPy(C6)**.

Poly(2,3-bis(4-(octyloxy)phenyl)thieno[3,4-b]pyrazine)

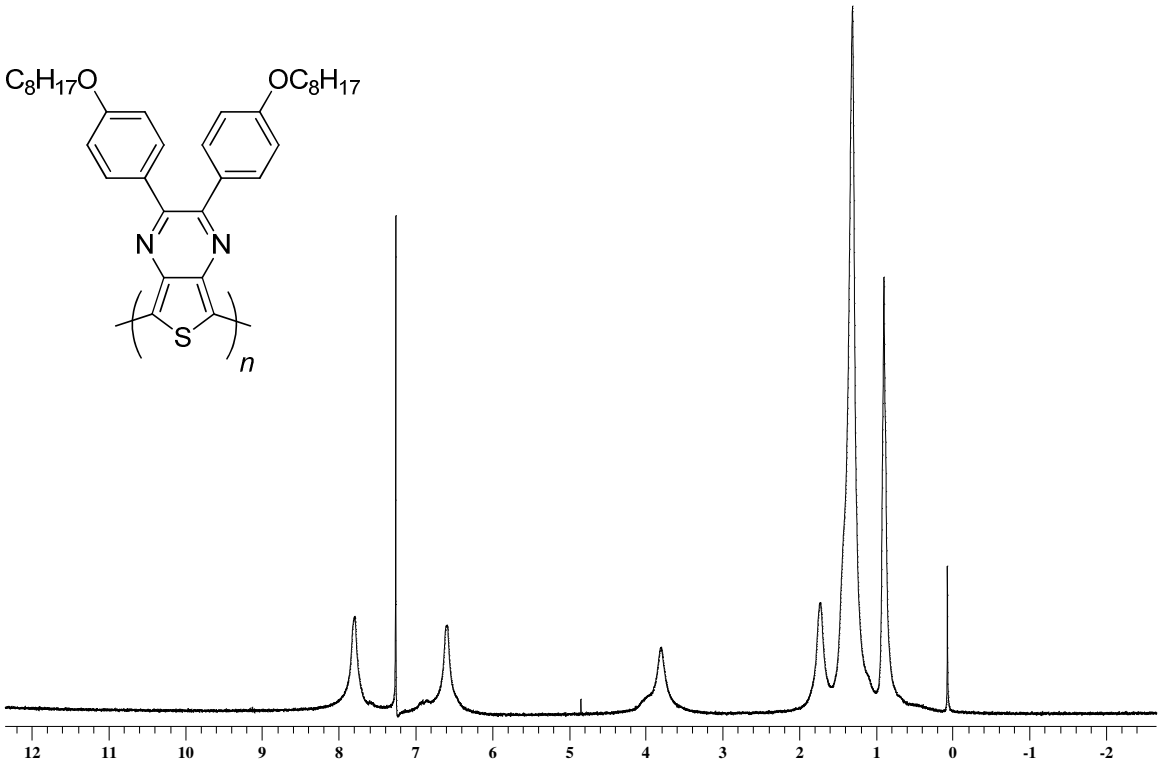

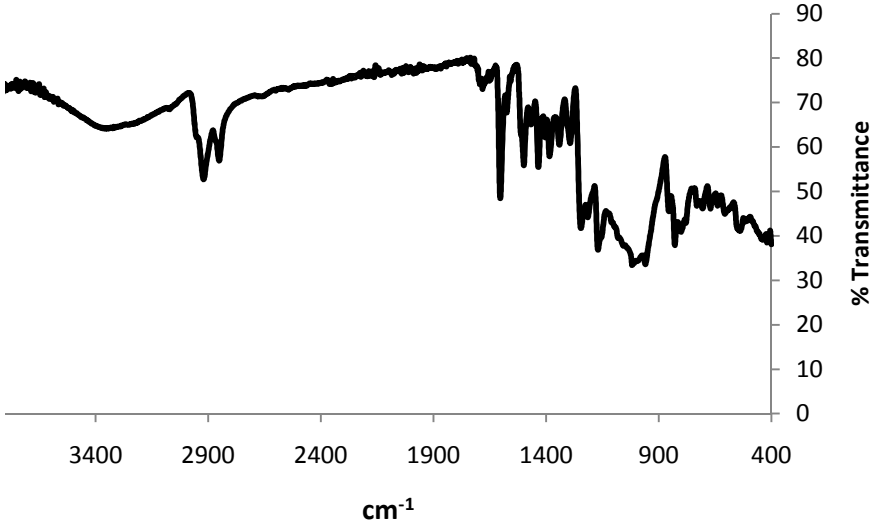

Figure E.9. [1]H NMR and IR spectrum for poly(2,3-bis(4-(octyloxy)phenyl)thieno[3,4-b]pyrazine), **PThPy(ArC8)**.

P3OT-*block*-PThPy(ArC8)

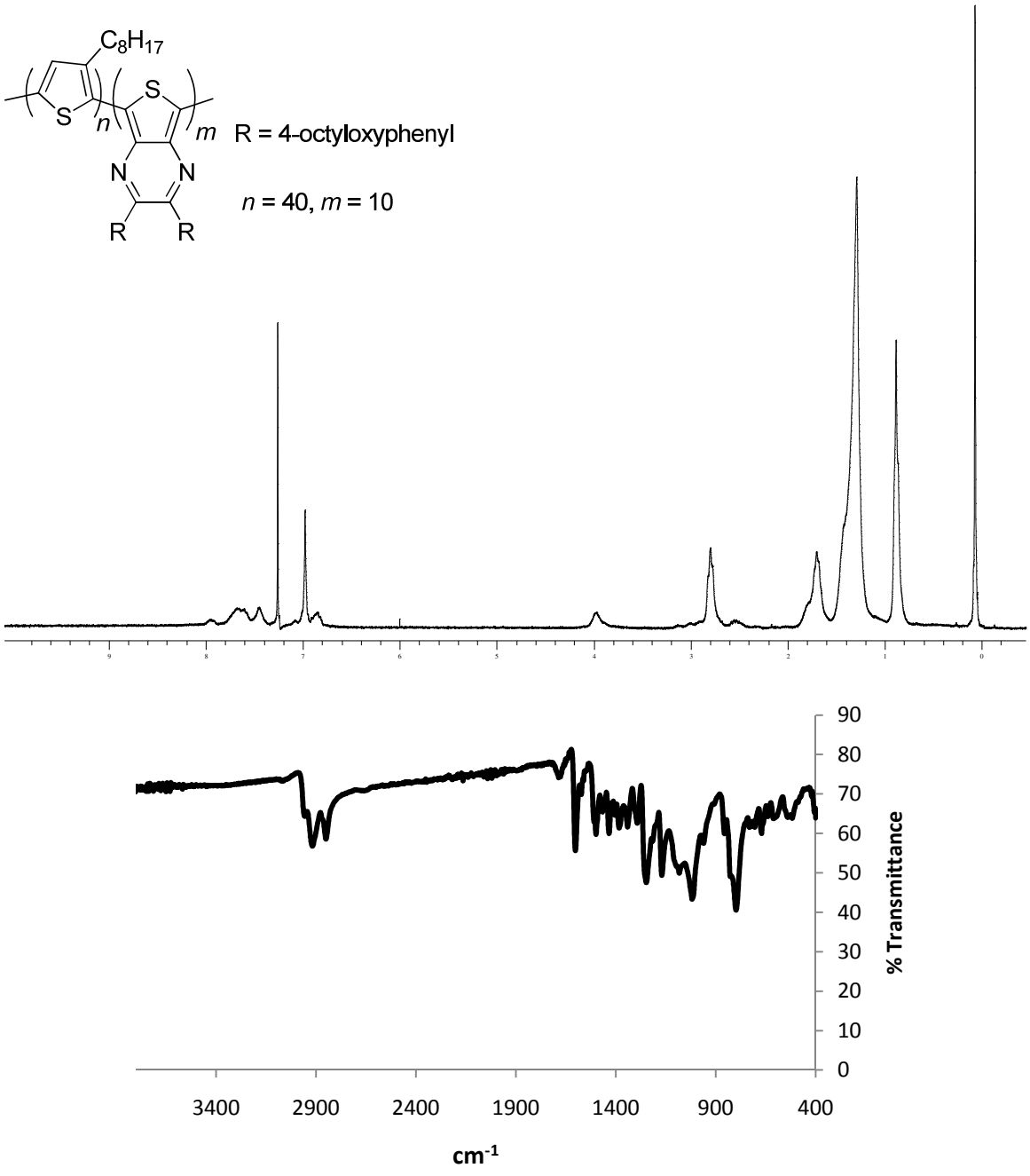

Figure E.10. ^{1}H NMR and IR spectrum for **P3OT-*block*-PThPy(ArC8)**.

APPENDIX F: ^{1}H AND ^{13}C NMR, IR AND MASS SPECTRA OF MONOMERS AND POLYMERS DESCRIBED IN CHAPTER 6

^{1}H NMR spectra were collected on a Varian Mercury Vx 300 MHz instrument using $CDCl_3$ as a solvent unless otherwise stated. ^{13} C NMR spectra were obtained at 75.5 MHz. IR analyses were performed on a Nicolet 4700 FTIR with an ATR attachment from SmartOrbit Thermoelectronic Corporation. Compounds **VI-2b** and **VI-3b** can be found in Appendix D.

5,8-dibromo-2,3-bis(4-(2-ethylhexyloxy)phenyl)quinoxaline

A.

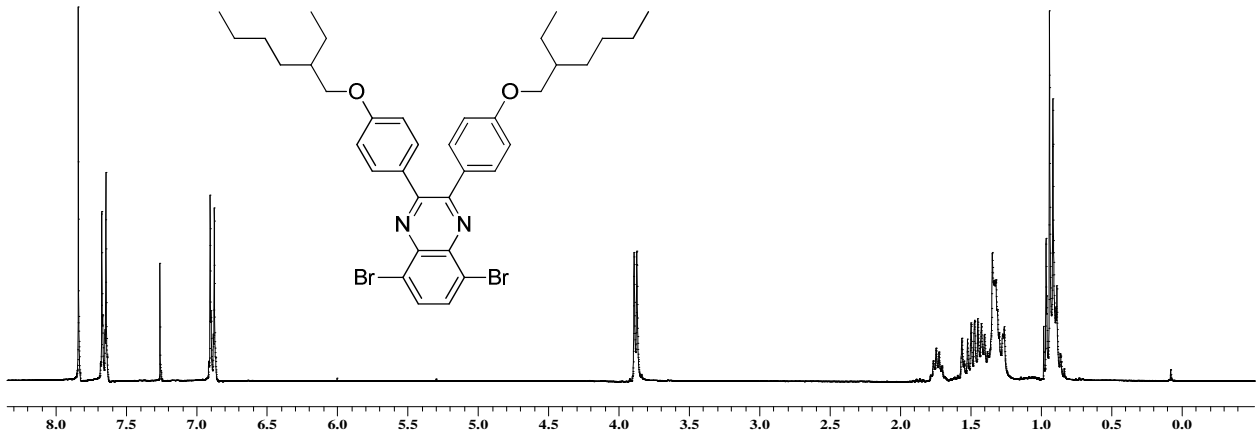

B.

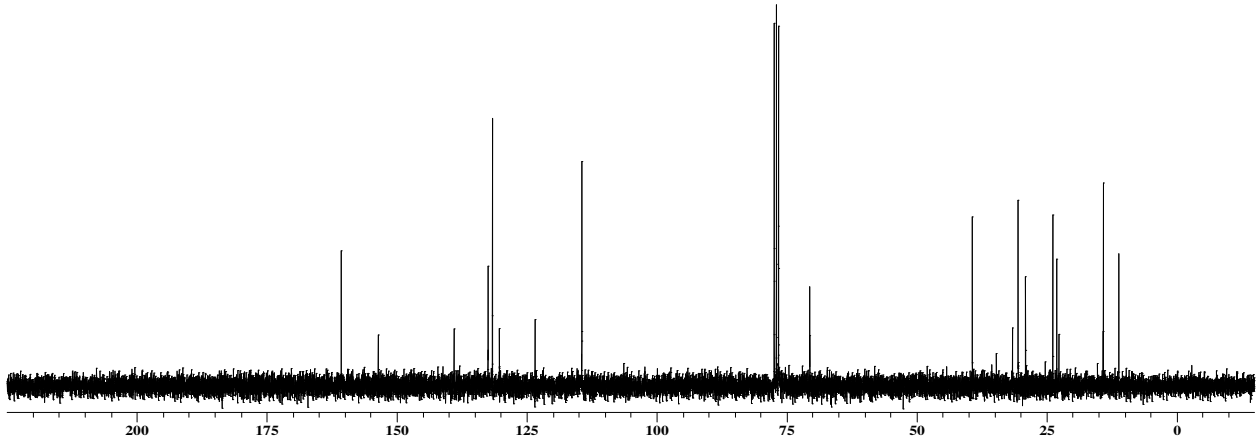

C.

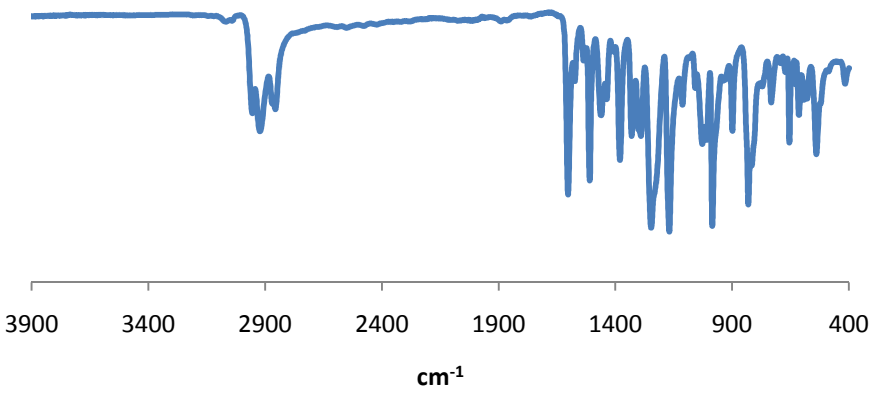

D.

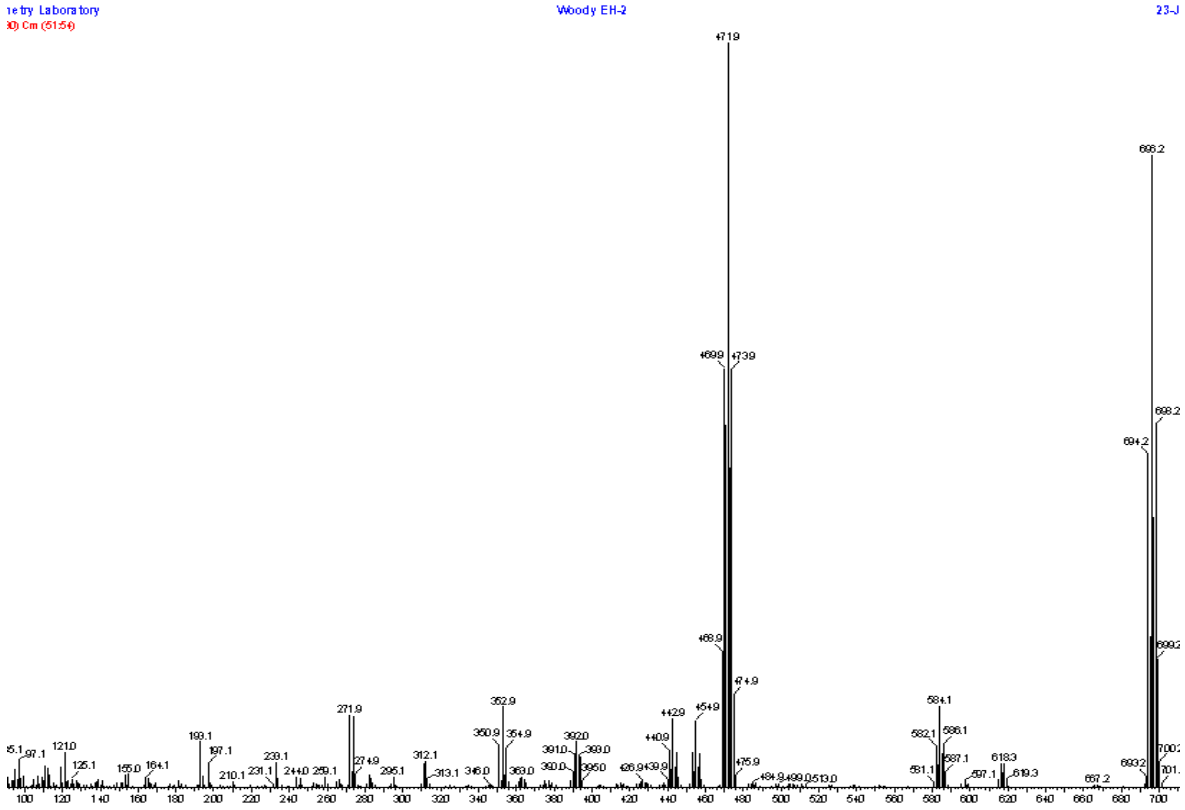

Figure F.1. ^{1}H NMR (A), ^{13}C NMR (B), IR spectrum (C) and EI mass spectrum (D) for 5,8-dibromo-2,3-bis(4-(2-ethylhexyloxy)phenyl)quinoxaline (**VI-3a**).

2,3-bis(4-(2-ethylhexyloxy)phenyl)-5,8-bis((trimethylsilyl)ethynyl)quinoxaline

A.

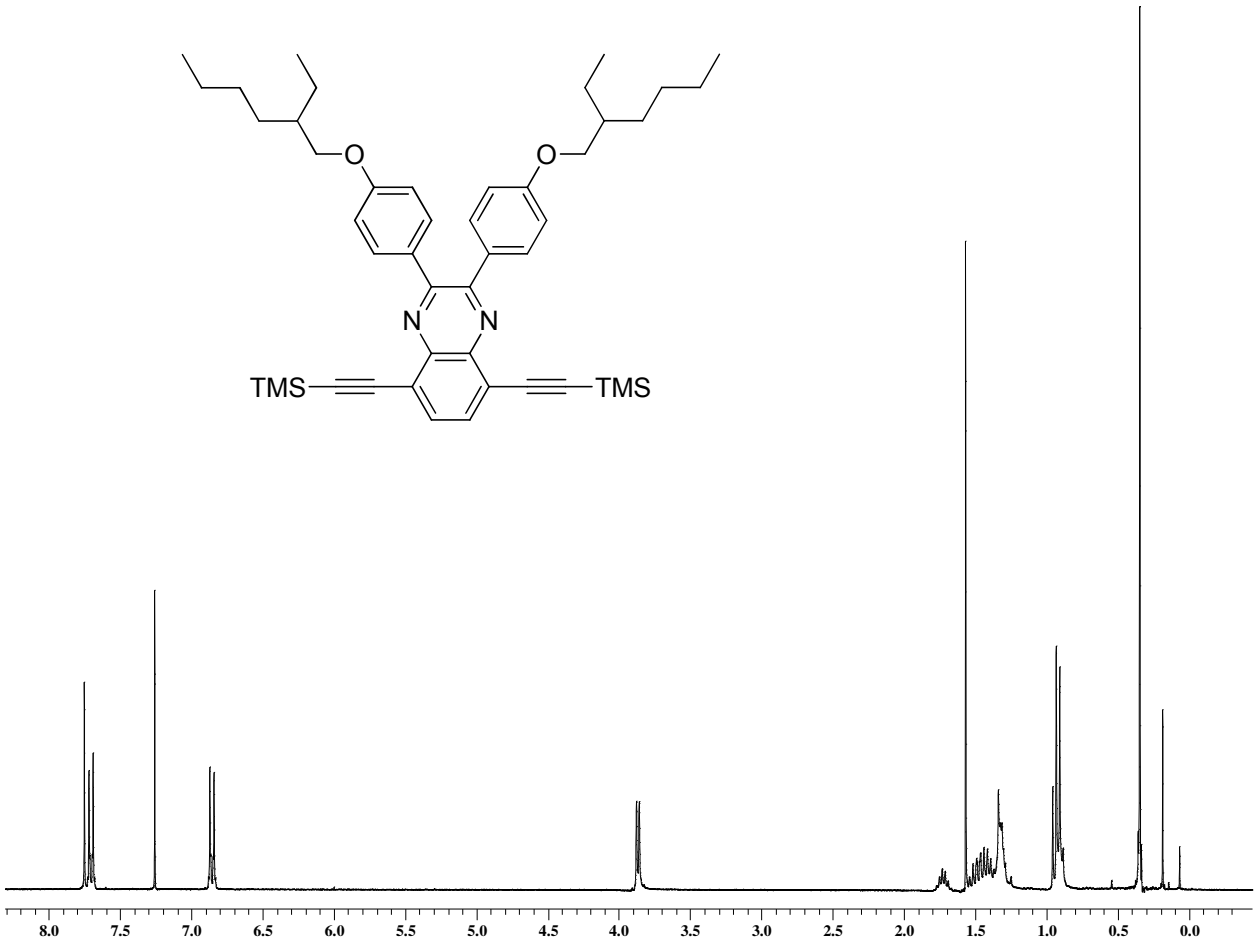

B.

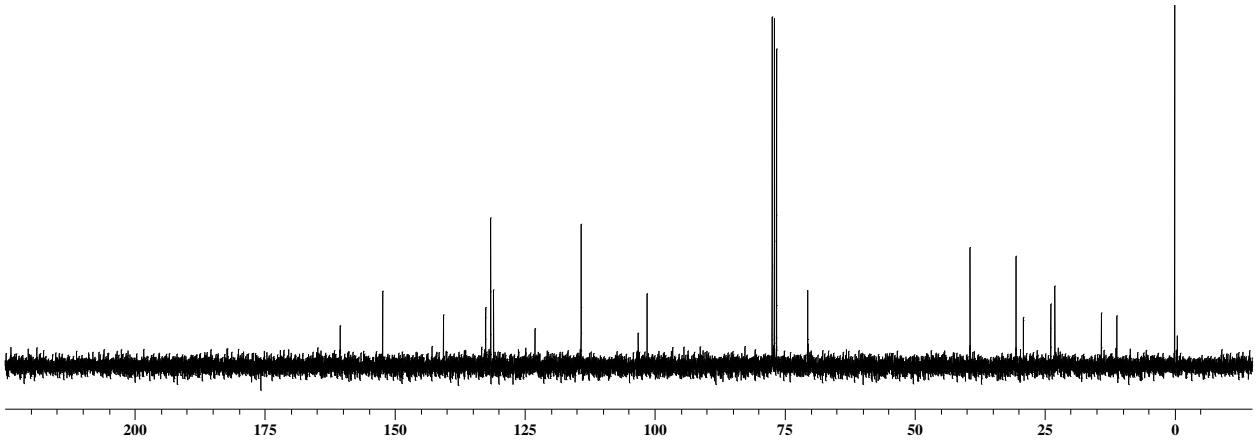

C.

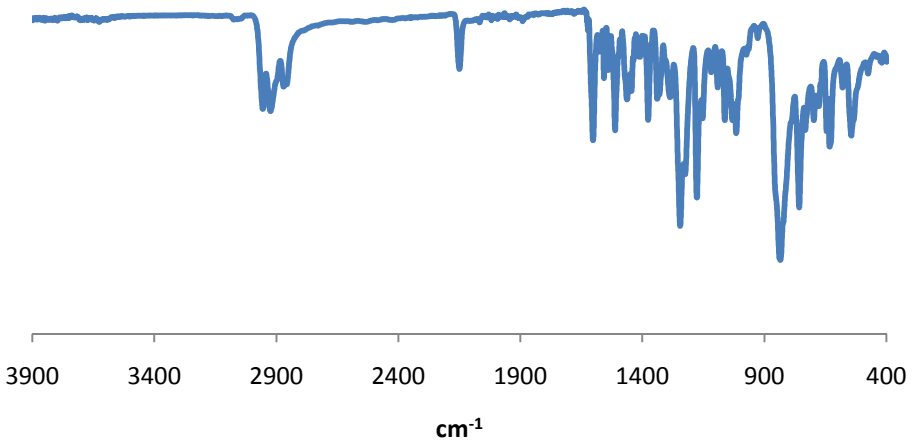

D.

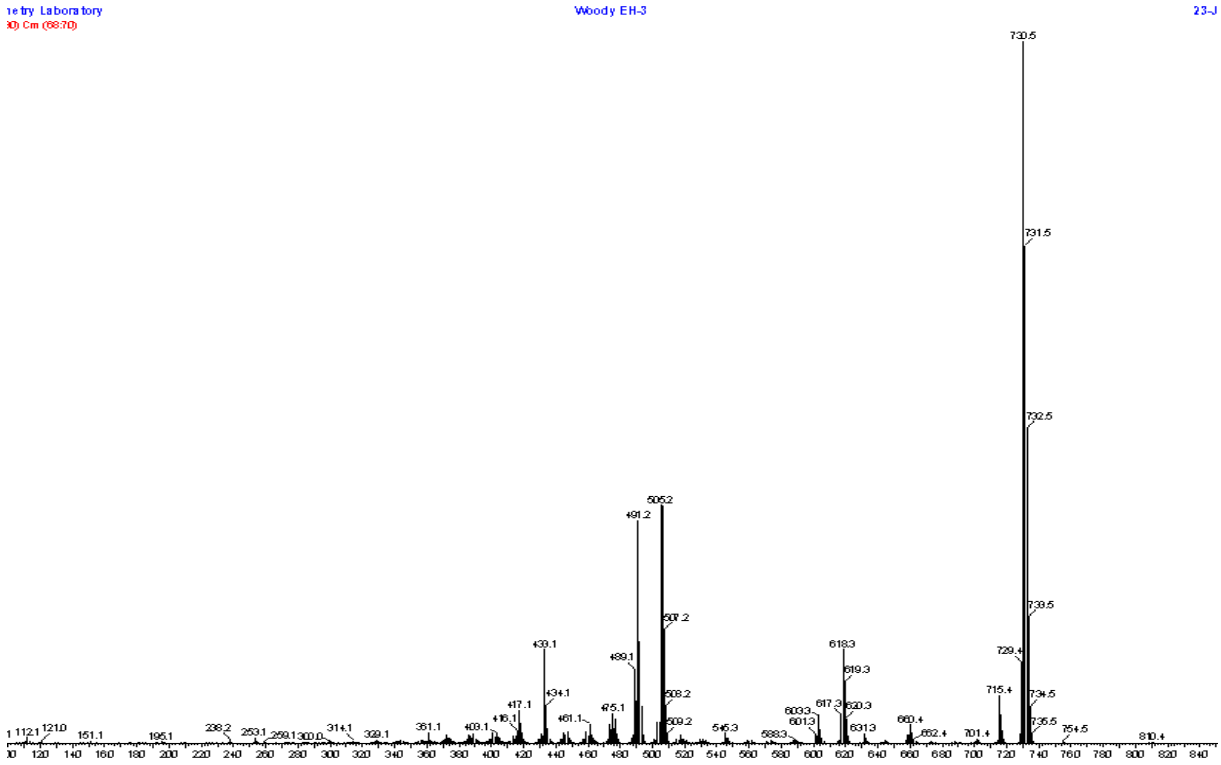

Figure F.2. ^{1}H NMR (A), ^{13}C NMR (B), IR spectrum (C) and EI mass spectrum (D) for 2,3-bis(4-(2-ethylhexyloxy)phenyl)-5,8-bis((trimethylsilyl)ethynyl)quinoxaline (**VI-4a**).

2,3-bis(4-(octyloxy)phenyl)-5,8-bis((trimethylsilyl)ethynyl)quinoxaline

A.

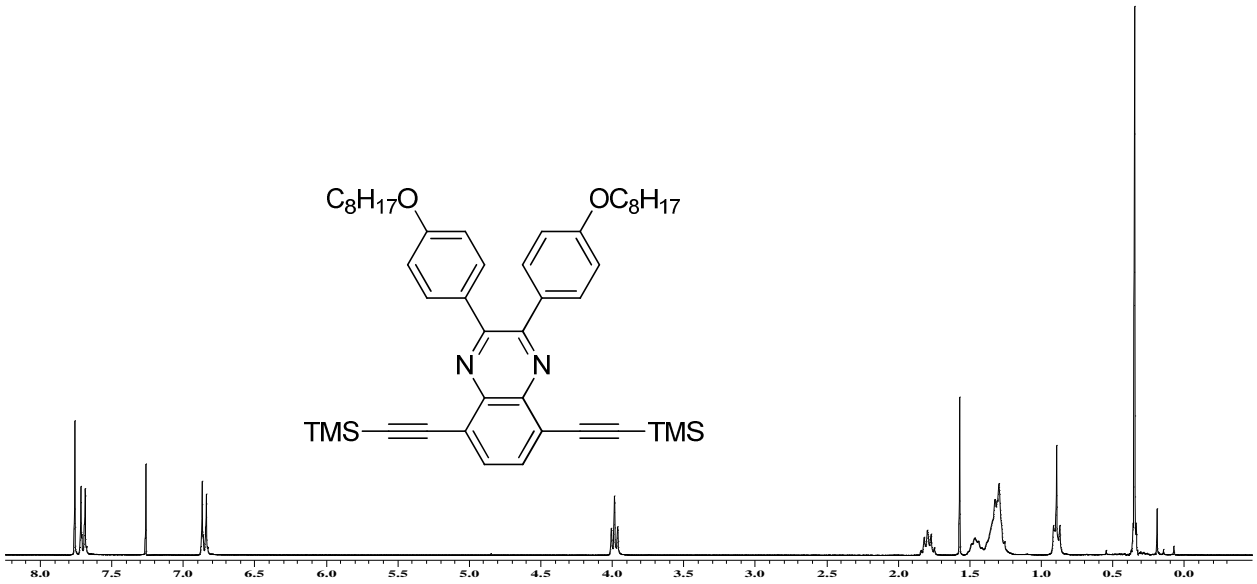

B.

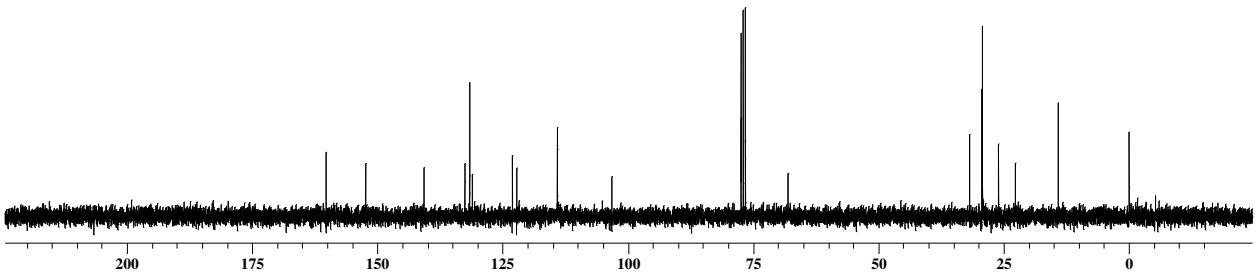

C.

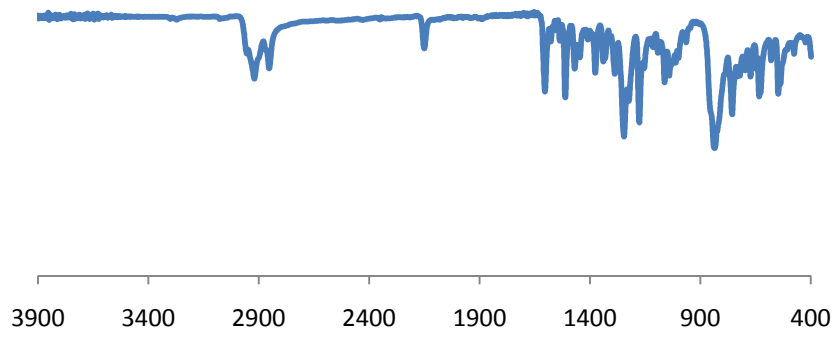

Figure F.3. ^{1}H NMR (A), ^{13}C NMR (B) and IR spectrum (C) for 2,3-bis(4-(octyloxy)phenyl)-5,8-bis((trimethylsilyl)ethynyl)quinoxaline (**VI-4b**).

5,8-diethynyl-2,3-bis(4-(2-ethylhexyloxy)phenyl)quinoxaline

A.

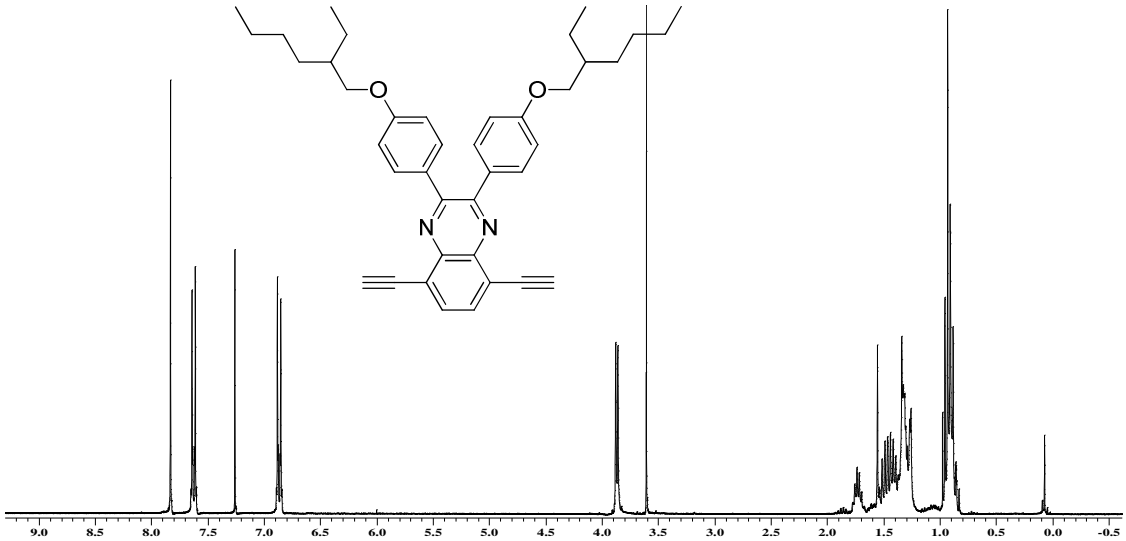

B.

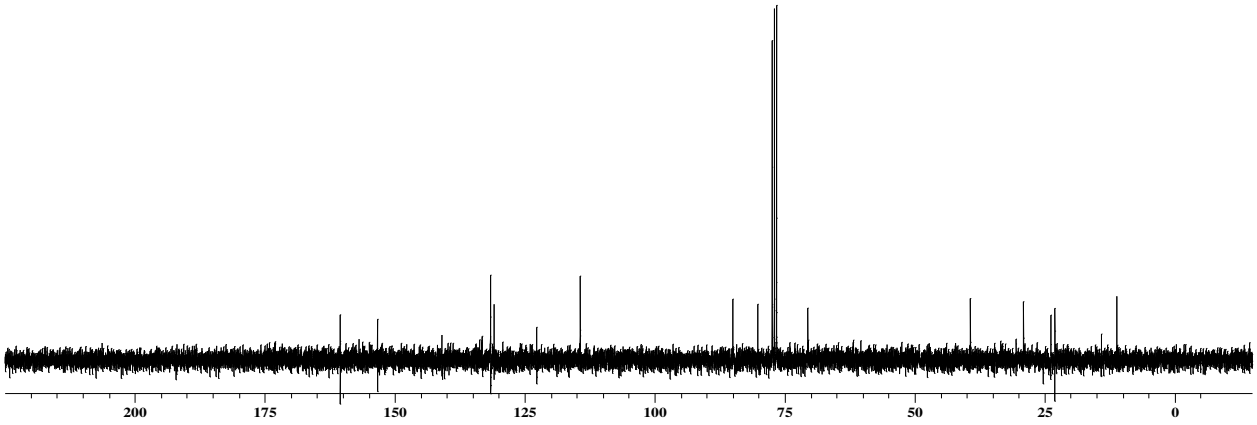

C.

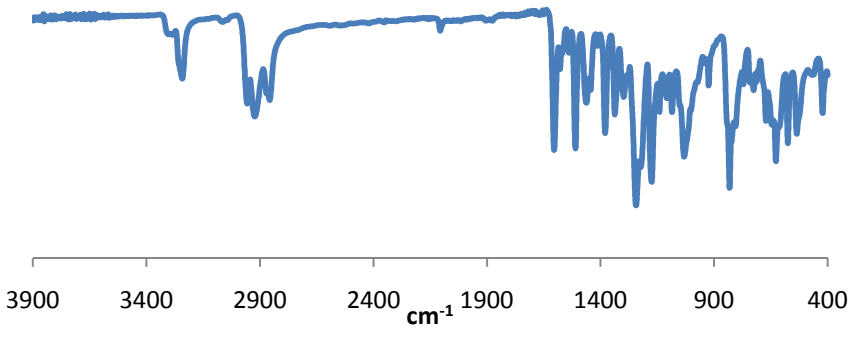

Figure F.4. ^{1}H NMR (A), ^{13}C NMR (B), and IR spectrum (C) for 5,8-diethynyl-2,3-bis(4-(2-ethylhexyloxy)phenyl)quinoxaline (**VI-5a**).

5,8-diethynyl-2,3-bis(4-(octyloxy)phenyl)quinoxaline

A.

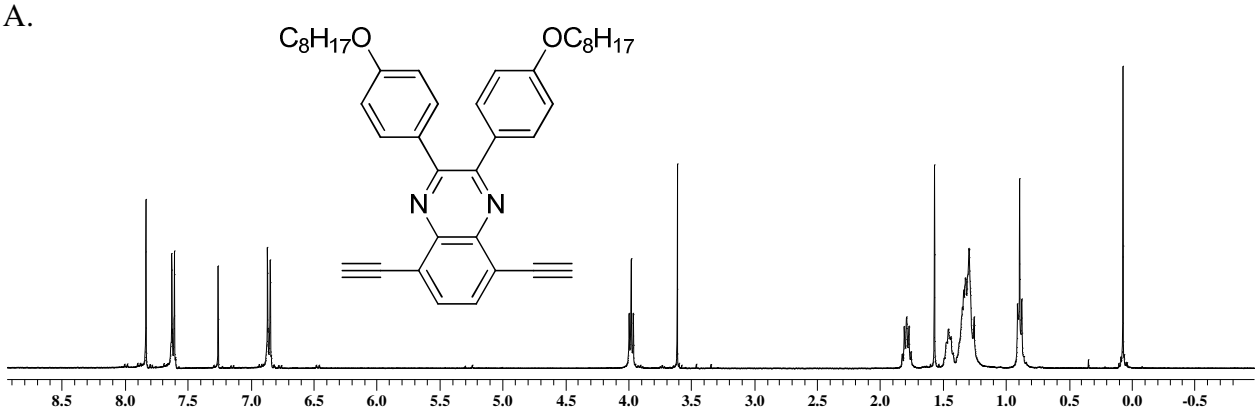

B.

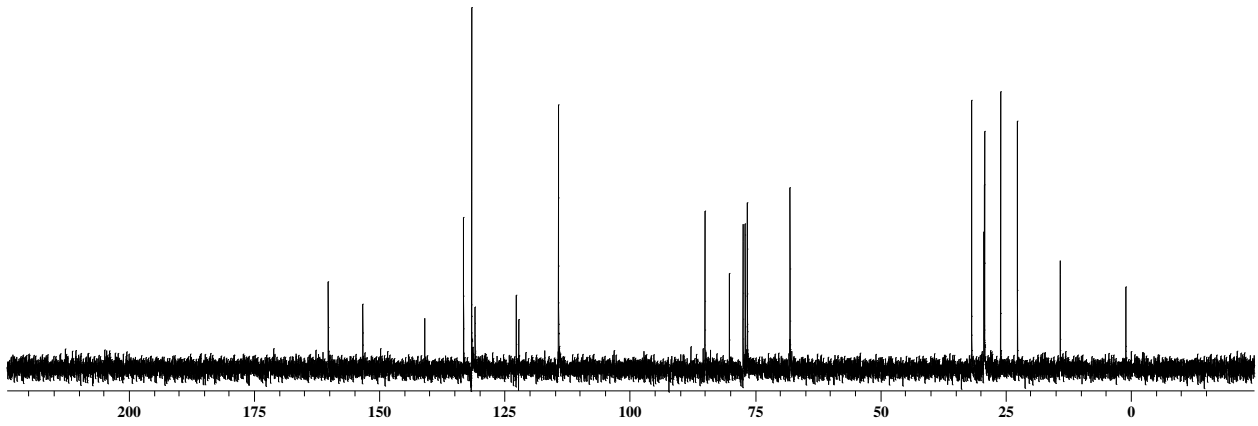

C.

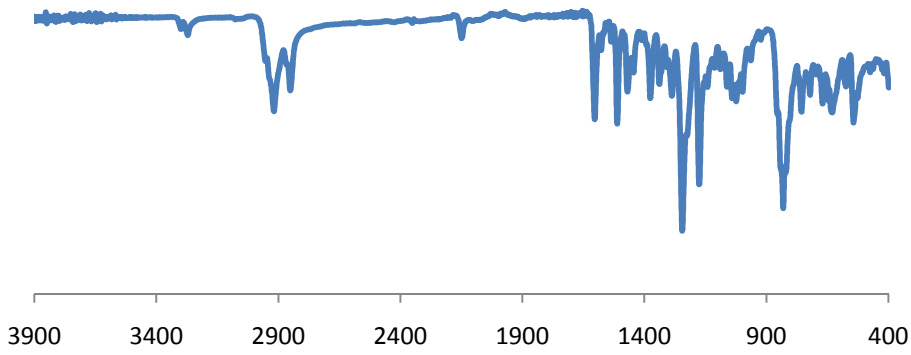

Figure F.5. ^{1}H NMR (A), ^{13}C NMR (B), and IR spectrum (C) for 5,8-diethynyl-2,3-bis(4-(octyloxy)phenyl)quinoxaline (**VI-5b**).

A.

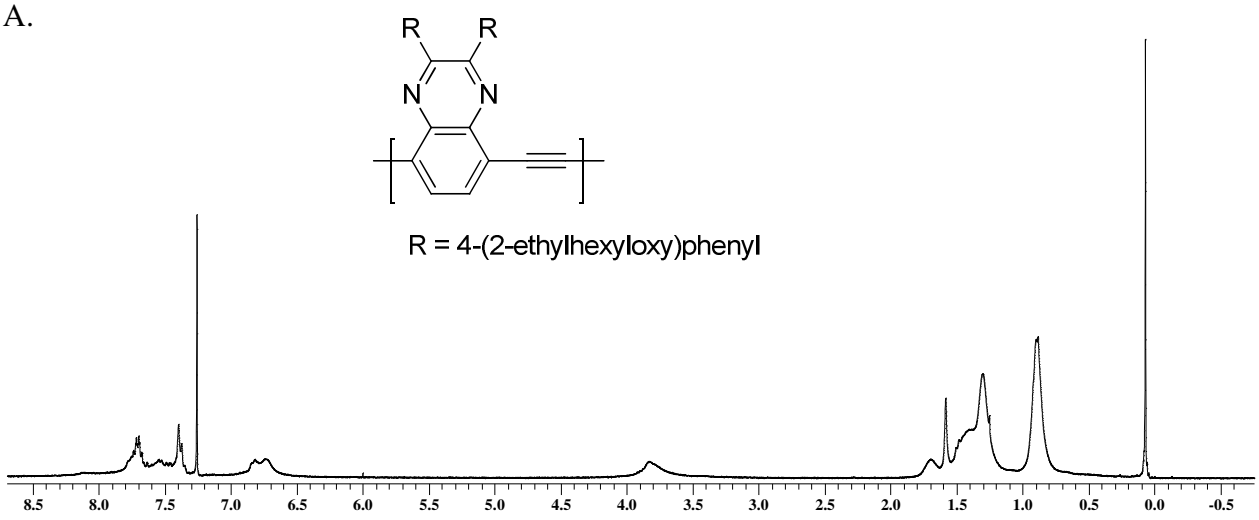

B.

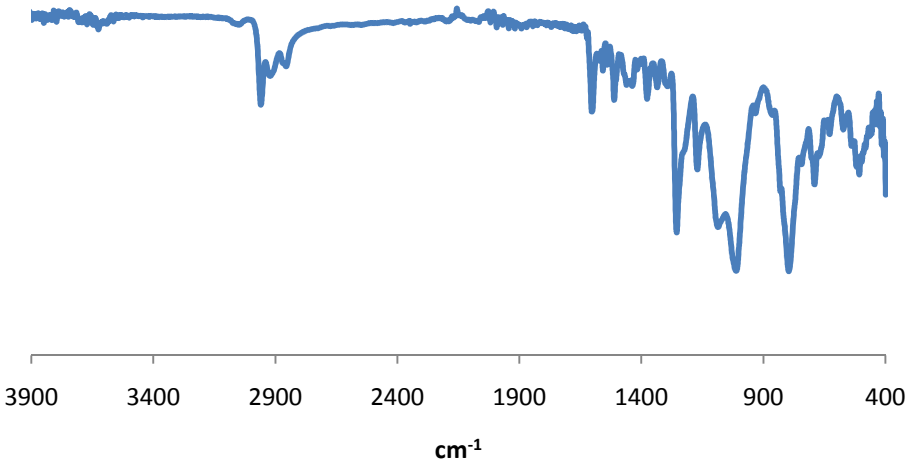

Figure F.6. ^{1}H NMR (A) and IR spectrum (B) for poly(5,8-quinoxaline ethynylene) **PQE(EH)**.

A.

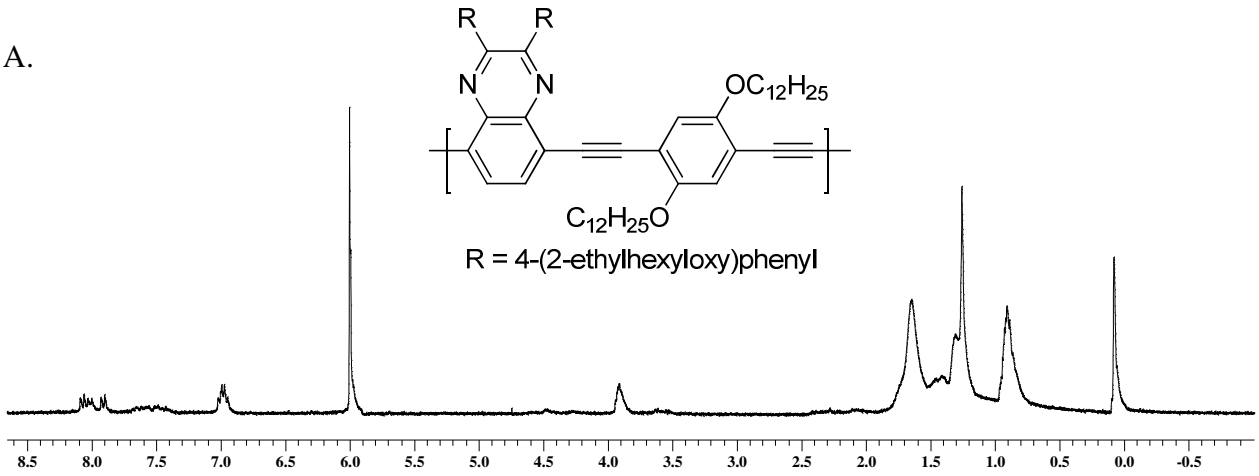

B.

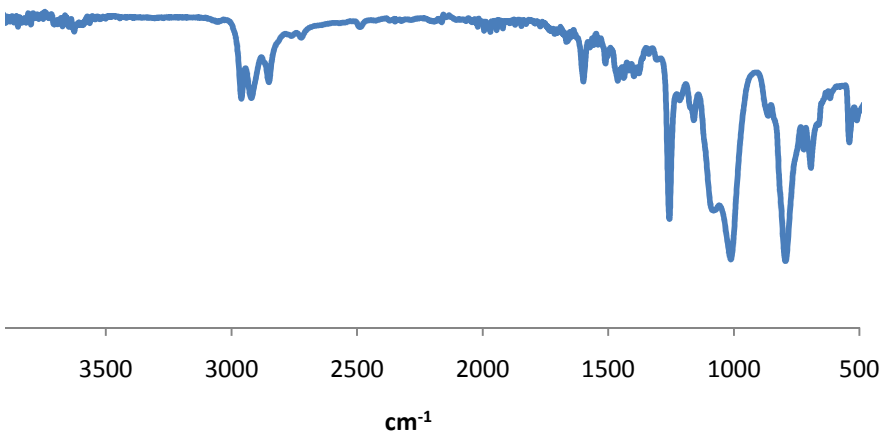

Figure F.7. ^{1}H NMR (A) and IR spectrum (B) for **PQE(EH)-*alt*-PPE(C12)** (^{1}H NMR solvent is 1,1,2,2-tetrachloroethane-D_2).